Daniel Gutierrez Rojas

ANOMALY DETECTION IN CYBER-PHYSICAL APPLICATIONS

ACTA UNIVERSITATIS LAPPEENRANTAENSIS 1074

Daniel Gutierrez Rojas

ANOMALY DETECTION IN CYBER-PHYSICAL APPLICATIONS

Dissertation for the degree of Doctor of Science (Technology) to be presented with due permission for public examination and criticism in the Auditorium 1316 at Lappeenranta–Lahti University of Technology LUT, Lappeenranta, Finland on the 25th of May, 2023, at noon.

Acta Universitatis
Lappeenrantaensis 1074

Supervisors Associate Professor Pedro Juliano Nardelli
LUT School of Energy Systems
Lappeenranta–Lahti University of Technology LUT
Finland

Professor Yongheng Yang
College of Electrical Engineering
Zhejiang University
China

Dr. Gonçalo Mendes
LUT School of Energy Systems
Lappeenranta–Lahti University of Technology LUT
Finland

Reviewers Professor Isabel Praça
School of Engineering
Polytechnic of Porto-ISEP
Portugal

Assistant Professor Mateus Giesbrecht
School of Electrical and Computing Engineering
University of Campinas
Brazil

Opponent Assistant Professor Mateus Giesbrecht
School of Electrical and Computing Engineering
University of Campinas
Brazil

ISBN 978-952-335-933-8
ISBN 978-952-335-934-5 (PDF)
ISSN 1456-4491 (Print)
ISSN 2814-5518 (Online)

Lappeenranta-Lahti University of Technology LUT
LUT University Press 2023

Abstract

Daniel Gutierrez Rojas
Anomaly detection in cyber-physical applications
Lappeenranta 2023
68 pages
Acta Universitatis Lappeenrantaensis 1074
Diss. Lappeenranta–Lahti University of Technology LUT
ISBN 978-952-335-933-8, ISBN 978-952-335-934-5 (PDF), ISSN 1456-4491 (Print), ISSN 2814-5518 (Online)

Anomaly detection is a crucial task in many industrial environments as it enables a safer and more reliable operation of different processes; it is usually seen as a separate process from the industrial system design. Performance improvements mostly rely on detection methods. Therefore, anomaly detection can be seen as an end in itself. In this context, the focus of this doctoral dissertation is to highlight the importance of anomaly detection considering different, often neglected, subfunctions such as sampling, network architecture, and planning support. These subfunctions, along with an analysis of detection performance and upcoming communication technologies, are merged to ultimately improve anomaly detection. This is achieved by the integration of anomaly detection in the cyber-physical system composed of three articulated layers: a physical layer, a data layer, and a decision layer, where the layers have specific tasks that could be enhanced or modified, thereby providing additional flexibility and scalability. Simple adjustments to the physical layer like an increase in the number of sensors or changing the sampling methodology may result in an average improvement of the data transmission rate. In the data layer, the data aggregation method to be used has an impact on the anomaly detection accuracy. The results presented in this doctoral dissertation were obtained in specific cyber-physical applications, such as a microgrid, a chemical process, and a power transmission system. The three-layer model applied to the Tennessee Eastman process shows how it benefits the levels of data processing, pointing out in which layer greater improvements can be made even including details of the communication network and the computing platform. In the physical layer, the event-driven method used to transmit samples from the sensors yielded gains in the data transmission rate of 20% and improved anomaly detection in five out of six hard-to-detect faults. In a transmission line application, in the data layer, the quantitative association rule mining algorithm was able to maintain a 98% accuracy of anomaly detection while retrieving explainable results. Furthermore, in the decision layer, predictions of anomalies served as multiobjective chance constraint optimization, balancing resilience and economic objectives in a microgrid. Finally, an extensive analysis of protection in microgrids for anomaly detection showed that multiconnectivity of wired and wireless technologies, such as 5G, meets the requirements of wired networks, thereby improving the flexibility of this application.

Keywords: anomaly detection, cyber-physical systems, event-driven sampling, ML techniques and wireless communication

Acknowledgments

These four years spent at LUT university have been an amazing journey. I have had the opportunity to meet not only great professionals in the research community but also amazing human beings from whom I have continuously learned and grown as an engineer and as a person.

I would like to thank Pedro Nardelli for his huge support during my studies and research. All the constant encouragement to rolling up your sleeves, participate in projects or calls, and review carefully every research text I wrote was essential during my time as a doctoral student. I feel very lucky to have Pedro as my supervisor and friend, with whom I have shared a lot of moments during my time at LUT from project meetings to casual conversations having always the intent to grow and do a better job for society. Pedro's willingness to help students and anyone who comes asking for opportunities is beyond measure; I express my appreciation to him for receiving me in Finland as I never thought I would end up living in this country I call home today.

I am grateful to my co-supervisors Gonçalo Mendes and Yongheng Yang for their contributions to this work and the fruitful discussions for the directions of the research.

I would like to thank the dissertation reviewer, Prof. Isabel Praça and honored opponent and dissertation reviewer Prof. Mateus Giesbrecht for the careful examination of the topics in question; your feedback was on point and helped with the final work.

Thanks to all the FIREMAN project members with whom I collaborated close in research activities. To the researchers Charalampos, Constantinos, Hirley, Ioannis, Gustavo, Nicola, Pavol, Merim and Subham for the valuable insights into the research carried out and some of whom I had the opportunity to meet during project trips. Special thanks to the NTUA members in Athens for the project research done, to Alkistis and Dimitris: your comments on work included in this dissertation were highly relevant.

This research work was mainly funded by the Academy of Finland via FIREMAN consortium n.326270 as part of the CHIST-ERA grant CHIST-ERA-17-BDSI-003; the EnergyNet Fellowship n.328869/n.352654; the X-SDEN project n.349965; and the ee-IoT project n. 319009. The finantial support of Elisa Oy, LUT Research Foundation and ERIGrid 2.0 is greatly acknowledged.

These years have been definitely way easier with the support of my partner Elisa. All the special moments have contributed to my adaptation to Finland and brought a lot of happiness that ultimately permeates the professional field—I love you for putting up with everything and for the years to come.

Most of my time as a researcher at LUT I spent working from home because of COVID-19 and can't say I was lonely because I had the amazing company of Doris and Nessie

(our dogs), making it very fun to work during those difficult times. Special thanks to Heli and Mikko Mutanen for their support in these years and welcoming to their family always with a positive attitude.

Despite being so far away, I have always counted on the support of my family in Colombia, especially my mom Angela, my brother Andres, and my abuela Paulina, who send their constant love, and I count on them in every matter of life.

I had the opportunity to collaborate with great researchers in the Cyber-Physical Systems Group, such as Arthur, Mehar, Majid, Arun, Pedro G, Mohammed, Ali, Cassia, Daynara, Dick, and those in other LUT research groups, such as Salla, Aleksei, Mirika, Christina, Pekka, Daniel Texidor and Nelli. Thanks to Dr. Hanna Niemelä for the language review of the research done and this dissertation. Special thanks to the LES secretaries Marika Hyrylä, Päivi Nuutinen, LES staff member Tarja Sipiläinen, and doctoral HR members Sari Damsten-Puustinen and Anu Honkanen—their work all together makes researchers' life way more easy to handle with bureaucracy and enhances the research quality of life.

Finally, I would like to thank the friends I have made on this journey. For all the social post-working afternoons to Leticia, who eventually became a research colleague at LES, Vaardan and Sankar, for the moments inside and outside university and football discussions. And others, such as Ana, Clara, Asiia, Viktor, Eeva, Harri, Appo, Oki, and long-distance friends Pablo, Santiago, and Federico, who one way or another have accompanied me in this wonderful adventure we call life.

Thanks.

Daniel Gutierrez Rojas
March 2022
Lappeenranta, Finland

Dedicated to my grandmother and my mother,
Maria Paulina Rojas and Angela Maria Rojas

Con amor, Dani

Contents

List of publications

Publication I

Gutierrez-Rojas, D., Ullah, M., Christou, I.T., Almeida, G., Nardelli, P., Carrillo, D., Sant'Ana, J. M., Alves, H., Dzaferagic, M., Chiumento, A. and Kalalas, C. (2020). Three-layer Approach to Detect Anomalies in Industrial Environments based on Machine Learning. In: *2020 IEEE Conference on Industrial Cyberphysical Systems (ICPS)*, pp. 250–256.

The author developed the general framework and wrote most of the publication.

Publication II

Gutierrez-Rojas, D., Mashlakov, A., Brester, C., Niska, H., Kolehmainen, M., Narayanan, A., Honkapuro, S. and Nardelli, P. H. J. (2021). Weather-Driven Predictive Control of a Battery Storage for Improved Microgrid Resilience. *IEEE Access*, vol. 9, pp. 163108–163121.

The author developed the resilience framework, evaluated the models, and wrote most of the publication.

Publication III

Gutierrez-Rojas, D., Christou, I.T., Dantas, D., Narayanan, A., Nardelli, P. H. J. and Yang, Y. (2022). Performance evaluation of machine learning for fault selection in power transmission lines. *Knowledge and Information Systems*, 64, pp. 859–883.

The author surveyed the literature, developed the fault identification model, and wrote the publication.

Publication IV

Gutierrez-Rojas, D., Räsänen, P., Belisario, A. B., Dzaferagic, M., Almeida, G. M. and Nardelli, P. H. J. (2022). Improving Fault Detection in Industrial Processes by Event-Driven Data Acquisition. *IEEE Access*, vol. 10, pp. 80918–80931.

The author developed the event-driven models, prepared the datasets, produced the results, and wrote most of the publication.

Publication V

Gutierrez-Rojas, D., Nardelli, P. H., Mendes, G., and Popovski, P. (2021). Review of the State of the Art on Adaptive Protection for Microgrids Based on Communications. *IEEE Transactions on Industrial Informatics*, vol. 17, no. 3, pp. 1539–1552.

The author surveyed the literature, compiled the requirements, and wrote most of the paper.

Other publications

The following publications have been produced during the doctoral studies. The author has contributed as a main researcher or co-author to these papers, but they are not included in this dissertation, because the topics are not relevant to the research questions, or they are embedded in the included publications.

Journal papers

Gutierrez-Rojas, D., Demidov, I., Kontou, A., Lagos, D., Sahoo, S., and Nardelli, P. H. (2023). Operational Issues on Adaptive Protection of Microgrids due to Cyber Attacks. *IEEE Transactions on Circuits and Systems II: Express Briefs*, Early Access.

Narayanan, A., Sousa De Sena, A., **Gutierrez-Rojas, D.**, Carrillo Melgarejo, D., Hussain, M., Ullah, M., Bayhan, S., and Nardelli, P. H. (2020). Key Advances in Pervasive Edge Computing for Industrial Internet of Things in 5G and Beyond. *IEEE Access*, vol. 8, pp. 206734–206754.

Castro Tomé, M. d., **Gutierrez-Rojas, D.**, Nardelli, P. H., Kalalas, C., d. Silva, L. C. P., and Pouttu, A. (2022). Event-Driven Data Acquisition for Electricity Metering: A Tutorial. *IEEE Sensors Journal*, vol. 22, no. 6, pp. 5495–5503.

Narayanan, A., Korium, M., Carrillo Melgarejo, D., Hussain, M., Sousa De Sena, A., Goria, P., **Gutierrez-Rojas, D.**, Ullah, M., Esmaeelnezhad, A., Rasti, M., Pournaras, E., and Nardelli, P. H. (2022). Collective Intelligence using 5G: Concepts, Applications, and Challenges in Sociotechnical Environments. *IEEE Access*, vol. 10, 70394-70417.

Ullah, M., **Gutierrez Rojas, D.**, Inkeri, E., Tynjälä, T., and Nardelli, P. H. J. (2022). Operation of Power-to-X related processes based on advanced data-driven methods: A comprehensive review. *Energies*, vol. 21, 1-17.

Conference proceedings

Ullah, M., Karuppannan Gopalraj, S., **Gutierrez-Rojas, D.**, Nardelli, P., and Kärki, T. (2021). IoT framework and requirement for intelligent industrial pyrolysis process to recycle CFRP composite wastes: application study. In: *International Conference on Production Research (ICPR 26)*, Taichung, Taiwan.

Mulinka, P., Kalalas, C., Dzaferagic, M., Macaluso, I., **Gutierrez Rojas, D.**, Nardelli, P., and Marchetti, N. (2021). Information Processing and Data Visualization in Networked Industrial Systems. In: *2021 IEEE 32nd Annual International Symposium on Personal, Indoor and Mobile Radio Communications (PIMRC)*, pp. 1–6, Helsinki, Finland.

Beattie, A., Mulinka, P., Sahoo, S., Christou, I. T., Kalalas, C., **Gutierrez Rojas, D.**, and

Nardelli, P. (2022). A Robust and Explainable Data-Driven Anomaly Detection Approach For Power Electronics. In: *IEEE International Conference on Communications, Control, and Computing Technologies for Smart Grids*, pp. 1–6, Singapore.

Book chapters

Rojas, D. G. and Mendes, G. P. (2021). Smart Grid Prediction and Restoration Advancements for the Achievement of Sustainable Development Goals. In: Leal Filho, W., Azul, A.M., Brandli, L., Lange Salvia, A., Wall, T. (Eds.). *Industry, Innovation and Infrastructure. Encyclopedia of the UN Sustainable Development Goals.* Cham, Switzerland: Springer.

Nomenclature

Abbreviations

AI	artificial intelligence
ANN	artificial neural networks
BESS	battery energy storage system
CPS	cyber-physical systems
DFT	Discrete Fourier transform
DL	deep learning
DM-DFT	delta method discrete Fourier transform
XAI	explainable artificial intelligence
EDM	event-driven method
EeMBB	enhanced mobile broadband
FAR	false alarm rate
MDR	missed detection rate
MI	mutual information
ML	machine learning
mMTC	massive machine-type communications
PCA	principal component analysis
Q	Q statistic
QARMA	quantitative association rule mining algorithm
SoA	send-on-area
SoD	send-on-delta
SoE	send-on-energy
SoP	send-on-prediction
T^2	Hotelling's T-squared distribution
TEP	Tennessee Eastman process
URLLC	ultrareliable low-latency communications

1 Introduction

1.1 Motivation and objectives

Prediction and detection of anomalies in any industrial applications are everyday tasks that require multiple resources to effectively mitigate the anomaly and continue operation. Some of the anomalies are considered trivial and are in many cases solved manually without any countermeasure or prediction that would increase the long-term economic impact for a given industry. Examples of anomalies affecting industrial applications that require attention or have an impact on their operation are faulted machines, electrical faults, extreme weather conditions, cyberattacks, and chemical faults, among others. Early detection of such faults plays a significant role to increase the operating time of the process and thereby reduce the overall energy consumption caused by the high energy requirements in case of stopping of the system process and restart.

In this context, technology transformation and current advances in topics such as sensors, storage and processing units, fault detection methods, sampling techniques, and communication have opened a path for the emergence of industrial cyber-physical systems (CPSs) (Nardelli, 2022). CPSs are fundamental for Industrial Revolution 4.0 and will contribute to achieving the goals of growing demand and efficient supply chains and be the backbone of production from both economic and sustainable aspects (Leitao et al., 2016). The innovative aspect of Industrial Revolution 4.0 is the logical (symbolic) interactions between different machines through their integration into digital platforms, which create new business models and confront techno-economic challenges by the introduction of a new generation of factories. Industrial CPSs will contribute to achieving global goals such as ending reliance on fossil fuels, reduction of carbon emissions, and promotion of sustainability by using real-time data analytics, advanced control systems, and smart sensors helping to reduce energy consumption, optimize supply chain management, reduce waste, and promote the use of renewable energy sources.

1.2 State-of-the-art

Anomaly detection in industrial environments was first approached as an intrusion detection real-time model, where the goal was to detect violations from outsiders in an attempt to break security (Denning, 1986). According to Denning (1986), the model is based on the following hypothesis:

Hypothesis 1 *"Exploitation of a system's vulnerabilities involves abnormal use of the system"*

This statement is the building block for anomaly detection. Monitoring of the current state of the process becomes a key aspect, even in cases known as "rare events" where the disturbance source is sometimes not located because of the lack of sensors in the process or incorrect monitoring. The definition can also be rephrased in computer science

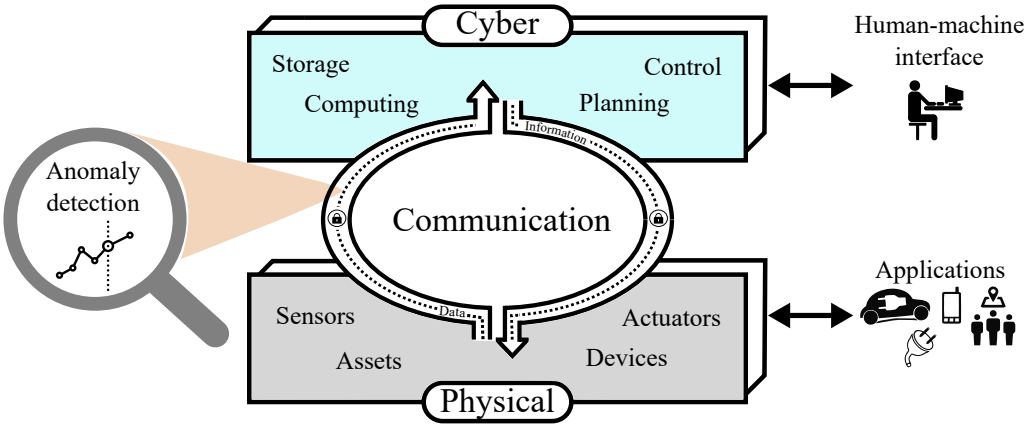

Figure 1.1: Schematic of anomaly detection in a CPS.

as: "An outlying observation, or 'outlier', is one that appears to deviate markedly from other members of the sample in which it occurs" (Grubbs, 1969). The importance of such a statement lies in the fact that nowadays almost any industrial process is monitored by computational means, and it involves a flow of data from one end to another. This development of digitalization, even in its early stages, has created a need to provide security. Many scientific approaches have been proposed to solve security and reliability issues, focusing on protecting the information in all the steps of the dataflow. When the CPS involves data flowing in various directions, it can be prone to attacks from intruders at many levels, and the system's capability to respond to those attacks in a secure and fast manner is critical and challenging (Teng et al., 1990).

To visualize the realm of anomaly detection, Fig. 1.1 shows the different CPS layers and how anomaly detection is integrated into the larger scheme of industrial process monitoring. This is an overview of some aspects of both physical and cyber layers, which can be integrated into any application. In the physical layer, we can find elements like sensors, the task of which is to measure desired variables from any industrial process application, after which these data are sent to the cyber layer for computing. When the data reach the cyber layer, they can be monitored, stored, processed, or even sent back as feedback information to the actuators of the application for control or action purposes. Anomaly detection intervenes as a monitoring action carried out as part of an automatic task (supervised or unsupervised methods (Munir et al., 2019)) or manually by humans at proper interfaces. Depending on the application and the communication requirements, anomaly detection can also be performed in real time or offline (Kühnlenz and Nardelli, 2016).

1.3 Research questions

This doctoral dissertation aims to answer research questions in the context of anomaly detection from various perspectives, covering current computational methods used in anomaly detection, application of anomaly detection to different industrial technologies,

its value in energy and communication gains, and its impacts on planning energy dispatch.

RQ1 *How to reformulate the three-layer model framework from (Kühnlenz and Nardelli, 2016) in order to perform anomaly detection in industrial applications?*

The first research question aims to define the boundaries in a framework for anomaly detection. From the design perspective, the focus is on reviewing the steps in an anomaly detection methodology to be improved, which are applicable to any industrial process. This means that independent of the application, the framework can either be implemented or adjusted to find the solutions needed in the field, thereby contributing to the operation of the industrial process and energy savings.

RQ2 *How can the proposed anomaly detection framework support management and control of energy resources by the integration of data platforms?*

A general framework usually gives quite straight answers to design a cyber-physical infrastructure for anomaly detection. Once the framework is established and a given industrial application is running, the value of support it gives to other tasks in the process is often bypassed. An anomaly detection framework does not only improve operational times as a static task, but also provides knowledge for expert systems to carry out control tasks in energy resources, thereby increasing resilience.

RQ3 *What is the advantage (if any) of employing the proposed framework for fault detection and/or classification in the operation of high-voltage transmission systems?*

A more detailed application to energy systems in the field of power systems is used to understand the advantages of the framework established in this study. Protection in power transmission lines is usually performed by devices known as relays, which isolate and clear a fault when it occurs. However, on some occasions they fail to identify specific faults because of the techniques employed. The challenge here is to define under which conditions an anomaly detection framework can maintain or improve security in power lines by including communication technologies or artificial intelligence (AI) methods replacing or strengthening the traditional methods such as phasor angle measurement.

RQ4 *In which circumstances can event-driven data acquisition be included in the proposed framework to improve fault detection in a complex industrial environment?*

Samples coming from sensors are of importance for anomaly detection. Understanding concepts like sampling frequency and signal reconstruction plays a vital role in detection performance. This research aims to answer how sampling techniques can improve the performance of detection and identification of anomalies while saving communication resources. A chemical industrial process largely used in the literature is studied as a use case.

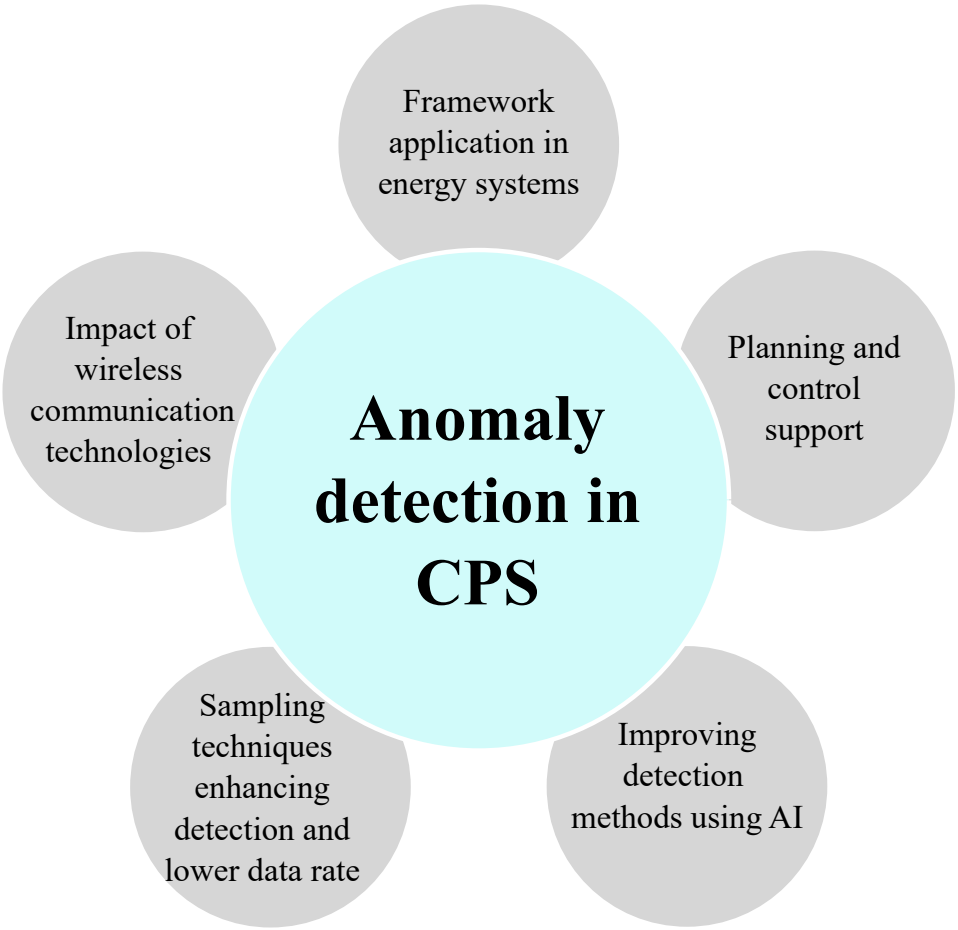

Figure 1.2: Overview of the topics under study.

RQ5 *What is the expected impact of most recent (wireless) communication technologies for adaptive protection in microgrids following the proposed framework?*

Communication technologies are the link between layers in a CPS. Usually, they are taken as a black box in anomaly detection applications. However, within the objectives of the investigation, it is shown that improving or replacing the communication technologies by following the framework can benefit the process both technically and economically. A power system application is investigated in this case.

This doctoral dissertation studies various aspects of anomaly detection, not limiting to particular techniques to perform detection. Fig. 1.2 shows the topics under study and the research questions to be answered. It is worth mentioning that these topics are not the only ones regarding anomaly detection; in contrast, there are many further aspects involved and thus, much research potential.

1.4 Dissertation outline

This doctoral dissertation is organized as follows:

Chapter 2 presents the background and mathematical support of the anomaly detection methods used in this doctoral dissertation.

Chapter 3 explains the main results of each publication used to answer the five research questions.

Chapter 4 provides a general discussion of the results, the conclusions of the doctoral dissertation, and future work.

2 Background

2.1 Introduction

The anomaly detection framework established in this study is based on a three-layer model: a physical layer, a data layer, and a decision layer. Under this model, seven questions are examined from a design point of view within the layers; these questions can be applied to any industrial process. A key aspect of the framework is integration between the layers. In order to have more efficient anomaly detection, a well-structured flow of data and information between layers is necessary. In Table 2.1, the questions applied to an industrial process using an anomaly detection framework are presented.

Table 2.1: Questions that can be answered by the proposed framework (adapted from (Gutierrez-Rojas et al., 2020)).

Q#	**Topic**	**Question**
Q0	Anomaly	What is the problem? Is the event known or unknown?
Q1	Sensors	What kinds of sensors will be used? How many of each can be used and where can they be located?
Q2	Sampling	Which type of sampling will be used? Periodic, event-driven, or mixed (hybrid)?
Q3	Communication	Which type of communication system (access and network technologies) will be used?
Q4	Data storage	Where are the data from sensors stored and processed?
Q5	Data fusion	How should the data be clustered/aggregated/structured/suppressed?
Q6	Anomaly detection	How to achieve ultrareliable anomaly detection based on ML algorithms?

The questions presented in Table 2.1 are intended to provide the first step for a particular industrial process that requires an infrastructure for anomaly detection. Some industrial processes that are up and running have experienced failures in their system that cannot be detected by their current methods or machinery. By answering the questions, or at least partially, an industrial process will be able to establish the foundations to implement anomaly detection. Question $Q0$ is related to whether the source of the anomaly is known or if the current measurement devices are recording it. If $Q0$ is unknown, then we can proceed to question $Q1$, where there is a possibility that new sensors might be installed so that the source of events can be recorded. In question $Q2$, the target is to define what kind of sampling is carried out, depending on the needs and capabilities of the industry and the nature of the anomaly. Then, question $Q3$ is the link between physical and cyber layers, the specific technology that will be used to send the data to the management center. It usually depends on the size of the industrial process, distances, and technical requirements. Question $Q4$ relates to the cyber layer, i.e., whether data are processed and stored in the cloud or in local physical devices located at the plant. Questions $Q5$ and $Q6$

are about the preprocessing and data manipulation before they are used in the detection algorithms and what kinds of methods will be used to perform the detection.

2.1.1 Previous approaches

The idea of a multilayer system in a CPS comes from (Kühnlenz and Nardelli, 2016). The main contribution is to model a system where the components are *"simple and easy to understand."* Under this concept, the multilayer system is designed to emulate the characteristics of a real-world system, where the layers are connected between them. These layers are the physical layer, the communication layer, and the decision layer. Kühnlenz and Nardelli (2016) state that there is no need to find explanations that are external to the system, and therefore, everything is built within the boundaries of the system.

The method of decomposing a complex system into smaller layers might simplify the problem and potentially find solutions to problems that might be difficult to deal with. The interaction between layers is also an important part, as in some cases, an individual layer can dominate, and a strong dependence on the entire system might occur. In those cases, higher security measures can be taken by designing the specific layer accordingly.

The multilayer concept is the basis of the approach of the CPS carried out in this study on anomaly detection. It is the base that helps to answer the research questions by providing support in each of the performed tasks that are designed to successfully detect and prevent system failures.

A more business-oriented approach can be seen in RAMI 4.0[1]. This multilayer architecture proposal was made in a joint collaboration by German Electrical and Electronic Manufacturers Association, which, among others, possesses a set of standards, practices, and references.

The model is composed essentially of three layers, each layer being divided into two sublayers. The model has two axes (see Fig. 2.1), a hierarchy axis and a layer axis. The hierarchy axis is an organizational and business description of the system process, its levels being the following:

- The product level considers the final product as part of the system, interacting with the upper levels.
- The field device level represents the devices in the field that support the manufacturing processes, such as sensors and meters.
- The control device level includes the monitoring infrastructure that controls the equipment.

[1] https://www.isa.org/intech-home/2019/march-april/features/rami-4-0-reference-architectural-model-for-industr

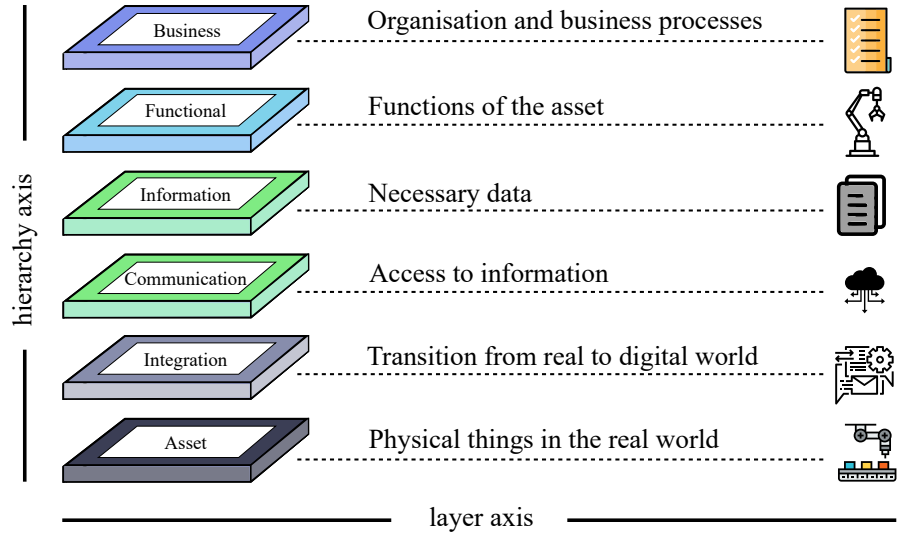

Figure 2.1: RAMI schematic 4.0 (adapted from (Bastos et al., 2021)).

- The station level represents the inputs of multiple modules that form a complex system.
- The work center level is composed of multiple stations dedicated to production.
- The enterprise level refers to the interactions performed by the other layers and represents administrative functions sending data back and forth.
- The connected world level represents the interaction between the factory and the outside, i.e., clients or supplementary services.

On the layer axis, the properties that classify the asset can be found; it focuses on the technical aspects related to the methodology. Under the layer axis (see Fig. 2.1), asset and integration layers refer to the devices exclusive to the physical world and the transition from the physical to the cyber world, respectively. Communication and information layers are where the data exchange and access take place. Under the information layer there are identification and routing of the assets, enabling transitions between devices at different layers. Finally, functional and business layers refer to the actions performed by the assets defined, where the higher-level specifications that are business-oriented processes for the assets are taking place.

The concepts given under the RAMI model in the context of Industry 4.0 aim to create integrated solutions for different applications in many fields, like in (Alemão et al., 2022), where a manufacturing scheduling problem is tackled by proposing a set of functional requirements. RAMI 4.0 simplifies the interaction between the layers and is able to handle the phases and aspects from assets (physical devices) to the decision-making of the process. An important aspect is that by defining each of the process requirements, it

will contribute to the development of the subsequent tasks performed in each of the layers.

RAMI 4.0 can be used in anomaly detection to structure tasks in industries that do not rely on any existing methodology to detect faults in a system. The real-world challenges that factories are facing to perform anomaly detection can be minimized by following the methodology of structuring the problem from the physical world to the decision-making by layers matching the architecture model of RAMI 4.0.

2.2 Sampling

Most of control and anomaly detection in modern industrial processes has relied on synchronous time-based sampling. These methods have shown reliability in the majority of cases. However, the infrastructure built for continuous sensors lacks flexibility and could represent a nonviable economic decision from the design perspective. Another reason why time-based approaches are expensive is the increased need for data storage facilities and congestion of the communication network. Thus, efficient utilization of resources is a priority, and it can have an impact on the overall use of energy of a given industrial process.

The event-driven method (EDM) for sampling has attracted a lot of attention in recent years mainly because of the gains in resource utilization, and it can also provide the same effectiveness while increasing flexibility and ease of extension (Sánchez et al., 2009). The EDM is not considered a new topic of research, but it has many challenges, as developing a standardized sampling methodology might be difficult. Nonetheless, in the field of anomaly detection, it is an interesting choice and may not only increase the accuracy of the detection methods but also provide better control capabilities for the industrial process. In this research project, time-based and event-driven methods and their impact on the anomaly detection are investigated and compared.

2.2.1 Time-based method

In time-based methods, the sampling is done at the start of a timer, and the duration is either at the end of the timer or the sample count. This type of sampling is also known as continuous sampling, because the signals are constantly measured from the start of the process until the end. The length of the sampling interval is the sampling period. The sampling period may vary from milliseconds to minutes or hours, depending on the application. Commonly, a short period between samples means that the resolution of the signal is high and thus, it can improve anomaly detection. However, in some industrial environments (e.g., chemical processes), the granularity of the data points might not be beneficial when using statistical detection techniques, because the data captured by smaller intervals do not have a good representation when a fault occurs.

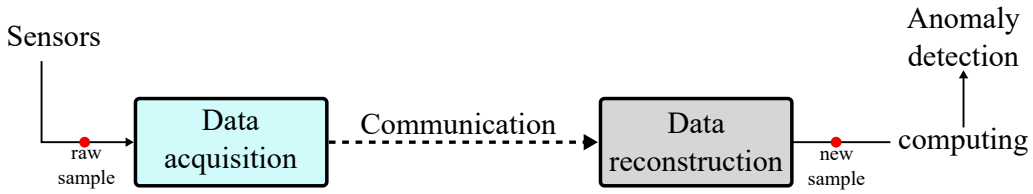

Figure 2.2: Overview of EDM method for sampling.

2.2.2 Event-driven method

The event-driven method (EDM) is a sampling method, and it is performed at the sensor end (data acquisition). An overview of the method is given in Fig. 2.2. The reconstruction block is where the samples that have already been processed reach by any communication means, and the output of this block is used to perform anomaly detection. The special interest in this method lies in the concept of saving transmission data from the acquisition to the reconstruction block. The main techniques in this method are: send-on-delta (SoD) (Miskowicz, 2006); send-on-prediction (SoP) (Staszek et al., 2011; Suh, 2007); send-on-area (SoA) (Nguyen and Suh, 2008); send-on-energy (SoE) (Miskowicz, 2010); and a simple definition of a threshold. In the SoD, the measurement is updated when a minimum difference between the current and the most recently transmitted signal value is reached. SoP is an extension of the SoD strategy. The difference is related to the use of a predicted value from the last update. SoA and SoE are two common extensions. The triggering criterion for the former is given by the integral of the absolute difference, and in the latter, by the energy of the difference. Another method is provided by a predefined threshold (Astrom and Bernhardsson, 2002). In this case, the event trigger is given when the current signal value crosses a cutoff point. Their paper investigated the threshold and delta event-based strategies.

In the context of EDM methods, many contributions have been made by Simonov and his collaborators in a series of papers (Simonov, 2013, 2014; Simonov et al., 2017a,c,b); in the present study, we followed and continued these strategies. It is noteworthy that when a sample is not received at the reconstruction block (Fig. 2.2), it is also informative in the EDM. If no sample is received or lost in the reconstruction block, the samples are assumed to be constant during the respective window defined by the sampling period T, as it never exceeds the thresholds that trigger either of the mentioned techniques.

Threshold-based technique

The threshold-based method employs a cutoff value as a decision rule for data acquisition. That is, the sampled value of the variable is only updated if it exceeds this reference level.

First, the following statistics of the continuous signal (S) under normal operating condition are obtained: mean (S_{avg}), minimum (S_{min}), and maximum (S_{max}). The lower (T_l) and upper (T_u) thresholds are given in Equation 2.1 as a function of the parameter p, with $0 < p < 1$. The larger the parameter is, the smaller the number of updated samples is.

$$T_u = S_{\text{avg}} + (S_{max} - S_{avg}) \times p \tag{2.1a}$$
$$T_l = S_{avg} - (S_{avg} - S_{min}) \times p \tag{2.1b}$$

The signal reconstruction (S'_t) is then performed for each sample as shown in Equation 2.2. If the variable value exceeds one of its respective lower and upper thresholds, it is updated (with S_t), otherwise, the last sent value (S_{t-1}) is kept.

$$S'_t = \begin{cases} S_t, & \text{if } (S_t < T_l) \text{ or } (S_t > T_u) \\ S_{t-1}, & \text{if } T_l \leq S_t \leq T_u \end{cases} \tag{2.2}$$

The threshold method (with $p = 50\%$) is illustrated in feed A (stream 1), which is one of the case study process variables. The optimal threshold percentage is chosen from the industrial process historical data.

Delta-based technique

The SoD method is based on the difference between the current value and the one previously sent by the data acquisition system. For fault detection, this difference is calculated from a signal in normal operating conditions (NOC). Equation 2.3 gives the maximum absolute difference ($\Delta \max$) between consecutive sample values ($t, t-1$) of the continuous signal (S). The parameter p is used as before. This procedure is applied to each variable separately.

$$\Delta \max = \max(\mid S_t - S_{t-1} \mid) \times p \tag{2.3}$$

The next step concerns the reconstruction of the signal (S'_t), which is done according to Equation 2.4. The variable value (S_t) is passed only if it is greater than $\Delta \max$, otherwise, the last sent value (S_{t-1}) is repeated.

$$S'_t = \begin{cases} S_t, & \text{if } \mid S_t - S_{t-1} \mid > (\Delta \max) \\ S_{t-1}, & \text{if } \mid S_t - S_{t-1} \mid \leq (\Delta \max) \end{cases} \tag{2.4}$$

An example of both methods used in the study, Threshold and Delta, is illustrated in Fig. 2.3. The data of one of the variables are presented in the Tennessee Eastman process, where both methods are easy to perceive. The level of data compression can vary according to the percentage of the threshold chosen, or the percentage of the variation given as p in Equations 2.1 and 2.3.

2.3 Communication

In the cyber-physical domain, the communication network is a relevant aspect as it is the means by which the data flow from one layer to another. Traditionally, communication systems have had a significant impact on different industrial processes as they have been

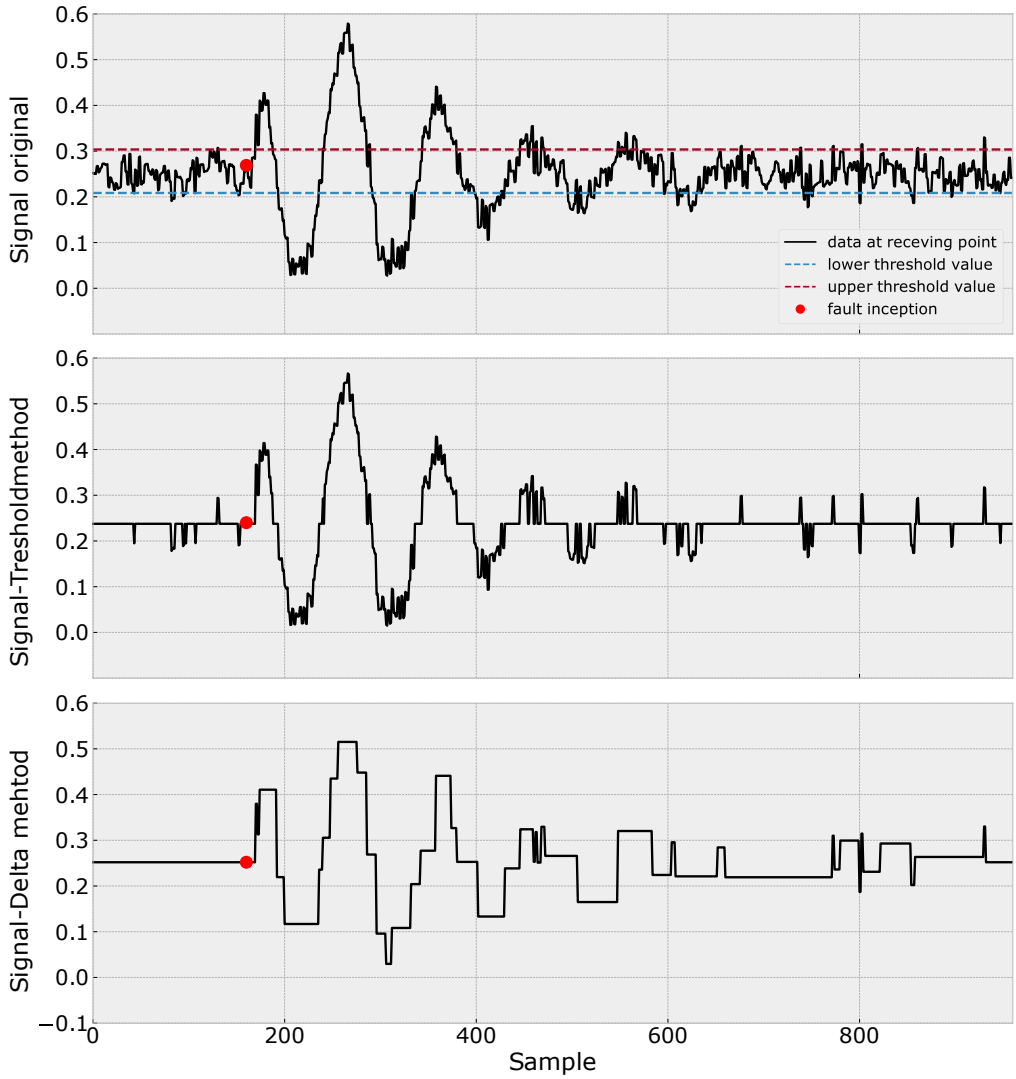

Figure 2.3: Examples of a signal coming from a sensor with the threshold and delta EDM.

a limiting factor in terms of the speed of data flow, usually requiring a large infrastructure inside factories to perform simple tasks. The infrastructure usually relied on Ethernet communication, copper cables, or optic fiber, which could significantly increase the area of operation and costs. Moreover, detecting communication failures or maintenance is a time-consuming task.

Modern technologies have opened a new scheme of opportunities for industries. Many anomaly detection and control tasks that have usually been performed manually are now being executed automatically as the data reach from sensors to the management systems on the timescale of milliseconds. In addition, faster processors are capable of delivering decisions preventing the processes from interruptions or physical harm to industries or personnel. Among such new technologies, cellular LTE 4G and 5G communication technologies that have shown promising results, and given the flexibility they support, are a well-rounded choice to implement.

Especially, advances in 5G are set to offer a wider bandwidth, faster data transmission, and improved spectral efficiency while being supported by local private networks (Esposito et al., 2017). 5G specifications are still being deployed worldwide, and they are able to support a wide range of applications that impose different requirements, such as smart homes, industrial automation, augmented reality, and 3D videos, among others (Narayanan et al., 2022). The above-mentioned applications can be classified into three major classes that are a signature of 5G communications:

- enhanced mobile broadband (eMBB);
- massive machine-type communications (mMTC);
- ultrareliable low-latency communications (URLLC).

Enhanced mobile broadband (eMBB) usually contains applications that have an ultra-high data rate in both upload and download links, even exceeding 1 Gbits per second, and applications like video games and augmented reality; also communication between routers in industrial facilities may require such a high rate. Massive machine-type communications (mMTC) focuses on enabling the connection between a massive number of devices that have low power and low data rate requirements; such devices can be smartphones that are being used together for a specific application like localization or even performing edge computing. mMTC is of particular importance for large factories that have multiple processes requiring constant monitoring, as communication between sensors to the central management system could play an important role, bringing flexibility without neglecting the economic aspect. The ultrareliable low-latency communications (URLLC) class contains applications that are mainly used in critical applications, thus having more stringent requirements in latency, reliability, and availability. The applications that can be supported by this class are, e.g., industrial internet, fault location and clearance, and remote surgery.

Moreover, 5G embraces a network architecture type called network slicing. It creates virtualized and independent networks inside the same infrastructure domain. Each slice is a self-contained, logically separated, and secured part of the network that fulfills diverse requirements required by specific applications. In anomaly detection, network slicing is particularly important as the requirements might vary from the rest of the control and communication tasks inside the factory; in cases like electrical circuits, detecting faults might require a low latency and a small data rate to protect the equipment and trigger protective functions in a matter of milliseconds. Alternatively, some chemical processes require a higher data rate while being connected to multiple sensors, and if both applications reside next to each other, 5G network slicing can provide both needs within the same network architecture.

2.4 Data fusion

Anomaly detection in cyber-physical environments requires data from different sources or sensors to an aggregated unit and thus increases the effectiveness of the detection methods by having more meaningful data (Hall and Llinas, 1997). This aggregation is performed at the cyber layer, and it is known as data fusion. This technique not only offers statistical gains and data reduction but also improves the accuracy of anomaly detection.

Many models haven been employed to perform data fusion (Esteban et al., 2005), some of which are data-driven or knowledge-based methods. Choosing either of the methods depends on the application, and a larger framework is usually necessary, especially in industrial environments to cover the entire operating process. A whole data fusion architecture model is outside the scope of this study; consequently, data fusion is considered as part of the data preprocessing, where mathematical methods are used to aggregate the data incoming the cyber layer. The aggregation methods used are:

Principal component analysis (PCA)

Principal component analysis (PCA) is a dimensionality reduction technique, and it gives a lower-dimension representation of the data by keeping the correlation between the original variables (Chiang et al., 2001). The variables are signals coming from the sensors, and the dimensional reduction can be chosen accordingly to maintain a good percentage that can represent the original dimension signals. This technique is widely used in anomaly detection for process monitoring (El Koujok et al., 2020; Jiao et al., 2020; Marino et al., 2020; Chen et al., 2019).

Delta Method Discrete Fourier Transform (DM-DFT)

This technique is used to extract fault features. First, the Discrete Fourier Transform (DFT) is performed on the signal (instantaneous electric current); then, a recording instant is selected from the signal in the frequency domain; and finally, two signals coming from two sensors are compressed, resulting in just an 8-dimension data point for the dataset. The DFT maps a given point of the input signal (i.e., current or voltage) into two points in the output signal. For N samples, considering the pair x_n (input signal) and X_k (its

DFT):

$$X_k = \sum_{n=0}^{T-1} x_n e^{-2\pi i k n/T}, \tag{2.5}$$

where $0 \leq k \leq T-1$, and T is the number of samples per cycle. The DM-DFT uses a moving window of length T instead of the complete signal, thus allowing faster fault recognition. Once the DFT is calculated, variations in the frequency domain can be detected as

$$\Delta S_n = |S_{n(j)} - S_{n(j+T)}|, \tag{2.6}$$

$$F_i = j + T \leftrightarrow \Delta S \geq 0.5 S_{n(j)}. \tag{2.7}$$

in which ΔS_n is the changes in the current signal, $S_{n(j)}$ is the current Fourier value of the jth sample with $0 \leq j \leq N - T$ and F_i indicates the instant at which the values are recorded.

A different threshold value is selected based on experimental results for different fault conditions. In a multiphase system, if any of the phases ΔS_n are above the threshold, the recording instant is chosen from the phase n that has the highest value. If $\Delta S_n = 0$ for all signals, then it is assumed that there is no fault and the feature extraction is taken randomly from one of the samples of each signal.

Note that the DFT phasor estimation is less sensitive to noise than the individual measurements, and it is robust to the presence of harmonics or noise (Junior et al., 2016). However, the DFT is dependent on the sample frequency, which might be problematic for real-time applications because of the computational time limitations.

2.5 Anomaly detection

The increasing power capacity of large industrial environments has led to a need to deliver better-quality goods while increasing efficiency. This means that operating times will play a key part as an interruption in the processes will result in economic losses. Interruptions caused by anomalies are becoming harder to detect as the modern industries rely more on automated processes working under closed-loop control and multiple parametrizations. Moreover, the number of sensors may be either redundant like in the case of a wrong loop control because of a faulty sensor or because there may not be enough sensors, and thus, the anomaly cannot be identified by current sensing devices.

The different methodologies employed to perform anomaly detection in industrial CPSs are also known as process monitoring methods (Chiang et al., 2001). Anomaly detection methods are important to inform operators and automated robots in charge of maintenance or to ensure safety of the system elements. In this study, two different anomaly detection methods are explored.

Data preprocessing is an important part of anomaly detection methods. It can be performed at the data fusion stages to prepare the datasets by eliminating outliers or by autoscaling. This allows the detection algorithms to have a better accuracy once redundant or not valuable information is removed.

2.5.1 Standard statistical methods

In this category, two methods are used to perform anomaly detection. In this work, data preprocessing includes EDM and PCA to reduce the space dimensionality. Other techniques performing dimesion reduction are, e.g., nonnegative matrix factorization, linear discriminant analysis, generalized discriminant analysis, autoencoder, and t-distributed stochastic neighbor.

Hotelling's T-squared distribution (T^2)

This is a multivariate statistical method that relies on a threshold to perform anomaly detection (Hotelling, 1931). The threshold is based on the level of significance α. Calculation in T^2 is done as follows:

Given a training dataset of n variables and m samples stacked into a matrix X as

$$X = \begin{bmatrix} x_{11} & \dots & x_{1m} \\ \vdots & \ddots & \vdots \\ x_{n1} & \dots & x_{nm} \end{bmatrix}, \tag{2.8}$$

the sample covariance matrix can be calculated as

$$S = \frac{1}{n-1} X^T X, \tag{2.9}$$

and the eigenvalue decomposition of the matrix S is expressed as

$$S = V \Lambda V^T, \tag{2.10}$$

where Λ is a diagonal and V an orthogonal matrix, respectively. Assuming that S can be inverted and x is an observable vector that belongs to the domain of the matrix X, z is calculated as

$$z = \Lambda^{-1/2} V^T x, \tag{2.11}$$

and finally, we can obtain Hotelling's T^2 statistic as

$$T^2 = z^T z \tag{2.12}$$

The conversion of the covariance matrix yields a two-dimensional observation space of all the m variables, and it can be graphically represented in an X-Y plot.

Q statistic (Q)

Another estimator for the upper limits after PCA is given by Jackson and Mudholkar (1979) by means of normal approximation. It is calculated as

$$Q = r^T r \tag{2.13}$$

$$r = (I - PP^T)x, \tag{2.14}$$

then, the threshold is given as

$$Q_\alpha = \theta_1 \left[\frac{h_0 c_\alpha \sqrt{2\theta_2}}{\theta_1} + 1 + \frac{\theta_2 h_0 (h_0 - 1)}{\theta_1^2} \right]^{\frac{1}{h_0}}, \tag{2.15}$$

where

$$\theta_i = \sum_{j=a+1}^{n} \sigma_j^{2i} \tag{2.16}$$

$$h_0 = 1 - \frac{(2\theta_1 \theta_3)}{3\theta_2^2} \tag{2.17}$$

and c_α is the normal of $(1 - \alpha)$ percentile.

2.5.2 Machine learning methods (ML)

Many machine learning methods have been developed in recent years to perform anomaly detection and classify those anomalies. They are usually known as black box methods, where they learn based on fault–symptom relationships on the available data. Examples of these methods include, e.g., pattern recognition, support vector machine, artificial neural networks (ANN), rule-based methods, and tree search. These methods have several advantages as some of them are robust against parametrization and outliers. This means that they can be applied to a wide range of applications in CPSs; however, they usually require a lot of data to train the model. Time and resources might be expensive, and the interpretation of results is not straightforward. Two knowledge-based ML methods are used in this study.

Deep Learning (DL)

Deep learning (DL) is a machine learning method that learns representations from data, putting emphasis on subsequent layers, which increases the meaningful representations (Chollet, 2018). The representations are learned from an input dataset, which is usually divided into training and testing, once the training is done and validated by means of a loss function. Once the model of representation is achieved, the testing dataset is corroborated and the accuracy for the model is obtained. In Fig. 2.4, an overview of the DL process can be seen. As for the training procedure, the inputs are passed through the layers where they have random assign weights, and thus, initially, the transformations within the network of layers are random. Then, the predictions and true targets are computed in the loss function and the optimizer adjusts the weights, known as $backpropagation$. Finally, the

objective is to find a network that yields the minimal losses.

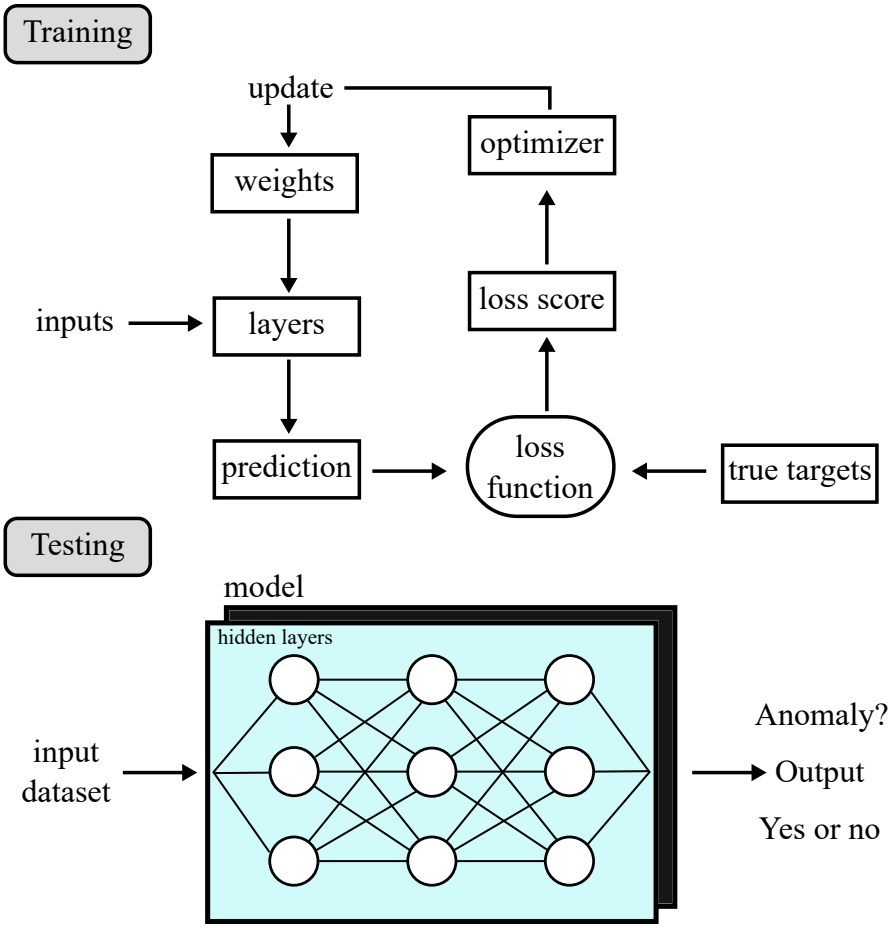

Figure 2.4: Exemplification of a signal coming from a sensor with the threshold and delta methods of the EDM applied.

The results achieved by DL in different applications are extremely useful for anomaly detection as they can provide a good accuracy with relatively simple algorithms vastly implemented by the research community and shared in open software libraries and codes online.

Quantitative Association Rule Mining Algorithm (QARMA)

Quantitative Association Rule Mining Algorithm (QARMA) was defined in (Christou et al., 2018; Christou, 2019), and it is a family of efficient novel cluster–parallel algorithms for mining quantitative association rules with a single consequent item, and many antecedent items with different attributes in large multidimensional datasets. Using the standard support-confidence framework of qualitative association rule mining (Adamo,

2001), it extends the notions of support, confidence, and many other "interestingness" metrics so that they apply to quantitative rules.
QARMA is configured to produce rules of the form

$$I_1.attr_1 \in [l_{1,1}, h_{1,1}] \wedge \cdots \wedge I_n.attr_m \in [l_{n,m}, h_{n,m}] \implies J_0.p \in [l_0, h_0] \tag{2.18}$$

or alternatively, to produce rules of the form

$$I_1.attr_1 \in [l_{1,1}, h_{1,1}] \wedge \cdots \wedge I_n.attr_m \in [l_{n,m}, h_{n,m}] \implies J_0.p = v. \tag{2.19}$$

The latter form is very useful in supervised classification problems, where the value of the target item attribute is essentially the class variable that is being learned.

QARMA learns a small set of different features from the training historical dataset by extracting the rule and then provides simple decision rules (similar to decision trees), and it is robust against noise. The quantitative rules generated by QARMA are easier to understand than other ML models, making it comprehensible to humans. All the extracted rules are validated in the training dataset, and one would be able to understand the meaning because the space of validation for each rule is within certain given boundaries. Understanding the rules of ML approaches is very attractive to the scientific community, and multiple early attempts have been made to light the black box (Towell and Shavlik, 1994). Therefore, QARMA is, in general, a particularly good fit for the newly emerging "eXplainable Artificial Intelligence" (XAI) paradigm. The term "explainable" means that the resultant model that the algorithm produces can be easily understood by humans.

3 Results

3.1 Publication I: Three-layer Approach to Detect Anomalies in Industrial Environments based on Machine Learning

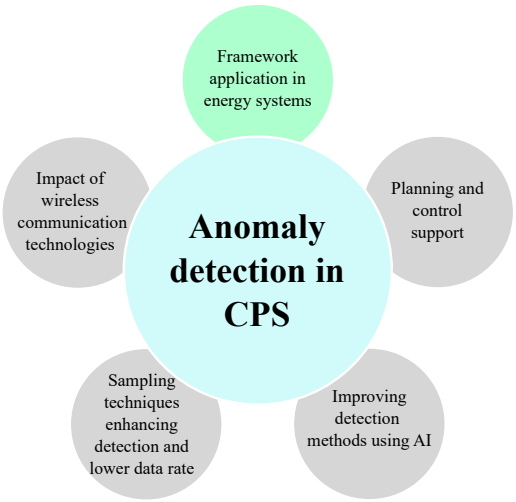

Figure 3.1: Topic studied in Publication I

In this publication, research question RQ1 was answered by studying how to represent an anomaly detection framework that can be generalized to any industrial application. In order to do this, a set of questions were proposed, which would help, from a design point of view, in obtaining information about a specific application, and in applying the concepts of anomaly detection that is suitable for the purposes of all the aspects under study (e.g., sensors, network, data processing, decision-making).

Tennessee Eastman process (TEP)

The three-layer model was applied to the Tennessee Eastman process, a dataset of a chemical process generated in a process simulator widely used in process monitoring[2]. Despite being a dataset generated in the 1990s, it still attracts the attention of the research community in anomaly detection and fault classification.

The dataset is described as follows: 52 process variables (11 manipulated and 41 measured) and 21 different faults of a chemical industrial plant, producing a Tennessee Eastman problem (Downs and Vogel, 1993). The Tennessee Eastman process consists of five major equipment units: a condenser, a vapor–liquid separator, a reactor, a product stripper, and a recycle compressor (Fig. 3.2). Its objective is to obtain products G and H from reactants A, C, D, and E. This is reached by a set of four chemical reactions, in which components B and F are an inert and a byproduct, respectively. A full description

[2]https://github.com/camaramm/tennessee-eastman-profBraatz

of the process can be found in (Yin et al., 2012; Chiang et al., 2001). There has been a substantial interest by the research community to evaluate process monitoring schemes and control and anomaly detection strategies based on data-driven techniques. Besides the normal operation file in the dataset, another 21 fault conditions caused by common disturbances in practice after a given time slot are simulated (Russell et al., 2000). When a fault occurs in the system, the values on the variables can either change dramatically or slightly (depending on the fault type).

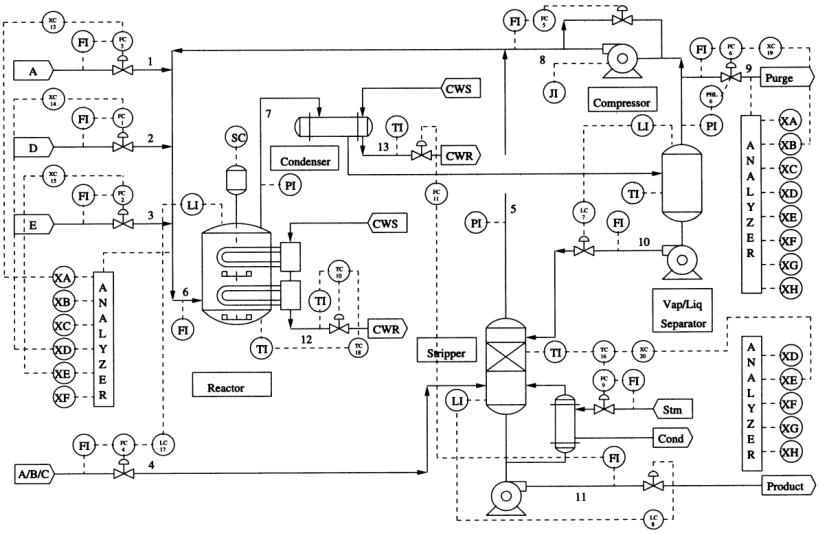

Figure 3.2: Process flow diagram of the Tennessee Eastman problem (Chiang et al., 2001).

The fault files constitute a shift from the reference condition. Sample acquisition is carried out every 3 min with Gaussian noise. In total, there are 960 samples of each of the 52 variables for a process duration of 48 h. Each fault file begins in normal operation until the sample number reaches 160 (8 h after the process has started).

Anomaly detection framework

The first task consists of answering the questions proposed in the framework. Table 3.1 presents these answers applied to the TEP, which provides the boundary conditions of the anomaly detection design.

For the second task, the related data acquisition event-driven methods were applied. In the threshold technique, the margin is chosen based on the average of each signal and the percentage value to the minimum or maximum of that variable given in normal operation conditions. The value of those limits are shown in Fig. 3.3a. In this case, the parameter p takes the value 90%. The transmitted samples are only the ones that are outside the limits. This threshold EDM approach allows to send less data to the receiving end by any communication means. In Fig. 3.3a, the compression rate is around 92.60%, meaning that only around 72 samples (from 960 in total) are transmitted to the receiving end during the sampling period. Once the threshold is achieved and the samples are transmitted, they

Table 3.1: Proposed framework applied in the TEP.

Q#	**Answer**
Q0	Lack of accuracy to detect anomalies (21) from measurements
Q1	Each of the 52 variables are sensors, no other can be added
Q2	Periodic sampling; all 52 variables are in sync (3 min)
Q3	It can be considered as in (Liu et al., 2019)
Q4	Not constrained; freedom to test as in (Dai et al., 2019)
Q5	Open question; focus of research in the field
Q6	Open question; focus of research in the field

will be used as inputs for the data fusion. This means the use of any method, such as ML or statistical analysis, to perform anomaly detection.

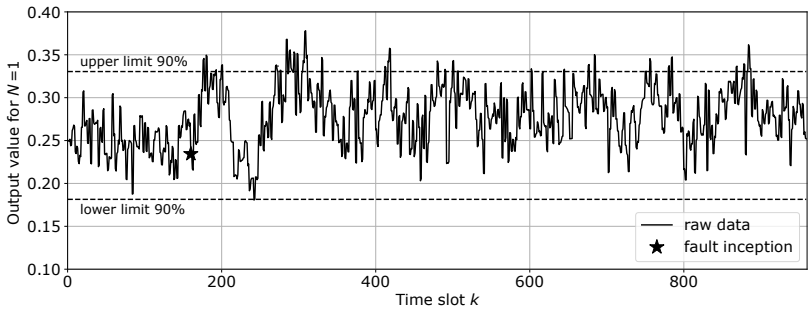

(a) Signal from variable 1 at the data acquisition point (before transmission) for fault number 2 of the Tennessee Eastman dataset.

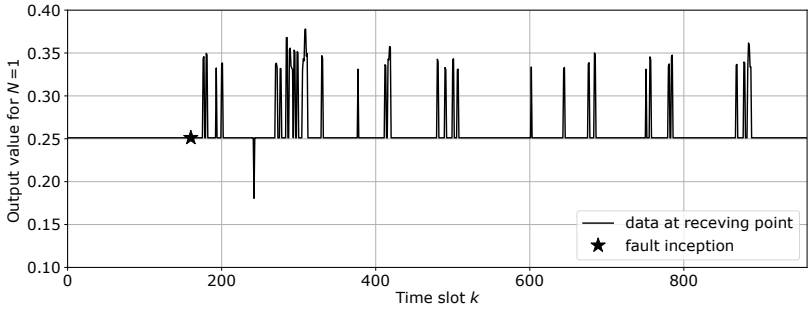

(b) Signal from variable 1 at the data fusion point (after transmission) for fault number 2 of the Tennessee Eastman dataset.

Figure 3.3: Data acquisition EDM applied to the TEP.

For the third task, in order to further reduce the amount of processing required for fault detection, data fusion based on Mutual Information (MI) was carried out on the TEP dataset. It measures the mutual dependence between the process variables. In the case of

the Tennessee Eastman dataset, dependences are obtained automatically from the variable measurements.

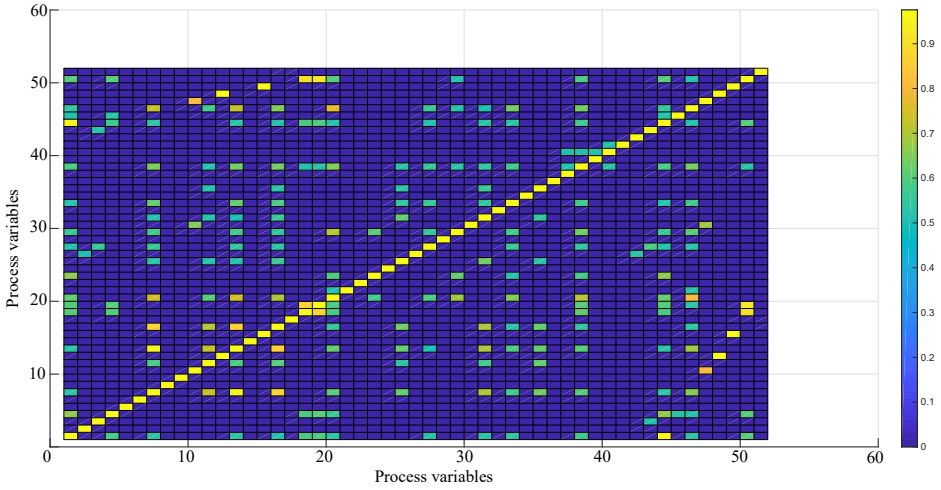

Figure 3.4: Correlation between process variables.

In this application, the objective is to maximize the MI and thereby increase dependences between the variables (Chiumento et al., 2018).

In this work, statistical closeness was used to obtain correlations between variables. First, it quantifies correlations by producing links between the measured sample variables and the assigning directionality (Villaverde et al., 2014). In Fig. 3.4, a form of autocorrelation between the variables is shown. It presents a strong correlation (about 80%) between 12 out of the 52 variables, and a slight correlation (about 50%) on 34 of them. This result implies that in some of the fault cases, the MI carried out on the process variables is helpful to reduce data and computational load.

Finally, in the last step, anomaly detection using QARMA was implemented. During this step, no qualitative association mining was performed as all the rows from the samples contain values. Because of the time-dependent nature of the data, i.e., the previous value has dependences with the next, the data were expanded for each feature, using the difference between the current values and two previous time slots, obtaining 156 fully dense features. Then, QARMA was run for several days, producing a total of 63008 non-dominated rules. The rules predict all different faults with the exception of the normal operation mode and hard-to-detect faults 3, 9, 15. By using QARMA, the overall rule accuracy was 62% on the test set, and it is significantly better than the one reported by the decision tree or the ANN, which was less than 50%.

In the minimum cardinality tests, it was found that an appropriate set of rules that explains

85% of the dataset is enough with 14 of the 156 expanded variables obtained. This result implies the need to monitor a much smaller set of variables, which will ultimately make it possible to draw safer conclusions about the state of the process. Despite the preprocessing of the variables and the computational time the algorithm takes, QARMA is a powerful tool that can bring explainability to the behavior of the sampling measurements, unlike traditional statistical techniques, such as PCA, that lack this characteristic.

In summary, this study, as a continuation of the model proposed by Kühnlenz and Nardelli (2016), serves as a generalized framework for anomaly detection in cyber-physical systems. In this study, a specific application was addressed, and it was investigated how each step of the framework helps to identify and design a proper methodology and to implement it from a design point of view. With the studied application, it was possible to answer questions such as whether more sensors are needed in an industrial process that would be the input of the anomaly detection methods, what communications technologies are the link between the physical and cyber layers, and how the sampling can be beneficial for the process. This type of knowlegde derived from the three-layer model demonstrates that it is possible to perform reliable anomaly detection in any cyber-physical application.

3.2 Publication II: Weather-Driven Predictive Control of a Battery Storage for Improved Microgrid Resilience

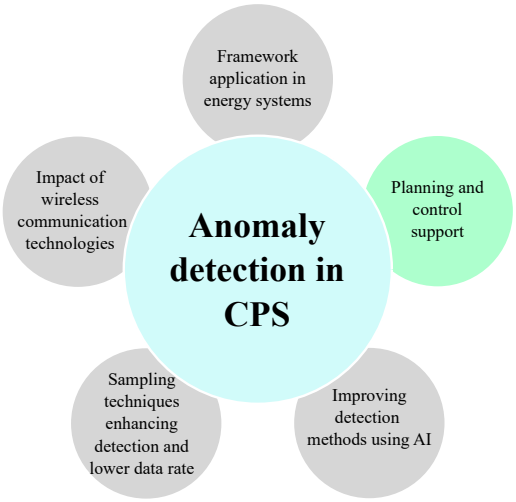

Figure 3.5: Topic studied in Publication II

In this publication, research question RQ2 was answered by studying the outcomes of anomaly detection. The interaction of anomaly detection and prediction and/or control tasks in the cyber layer are key aspects that can support resilience in smart grid applications.

Most of the anomaly detection framework developed in this work was applied to obtain results of improving resilience in microgrids. The only aspect that was not explored further was communication as it was assumed to be perfect with no delays in the data. Here, the task was not only to perform anomaly detection/prediction based on weather, but also use that information to control the energy exchange in a microgrid to make it more resilient against such anomalies whenever they occur. The ultimate goal during this research was to manage a Battery Energy Storage System (BESS) in a microgrid to improve its resilience. The research involved a multitask step procedure.

The first task was to obtain fault data (occurrences and locations) from Elenia (a Finnish local distribution operator) and match that information with their closest weather station. In Fig. 3.6, we observe the clusters created in a portion of the Finnish territory; the reason behind the cluster is that the fault data are spread over several kilometers, and the weather predictions must be accurate. The final outcome of this task was to find the best location for a virtual microgrid where the follow-up investigations were going to be carried out. This location was chosen for the comparison of five clusters that achieved the best model test accuracy, and the corresponding microgrids were placed in the centroid of those clusters. The coordinates of the microgrid locations are used to later predict faults based on the weather condition information obtained from the nearest weather station.

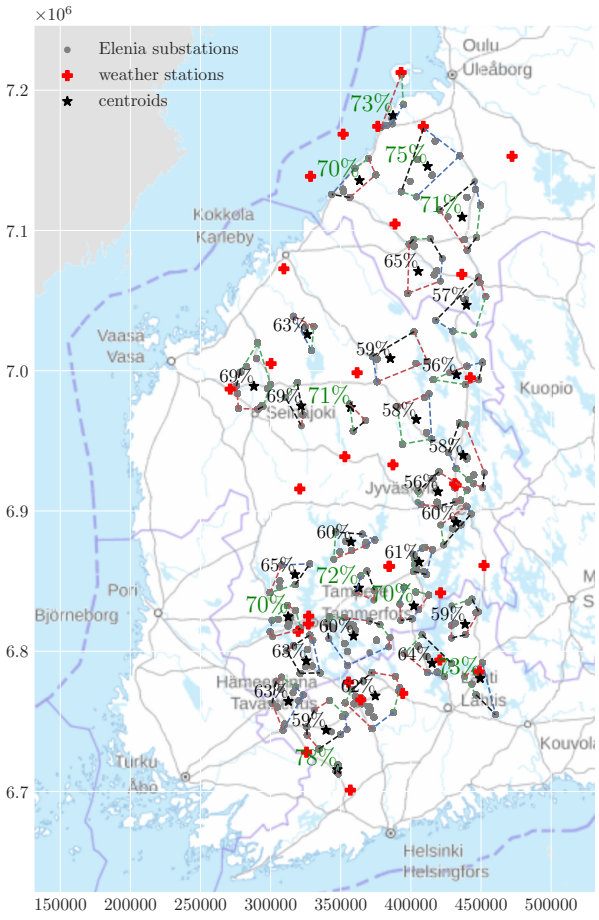

Figure 3.6: Clusters of Elenia's substations, the closest weather stations, and the test accuracy achieved by the predictive model. The underlying map in the ETRSTM35FIN coordinate system is taken from the website of the National Land Survey of Finland.

The second task was to predict the energy flow in the microgrid by making a load and generation model. Fig. 3.7 illustrates the target series in hourly resolution for the year 2013 on the virtual microgrid, the load demand from the microgrid in red and the solar PV production for that year in gray. This information is critical because based on the anomaly prediction, the BESS will be charged accordingly.

In the third task, energy optimization for the microgrid was performed, considering four different scenarios. In the economical and reliable scenarios, the optimization considered the objective function of cost reduction. The predicted scenario included both economical aspects and uncertainty of outage probability (λ), while λ was known in advance.
In the fourth and fifth tasks, a resilience metric was calculated based on the energy op-

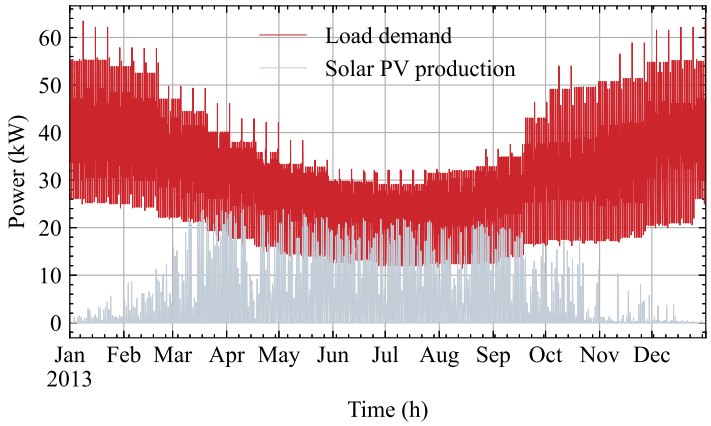

Figure 3.7: Time series of the microgrid load demand and solar production.

timization for the whole year in the occurrence of an outage. The results for the daily resilience depicted in Fig. 3.8 show the predicted scenarios, where both the economical and anomaly prediction weights have a better performance on average than the other three scenarios. It was considered to have 1-hour and 2-hour operation of the BESS when the microgrid is completely disconnected from the grid during an outage. In the violin plot presented in Fig. 3.9, a closer look for the yearly dependence (metric of resilience) is taken. It is observed that the economical and foresight approaches have lower adjacent values. The dependence in the economical approach is more distributed in the y-axis, indicating that it is not dependent on resilience. In the other approaches, the medians are almost the same and the variations lie in the first and third quartiles, the predictive approach having greater values close to 1. The difference between the clusters is also almost negligible as the accuracy results seen in Fig. 3.6 are quite close to each other.

The results obtained in this research indicate that anomaly prediction based on weather conditions for distribution networks is an important task that can benefit the energy control in a microgrid and improve the resilience against severe weather events. Moreover, it was proved that anomaly detection in cyber-physical systems is capable of not only serving as a reactive maintenance tool but also providing valuable information to support control tasks that keep the whole system reliable and secure. By development of a smart approach, it was shown that technical aspects of anomaly prediction can be combined to support an economical scheduling mechanism of a microgrid and thereby obtain benefits in multiple functions.

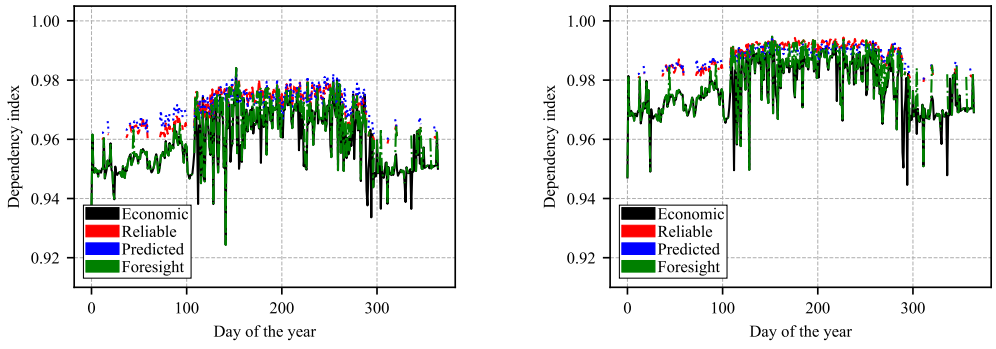

(a) 1 h energy storage for cluster 1

(b) 2 h energy storage for cluster 1

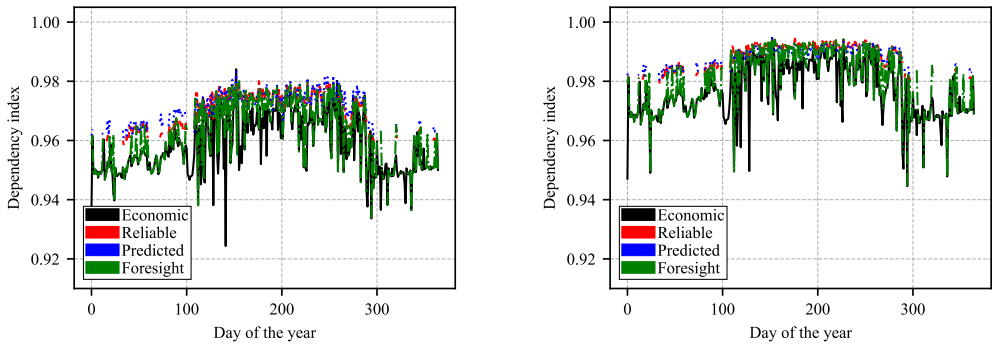

(c) 1 h energy storage for cluster 6

(d) 2 h energy storage for cluster 6

Figure 3.8: Daily dependence index (R_L) for the year 2013.

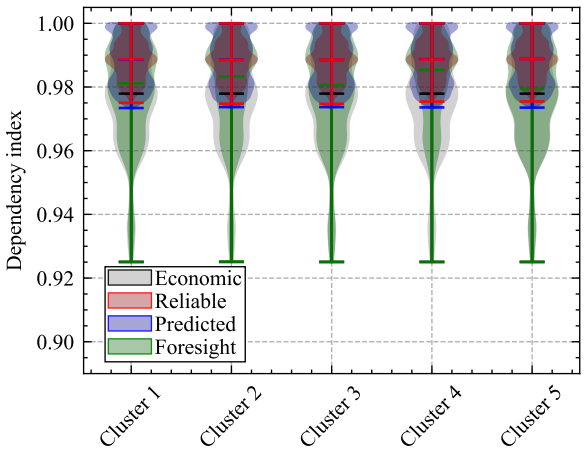

Figure 3.9: Violin plot for R_L in the highest accuracy clusters for the year 2013.

3.3 Publication III: Performance evaluation of machine learning for fault selection in power transmission lines

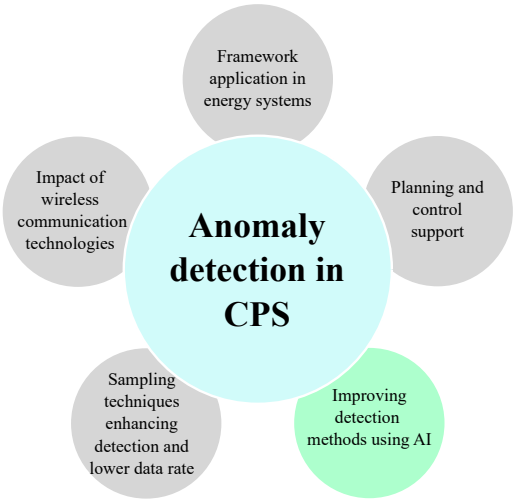

Figure 3.10: Topic studied in Publication III

In this publication, research question RQ3 was answered by studying an application in energy systems related to protection in power lines and comparing the current and classic methods in anomaly detection.

The results were obtained from a two-stage methodology. In the first stage, a DM-DFT is used for preprocessing the nonfaulty and faulty data coming from a simulated double-circuit transmission line. The second stage involves an accuracy analysis applying machine learning algorithms to fault selection. The analysis was conducted in terms of accuracy and explainability. To test the methodology, in addition to the simulation data, the ML model was tested on a real fault file. In order to be more computationally efficient, all ML algorithms were ran on the same machine, being fully parallel and taking advantage of all CPU cores. In the second stage, multiple ML algorithms were compared against QARMA. The reason is that most the of widely used ML algorithms in the literature are easy to implement. Despite usually having a high accuracy for certain applications, they lack explainability. The correlation between variables and outcomes might be important in an electrical application as the correlation chart presented in this research can help engineers to effectively choose the sensors that will monitor the variable while maintaining a high accuracy in the fault selection task.

In the case of QARMA, it does not require any hyperparameters to run. However, regarding ANNs, parametrization is an important task, and in many cases, the tuning requires many rounds of experimentation. The parameters of the ANN used in this study were found by a repeated set of experiments, and thus, they might not be the most optimal ones as the accuracy provided was above 98%. Moreover, as for the hyperparametriza-

tion of the rest of the algorithms used for comparison, they either require no parameters, or the ones typically used in the literature were used in this work. The simulation scenarios are based on usually employed power system transmission topologies and are widely exploited in the literature for fault location and selection.

3.3.1 Test system 1

The first test system simulation consists of a double transmission line. The data were split into 75% for training and 25% for testing. After 5-fold cross-validation experiments, the results obtained were similar. Table 3.2 shows the accuracy results of the above-mentioned algorithms including QARMA; the matrix of fault selection performed by the best result achieved by ANN can be seen in Fig. 3.11.

The best results in terms of accuracy obtained with the DL were 98.33%. They were achieved by trial and error, and they are particularly high because of having enough layers to produce a representation of the data and the final layer being able to correctly classify most of the faults. The statistical methods and probabilistic classifiers Naïve Bayes, logistic regression, and AdaBoost did not perform well; the reason for this is that algorithms of this type are very susceptible to noise. The similitude between some of the features contributes to reducing the accuracy of the results. The high results obtained with rule-based methods and ANNs in particular are a product of a well-balanced dataset and all the features being available. During the fault point extraction, synchronization and problems related to communication were not considered. It is important to note that once fewer features become available in the dataset, the accuracy decreases substantially as seen in Fig. 3.12. However, when only the currents of one end are available, the validation error is within an acceptable range. This happens because the fault information contained in the current features is greater than in the voltage features. This knowledge is relevant for the application as the current transformers that sense the currents from transmission lines are a vital aspect for protection tasks. The list of features tested for each round in Fig. 3.12 is given in Table 3.3.

Table 3.2: ML Results on the Fault-Grid Dataset.

Classifier	**Accuracy**
Decision Tree	94.62%
ANN (1 hidden layer)	95.18%
ANN (3 hidden layer)	**98.33%**
SVM	89.05%
Ripper-k	86.17%
Naïve Bayes	59.42%
Logistic Regression	78.47%
AdaBoost.M1	17.81%
QARMA	**98%**

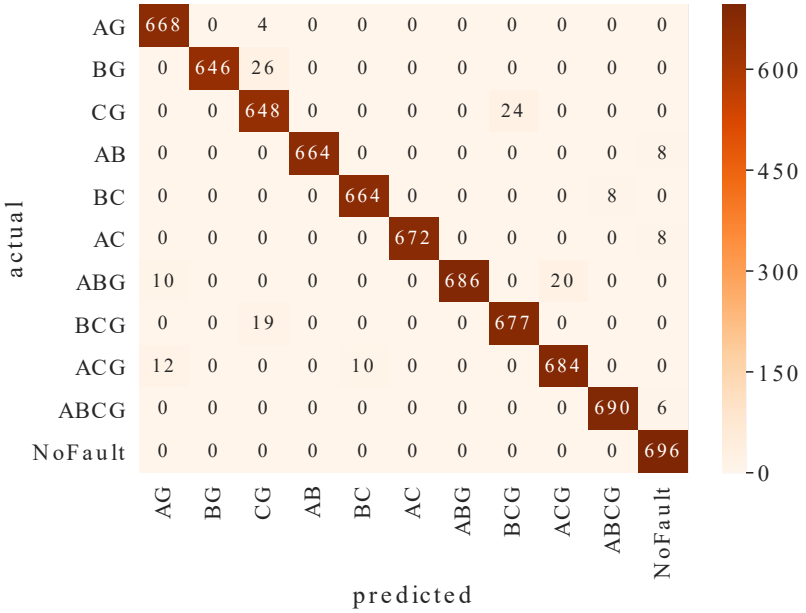

Figure 3.11: Fault classification task confusion matrix for test system 1.

As the experiments ran in QARMA on the dataset, the algorithm was able to obtain 5333 rules that cover 97.8% of the training dataset. The resultant accuracy of QARMA was around 98%, and for a small number of cases, QARMA did not classify correctly because of the rules that were triggering the classification. However, in more highly skewed datasets, QARMA is expected to outperform ANN classification by its decision-making.

Table 3.3: Feature selection on the original dataset.

Round	Feature
1	all features (local and remote current and voltages including I_R)
2	$L_{I_A}, L_{I_B}, L_{I_C}, L_{I_R}$
3	$R_{I_A}, R_{I_B}, R_{I_C}, R_{I_R}$
4	$L_{I_A}, L_{I_B}, L_{I_C}, L_{V_A}, L_{V_B}, L_{V_C}$
5	$R_{I_A}, R_{I_B}, R_{I_C}, R_{V_A}, R_{V_B}, R_{V_C}$
6	$L_{I_A}, L_{I_B}, L_{I_C}$
7	$R_{I_A}, R_{I_B}, R_{I_C}$
8	$L_{V_A}, L_{V_B}, L_{V_C}$
9	$R_{V_A}, R_{V_B}, R_{V_C}$

In this system test, a sensitivity experiment was also performed. It was tested how resilient the ANN is to measurement noise by progressively adding Gaussian white noise to all the features in the training and test datasets. The results obtained in Table 3.4 indicate

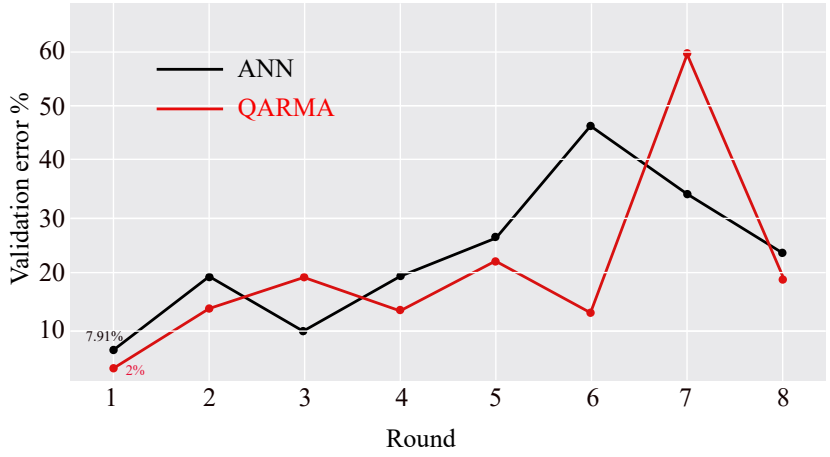

Figure 3.12: Validation error obtained with the same model parameters using fewer features.

that ANNs are still able to classify the fault, achieving almost the same accuracy as that without noise, but the accuracy significantly drops to 20.67% error when sigma (σ) is equal to 100 in the training dataset. This is important in the sense of measurements in a real scenario (different from simulated) that is susceptible to different noise conditions in the system. In the sensitivity test, QARMA results outperformed ANN, and with the different values of σ, the error was always below the 3% error, making the system very robust against noise.

Table 3.4: Neural network and QARMA performance under different noise levels in the data.

training σ	**testing σ**	**NN error%**	**QARMA error%**
0	0.01	2.98	2
0	1	3	2
0	10	3.14	2.01
0	100	11.7	2.23
0.01	0	3.04	2
1	0	3.04	2
10	0	6.1	2.01
100	0	17.84	2.47
100	100	20.67	2.89

This difference in robustness still requires more research, but we may assume that the underlining complexity of the ANNs subfunctions might be more susceptible to noise and easy to overfit, while the rules extracted by QARMA provide a simpler decision-making, and likely they hold true in the presence of noise.

Another advantage of QARMA is that it belongs to a fairly new concept called ”eXplainable Artficial Intelligence” (XAI), which states that the outcomes of such models are

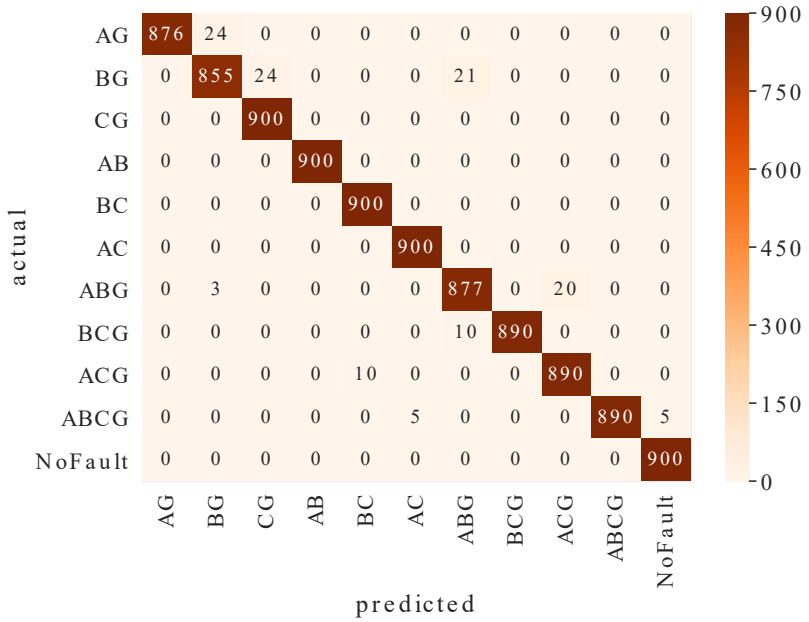

Figure 3.13: Fault classification task confusion matrix for test system 2.

easily understandable by humans. Under XAI, the rules created by QARMA from the dataset are trivially checked against the training dataset. These rules are usually bounded, and the rule attributes can easily be interpreted by humans as the extracted knowledge is based on the antecedents of the features. This is not the case for ANN, where this type of knowledge is embedded in the internal connections between the layers.

3.3.2 Test system 2

The objective of the test system number 2 was to test the generalization of the proposed ML approaches, more specifically QARMA and ANN. The system is a single-circuit 400 kV transmission line. The difference is that it does not have a mutual impedance between circuits as in the double-line case, which ultimately impacts the fault current behavior. The accuracy obtained with ANN was 98.8% and with QARMA 98.1%, slightly better than with the first test system, indicating that both models can be used for this type of problem independently of the test system. The confusion matrix of the above-mentioned test is illustrated in Fig. 3.13.

The improved results in this test can be explained by the fact that the fault currents are less attenuated from the contributions of mutual impedances, which are not so significant as in the case of a double-line system. Therefore, the features are able to better capture the characteristics of the fault.

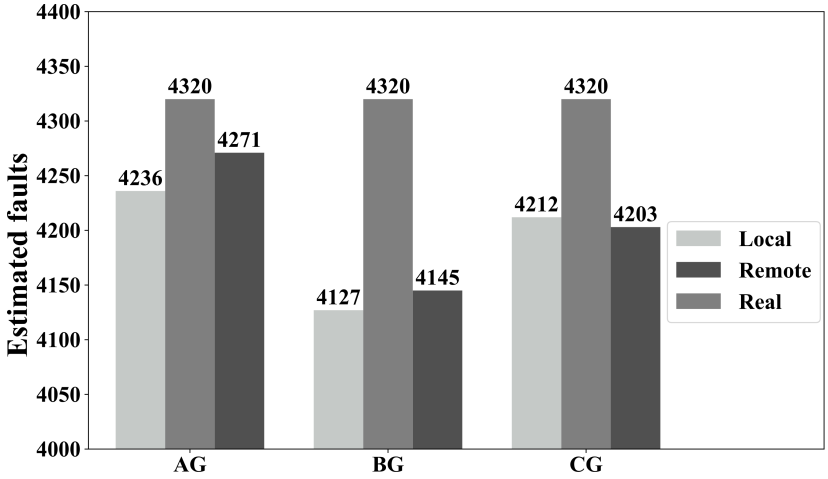

Figure 3.14: Fault classification by the symmetrical angle method.

Table 3.5: Results obtained by replicating the symmetrical method.

	Dependability		**Security**	
	Local end	Remote end	Local end	Remote end
AG	98.05%	98.86%	910	910
BG	95.53%	95.94%	896	909
CG	97.50%	97.29%	880	880

3.3.3 Symmetrical method

A symmetrical algorithm method using the system 1 model dataset was performed during the experiments. The purpose of using this method is to serve as a comparison with the ML methods employed in the research. The symmetrical method is often used by relay manufacturers to perform fault selection in real transmission scenarios, where the task is important. The results are presented in Fig. 3.14 (note that a confusion matrix like the one presented in Fig. 3.13 cannot be used to compare all faults using the symmetrical method because the datasets have different lengths; only AC, BC, and CG faults can be compared). The symmetrical method is only applicable during single-phase faults. The accuracy of this method for single-phase faults can be represented in Table 3.5 showing the false positives. In some situations, the symmetrical component method classified the fault as a single-phase fault, given that at least two phases were involved. Overall, this mistake can lead to some security errors in the protection system; the error can be single-pole tripping of transmission lines, which eventually leads to three-phase tripping that would require manual reclosure. In some cases with congested lines on highly interconnected and dependent systems, it can lead to further system failures.

3.3.4 Real fault file

It was possible to obtain a real fault file from a transmission system located in Brazil. This was extremely important for the research as we could test the model on a potential real scenario. Once the file is preprocessed and the voltage and current matrices are obtained, they can be injected into the DM-DFT algorithm that yields the fault point and extracts the features as shown in Fig. 3.15.

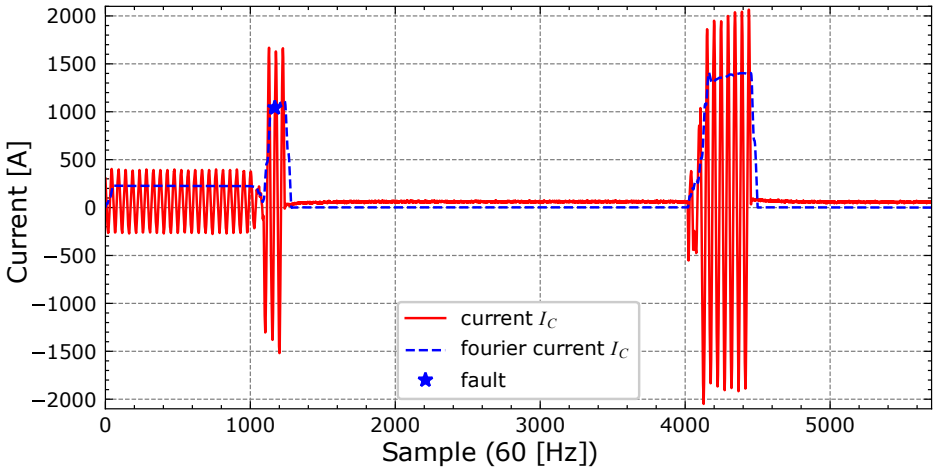

Figure 3.15: Phase C and DFT of a real transmission system fault.

In real situations, faults can suddenly reappear for such reasons as reclosure or reinsertion. This is the case in the CG-type fault shown in Fig. 3.15. The algorithm successfully detects the first fault occurrence, the second algorithm being able to classify both instances. The ANN and QARMA models were applied in the real fault data with a successful result: both correctly classify the fault as CG. In the case of QARMA, it yielded 1100 rules that predicted the class of the fault, which resulted in the overall correct classification of the test case. One of the highest confidence rules for this test case was:

$$\begin{aligned} & [local\_voltage_A >= 235730.0266612848] \\ AND\ & [local\_voltage\_B >= 231130.0132737731] \\ AND\ & [remote\_ir >= 321.3212781340371] \\ \Rightarrow\ & [fault\_type = CG]. \end{aligned} \tag{3.1}$$

The support of this rule on the training set is 2.72%, and it holds with a confidence level of 100%.

The results obtained during the real fault test proved that once the models are created based on historical data, they can serve as a fault selector with a proper computational infrastructure to perform this critical protective task. Even with the conditions in this case

where the model was created based on simulated data and a different test system than the real fault, it was able to obtain the correct phase involved during the fault.

Having the generalized framework as a base study to improve detection in the cyber-physical application is an important tool to compare between classic methods and the recent ML methods. Improving the detection method for a particular application is no less important than being able to create a closer relationship between the cyber and physical layers by providing explainability with ML methods. Human understanding of the influence of features regarding the outcome of anomaly detection has a significant impact on the prediction and mitigation of future events.

3.4 Publication IV: Anomaly detection by event-driven data acquisition

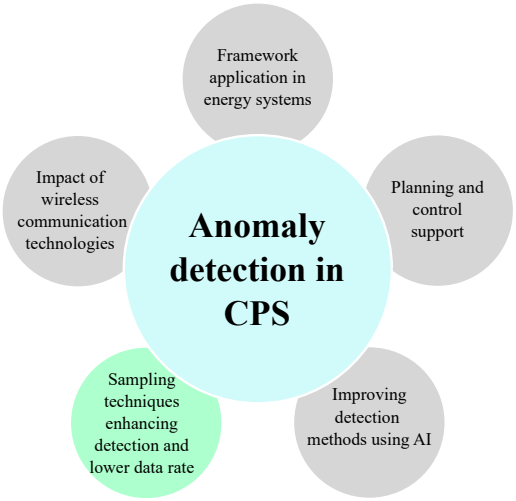

Figure 3.16: Topics studied in Publication IV.

In this publication, research question RQ4 was answered by studying the impact of sampling techniques on anomaly detection in cyber-physical systems under different scenarios.

To further develop the initial results presented in Section 3.1, these results present the advantage of event-driven strategies in anomaly detection. The results were obtained by using delta and threshold approaches on the TEP, compared with the classic time-based approach. PCA was employed to perform anomaly detection using T^2 and Q statistics.

Based on the comparison of the methods, the performance of the threshold method for anomaly detection was slightly better for all the values of the parameter p (percentage of variation). The benefit in this case is in the use of a much smaller amount of data, which favors online applications, especially nowadays, given the era of big data.

As for the delta method, the performance was remarkably better compared with the threshold- and time-based approaches. The results are explained by the fact that the delta approach can record not only the greater changes within the original signal but also some slight changes that are a product of faults that are very hard to detect. If the value is not recorded at a specific time slot, the delta EDM maintains the previous value, and thus, the system is working as it were in normal operation. Ultimately, the slight or greater changes made after the anomaly are placed in the process, and then used as an input vector for the PCA detection method.

Tables 3.6 and 3.7 show the missed detection rate (MDR) obtained with the delta rule

for the statistics T^2 and Q, respectively. The best result for each fault is given in bold. For example, the best MDR values for fault 5 were equal to 0.604 (for T^2 and p = 0.90) and 0.001 (for Q and p = 0.80). Absolute differences from the respective MDR values obtained with the periodic approach are also presented. The greater this difference is, the better is the result obtained by the delta rule. For example, the gains for fault 5 were equal to about 17% ($= 0.775 - 0.604$) and 74% ($= 0.746 - 0.001$) for the statistics T^2 and Q, respectively. For the statistic Q, it can be seen that the MDR value obtained with the event-driven delta rule is very close to zero (0.001), as desired, while the corresponding value for the time-fixed procedure is considerably high (0.746). A gray cell means that the result was not considered valid because of a false alarm rate (FAR) above 5%.

Table 3.6: MDR (missed detection rate) for the statistic T^2.

Fault	Time-based approach	Event-based delta approach (p in %)											Absolute gain
		5	10	20	30	40	50	60	70	80	90	95	
1	0.008	**0.008**	**0.008**	**0.008**	**0.008**	**0.008**	**0.008**	0.009	**0.008**	**0.008**	0.010	0.010	0%
2	0.020	**0.020**	**0.020**	**0.020**	**0.020**	0.023	0.023	**0.020**	0.023	0.023	0.023	0.023	0%
3	0.998	0.999	0.996	0.996	1.000	**0.993**	1.000	1.000	0.996	1.000	1.000	1.000	1%
4	0.956	0.961	0.959	0.960	0.973	0.969	0.939	0.934	**0.905**	0.999	0.999	0.999	**5%**
5	0.775	0.774	0.771	0.770	0.766	0.764	0.766	0.773	0.729	0.683	**0.604**	0.701	**17%**
6	0.011	0.011	0.011	0.011	0.011	0.011	0.011	**0.008**	0.009	0.009	0.009	0.009	0%
7	0.085	0.079	0.076	0.079	0.065	0.045	0.051	0.161	**0.000**	**0.000**	**0.000**	**0.000**	**9%**
8	0.034	0.033	**0.031**	0.034	**0.031**	0.033	**0.031**	**0.031**	**0.031**	0.043	0.054	0.045	0%
9	0.994	0.998	0.996	0.991	0.993	0.998	0.984	0.984	**0.979**	1.000	1.000	1.000	2%
10	0.666	0.653	0.653	**0.646**	0.655	0.671	0.678	0.679	0.694	0.744	0.806	0.826	2%
11	0.794	0.789	0.786	0.796	0.793	0.794	0.761	**0.688**	0.876	0.886	0.899	0.926	**11%**
12	0.029	0.021	0.021	0.023	**0.019**	0.024	0.026	0.021	0.035	0.034	0.059	0.056	1%
13	0.060	**0.060**	**0.060**	0.061	0.061	0.061	0.061	0.063	0.061	0.063	0.076	0.078	0%
14	0.158	0.120	0.125	0.111	0.114	0.096	**0.094**	0.106	0.095	0.154	0.149	0.154	**6%**
15	0.988	0.979	0.978	0.984	0.983	0.993	**0.940**	0.974	0.984	0.996	1.000	1.000	**5%**
16	0.834	0.833	0.833	0.851	0.844	0.834	0.860	0.809	**0.733**	0.920	0.934	0.946	**10%**
17	0.259	0.254	0.251	0.258	0.260	**0.249**	0.261	0.255	0.273	0.338	0.261	0.324	1%
18	0.113	0.113	0.113	0.111	**0.110**	0.113	0.116	0.118	0.113	0.113	0.121	0.121	0%
19	0.996	0.999	0.999	1.000	0.999	0.996	0.993	0.998	**0.885**	0.988	0.996	1.000	**11%**
20	0.701	0.704	0.710	0.709	0.718	0.725	0.684	0.731	**0.650**	0.766	0.754	0.805	**5%**
21	0.736	0.694	0.693	0.691	0.691	0.696	0.690	**0.651**	0.716	0.786	0.865	0.876	**8%**

Gray cells: False alarm rate $> 5\%$.

Moreover, faults 10, 15, and 16 showed significant MDR gains, given the statistic Q (Table 3.7). Thus, they also showed considerable gains in terms of detection time. Faults 10 and 16 are hard-to-detect (group 3), and fault 15 is very hard-to-detect (group 4). Intermediate faults 17 and 18 (group 2), with MDR gains of 7% (Table 3.7), also presented reasonable gains for detection time, given the statistic Q, with FAR values close to zero.

To visualize the impact of delta EDM compared with the time-based approach, Fig. 3.17 shows the Q control charts obtained with the event-based delta rule for faults 5, 10, 16, and 20 (on the left). Corresponding charts for the same fault and variables in the time-based approach are also presented for comparison (on the right).

The values that are not sent or transmitted by using the delta EDM are replaced by the previous ones sent to signal reconstruction. The signal obtained and its input vector normally have more deviations than the one obtained in the time-based approach because of

Table 3.7: MDR (missed detection rate) for the statistic Q.

Fault	Time-based approach	Event-based delta approach (p in %)											Absolute gain
		5	10	20	30	40	50	60	70	80	90	95	
1	0.003	0.003	0.003	0.003	0.003	**0.001**	0.003	0.003	0.003	0.006	0.004	0.004	0%
2	0.014	0.014	0.014	0.015	0.011	0.011	**0.010**	0.018	0.000	0.023	0.023	0.023	0%
3	0.991	0.990	0.990	0.985	0.975	0.830	0.949	0.160	0.461	**0.876**	0.926	0.995	**11%**
4	0.038	0.035	**0.031**	0.040	0.038	0.031	0.033	0.046	0.006	0.063	0.000	0.470	1%
5	0.746	0.745	0.743	0.743	0.720	0.644	0.303	0.164	0.000	**0.001**	0.000	0.008	**74%**
6	0.000	**0.000**	**0.000**	**0.000**	**0.000**	**0.000**	0.000	**0.000**	**0.000**	**0.000**	**0.000**	**0.000**	0%
7	0.000	**0.000**	**0.000**	**0.000**	**0.000**	**0.000**	**0.000**	**0.000**	**0.000**	**0.000**	**0.000**	**0.000**	0%
8	0.024	0.025	0.025	0.021	0.023	**0.019**	0.025	0.000	0.025	0.025	0.026	0.026	1%
9	0.981	0.979	0.983	0.979	0.966	0.915	0.675	0.711	0.484	**0.501**	1.000	1.000	**48%**
10	0.659	0.650	0.653	0.648	0.578	0.465	0.255	**0.061**	0.065	0.226	0.454	0.464	**60%**
11	0.356	0.340	0.335	0.335	0.329	0.290	0.198	**0.099**	0.320	0.313	0.519	0.635	**26%**
12	0.025	0.025	0.025	0.029	0.031	0.018	**0.009**	0.005	0.014	0.016	0.016	0.016	2%
13	0.045	0.045	0.045	0.045	0.048	**0.041**	0.044	0.054	0.053	0.055	0.055	0.060	0%
14	0.000	**0.000**	**0.000**	**0.000**	**0.000**	**0.000**	**0.000**	0.001	0.001	0.001	0.001	0.001	0%
15	0.973	0.970	0.971	0.968	0.948	0.855	0.756	0.251	**0.279**	0.954	0.956	0.884	**69%**
16	0.755	0.744	0.740	0.728	0.661	0.574	**0.290**	0.210	0.174	0.536	0.633	0.546	**47%**
17	0.108	0.098	0.103	0.100	0.100	0.064	**0.034**	0.054	0.043	0.083	0.086	0.094	**7%**
18	0.101	0.103	0.100	0.101	0.096	0.076	0.031	0.048	**0.034**	0.063	0.114	0.114	**7%**
19	0.873	0.863	0.856	0.869	0.821	0.666	0.539	**0.526**	0.628	0.845	0.711	0.740	**35%**
20	0.550	0.546	0.538	0.529	0.509	0.448	0.286	0.169	**0.135**	0.138	0.376	0.354	**42%**
21	0.570	0.578	0.571	0.570	0.535	**0.456**	0.309	0.505	0.555	0.610	0.614	0.704	**11%**

Gray cells: False alarm rate $> 5\%$.

the filtering, leaving larger variations from the original input signal. This fact is what ultimately provides a better performance for anomaly detection in the PCA algorithm. This means that after a fault has occurred in the system, the most relevant changes come faster in the detection. For the specific case of the TEP, the best results for the parameter p are obtained in intermediate values of around 40% to 60%. When the parameter p is close to 0, the results are the same as in the time-based approach, and when p approaches 1, it yields a very harsh constraint for fault detection, recording only major changes. Thus, p is seen as a sensitivity parameter for data rate transmission that has a great impact on anomaly detection. The most important achievement for the EDM delta approach was on hard-to-detect faults.

In terms of data transmission rate, the EDM approach provides significant savings. The process changes do not necessarily depend on periodic measurement. Fig. 3.18a shows the average transmission rate in each time slot using the EDM delta approach from all the 52 variables in the TEP process. At 0%, in any given time slot, all variables are transmitted, and once the parameter p increases just to 5%, there is a dramatic drop saving almost half of the initial transmission rate. Similarly, it is possible to obtain for the parameter p the best MDR results for both statistics T^2 and Q (see Fig. 3.18b). By further analyzing the results from Fig. 3.18, it is possible, from a design point of view, to retrieve a p parameter from the EDM technique that can meet the requirements of the FAR and the MDR while considerably reducing the transmission traffic to the desired levels.

The implications of the results rely on the increasing network demand for communication traffic and the fact that EDM techniques can substantially leverage the network traffic

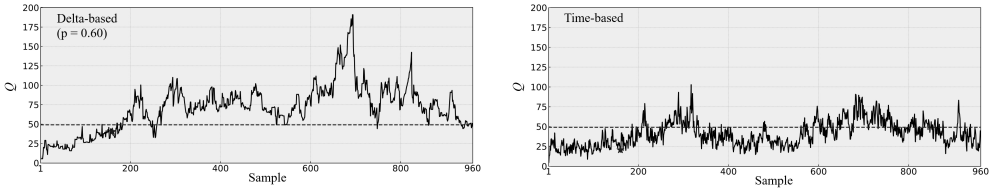

(a) Fault 10.

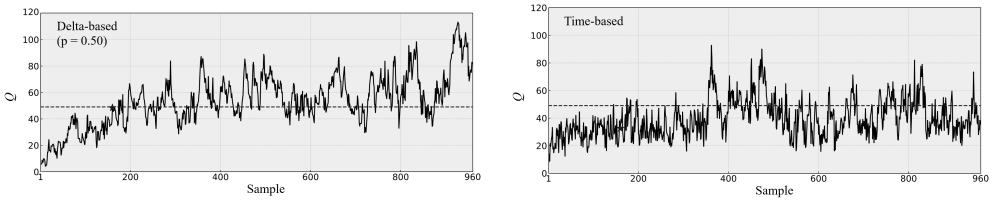

(b) Fault 16.

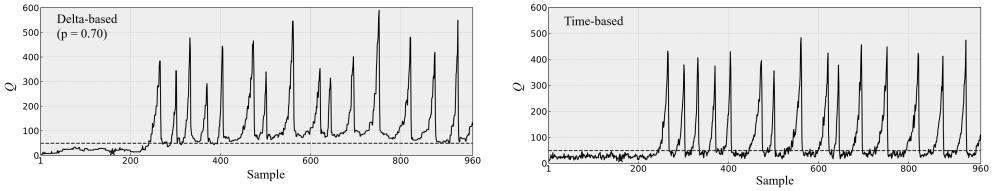

(c) Fault 20.

Figure 3.17: Q control charts for the event-based delta method (on the left) and the time-based approach (on the right) for hard-to-detect faults ($\star$: Fault start up at $t = 160$).

while improving anomaly detection tasks. All are important for current applications and in the frame of Industry 4.0. Following the framework presented in this research work for improving anomaly detection, the use of the EDM might be attractive for other process industries that require a large amount of transmitted data in short periods of time.

In summary, before the raw samples coming from physical sensors in the chemical process reach the cyber layer, EDM sampling techniques performed locally have a huge potential to support the data rate and improve anomaly detection techniques. From the general framework perspective, this is a task done in the data layer, which eventually can change the course of actions in the decision layer. The raw measurements do not always provide significant information. Meanwhile, the two methods proposed for the EDM take advantage of the data points that are far from the median or increased variation. The recording of these data has a statistically more significant impact on the detection algorithms enhancing their performance against hard-to-detect anomalies. It is important to note that prior knowledge of the application is required to efficiently choose the EDM in order to have gains. This means to choose a percentage threshold or percentage variation for the delta technique that yields best results (accuracy and data transmission rate). In this study, we demonstrated that it is possible to gain as much as 20% on average in data rate transmission from the sensors (physical layer) to the reconstruction block (data layer). The data

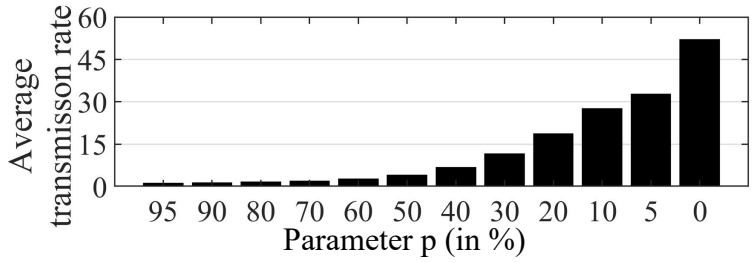

(a)

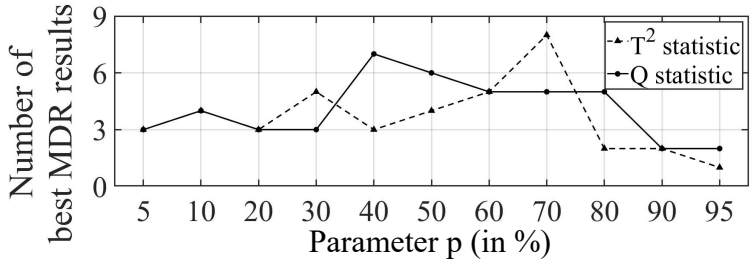

(b)

Figure 3.18: Effect of the parameter p (Equation 2.3) (a) on the average number of sampled values transmitted per sampling unit and (b) on the number of best MDR results, given the event-based delta rule.

reduction was obtained while maintaining or improving the anomaly detection accuracy (subjected to the percentage applied) using the classic statistical technique PCA. Recent ML techniques also have potential to be adopted by this methodology, but they were not used during the publication for fair comparison as ML is still fairly new to approach the TEP anomaly detection problem.

3.5 Publication V: Review of the State of the Art on Adaptive Protection for Microgrids Based on Communications

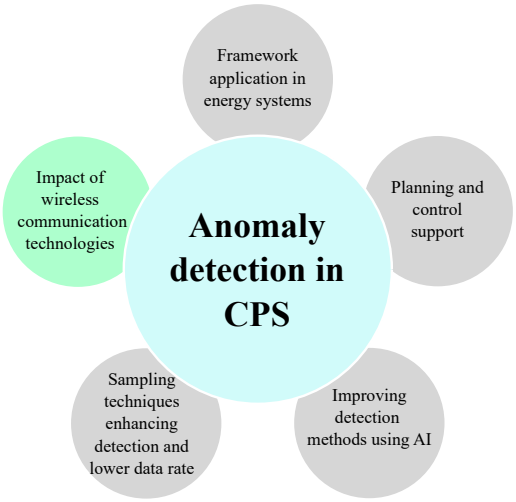

Figure 3.19: Topic studied in Publication V.

In this publication, research question RQ5 was answered by studying the current tendency of communication technologies in adaptive protection for microgrids specifically as an anomaly detection task. The current requirements of this application were also investigated in comparison with what 5G cellular communication can offer.

The investigation also focused on how recent cellular communication technologies can support a power application for anomaly detection. In particular, adaptive protection is a commonly used strategy in distribution networks to successfully identify and clear electrical faults in the case of topology or energy variations by changing the protective settings of the relays or IEDs according to the current state of the grid. An adaptive protection task requires communication between its IEDs to synchronize its settings. Communication technologies have a great impact because of the latency, and delay requirements are usually met by means of Ethernet cabling or optic fiber.

The research relevant to the topic of this study covers around 71 papers from 2015 to 2018. There is still a predominance of wired communication technologies in microgrids to perform adaptive protection and control. This is particularly ineffective, and wired technologies do not possess the required flexibility when there is a need to increase the penetration of renewable energy resources or additional loads. On the other hand, the research shows how emerging wireless technologies, such a cellular LTE 4G or 5G communication, can support those tasks, while maintaining the latency requirements.

In terms of communication standards that are essential in power systems, IEC 61850 is already widely used and seems promising because other communication protocols, such as

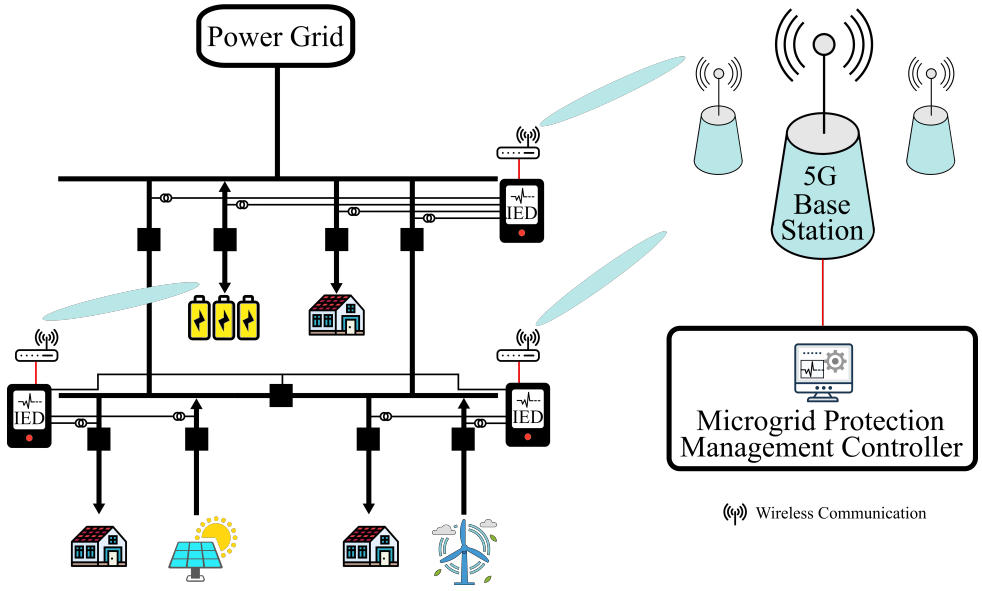

Figure 3.20: Deployment of wireless 5G communications with interface diversity in an overcurrent adaptive protection scheme.

sampled measured values (SMV) and generic object-oriented substation event (GOOSE), are annexed, and they have the necessary requirements for data transmission for intrarelay coordination with station-bus communications. The communication requirements for protection are very stringent, usually bounded to 12 ms from the event occurrence to the data transmission. With the current state of cellular communications, the requirements can be met by these wireless technologies, in particular, reliability of 99.999% with a low latency down to 4 ms.

One of the disadvantages of relying more on the cyber domain rather than the physical one, brought by the inclusion of wireless technologies, is that the system is more prone to cyberattacks. In a critical infrastructure like power systems, security is the main aspect when designing any application. Despite the vulnerabilities, a potential wireless system should have a robust architecture that is able to prevent or avoid possible cyberattacks.

Overall, an adequate way to incorporate wireless technologies into substation automation and control is through multiconnectivity (see Fig. 3.20) capable of performing anomaly detection tasks by delivering information adequately and timely from the physical layer to the data layer. This means hybrid ways between wired and wireless technologies that are able to meet the requirements while keeping the communication network secure. The coexistence of technologies should make economically viable the option of integration into new resources and slowly develop to a fully wireless system, which can greatly reduce the cost. A smooth transition will not only bring technical benefits but also be economical in the long run.

4 Conclusions

So far, most of the use cases addressed in the dissertation are related to energy applications. Data from those cases were found by means of simulations or datasets available for the public on different platforms. One distribution fault dataset that was provided by the distribution operator Elenia was used extensively for the development of the papers, but typically, obtaining such data requires an enormous amount of bureaucracy when companies are involved.

This research work showed the potential of the proposed three-layer scheme in cyber-physical systems to perform anomaly detection. It explored in detail some characteristics of each layer in data acquisition, data fusion, analytics, and decision-making. Almost every industrial application can be seen as a cyber-physical system, where data coming from sensors must be processed to deliver a specific task. The integration of the layers in a cyber-physical system has a significant impact on the outcomes of fault detection and prevention. The results obtained in terms of data acquisition for anomaly detection in the Tennessee Eastman process show that event-driven approaches can benefit the detection and classification of faults as they can record the important features that will be later injected as inputs into the detection algorithms. Moreover, event-driven acquisition is seen as a data filtering method where reconstruction of the signal implies that less data are transmitted over the communication network from the sensor to the management center. The reduction in the data transmission rates was around 20% on average, at the same time improving anomaly detection. Approaches of this kind can be very interesting for different companies, especially for those who deal with a lot of possible shutdowns in operation resulting from faults in the process. The complexity of some industries that involve considerable measurements makes it hard to effectively detect, select, and isolate faults. This is mainly due to the enormous amount of measurement variables that usually do not have any type of filtering, or simply the storage and data transmission infrastructure is not sufficient. Using event-driven approaches will ease the load of data inside those types of environments and support various control and operational tasks.

In terms of evaluating different algorithms existing for an application in power assets, the research conducted in this doctoral dissertation proved that the emerging techniques in machine learning and rule-based algorithms can outperform the classic ones. Under this approach, a methodology was developed to first identify the instant when a fault in power transmission lines occurs, and then, a procedure was established that selects based on machine learning algorithms. The accuracy achieved with artificial neural networks was 98.33%, while QARMA reached 98%. The slight difference in accuracy between the two techniques is irrelevant, and the main advantage of QARMA is the explainability it brings from the problem. Finding easy connections in the rules between the features and the anomaly detection outcomes that are understandable for humans are key factors. It can help engineering, e.g., to adequately measure and design a more robust system, place more sensors in the system, and thereby reduce operational times in the industrial processes.

Anomaly detection is not only useful for reducing shutdown times, but it can also support other control tasks leading to energy efficiency, and ultimately, reducing costs. In this work, it was shown how anomaly detection and prevention based on weather forecasts is one of the inputs to economically control a battery energy storage system in a microgrid. Using different computational techniques, such as machine learning methods, to predict anomaly occurrences in a power distribution system, a battery was optimized to store as much energy as possible in the occurrence of fault events. The events cause the microgrid to be isolated from the main grid and operate solely on the battery. When the energy of the battery is charged almost to full prior those events (while keeping an economical approach), the microgrid load is capable of continuing operation for longer times and thereby having less or no impact on the users connected to the microgrid. Anomaly prediction in distribution systems is relevant information for the operators as they can effectively prepare their maintenance team or allocate resources to specific areas to clear faulted networks and increase the overall resilience of the grid.

Dataflows in cyber-physical systems are supported by communication technologies. In this dissertation, it was analyzed how in an energy application, such as protection in power systems, there is still a tendency to rely on wired communication. This conventional technology requires a heavier infrastructure and thereby an expensive solution. With the constant changes in electricity networks and the penetration of renewable energy, flexibility for communication is an important aspect. Decentralization of electricity networks calls for more automation, and this is only possible when the bidirectional dataflow meets the necessary requirements for latency and delays. For the case of protection of a power system, those requirements are met by emerging technologies, such as cellular 4G LTE and 5G communication. The important factor will be how to merge the technologies into a multiconnectivity application, where the technical aspects have enough flexibility supporting one or many applications while increasing the economical benefits to the industry.

The overall aim of the doctoral dissertation was the articulation of anomaly detection in a CPS in three layers for performance improvement. The importance of clearly integrating the problem space into these layers lies in the fact that a small improvement in each layer can have a significant impact on the anomaly detection outcome. Identifying the key factors in each layer can help engineers in ranking priorities and thereby improving accuracy and dataflow in different industrial applications that would benefit from more effective anomaly detection.

For future work, the research directions have plenty of potential in the five edges that were investigated, namely the generalization framework, planning and control support, detection methods, sampling techniques, and communication technologies.

In terms of framework application, new tests could include electric drives, methanol processes, mechanical machines, measurement of CO_2 inside industrial facilities, and automotive machinery failures during operation. This last automotive application was one of

the initial motivations to carry out this research, but a project with the automotive industry to gather the data by employing new sensors could not be carried out in the 4-year span of this doctoral dissertation. Futhermore, data availability from critical applications like transmission power lines, which is usually limited for industrial security reasons, could play a key role in developing interventions as subsequent tasks after anomaly detection. Advances in hyperparametrization of AI techniques could also significantly improve the accuracy of detection. Finally, for sampling techniques, advances in data reduction in combination with communication technologies, e.g., asnew wireless standards, could not only improve the detection accuracy but also reduce the need for data storage and overall transmission. All these opportunities give some indication of the different paths that the work reported here has introduced.

References

Adamo, J.M. (2001). *Data mining for association rules and sequential patterns*. Springer Media, NY, NY.

Alemão, D., Rocha, A.D., Nikghadam-Hojjati, S., and Barata, J. (2022). How to Design Scheduling Solutions for Smart Manufacturing Environments Using RAMI 4.0? *IEEE Access*, 10, pp. 71284–71298. doi:10.1109/ACCESS.2022.3187974.

Astrom, K.J. and Bernhardsson, B.M. (2002). Comparison of Riemann and Lebesgue sampling for first order stochastic systems. In: *Pro. of the 41st IEEE Conf. on Decision and Control, 2002.*, vol. 2, pp. 2011–2016.

Bastos, A., Sguario Coelho De Andrade, M.L., Yoshino, R.T., and Santos, M.M.D. (2021). Industry 4.0 Readiness Assessment Method Based on RAMI 4.0 Standards. *IEEE Access*, 9, pp. 119778–119799. doi:10.1109/ACCESS.2021.3105456.

Chen, Z., et al. (2019). A distributed canonical correlation analysis-based fault detection method for plant-wide process monitoring. *IEEE Trans. on Industrial Informatics*, 15(5), pp. 2710–2720.

Chiang, L.H., Russell, E.L., and Braatz, R.D. (2001). *Fault detection and diagnosis in industrial systems*. Springer.

Chiumento, A., Reynders, B., Murillo, Y., and Pollin, S. (2018). Building a connected BLE mesh: A network inference study. In: *2018 IEEE Wireless Communications and Networking Conference Workshops (WCNCW)*, pp. 296–301.

Chollet, F. (2018). *Deep learning mit python und keras: Das Praxis-Handbuch vom Entwickler der Keras-Bibliothek*. MITP-Verlags GmbH & Co. KG.

Christou, I.T. (2019). Avoiding the Hay for the Needle in the Stack: Online Rule Pruning in Rare Events Detection. In: *2019 16th International Symposium on Wireless Communication Systems (ISWCS)*, pp. 661–665.

Christou, I.T., Amolochitis, E., and Tan, Z.H. (2018). A parallel/distributed algorithmic framework for mining all quantitative association rules. *arXiv preprint arXiv:1804.06764*.

Dai, W., et al. (2019). Industrial Edge Computing: Enabling Embedded Intelligence. *IEEE Industrial Electronics Magazine*, 13(4), pp. 48–56.

Denning, D.E. (1986). An Intrusion-Detection Model. In: *1986 IEEE Symposium on Security and Privacy*, pp. 118–118.

Downs, J.J. and Vogel, E.F. (1993). A plan-wide industrial process control problem. *Computers and Chemical Engineering*, 17(3), pp. 245–255.

El Koujok, M., Ragab, A., Ghezzaz, H., and Amazouz, M. (2020). A Multi-Agent-Based Methodology for Known and Novel Faults Diagnosis in Industrial Processes. *IEEE Trans. on Industrial Informatics*.

Esposito, C., Castiglione, A., Pop, F., and Choo, K.K.R. (2017). Challenges of Connecting Edge and Cloud Computing: A Security and Forensic Perspective. *IEEE Cloud Computing*, 4(2), pp. 13–17. doi:10.1109/MCC.2017.30.

Esteban, J., et al. (2005). A Review of data fusion models and architectures: towards engineering guidelines. *Neural Computing and Applications*, 14(4), pp. 273–281.

Grubbs, F.E. (1969). Procedures for Detecting Outlying Observations in Samples. *Technometrics*, 11(1), pp. 1–21.

Gutierrez-Rojas, D., et al. (2020). Three-layer Approach to Detect Anomalies in Industrial Environments based on Machine Learning. In: *2020 IEEE Conference on Industrial Cyberphysical Systems (ICPS)*, vol. 1, pp. 250–256.

Hall, D. and Llinas, J. (1997). An introduction to multisensor data fusion. *Proceedings of the IEEE*, 85(1), pp. 6–23.

Hotelling, H. (1931). The Generalization of Student's Ratio. *The Annals of Mathematical Statistics*, 2(3), pp. 360–378.

Jackson, J.E. and Mudholkar, G.S. (1979). Control Procedures for Residuals Associated With Principal Component Analysis. *Technometrics*, 21(3), pp. 341–349.

Jiao, J., Zhen, W., Zhu, W., and Wang, G. (2020). Quality-related Root Cause Diagnosis Based on Orthogonal Kernel Principal Component Regression and Transfer Entropy. *IEEE Trans. on Industrial Informatics*.

Junior, G.M., Di Santo, S.G., and Rojas, D.G. (2016). Fault location in series-compensated transmission lines based on heuristic method. *Electric Power Systems Research*, 140, pp. 950–957.

Kühnlenz, F. and Nardelli, P.H. (2016). Dynamics of complex systems built as coupled physical, communication and decision layers. *PloS one*, 11(1), p. e0145135.

Leitao, P. et al. (2016). Smart agents in industrial cyber–physical systems. *Proceedings of the IEEE*, 104(5), pp. 1086–1101.

Liu, Y., et al. (2019). Wireless Network Design for Emerging IIoT Applications: Reference Framework and Use Cases. *Proceedings of the IEEE*, 107(6), pp. 1166–1192. ISSN 1558-2256.

Marino, R., et al. (2020). A Machine Learning-based Distributed System for Fault Diagnosis with Scalable Detection Quality in Industrial IoT. *IEEE Internet of Things Journal*.

Miskowicz, M. (2010). Efficiency of event-based sampling according to error energy criterion. *Sensors*, 10(3), pp. 2242–2261.

Miskowicz, M. (2006). Send-On-Delta Concept: An Event-Based Data Reporting Strategy. *Sensors*, 6(1), pp. 49–63.

Munir, M., Siddiqui, S.A., Dengel, A., and Ahmed, S. (2019). DeepAnT: A Deep Learning Approach for Unsupervised Anomaly Detection in Time Series. *IEEE Access*, 7, pp. 1991–2005.

Narayanan, A., et al. (2022). Collective Intelligence Using 5G: Concepts, Applications, and Challenges in Sociotechnical Environments. *IEEE Access*, 10, pp. 70394–70417. doi:10.1109/ACCESS.2022.3184035.

Nardelli, P. (2022). *Cyber-physical systems: Theory, methodology and applications*, IEEE Press. Hoboken, NJ: Wiley-Blackwell.

Nguyen, V.H. and Suh, Y.S. (2008). Networked estimation with an area-triggered transmission method. *Sensors*, 8(2), pp. 897–909.

Russell, E.L., Chiang, L.H., and Braatz, R.D. (2000). Fault detection in industrial processes using canonical variate analysis and dynamic principal component analysis. *Chemometrics and intelligent laboratory systems*, 51(1), pp. 81–93.

Sánchez, J., Guarnes, M., and Dormido, S. (2009). On the Application of Different Event-Based Sampling Strategies to the Control of a Simple Industrial Process. *Sensors*, 9(9), pp. 6795–6818.

Simonov, M. (2013). Event-driven communication in smart grid. *IEEE Communications Letters*, 17(6), pp. 1061–1064.

Simonov, M. (2014). Hybrid scheme of electricity metering in smart grid. *IEEE Systems Journal*, 8(2), pp. 422–429.

Simonov, M., Chicco, G., and Zanetto, G. (2017a). Event-driven energy metering: Principles and applications. *IEEE Transactions on Industry Applications*, 53(4), pp. 3217–3227.

Simonov, M., Chicco, G., and Zanetto, G. (2017b). Real-time event-based energy metering. *IEEE Transactions on Industrial Informatics*, 13(6), pp. 2813–2823.

Simonov, M., Li, H., and Chicco, G. (2017c). Gathering Process Data in Low-Voltage Systems by Enhanced Event-Driven Metering. *IEEE Systems Journal*, 11(3), pp. 1755–1766. ISSN 1932-8184.

Staszek, K., Koryciak, S., and Miskowicz, M. (2011). Performance of send-on-delta sampling schemes with prediction. In: *Proc. IEEE Int. Symp. on Industrial Electronics*, pp. 2037–2042. IEEE.

Suh, Y.S. (2007). Send-on-delta sensor data transmission with a linear predictor. *Sensors*, 7(4), pp. 537–547.

Teng, H., Chen, K., and Lu, S. (1990). Adaptive real-time anomaly detection using inductively generated sequential patterns. In: *Proceedings. 1990 IEEE Computer Society Symposium on Research in Security and Privacy*, pp. 278–284.

Towell, G.G. and Shavlik, J. (1994). Knowledge-based artificial neural networks. *Artificial Intelligence*, 70(1–2), pp. 119–165.

Villaverde, A.F., Ross, J., Morán, F., and Banga, J.R. (2014). MIDER: Network Inference with Mutual Information Distance and Entropy Reduction. *PLOS ONE*, 9(5), pp. 1–15. doi:10.1371/journal.pone.0096732.

Yin, S., et al. (2012). A comparison study of basic data-driven fault diagnosis and process monitoring methods on the benchmark Tennessee Eastman process. *Journal of Process Control*, 22(9), pp. 1567 – 1581. ISSN 0959-1524.

Publication I

Gutierrez-Rojas, D., Ullah, M., Christou, I.T., Almeida, G., Nardelli, P., Carrillo, D., Sant'Ana, J. M., Alves, H., Dzaferagic, M., Chiumento, A. and Kalalas, C.
Three-layer Approach to Detect Anomalies in Industrial Environments based on Machine Learning

Reprinted with permission from
2020 IEEE Conference on Industrial Cyberphysical Systems (ICPS)
Vol. 1, pp. 250–256, Dec. 2020

Three-layer Approach to Detect Anomalies in Industrial Environments based on Machine Learning

Daniel Gutierrez-Rojas[1], Mehar Ullah[1], Ioannis T. Christou[2], Gustavo Almeida[3], Pedro Nardelli[1], Dick Carrillo[1], Jean M. Sant'Ana[4], Hirley Alves[4], Merim Dzaferagic[5], Alessandro Chiumento[5], Charalampos Kalalas[6]
[1]LUT University, Finland
[2]Athens Information Technology, Greece
[3]Federal University of Minas Gerais, Brazil
[4]6G Flagship, University of Oulu, Finland
[5]Trinity College Dublin, Ireland
[6]Centre Tecnològic de Telecomunicacions de Catalunya (CTTC/CERCA), Spain

***Abstract*—This paper introduces a general approach to design a tailored solution to detect rare events in different industrial applications based on Internet of Things (IoT) networks and machine learning algorithms. We propose a general framework based on three layers (physical, data and decision) that defines the possible designing options so that the rare events/anomalies can be detected ultra-reliably. This general framework is then applied in a well-known benchmark scenario, namely Tennessee Eastman Process. We then analyze this benchmark under three threads related to data processes: acquisition, fusion and analytics. Our numerical results indicate that: (i) event-driven data acquisition can significantly decrease the number of samples while filtering measurement noise, (ii) mutual information data fusion method can significantly decrease the variable spaces and (iii) quantitative association rule mining method for data analytics is effective for the rare event detection, identification and diagnosis. These results indicates the benefits of an integrated solution that jointly considers the different levels of data processing following the proposed general three layer framework, including details of the communication network and computing platform to be employed.**

***Index Terms*—cyber-physical systems, fault detection, industrial IoT, Tennessee Eastman Process**

I. Introduction

Detection and prediction of anomalies in industrial environments are important for both economic and security reasons. However, these tasks are far from trivial since anomalies are usually *rare events* within datasets so that most existing algorithms fail to identify them with (ultra-)reliability, either favoring false-alarms or misdetections [1], [2]. Even worse, in the special cases where effective solutions can be found, generalization is not straightforward. The challenge situation becomes: general approaches usually lead to false alarms and misdetections while effective solutions are very particular and cannot offer direct guidelines to other cases.

In this paper we deal with this problem by proposing a general frame to model a wide range of cases based on the advances in Industrial Internet of Things (IIoT) networks and Machine Learning (ML) algorithms [3]. In particular, we approach the problem by using a theory that considers three autonomous (but strongly dependent) layers of cyber-physical systems (CPS), namely physical, data and regulatory. By doing so, we are capable of analyzing in a more general way the steps of data acquisition, transmission, fusion and analytic that will allow an effective anomaly detection. Before going into details, we provide next a brief review of the state-of-the-art in industrial CPS and rare event detection.

Industrial CPS have been studied for many years, including already several deployed solutions [4], [5]. Most of the current research focuses on how to incorporate data flows so the industrial physical processes can run in a more efficient way, particularly focusing on multi-agent systems and the concept of digital twins. The most promising solutions would involve real-time monitoring and control [6], industrial edge computing [7] and software-defined wireless communications [8].

When dealing with CPS [9], three basic steps (in addition to transmission) are taken in relation to data: acquisition, fusion and analytics. In the data acquisition phase, sensors map physical processes into data, which can be sampled based on periodic measurements (e.g., sample every second), or event-driven ones (e.g., sample every threshold crossing), or a hybrid between both (e.g., [10]–[12]). In the fusion phase, acquired data shall be structured, disseminated and stored [13]. In this phase, heterogeneous data streams might be compressed/aggregated via ML algorithms. This phase includes possible issues related to communications and also communication network technologies including low-power networks, (beyond) 5G and IoT platforms [14], [15]. The analytics phase is also related to the ML algorithms that are now designed to detect or predict particular patterns or events [16], [17]; in particular the algorithms based on associative rules have been studied to identify anomalies and rare events with high performance [18], [19]. Data fusion and analytics are also related to the computing paradigm to be employed, particularly cloud or edge [7].

This paper focus on the combination of these three basic steps following a generalized framework that defines the boundary conditions that the proposed solution for anomaly detection shall be designed.

978-1-7281-6389-5/20/$31.00 ©2020 IEEE

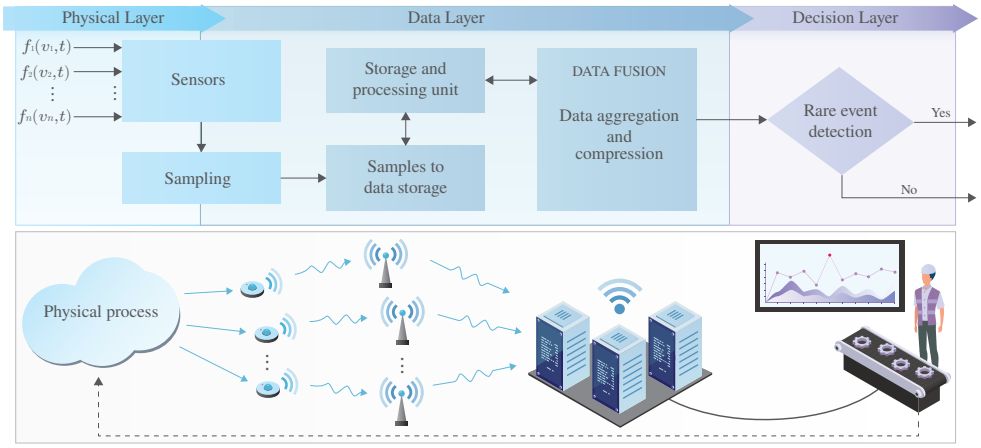

Fig. 1: Three layer framework for rare event detection.

Our specific contributions are:

- Propose a general framework based on the 3-layer model of CPS, as presented in Fig. 1, from where a set of general questions related to the data acquisition, fusion and analytic steps are defined (Sec.II).
- Employ the proposed framework in a well-known benchmark scenario from process engineering called Tennessee Eastman Process (TEP) [17], [20], [21] (Sec. III).
- Evaluate numerically the benefits of: event-driven data acquisition, mutual information data fusion and quantitative association rule data analytics (Sec. IV).
- Discuss different aspects about communication networks and computing paradigm usually considering perfect for this kind of studies (Sec. V).

II. Proposed framework

There are several methods for detecting anomalies and faults in industrial settings based on data. However, with the steep growth of information and communication technologies, more sensors with lower time granularity are becoming commonplace, generating the so-called big data. This, however, brings a generalized misunderstanding: “the bigger data, the better". In particular, in situations where the target is to reliably detect rare events in the dataset, the situation becomes more critical since the goal is to identify outliers with minimum chances of false alarm and misdetection.

Under this new condition, the usual fragmentation between data acquisition, fusion and analytic steps needs to be reviewed. For instance, the analytics algorithm requires structured good quality data (not necessarily “big data") to more reliably detect anomalies. The structured (time stamped) data, in their turn, is attained in the fusion step by disseminating, aggregating and/or eliminating data based on the needs of the rare-event detection algorithm. But, before data is fused, it needs to be acquired by sensors that map different (usually well-defined) physical processes; sensors may be located in different places (spatial domain) and sampled (temporal domain) in potentially different ways (e.g., periodically or not).

Our main motivation here is then to build a tailored integrated solution based on these three steps looking, for example, data compression/reduction can offer to the analytics algorithm better quality data to identify rare events. Notwithstanding, the solution to be designed for particular shall be derived from a general framework. In this case, the proposed framework consists of modeling CPS using three interrelated layers, namely physical, data, and decision. This approach was proposed in [22], [23] to assess the dynamics of physical systems that are regulated based on a decision-making processes that depend on data processing. The previous contributions were mainly focused on theoretical toy-models, though. Here, we will extend this approach to focus on realistic industrial settings. Fig. 1 depicts the proposed 3-layer model, together with the underlying communication network topology.

The proposed general framework is based on key questions that must be answered before the specific solution for detecting rare-events is designed. The questions are present in Table I. The idea is to define the viable designing options that we need to consider to have an effective solution for a particular industrial processes, as well as practical limitations imposed by industry itself (e.g., preference for private networks, or already deployed wired communication system).

The questions are structured in steps that follow the three-layer model. The first step is to identify the rare event(s) under consideration, also considering whether the problem is known beforehand. To have a quantitative evaluation of the related physical processes related to the event, sensors are needed

TABLE I: Related questions that can be answered by the proposed framework

Q#	**Topic**	**Related Question**
Q0	Anomaly	What is the problem? Is the Rare Event known or unknown?
Q1	Sensors	What kinds of sensors will be used? How many of each can be used and where they can be located?
Q2	Sampling	Which type of sampling will be used? Periodic, event driven or mixed (hybrid)?
Q3	Communication	Which type of communication system (access and network technologies) will be used?
Q4	Data storage	Where the data from sensors are stored and processed?
Q5	Data fusion	How the data should be clustered/aggregated/structured/suppressed?
Q6	Event detection	How to make the ultra-reliable rare event detection based on ML algorithms?

to map the physical to the data layer. Here the question is what kind of sensors can be used? How many should be used and where they should be located? After the locations are confirmed, the next phase is the sampling strategy from those sensors: it may be periodic, event-driven (non-periodic) or a mix between them. We then need to determine the time granularity and/or the event that trigger a sampling. The next phase is to define the communication system to be used. Particularly, the type of access technology (wireless or wired), the network (internet or private network) and storage (local database, cloud, private cloud). Once the data is stored, data should be aggregated, as other variables are stored with the same timestamp. Depending on the information of variables monitored, some of them could be suppressed. The question here is how data should be clustered/aggregated/structured/suppressed (fused)? The information gathered after the data fusion will be used to detect the event, when adding variables that monitor physical condition of the grid. Here the question arises is how to make the ultra-reliable rare event detection for our problem? In the following section, we will briefly present the Tennessee Eastman benchmark process and then apply the proposed approach on it.

III. Tennessee Eastman Process

The dataset material consists of several faulty cases of an industrial plant, as produced by the Tennessee Eastman problem [24]. The process has five major equipments, namely a condenser, a vapor-liquid separator, a reactor, a product stripper, and a recycle compressor (Fig. 2). Its objective is to obtain the products G and H from the reactants A, C, D and E. This is reached by a set of four chemical reactions, in which components B and F are, respectively, an inert and a byproduct. More details can be found in [25], [26]. This benchmark is suitable to evaluate process monitoring schemes and control strategies based on data driven analysis. Besides the normal operation, 21 abrupt or incipient faulty conditions caused by common disturbances in practice are simulated [20]. There are 52 monitoring variables or features, being 11 manipulated variables and 41 measured variables. Once a faulty condition occurs, all are generally affected with changes in their respective values.

The Tennessee dataset was generated in a process simulator that has been widely used by the process monitoring community[1]. It is composed by 22 subsets named *dXX_te.dat*, where $XX = 0, 1, 2, \cdots, 21$. The file *d00_te.dat* refers to the normal operating condition. Each of the other ones regards to

[1]https://github.com/camaramm/tennessee-eastman-profBraatz

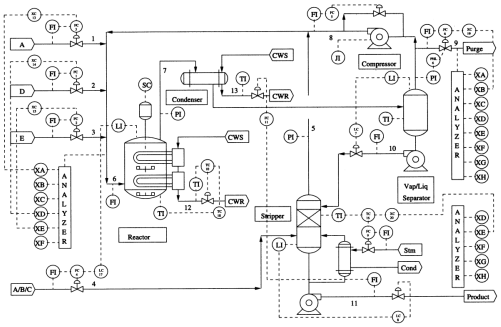

Fig. 2: Process flow diagram of the Tennessee Eastman problem [26].

TABLE II: Proposed framework applied in TEP

Q#	**Answer**
Q0	Lack of accuracy to detect anomalies (21) from measurements
Q1	Each of the 52 variables are sensors, no other can be added
Q2	Periodic sampling; all 52 variables are sync (3 min.)
Q3	It can be considered as in [27]
Q4	Not constrained; freedom to test as in [7]
Q5	Open question; focus of research in the field
Q6	Open question; focus of research in the field

a particular fault, that is, a different shift from this reference condition. The subsets consist of 960 observations of the 52 variables, which are sampled every 3min with a Gaussian noise. The faults are introduced after 8 simulation hours. Table II presents the proposed framework applied in TEP, which provides the boundary conditions of the anomaly detection design.

IV. Numerical results

A. Event-driven data acquisition

The main idea of an event-driven approach for this application is to perform data compression in order to transmit the meaning of information from the data acquisition point to the data fusion point. This approach can be described using the following steps: (1) input data from all 52 sensors (N); (2) variable average estimation and margin selection (90% of lowest/highest values) from normal operation; (3) at every time slot (k) for each variable, if the values are out of the margins the sample is transmitted, otherwise, if nothing is received at the data fusion point the variable will maintain the average value estimated from the previous step; (4) compression rate calculation for each variable. The limit values for margin selection for each variable were chosen arbitrarily. An example of this approach is seen in Fig. 3 where

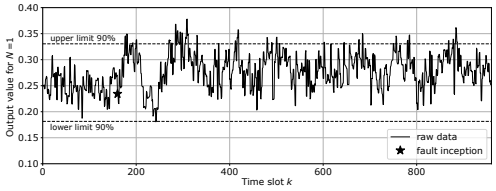

Fig. 3: Signal from variable 1 at data acquisition point (before transmission) for fault number 2 of Tennessee Eastman dataset.

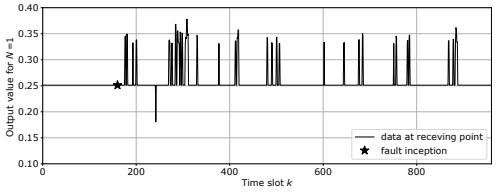

Fig. 4: Signal from variable 1 at data fusion point (after transmission) for fault number 2 of Tennessee Eastman dataset.

the signal obtained from the sensors is shown with its limits. The samples transmitted are only the ones that are out of the upper and lower limits as seen in Fig. 4.

This setup allows to transmit less data via any communications system. In the example mentioned above the compression rate is 92.60%, this means only about 7.4% of the samples are transmitted. The pre-processed time series based on the proposed event-driven method will serve as inputs to the data fusion and analytics, where anomalies should be detected, identified and diagnosed.

B. Data fusion based on Mutual Information

In order to further reduce the amount of processing required for fault detection, on top of the time-series compression as proposed by the event-driven approach, the proposed framework determines how the process variables are related to each other to discover and exploit their dependencies. The interdependencies between the process variables are determined automatically from the sampled measurements in the Tennessee datasets. Specifically, Mutual Information (MI) entropy reduction technique is used to infer how variables are correlated. The MI quantifies the amount of information that each variable contains about the other ones [28].

The tools used to determine correlations among the variables used in this work represents the distances between variables in terms of their statistical closeness, then it quantifies the correlation by providing links between the variables. Finally, it assigns directionality to the links [29]. Fig. 5 shows that aside form the auto-correlation, strong cross-correlation is present between a high number of variables; in fact, a high correlation above 80% is present in 23% of the variables (12 out of 52) while a modest correlation above 50% is present in 65% of the variables (34 out of 52).

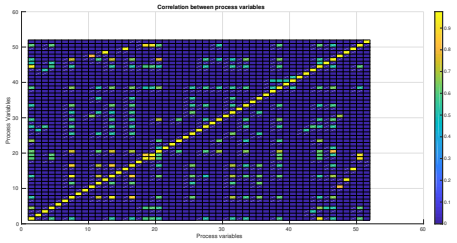

Fig. 5: Correlation between Process Variables

As an example of statistical closeness, Fig. 5 presents the correlation for the 52 process variables in the Tennessee datasets. This result showcases that not every single variable needs to be observed at every given moment but, depending on the fault under investigation, it is possible to observe variables carrying a high amount of MI with other variables involved in the process. This reduces both data and computational load considerably.

C. Quantitative association rule method for anomaly detection

Quantitative association rule mining is a natural extension of classical qualitative association rule mining where the difficult task is the extraction of frequent itemsets from a dataset containing transactions. The extracted rules are statistical rules of the form $Item_1 AND Item_2 ... AND Item_k \implies Item_n$, that hold with certain support and confidence values (or other metrics) that are above user-defined thresholds. Association rule mining is one of the most heavily researched areas in data mining to this date. In our context, items correspond to the features in our dataset, and transactions are in one-to-one correspondence with the rows of the dataset; the consequent item ($Item_n$) in particular is constrained to always be the target variable in our dataset. The problem then becomes one of quantifying each item in each (qualitative) rule extracted from the dataset by constraining its value to lie in a specified interval, so that the target variable assumes a particular value. This is achieved by a modified parallel Breadth-First Search (BFS) algorithm, called QARMA, which guarantees that all (and none other) non-dominated quantitative association rules that hold in the dataset will be found (see [30]).

In the case of the Tennessee dataset in particular, the dataset is fully dense in the sense that every row contains values for every dataset feature, which makes the application of the qualitative association rule mining part useless. Instead, we construct all itemsets of size less than 4, and quantify each one of them separately, and in parallel, making sure that all itemsets of size s are fully processed before starting to process itemsets of size $s+1$. To take into account the time-dependent nature of the data, whereby the values of any feature in the dataset are to some degree dependent on the values at the immediate previous times, we expanded the data to include for each feature, the difference between the feature's value and

the feature's value in the previous 2 time-steps, resulting in a dataset having 156 different fully dense features. The QARMA algorithm took several days to run on this expanded Tennessee dataset, producing a total of 63008 non-dominated rules, that could predict all different modes of operation except mode 0 (normal operation), and hard-to-detect faults 3, 9 and 15 (none of the 63008 rules imply faults 3, 9 or 15). The distribution of the rules among the faults is also highly skewed: faults 6 and 18 are implied by 23624 and 23884 rules respectively, whereas faults 5, 10 and 21 are implied by 9, 3, and 8 rules respectively. During testing, an instance for which more than 10 rules fire, is predicted to belong to the fault that is specified by the majority of rules firing on that instance. Using this majority vote rule ensemble, we obtained an overall rule-accuracy that exceeds 62% on the test set. This accuracy is significantly better than the one reported by decision trees (J48), or artificial neural networks (MultiLayerPerceptron) as implemented in the WEKA ML/DM software suite, all of which reported accuracy less than 50% on the test set.

We also implemented another modified BFS algorithm to search to find a minimum cardinality set of variables that contain all the variables necessary for an appropriate subset of the discovered rules to cover 85% of all instances that the entire set of rules cover; we say that "rule r covers instance i" if and only if in the instance i the values of the features that form the antecedents in rule r are within the intervals specified for them by the rule, and the instance indeed belongs to the operation mode (fault number) that is predicted by the rule. Interestingly, only 14 of the 156 variables are enough to "explain" 85% of the entire dataset covered by the rules found; this result implies that possibly a much smaller set of variables need be monitored in order to derive safe conclusions about the state of the process. The total rules found covered more than 70% of the training set.

We consider our first results as encouraging in that rules using only up to 2 features at a time are able to form an ensemble of rules that outperformed other well-known ML algorithms in test-set performance. We expect that dimensionality reduction will allow larger number of antecedent features to be examined and eventually provide much higher accuracies measured by detection rates/false alarm rates per class.

V. Discussions

A. Industrial communication networks in the TEP benchmark

Liu et al. proposed in [31] a description of how a communication network could be applied in TEP. They also proposed a more complete analysis of Industrial IoT settings, exemplified by TEP, in [27]. Other recent work focusing on how 5G could be employed in TEP for fault detection and diagnosis [32]. We expect to extend those works based on the proposed 3-layer model, where we can focus on the following aspects.

Physical layer: It presents mostly the communication between sensors and aggregators. In order to reach a possible massive number of sensors, wireless technologies seem to be an obvious choice, in special machine-type communications (MTC) [33]. Besides cellular massive MTC solutions [34], Long Range Low Power Networks (LPWAN) (e.g. LoRa, Sigfox, NB-IoT) recently gained attention for industrial indoor applications [27]. See that its high link budget is suitable for the coverage of industrial environments, where we find many floors, walls, and machinery that mitigates the signal propagation [35]. From this category, we see LoRa and LoRaWAN with great potential for industrial scenarios. Since LoRaWAN presents an open MAC protocol, it is easier to deploy aggregators (gateways) inside factories and thus have control over the whole network. Moreover, it enabled several works that evaluated LoRa's performance [36]–[38]. Even though we plan on a massive communication approach for mostly of sensors, there might be cases where they do not attend the reliability or latency requirements. Then, cellular ultra-reliable low-latency communications (URLLC) might come as a solution.

Data layer: The communication is based on the aggregators storing their data into a centralized unit, preceding the data fusion process. Since aggregators serve a massive number of sensors, there is a huge amount of traffic within this layer [34]. Thus, we plan most traffic to be enhanced Mobile BroadBand (eMBB). Similar to layer 1, we can rely on URLLC when there is reliability and latency constraints. Note that the packet size for URLLC is very limited, thus producing a small impact on the total aggregated traffic. Coexistence of MTC traffic can be mitigated by non-orthogonal solutions as in [39], or through network slicing [40] where orthogonal resources are dedicated to meet each service requirement (e.g., eMBB, URLLC and mMTC). Considering that communication in TEP is mostly done in uplink, the customization of grant-free access based on diversity scheduling of URLLC resources as proposed in [41], [42] could be optimized in terms of reliability and users density. Finally, we could alternatively employ wired/optical connection where aggregators are local to the storage unit.

Decision layer: It is highly dependent on the system topology. After the data fusion stage, the aggregator must send all compressed data to a decision controller. This is a sensitive stage, where losing one packet means giving up many compressed others. Moreover, it can lead to an inaccurate detection decision. Finally, the decision results can give automatic feedback to the machinery; thus, URLLC should be predominant.

B. Imperfect wireless medium

In industrial CPS empowered by wireless connectivity, the unreliable nature of the wireless medium introduces uncertainties in the achieved TEP fault detection performance and efficiency [43]. The complex fading conditions in indoor factory plants – usually rich in metallic surfaces and physical obstructions which result in high network dynamics and a harsh radio propagation environment – involving numerous IIoT components may significantly affect the accuracy of the transmitted sensor observations to the fusion center and result in transmission failures due to the high distortion levels. Although the millimeter-wave (mmWave) technology is continuously gaining momentum in industrial indoor environments for

providing high data rate, low-latency and high-reliability [44], mmWave frequencies (up to 100 GHz) are highly susceptible to blockage, diffraction, and scattering effects. In practical industrial deployments where no line-of-sight connectivity is possible, the installation of reconfigurable intelligent surfaces, capable of adaptively shaping the impinging radio waves based on the actual channel conditions, appears as a promising solution to circumvent the unreliability of high-frequency channels.

C. Communication-Computation Trade-off

The reliability and latency concerns related to Industrial IoT in addition to the increasing density deployment precipitate the need for new communication and computation paradigms in such environments. The increasing number of sensors and the heterogeneity of the datasets being collected pose new challenges during the data fusion and analysis. For example, the large number of sensors collecting information about the industrial processes have to transmit the collected datasets to the data fusion point, which results in high communication cost and affects the energy efficiency and computational delay. There are multiple ways to approach this problem. One approach is to move the data fusion points closer to the sensors that are acquiring the measurements and to perform the analysis in the cloud.

This approach results in lower communication overhead, and reduce the amount of raw measurements being sent throughout the network, which results in higher energy efficiency. However, there are problems associated with this solution. For example, the sensors performing the data fusion are potential single points-of-failure. These fusion points also use more energy due to the computation and communication with a large number of nodes. Therefore, depending on the energy source being used for these nodes (e.g., battery), they could potentially lead to parts of the network being disconnected from the rest of the deployment. Another possible problem with this solution is related to latency concerns. Since the data analysis is happening in the cloud, the combined delay associated with the communication and computation can not be neglected. For this reasons, authors have been proposing the idea of moving the processing from the cloud to the edge of the network [45]. This approach relies on both, fusion and analysis happening on the nodes that are very close to the acquisition sensors. However, while reducing the latency effect, this approach does not address the energy hole effect (i.e., nodes closer to the centralized fusion point drain their battery faster) [46].

The next logical step is to rely on in-network computing, in which data processing is distributed among the nodes of the network. An example is shown in [47], in which the authors place the computational nodes of a neural network on the physical sensor nodes. The placement relies on an optimized mapping procedure that minimizes either the total transmit power or the overall transmit time. Due to its flexibility, this approach allows us to eliminate the single point-of-failure problem, helps us to reduce the communication/computation latency and enables us to distribute the energy consumption across the IoT network. By taking advantage of the in-network computing paradigms we can tweak the trade-off between communication and computation.

D. Network Slices and Business Model

Nowadays, many wireless technologies are capable to replace wired communication in industrial applications. However, using these new technologies in real scenarios mean an increase cost in terms of CapEx and OpEx. So, an appropriate model that fairly distributes costs over multiple virtual operators, and also optimizes physical resource planning is introduced in [48]. Here, a new model of 5G isolated network slices of multitenant Mobile Backhaul (MBH) is proposed, based on a novel pay-as-you-grow model that considers the Total-Cost-of-Ownership (TCO) and the yearly generated Return-on-Investment (ROI). So, new business models that are coming with the wave of 5G and beyond have a big potential to boost the application of novel wireless communication technologies beyond the technical benefits.

VI. Conclusions

This paper shows the potential of the 3-layer approach to design anomaly detection, where data acquisition, fusion and analytics, together with the enabling communication network and computation paradigm, are jointly studied as subsequent steps. We presented initial results based on the TEP benchmark and we plan to extend this study to other scenarios, including a micro-grid and a car factory. All in all, we expect to demonstrate that the proposed framework is general so that it can be applied to provide ultra-reliable rare event detection in a wide range of industrial applications.

Acknowledgments

This work is supported by CHIST-ERA (call 2017) via FIREMAN consortium, which is funded by the following national foundations: Academy of Finland (n. 326270, n. 326301), Irish Research Council, and the Spanish Government under grant PCI2019-103780. This work is partially funded by Academy of Finland 6Genesis Flagship (n. 318927), ee-IoT (n.319009) and EnergyNet Research Fellowship (n.321265/n.328869). and was supported in part by the Research Grant from Science Foundation Ireland and the European Regional Development Fund under Grant 13/RC/2077 and the Catalan Government under grant 2017-SGR-891.

References

[1] H. He and E. A. Garcia, "Learning from imbalanced data," *IEEE Transactions on knowledge and data engineering*, vol. 21, no. 9, pp. 1263–1284, 2009.

[2] B. Krawczyk, "Learning from imbalanced data: open challenges and future directions," *Progress in Artificial Intelligence*, vol. 5, no. 4, pp. 221–232, 2016.

[3] P. Nardelli *et al.*, "Framework for the identification of rare events via machine learning and iot networks," in *2019 16th International Symposium on Wireless Communication Systems (ISWCS)*. IEEE, 2019, pp. 656–660.

[4] P. Leitao *et al.*, "Smart agents in industrial cyber–physical systems," *Proceedings of the IEEE*, vol. 104, no. 5, pp. 1086–1101, 2016.

[5] S. J. Oks, A. Fritzsche, and K. M. Möslein, "An application map for industrial cyber-physical systems," in *Industrial Internet of Things*. Springer, 2017, pp. 21–46.

[6] S. Yin, J. J. Rodriguez-Andina, and Y. Jiang, "Real-time monitoring and control of industrial cyberphysical systems: With integrated plant-wide monitoring and control framework," *IEEE Industrial Electronics Magazine*, vol. 13, no. 4, pp. 38–47, 2019.

[7] W. Dai, H. Nishi, V. Vyatkin, V. Huang, Y. Shi, and X. Guan, "Industrial edge computing: Enabling embedded intelligence," *IEEE Industrial Electronics Magazine*, vol. 13, no. 4, pp. 48–56, 2019.

[8] H. Hellstrom, M. Luvisotto, R. Jansson, and Z. Pang, "Software-defined wireless communication for industrial control: A realistic approach," *IEEE Industrial Electronics Magazine*, vol. 13, no. 4, pp. 31–37, 2019.

[9] C. Greer *et al.*, "Cyber-physical systems and internet of things," *NIST Special Publication*, vol. 1900-202, p. 61, 2019. [Online]. Available: https://doi.org/10.6028/NIST.SP.1900-202

[10] M. Mazo and P. Tabuada, "Decentralized event-triggered control over wireless sensor/actuator networks," *IEEE Transactions on Automatic Control*, vol. 56, no. 10, pp. 2456–2461, 2011.

[11] M. Miskowicz, *Event-based control and signal processing*. CRC press, 2015.

[12] X. Ge *et al.*, "Distributed event-triggered estimation over sensor networks: A survey," *IEEE Transactions on Cybernetics*, 2019.

[13] D. L. Hall and J. Llinas, "An introduction to multisensor data fusion," *Proceedings of the IEEE*, vol. 85, no. 1, pp. 6–23, 1997.

[14] F. Alam *et al.*, "Data fusion and iot for smart ubiquitous environments: a survey," *IEEE Access*, vol. 5, pp. 9533–9554, 2017.

[15] J. Cheng *et al.*, "Industrial iot in 5g environment towards smart manufacturing," *Journal of Industrial Information Integration*, vol. 10, pp. 10–19, 2018.

[16] J. Lee, B. Kang, and S.-H. Kang, "Integrating independent component analysis and local outlier factor for plant-wide process monitoring," *Journal of Process Control*, vol. 21, no. 7, pp. 1011–1021, 2011.

[17] S. Yin, S. X. Ding, A. Haghani, H. Hao, and P. Zhang, "A comparison study of basic data-driven fault diagnosis and process monitoring methods on the benchmark tennessee eastman process," *Journal of process control*, vol. 22, no. 9, pp. 1567–1581, 2012.

[18] J.-M. Adamo, *Data mining for association rules and sequential patterns: sequential and parallel algorithms*. Springer Science & Business Media, 2012.

[19] I. T. Christou, "Avoiding the hay for the needle in the stack: Online rule pruning in rare events detection," in *2019 16th International Symposium on Wireless Communication Systems (ISWCS)*. IEEE, 2019, pp. 661–665.

[20] E. L. Russell, L. H. Chiang, and R. D. Braatz, "Fault detection in industrial processes using canonical variate analysis and dynamic principal component analysis," *Chemometrics and intelligent laboratory systems*, vol. 51, no. 1, pp. 81–93, 2000.

[21] C. Zhang, K. Peng, and J. Dong, "An incipient fault detection and self-learning identification method based on robust svdd and rbm-pnn," *Journal of Process Control*, vol. 85, pp. 173–183, 2020.

[22] F. Kühnlenz and P. H. Nardelli, "Dynamics of complex systems built as coupled physical, communication and decision layers," *PloS one*, vol. 11, no. 1, p. e0145135, 2016.

[23] P. H. Nardelli and F. Kuhnlenz, "Why smart appliances may result in a stupid grid: Examining the layers of the sociotechnical systems," *IEEE Systems, Man, and Cybernetics Magazine*, vol. 4, no. 4, pp. 21–27, 2018.

[24] J. J. Downs and E. F. Vogel, "A plan-wide industrial process control problem," *Computers and Chemical Engineering*, vol. 17, no. 3, pp. 245–255, 1993.

[25] S. Yin, S. X. Ding, A. Haghani, H. Hao, and P. Zhang, "A comparison study of basic data-driven fault diagnosis and process monitoring methods on the benchmark tennessee eastman process," *Journal of Process Control*, vol. 22, no. 9, pp. 1567 – 1581, 2012. [Online]. Available: http://www.sciencedirect.com/science/article/pii/S0959152412001503

[26] L. H. Chiang, E. L. Russell, and R. D. Braatz, *Fault detection and diagnosis in industrial systems*. Springer, 2001.

[27] Y. Liu, M. Kashef, K. B. Lee, L. Benmohamed, and R. Candell, "Wireless network design for emerging iiot applications: Reference framework and use cases," *Proceedings of the IEEE*, vol. 107, no. 6, pp. 1166–1192, June 2019.

[28] A. Chiumento, B. Reynders, Y. Murillo, and S. Pollin, "Building a connected ble mesh: A network inference study," in *2018 IEEE Wireless Communications and Networking Conference Workshops (WCNCW)*, April 2018, pp. 296–301.

[29] A. F. Villaverde, J. Ross, F. Morán, and J. R. Banga, "Mider: Network inference with mutual information distance and entropy reduction," *PLOS ONE*, vol. 9, no. 5, pp. 1–15, 05 2014. [Online]. Available: https://doi.org/10.1371/journal.pone.0096732

[30] I. T. Christou, E. Amolochitis, and Z.-H. Tan, "A parallel/distributed algorithmic framework for mining all quantitative association rules," 2018.

[31] Y. Liu, R. Candell, K. Lee, and N. Moayeri, "A simulation framework for industrial wireless networks and process control systems," in *2016 IEEE World Conference on Factory Communication Systems (WFCS)*. IEEE, 2016, pp. 1–11.

[32] P. Hu and J. Zhang, "5g enabled fault detection and diagnostics: How do we achieve efficiency?" *IEEE Internet of Things Journal*, 2020.

[33] N. H. Mahmood, H. Alves, O. L. A. López, M. Shehab, D. P. M. Osorio, and M. Latva-aho, "Six Key Enablers for Machine Type Communication in 6G," pp. 1–14, 2019. [Online]. Available: http://arxiv.org/abs/1903.05406

[34] O. López, H. Alves, P. Nardelli, and M. Latva-aho, "Aggreg. and resource scheduling in mach.-type commun. netw.: A stochastic geometry approach," *IEEE Trans. Wireless Commun.*, vol. 17, no. 7, Jul 2018.

[35] P. Sommer, Y. Maret, and D. Dzung, "Low-power wide-area networks for industrial sensing applications," in *2018 IEEE International Conference on Industrial Internet (ICII)*, Oct 2018, pp. 23–32.

[36] A. Hoeller, R. D. Souza, H. Alves, O. L. Alcaraz López, S. Montejo-Sánchez, and M. E. Pellenz, "Optimum lorawan configuration under wi-sun interference," *IEEE Access*, vol. 7, pp. 170 936–170 948, 2019.

[37] J. S. Sant'Ana, A. S. Hoeller, R. D. Souza, S. Montejo-Sanchez, H. Alves, and M. Noronha, "Hybrid coded replication in LoRa networks," *IEEE Transactions on Industrial Informatics*, pp. 1–1, 2020.

[38] M. Rizzi, P. Ferrari, A. Flammini, E. Sisinni, and M. Gidlund, "Using LoRa for industrial wireless networks," in *2017 IEEE 13th International Workshop on Factory Communication Systems (WFCS)*, May 2017, pp. 1–4.

[39] P. Popovski, K. F. Trillingsgaard, O. Simeone, and G. Durisi, "5g wireless network slicing for embb, urllc, and mmtc: A communication-theoretic view," *IEEE Access*, vol. 6, pp. 55 765–55 779, 2018.

[40] S. E. Elayoubi, S. B. Jemaa, Z. Altman, and A. Galindo-Serrano, "5g ran slicing for verticals: Enablers and challenges," *IEEE Communications Magazine*, vol. 57, no. 1, pp. 28–34, January 2019.

[41] R. Kotaba, C. Navarro Manchón, T. Balercia, and P. Popovski, "Uplink transmissions in urllc systems with shared diversity resources," *IEEE Wireless Communications Letters*, vol. 7, no. 4, pp. 590–593, Aug 2018.

[42] G. Berardinelli, N. Huda Mahmood, R. Abreu, T. Jacobsen, K. Pedersen, I. Z. Kovács, and P. Mogensen, "Reliability analysis of uplink grant-free transmission over shared resources," *IEEE Access*, vol. 6, pp. 23 602–23 611, 2018.

[43] B. Martinez, C. Cano, and X. Vilajosana, "A square peg in a round hole: The complex path for wireless in the manufacturing industry," *IEEE Communications Magazine*, vol. 57, no. 4, pp. 109–115, April 2019.

[44] D. Solomitckii, A. Orsino, S. Andreev, Y. Koucheryavy, and M. Valkama, "Characterization of mmwave channel properties at 28 and 60 ghz in factory automation deployments," in *2018 IEEE Wireless Communications and Networking Conference (WCNC)*, April 2018, pp. 1–6.

[45] F. Bonomi, R. Milito, J. Zhu, and S. Addepalli, "Fog computing and its role in the internet of things," in *Proceedings of the first edition of the MCC workshop on Mobile cloud computing*, 2012, pp. 13–16.

[46] A.-F. Liu, M. Ma, Z.-G. Chen, and W.-h. Gui, "Energy-hole avoidance routing algorithm for wsn," in *2008 Fourth International Conference on Natural Computation*, vol. 1. IEEE, 2008, pp. 76–80.

[47] E. Di Pascale, I. Macaluso, A. Nag, M. Kelly, and L. Doyle, "The network as a computer: A framework for distributed computing over iot mesh networks," *IEEE Internet of Things Journal*, vol. 5, no. 3, pp. 2107–2119, 2018.

[48] N. Haddaji, K. Nguyen, and M. Cheriet, "Tco planning game for 5g multitenant virtualized mobile backhaul (v-mbh) network," *Journal of Lightwave Technology*, vol. 37, no. 24, pp. 6193–6206, Dec 2019.

Publication II

Gutierrez-Rojas, D., Mashlakov, A., Brester, C.,Niska, H., Kolehmainen, M.,
Narayanan, A., Honkapuro, S. and Nardelli, P. H. J.
Weather-Driven Predictive Control of a Battery Storage for Improved Microgrid Resilience

Reprinted with permission from
IEEE Access
Vol. 9, pp. 163108–163121, Dec. 2021

IEEE Access
Multidisciplinary ⋮ Rapid Review ⋮ Open Access Journal

Received November 17, 2021, accepted December 2, 2021, date of publication December 6, 2021,
date of current version December 17, 2021.

Digital Object Identifier 10.1109/ACCESS.2021.3133490

Weather-Driven Predictive Control of a Battery Storage for Improved Microgrid Resilience

DANIEL GUTIERREZ-ROJAS[1], (Student Member, IEEE), ALEKSEI MASHLAKOV[1], CHRISTINA BRESTER[2], HARRI NISKA[2], MIKKO KOLEHMAINEN[2], ARUN NARAYANAN[1], (Member, IEEE), SAMULI HONKAPURO[1], AND PEDRO H. J. NARDELLI[1], (Senior Member, IEEE)

[1]Department of Electrical Engineering, School of Energy Systems, LUT University, 53850 Lappeenranta, Finland
[2]Department of Environmental and Biological Sciences, University of Eastern Finland, 70210 Kuopio, Finland

Corresponding author: Daniel Gutierrez-Rojas (daniel.gutierrez.rojas@lut.fi)

This work was supported by the Academy of Finland through the EnergyNet Research Fellowship under Grant 321265 and Grant 328869, through the Analytics Project under Grant 324677, and through the FIREMAN Consortium (326270) and CHIST-ERA Grant CHIST-ERA-17-BDSI-003.

ABSTRACT This paper aims to introduce a predictive weather-based control policy for the microgrid energy management to improve the resilience of the microgrid. This policy relies on the application of machine learning models for the prediction of microgrid load demand and solar production and supply interruption in the upstream distribution network. The predictions serve as an input to multiobjective chance constraint optimization that balances the microgrid resilience and economic objectives based on the probability of a supply interruption. The interruption predictions are made with a decision-tree-based model that can predict an upcoming interruption in the distribution network with 78% of the maximum accuracy. The case study microgrid consisting of several customers, solar photovoltaic generation, and battery storage is applied to cluster areas located in Finland. Overall, the developed control policy shows an improvement in the daily resilience of the microgrid in regard to an interruption in the main grid when compared with economic dispatch only.

INDEX TERMS Microgrid resilience, weather prediction, machine learning, battery storage, chance constraint optimization.

I. INTRODUCTION

The use of distributed energy resources (DERs) has recently been increasing especially in microgrids (MGs) as they are known to improve the reliability of electricity supply in sparsely populated areas and contribute to the reduction of greenhouse gas emissions [1]. As the integration of DER and household loads increases, maintaining the power system stability and voltage profile as well as management of energy resources in a cost-effective way become more challenging [2]. Microgrids are capable of operating in two different modes: either grid connected or island. While operating in the grid-connected mode, the power is exchanged with the main grid from the distribution feeder, which ensures the power dispatch and contributes to the system stability. In case of power faults, natural disasters, or not meeting power quality requirements, the MG will operate in the island mode. In this mode, battery energy storage systems (BESSs) are used to cover load energy consumption [3]. The BESSs depend on installed load power and have several limitations, such as power rating, Boolean charging/discharging scenarios, and time-dependent energy content dynamics.

During MG operation, a BESS improves resilience during operation in the island mode. Resilience is a relatively new concept in power systems, and in recent years, it has had a significant impact on the definition of the reliability of electricity distribution networks [4]. The definition proposed by [5] involves energy systems being able to recover fast from events caused by external factors. Moreover, the definition provided by [6] for resilience relies on four aspects: foresee/avoid, absorb/withstand, respond/restore, and adapt/upgrade. These elements play a key role in the function of MGs for the modernization and decentralization of electricity grids.

The associate editor coordinating the review of this manuscript and approving it for publication was Shagufta Henna.

Many strategies to manage the power and improve the resilience of MGs have been proposed in the literature [1], [7], [8]. These strategies combine predictive models for optimal dimensioning of the BESS based on the DER power infeed forecast of photovoltaics (PVs) and wind turbines and control methods to maximize resilience when operating in the island mode and to maximize energy profits from energy dispatch [9]–[11].

Renewable energy in MGs brings new challenges in terms of how to deal with uncertainty in power generation. In [12], uncertainty quantification is used to facilitate integration of an energy storage and thereby mitigate the impacts of uncertain PV and wind generation. The array of prediction techniques is also growing as artificial intelligence algorithms and optimization methods are being developed. One of such techniques is reported in [13], where forecasting of solar radiance, temperature, and load is carried out in addition to particle swarm optimization to optimally control and manage power in an MG.

Although resilience in microgrids has been a topic of growing interest in the past few years with an exponential increase in publications, to the authors' knowledge, the application of predictive methods has been limited. An approach that uses outage decision-making for power management in smart homes is reported in [14]. Outage management can benefit MGs, which are very prone to interruptions, as well as remote areas of difficult access. In [15], a multilevel MG method is proposed that incorporates a stochastic islanding event into the operational optimization, thereby allowing to foresee the occurrence of interruptions. The model can be adopted for optimal scheduling by applying the uncertainty of loads, DER, demand-side management, and frequency control.

The traditional concept of reliability has also been shifting toward resilience to take into account more characteristics of power grids; still, as discussed in [16], [17], reliability plays an important role in grid management and brings certain benefits to the grid. In [18], these benefits include minimization of load curtailment, flexibility, and improvement in the reliability index. In their paper, the authors propose a general framework for the assessment of the reliability of distribution systems with multiple microgrids to quantify the impact of different operating schemes by using a model predictive control for power management. In [19], the authors develop a resilience-oriented stochastic scheduling method for microgrids considering economic metrics; the resilience index is improved by 16.5% by integrating resilience metrics, stochastic planning, and resilient operation of DER into the method. Further, in [20], a microgrid scheduling strategy is developed considering resilience requirements: operating costs, energy purchasing costs, and degradation cost of the BESS. The solution uses an optimization model ensuring resilience by facilitating possible MG interruptions by securing load supply and robustness in DER.

BESSs have shown efficacy to increase resilience in MGs, and to this end, correct sizing to meet the economic requirements is an important task. In [21], the authors use a linear optimization approach to determine the most cost-effective BESS sizing for different types of load and DER generation. In the optimization, it is necessary to use historical data and accurate forecast resources for DER. Insights into the obtained power-to-energy ratio can also enhance the design of new commercial BESSs, which could possibly benefit and standardize other MG systems.

A similar approach as presented in this paper can be found in [22], where the authors use a home energy storage management system for decision-making. This system enhances home resilience in the face of extreme events. The model decides in advance when to charge the BESS based on the condition of the network and the probability of an outage. The interruption model takes into account the wind speed to provide the probability of an interruption for the location; however, in the case of extreme events there might be also other variables involved. Our approach considers a set of different variables, and by using machine learning techniques, we are able to reliably predict an interruption for the next day, thereby improving the battery state-of-charge (SOC). Furthermore, the model is scalable to the size of the MG or the area of interest, being thus not limited to a single MG but being applicable also to multiple microgrids and large areas. This can greatly improve the resilience in the system to be able to withstand upcoming severe weather interruptions.

In this paper, a weather-based predictive control policy is used to improve the resilience of an MG when operating in the island mode. This method can predict the energy requirements for the BESS and schedule day-ahead optimal operation of the BESS based on predictions of machine learning models for load demand and solar PV power production. The proposed methodology takes into account the probability of an interruption for the prediction horizon based on weather conditions so that any decision taken beforehand to charge/discharge the MG battery will have a profound impact on the MG resilience when operating in the island mode. This will contribute to the MG decentralization paradigm, because the total output power supply from the main grid and the power from the DERs connected to the affected MG will be maximized. The contributions of this paper are:

- formulation of multiobjective optimization problem under uncertainty for an MG BESS that takes into consideration the interruption probability and economical charging and thus foresees upcoming island operating modes;
- methodology for machine learning predictions of the probability of a daily supply interruption in the upstream distribution network, microgrid load demand, and solar PV production that are integrated into the optimization problem;
- introduction of a daily dependency (resilience metric) for the MG that continuously estimates the withstanding capability of the MG in the face of extreme weather events;
- quantitative comparison of how different battery sizes can affect the degree of daily dependency in the MG.

The rest of the paper is organized as follows. In section II-A, we analyze previous approaches to resilience and optimization in microgrids. The methodology of the proposed approach is presented in Section II. The predictive interruption model and the machine learning model are described in Section III. Section IV addresses the techno-economic dispatch optimization problem for microgrid energy management. A case study MG placed in the clusters of the interruption model, results, and discussion are summarized in Section V. Finally, conclusions of the paper are presented in Section VI.

II. METHODOLOGY

A. BACKGROUND OF RESILIENCE

The resilience framework introduced in this paper is based on a model proposed by [23]. In this context, to improve the resilience of an MG, we use the blocks shown in Fig. 1. The four pillars of MG resilience are: methods, attributes, interruptions, and metrics. The first block, methods, refers to a variety of methods or techniques that contribute to the improvement of resilience, the ones used in this work including resource allocation, battery scheduling, energy optimization, fault prediction, and load and production predictions. In the second block we find attributes, which are the properties or characteristics of an MG. Understanding of the system attributes of any MG, such as islanding capacity, is important as these attributes play a significant role in the decision-making concerning microgrid components. These decisions, in turn, have a direct or indirect impact on the system recovery. In the third block there are interruptions. Here, external events are assumed to be weather dependent and influenced by the grid topology next to the MG connection. Finally, for the assessment of the MG we use one common metric in resilience: dependency [24]. It is an index that means ''a linkage or connection between two infrastructures, through which the state of one infrastructure influences or is correlated to the state of the other.'' This is a key attribute when using a battery storage, and in this work, it is adopted in order to quantitatively characterize dependency in each of the MG load by measuring the need for energy storage to achieve the resilience objective. First, we introduce an analogous availability measurement [24], which measures individual resilience of a load as

$$R_I = \frac{T_U}{T} = \frac{T_U}{(T_U + T_D)}, \tag{1}$$

where T_U is the time up (microgrid is connected to the main grid) and T_D is the time down (microgrid disconnected from the main grid). T_U is directly related to the withstanding capability, whereas T_D is the service recovery speed, which is influenced by cyber-physical processes and human-driven activities (e.g., maintenance, repair, availability of human resources). Then, analogous to Eq. (1), the degree of dependency of a load, and for the context of the MG, that of the entire MG load, R_L, is given by:

$$R_L = 1 - (1 - R_I)e^{-uT_S}, \tag{2}$$

where T_S is the energy capacity stored in the MG BESS, measured by autonomy when entering the island mode, and u is the equivalent rate of the power grid, inverse to T_D. The interdependency of battery and resilience is seen in Eq. (2). It shows that the BESS makes the MG more resilient to disruptions.

B. MICROGRID MANAGEMENT ROUTINE

The Methods block in Fig. 1 contains the elements of load prediction, interruption prediction, DER generation prediction, and BESS management. According to the control policy depicted in Fig. 2, the algorithm starts at day 1 at an interval of a day (from start to end) to analyze the resilience, and an scheduling based on the weather forecast models is made for the next 24 h. Based on the weather conditions, a coefficient for the probability of an interruption is calculated from the forecast model for the probability of interruption. To prepare for an eventual island mode, the MG and the BESS have to be scheduled based on the future output of the DER and load power estimation; the models described in Sections III-A and IV-A provide details of both steps. Once the day is over, the daily dependency is calculated as presented in Section II-A. This process can be continuously checked and updated on a daily basis. Fig. 3 shows the impact of a varying BESS SOC (or analogous T_S) on whole-year runs (n_S); the figure illustrates MG management without considering any prior cost-effective or precautionary charging of the BESS, which is seen as sudden fluctuations from day to day. The values are within a range that depends on the resilience index calculation period (a day) and T_S.

The dependency index metric is usually calculated based on historical data, and thereby, average T_U. When this metric is calculated on a daily basis, it will show a significant difference when compared with a method that does not take the interruption model into consideration because of variability in the charging of the BESS.

III. PREDICTIVE MODELS

A. RISK ANALYSIS OF THE PROBABILITY OF AN ELECTRICITY SUPPLY INTERRUPTION

The data provided by the Finnish DSO Elenia were used to predict the daily fault occurrence in the distribution networks of the following regions: Kanta-Häme and Päijät-Häme, Pirkanmaa, Central Finland, and Ostrobothnia. First, we defined clusters comprised of Elenia's substations so that the maximum distance between substations in a cluster was not larger than 50 km. Agglomerative hierarchical clustering, specifically complete-linkage clustering implemented in the scikit-learn library [25], ended up with 31 substation clusters, to which the MGs are connected in our study. Fig. 4 presents the clusters obtained and their centroids in the ETRS-TM35FIN coordinates. Additionally, the figure shows the weather stations closest to Elenia's network. The original data contained 36874 unique faults that occurred in the whole network of Elenia between January 2011 and

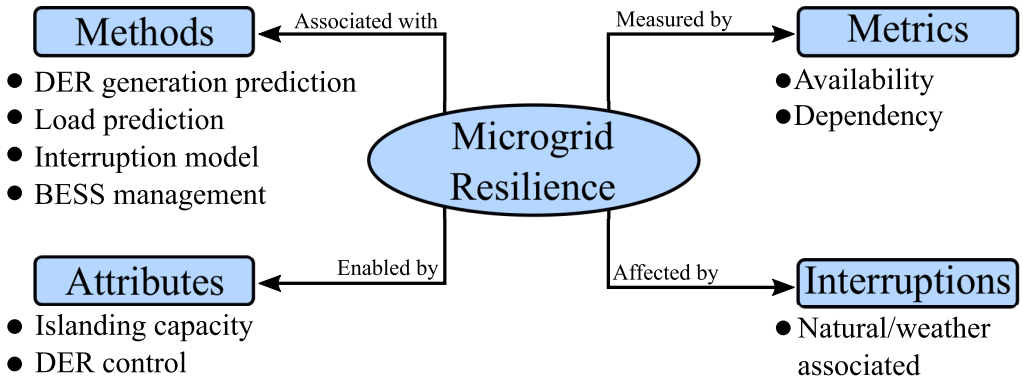

FIGURE 1. Framework of improving the resilience of a microgrid (adapted from [23] and revised).

December 2013. Faults associated with substations were summed up for the corresponding clusters with a daily time resolution. An additional categorical variable indicating the absence or presence of faults per day was introduced for each cluster. These binary variables worked as outcomes in the cluster fault prediction. Next, we created a set of predictors that included weather observations and time variables (see Table 1). The coordinates of the weather stations presented in Fig. 4 were used to collect historical weather observations from [26]. We transformed the coordinates into the *WGS84* system and retrieved the data applying the package *wwo − hist* [27], [28]. For each cluster, the weather observations were gathered and averaged over the weather stations closest to Elenia's substations. The set of input variables included 14 predictors similar to the previous study [29].

Predictive models were built separately for each cluster. The data collected in 2013 were reserved to test the models, whereas fault records from 2011 and 2012 were included in the training. As a learning algorithm, we chose Random Forest because of its useful properties: the ensemble-based nature aims to reach robustness and control overfitting [25], [30]. To reduce the model variance, we trained 250 trees in each ensemble. The maximum tree depth was tuned for each cluster: when varying the tree depth from 3 to 9, we selected one model trained on the data from 2011 that showed the highest accuracy on the validation data from 2012, and then switched around the training and validation years to select one more model. The outcomes of these two models on the test data were averaged to obtain the final estimate of the fault probability. Besides, to avoid tuning a cut-off for each cluster where the balance between days with and without faults differs, we oversampled the underrepresented class in the training years 2011–2012. As a result, 0.5 cut-off was applied within all clusters when estimating the model accuracy.

According to the previous study [29], the weather observations relevant to predicting faults are contained in a few recent measurements. Therefore, we tested one-, two-, and three-day historical weather as the model inputs and found that when predicting faults for the moment *t*, the weather observations from the moment *t* and *t-1* led to the highest maximum accuracy across clusters, i.e., 78%, and the highest number of clusters with the accuracy exceeding 70%, i.e., ten clusters. In the real use case scenario, historical weather observations should be substituted with the weather forecast. The resulting accuracy of the test data is presented in Fig. 4.

B. MACHINE LEARNING MODEL FOR LOAD AND SOLAR PV PREDICTION

The time series predictions of the load and solar PV production of the microgrid are required for the operation management of the microgrid BESS. Here, point forecasts (i.e., conditional mean of the predictive distribution) are produced for the next day with a 24 h ahead horizon and implemented with a Light Gradient Boosting Machine (LightGBM) regression [31] from the corresponding library [32]. The LightGBM model is a scalable and efficient gradient boosting framework that uses a decision-tree-based learning algorithm. In fact, the high accuracy of the LightGBM model was recently demonstrated in the M5 Accuracy competition [33]. The main difference of the model compared with the similar algorithms is the usage of a leafwise tree growth algorithm instead of the depthwise tree growth. This approach facilitates model convergence because of the faster finding of the best split points in each tree node but comes with higher chances for overfitting, i.e., poor generalization for unseen testing data. For instance, the unconstrained maximum depth and number of leaves can improve the training accuracy but also contribute to overfitting. Therefore, hyperparameter tuning is important to achieve a good model generalization with the LightGBM model. In this study, we apply a tree-structured Parzen estimator from the *hyperopt* library [34] to search for the hyperparameters affecting the model accuracy and overfitting. In particular, for the LightGBM model we tune

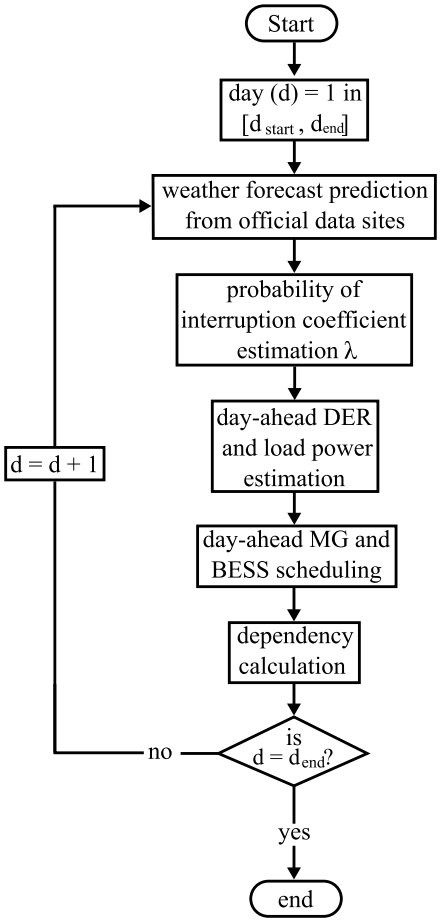

FIGURE 2. Flowchart of the control policy based on weather predictions for each cluster.

the learning rate, the number of boosting iterations (i.e., the number of trees to build), the maximum number of leaves in one tree (i.e., the maximum number of nodes per tree), and the maximum depth for a tree model (i.e., the maximum distance between the root node of each tree and a leaf node). The tuning is carried out with the hyperparameters presented in Table 2 using 500 iterations.

The target data for load demand represent an aggregated load of 29 customers from one Elenia secondary substation located in central Finland. The solar PV production data were retrieved from the same location using hourly PV simulations with the *renewable-ninja* platform [35]. The solar PV is simulated using the MERRA-2 (global) dataset for a system with 30 kWp installed capacity and 10% loss, the system facing south (azimuth angle 180°) and inclined from the horizon

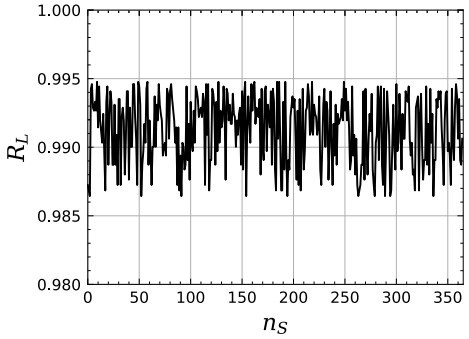

FIGURE 3. Daily dependency index with a fixed T_D and a varying T_S.

TABLE 1. Meteorological and time variables used for predicting faults.

Number	Variable
1	Air temperature, °C
2	Wind speed, km/s
3	Gust speed, km/s
4	Relative humidity, %
5	Wind direction (sine)
6	Wind direction (cosine)
7	Dew point temperature, °C
8	Snow depth, cm
9	Air pressure, mb
10	Horizontal visibility, km
11	Cloud cover, %
12	Month (sine)
13	Month (cosine)
14	Day of the month (sine)
15	Day of the month (cosine)

with a tilt angle of 35°. Fig. 5 illustrates the target series, both of which have an hourly resolution for the year 2013. Following the concept of weather-dependent operation of low-carbon power systems, we base our predictions solely on historical weather observations and time features presented in Table 3. The weather observations are obtained using open data of the Finnish Meteorological Institute [36].

The error of the point forecast for hour h on day d is estimated by the deviation between the actual observation $y_{h,d}$ and the prediction $\hat{y}_{h,d} = f(X_{h,d})$ as follows:

$$\varepsilon_{h,d} = y_{h,d} - \hat{y}_{h,d}. \tag{3}$$

The performance evaluation of the model is carried out using *k-fold cross-validation* with k = 12 folds separated per a particular month of a year. In such an arrangement, the model is trained using 11 months of a year and tested on an unseen month. Such a validation is repeated for each month. To quantify the statistical quality of the forecasts for all fold data, the metric of Mean Absolute Error (MAE) is employed:

$$\text{MAE} = \frac{1}{D \cdot H} \sum_{d=1}^{D} \sum_{h=1}^{H} |\varepsilon_{h,d}| \tag{4}$$

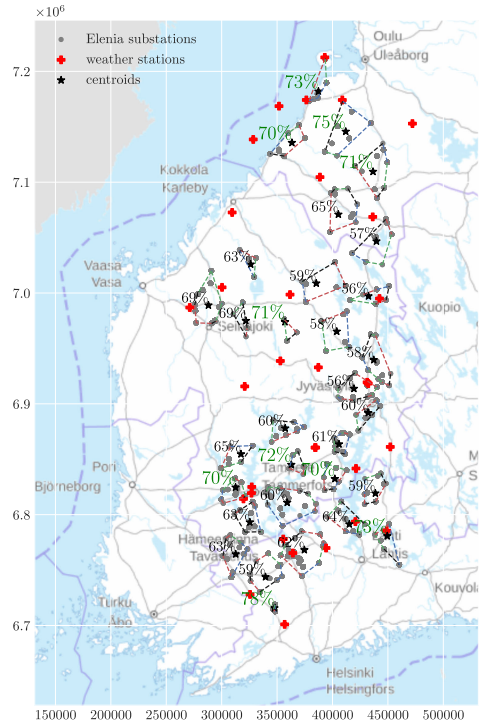

FIGURE 4. Clusters of Elenia's substations, the closest weather stations, and the test accuracy achieved by the predictive model. The underlying map in the ETRSTM35FIN coordinate system is taken from the website of the national land survey of Finland.

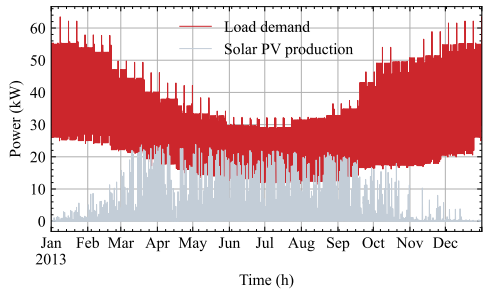

FIGURE 5. Time series of the microgrid load demand and solar production.

where $D \cdot H$ is the number of points for the evaluation equal to the number of hours per year. The lower the MAE, the better the model accuracy.

The results of the model performance are demonstrated in Table 4. The average point forecast error is close to 3 kW for the load demand and close to 2.5 kW[1] for the solar PV production. However, similar to the fault prediction, the historical weather observations should be substituted with the weather forecast data for the real use case.

[1]For nonzero hours of solar PV production.

TABLE 2. Details of the hyperparameter search space.

Hyperparameter	Search space	Stochastic expression
Maximum leaves	50:500:50	Quantized uniform
Maximum depth	1:10:1	Quantized uniform
Number of iterations	100:1000:100	Quantized uniform
Learning rate	0.001 – 0.3	Log-uniform

TABLE 3. Exogenous features used for demand and solar production forecasting.

Number	Variable
1	Air temperature, °C
2	Wind speed, m/s
3	Gust speed, m/s
4	Relative humidity, %
5	Precipitation amount, mm
6	Precipitation intensity, mm/h
7	Wind direction (sine)
8	Wind direction (cosine)
9	Dew point temperature, °C
10	Snow depth, cm
11	Air pressure (msl), hPa
12	Horizontal visibility, m
13	Cloud amount, (1/8)
14	Hour (sine)
15	Hour (cosine)
16	Day of the week (sine)
17	Day of the week (cosine)
18	Day of the month (sine)
19	Day of the month (cosine)
20	Holiday (binary)

TABLE 4. Model performance results for the testing folds.

Dataset	MAE, kW
load demand	3.04
solar PV production	2.53

Besides the values of point prediction, an optimization method in Section IV-A requires a covariance matrix of expected errors to produce stochastic scenarios. This covariance matrix is obtained for each target time series using post-hoc residual simulation; i.e., relying on the corresponding model prediction errors:

$$\Delta = \begin{bmatrix} \varepsilon_{1,1} & \cdots & \varepsilon_{1,d} & \cdots & \varepsilon_{1,D} \\ \vdots & \ddots & \vdots & \ddots & \vdots \\ \varepsilon_{h,1} & \cdots & \varepsilon_{h,d} & \cdots & \varepsilon_{h,D} \\ \vdots & \ddots & \vdots & \ddots & \vdots \\ \varepsilon_{H,1} & \cdots & \varepsilon_{H,d} & \cdots & \varepsilon_{H,D} \end{bmatrix} \tag{5}$$

where each row of the error matrix represents an hour of a day, and each column a single daily observation. A covariance

matrix $\Sigma \in \mathbb{R}^{H\times H}$ is then derived from the testing error matrix of all folds as follows:

$$\Sigma = \begin{bmatrix} \sigma_{1,1} & \dots & \sigma_{1,h_j} & \dots & \sigma_{1,h_J} \\ \vdots & \ddots & \vdots & \ddots & \vdots \\ \sigma_{h_i,1} & \dots & \sigma_{h_i,h_j} & \dots & \sigma_{h_i,h_J} \\ \vdots & \ddots & \vdots & \ddots & \vdots \\ \sigma_{h_I,1} & \dots & \sigma_{h_I,h_j} & \dots & \sigma_{h_I,h_J} \end{bmatrix} \tag{6}$$

where

$$\sigma_{h_i,h_j} = \frac{1}{D-1}\sum_{d=1}^{D}(\varepsilon_{h_i,d} - \hat{\varepsilon}_{h_i})(\varepsilon_{h_j,d} - \hat{\varepsilon}_{h_j})^T \tag{7}$$

is the variance of the marginal distributions of the prediction errors for look-ahead hours h_i and h_j. The covariance matrix illustrates the interdependence structure of prediction errors for each forecast horizon. For instance, Fig. 6 shows the examples of the target covariance matrices with a positive covariance between the prediction hours for both prediction targets. The positive covariance means that the prediction errors at two hours tend to increase or decrease in tandem. The covariance pattern has a distinct concentration along the diagonal line, especially marked for the peak hours of load demand and midday hours for solar PV production. Therefore, the model has difficulties in correctly predicting the target values at those hours. However, the covariances sharply decrease with an increase in distance from these forecast horizons.

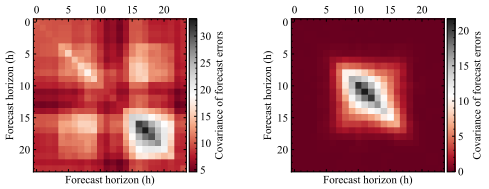

(a) Load demand (b) Solar PV production

FIGURE 6. Covariance matrices of forecast errors for the microgrid (a) load demand and (b) solar PV production for the next day forecast horizons.

IV. MICROGRID ENERGY STORAGE MANAGEMENT

A. OPTIMIZATION PROBLEM

The operation management of the MG aims to produce a BESS schedule for the next day using convex stochastic optimization with chance constraints, i.e., constraints that are required to hold with a high probability. The convex optimization problem is described with an objective in Section IV-A1 and a list of constraints in Section IV-A2.

1) OBJECTIVE FUNCTION

The objective function of the optimization problem considers a trade-off between cost reduction and outage prevention goals:

$$\begin{aligned} &\text{minimize} \quad \underbrace{(1-\lambda)\cdot f_{\text{Op}}}_{\text{cost reduction}} + \underbrace{\lambda \cdot \mathbb{E}f_{\text{Rel}}}_{\text{outage prevention}} \\ &\text{subject to} \quad \underbrace{(19)-(29)}_{\text{power balance and DER operational constraints}} \end{aligned} \tag{8}$$

where $\lambda \in [0, 1]$ is a weight coefficient that is equal to the probability of an outage occurrence, f_{Op} is an objective containing the operating costs of devices, and $\mathbb{E}f_{\text{Rel}}$ is an approximated expectation of the reliability of the supply objective. Intuitively, the higher the probability of an outage is, the more weight is given to the reliability of the supply goal. Otherwise, the optimization prioritizes the cost-effective load shifting with the BESS, e.g., by charging the BESS when the grid energy is cheap and discharging when it is expensive.

The operation objective at any time $t \in \mathcal{T} = \{1, 2, \dots, T\}$ is defined by the electricity costs at the point of common coupling (PCC) C_t^{pcc} and the degradation costs of BESS C_t^{b}:

$$f_{\text{Op}} = \sum_{t\in\mathcal{T}} C_t^{\text{pcc}} + \sum_{t\in\mathcal{T}} C_t^{\text{b}}. \tag{9}$$

The electricity costs are formed by selling the electricity to the grid and buying it from the grid, as well as assuming that the prices for the exported electricity C_t^{ex} are often lower than the prices of the imported electricity C_t^{im} from the grid [37], i.e., $C_t^{\text{im}} \geq C_t^{\text{ex}}$, $\forall t \in \mathcal{T}$:

$$C_t^{\text{pcc}} = (C_t^{\text{ex}} p_t + (C_t^{\text{im}} - C_t^{\text{ex}})(p_t + |p_t|)/2)\Delta t, \quad \forall t \in \mathcal{T} \tag{10}$$

where p_t is the power scheduled at the PCC of the MG [38] during the metering period Δt.

The MG purchase electricity price C_t^{im} (€/kWh) consists of the electricity network service charges C^{nsc} (€/kWh), the price of electrical energy, and the electricity tax C^{etax} (€/kWh). Here, the price of electrical energy is based on the wholesale market prices C_t^{ws} (€/kWh) and a retail margin. The network service charges and the market price include a value added tax (VAT, 24%). Finally, the purchase electricity price is formulated as follows:

$$C_t^{\text{im}} = C_t^{\text{ws}} + C^{\text{rm}} + C^{\text{nsc}} + C^{\text{etax}}, \quad \forall t \in \mathcal{T} \tag{11}$$

The MG electricity selling price C_t^{ex} consists of the wholesale market price C_t^{ws} (without VAT) and a network service charge for the feed-in generation C^{fic} (€/kWh):

$$C_t^{\text{ex}} = C_t^{\text{ws}} - C^{\text{fic}}, \quad \forall t \in \mathcal{T} \tag{12}$$

The degradation cost of the BESS during the operation is included by penalizing excessive charge–discharge cycling with a coefficient β as follows:

$$C_t^{\text{b}} = \beta |p_{d,t}^{\text{b}}| \Delta t \tag{13}$$

$$\beta = \frac{C^{\text{inv}}}{2 n_{\text{cyc}} DOD_{\max}} \tag{14}$$

where $p_{d,t}^{\text{b}}$ is a decision variable of scheduled battery storage power, C^{inv} is the investment cost of the BESS (€/kWh), n_{cyc}

is the estimated lifetime in equivalent cycles, and $DOD_{\max}$ is the maximum allowed depth of discharge (DoD). In addition, other market-related components can be added to the objective function, such as revenue from the provision of a BESS for the frequency regulation service [39]. This BESS application is especially demanding for a low-carbon power system with an increasing share of renewable generation.

The availability of self-supply and battery storage capacity enables the MG to withstand the outage event in the upstream grid by switching to island operation. In that case, the reliability objective function is formulated using expected energy not supplied (EENS), i.e., the amount of the net demand unsupplied by local resources during the outage:

$$f_{\text{Rel}} = C^{\text{ens}} \sum_{t \in \mathcal{T}} [p_t^{\text{out}}]^+ \Delta t, \tag{15}$$

where $[\cdot]^+ \equiv \max[\cdot, 0]$ is the elementwise ramp-up function, Δt is the metering period, C^{ens} is the unit cost of the energy not supplied, and p_t^{out} is the unsupplied net demand during an outage. In such a formulation, we consider an equal probability of an outage to happen at any hour of a day. The unsupplied demand at time t is calculated based on the local demand $p_{d,t}^{\text{load}}$, supply $p_{d,t}^{\text{solar}}$, and available active power $p_t^{\text{b,sup}}$ of the BESS as follows:

$$p_t^{\text{out}} = p_{d,t}^{\text{load}} - p_{d,t}^{\text{solar}} - p_{d,t}^{\text{b,sup}}, \quad \forall t \in \mathcal{T} \tag{16}$$

where

$$p_t^{\text{b,sup}} = \frac{e_t^{\text{b}} \eta}{\tau_{\max} \sum_{k=1}^{\tau_{\max}} \alpha^{1-k}}, \tag{17}$$

is the available active power in one time step if the BESS energy capacity e_t^{b} at time t is emptied at a constant power over the next $\tau_{\max}$ time periods with a self-discharge rate α and a discharge loss coefficient η [38]. The unknown variables (i.e., solar PV production p_d^{solar} and load demand p_d^{load}) are specified as normal random variables $p \sim \text{Normal}(\hat{p}, \Sigma)$ using the predicted mean and covariance matrix of prediction errors from Section III-B. The expectation of the reliability of the supply objective $\mathbb{E}f_{\text{Rel}}$ containing these random variables is then computed using scenario-based sample average approximation (SAA):

$$\mathbb{E}f_{\text{Rel}} \approx (1/N) \sum_{i=1}^{N} f_{\text{Rel}}(p_d^{\text{b,sup}}, p_{d,i}^{\text{solar}}, p_{d,i}^{\text{load}}), \tag{18}$$

where p_d^{b} serves as an optimization variable, whereas $p_{d,i}^{\text{solar}}$ and $p_{d,i}^{\text{load}}$ are random variables with $i = 1, \ldots, N$ scenarios that are drawn using the Markov chain Monte Carlo (MCMC) method.

2) CONSTRAINTS AND COMPONENT MODELS

The MG network power flow is described using a *static* direct current (DC) power flow formulation. The static setting of power flow assumes that the power flows are constant over the metering time interval, typically equal to one hour, whereas the DC formulation leaves out the reactive power flow and voltage phase angles. The network contains *devices* $d \in \mathcal{D}$ (e.g., generators, loads, storages, and power converters) that have one or more terminals providing a bidirectional power flow.[2] Here, the internal MG network structure is neglected assuming a single bus connection of all devices without connecting lines. The reasoning for such a simplification given in [40] concludes that an MG network with a limited capacity and proximity of devices does not typically provide the limiting constraints but complicates the formulation. Therefore, following the formal notation in [41] to describe the problem, a single bus of the MG is described by the *net* illustrated in Fig. 7. The net exchanges power between terminals of devices and guarantees power conservation over the connected terminals (i.e., the sum of the terminal powers is zero). The power balance in the net of the MG with M terminals in each time period can be expressed as follows:

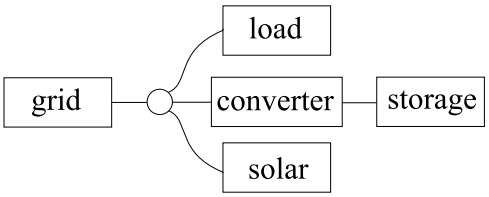

FIGURE 7. Schematic of a microgrid network in the modeling environment.

$$\sum_{d \in \mathcal{D}} p_{d,t} = 0, \quad \forall t \in \mathcal{T} \tag{19}$$

where $p_{d,t}$ is the scheduled power at time $t \in \mathcal{T}$ of a device at the connected terminal.

The devices modeled in the MG network include a grid tie, a renewable generator, an aggregated fixed-power load, and a lossy BESS. The grid tie is a single-terminal device modeled as a generator and representing a connection to an external power grid. The renewable generator is a single-terminal device that produces power, i.e., its terminal power $p_{d,t}$ satisfies $p_{d,t} < 0$. Similarly, the fixed load is also a single-terminal device that consumes a fixed amount of power $p_{d,t} > 0$. The power values at the terminals of the generator and the load devices correspond to the mean forecasts of production and demand of these devices. The lossy BESS is formulated as a composite device by connecting a constant-efficiency power converter that models the charge and discharge losses of the BESS and a storage with self-discharge losses. The internal energy state $e_t^{\text{b}} \in \mathbb{R}^+$ of the BESS is expressed as:

$$e_t^{\text{b}} = (1 - \alpha) e_{t-1}^{\text{b}} + p_{d,t-1}^{\text{b}} \Delta t, \quad \forall t \in \{2, 3, \ldots, T\} \tag{20}$$

where α is the (per-period) leakage rate limited by $0 < \alpha \leq 1$, and Δt is the time interval between time periods. Furthermore, we constrain the energy charge of the BESS

[2]Positive (negative) terminal power means power flows into (out of) the device at that terminal.

at the beginning and end of every optimization cycle to 50% of the available energy capacity of the BESS $\overline{E}^{\mathrm{b}}$:

$$e_1^{\mathrm{b}} = 0.5\overline{E}^{\mathrm{b}}, \tag{21}$$

$$(1-\alpha)e_T^{\mathrm{b}} + p_{d,T}^{\mathrm{b}}\Delta t \geq 0.5\overline{E}^{\mathrm{b}}, \tag{22}$$

which enables to decouple the results of daily experiments. The useful energy capacity is then limited by:

$$(1 - DOD_{\max})\overline{E}^{\mathrm{b}} \leq e_t^{\mathrm{b}} \leq \overline{E}^{\mathrm{b}}, \quad \forall t \in \mathcal{T} \tag{23}$$

The charge and discharge rate is limited by the restricted $\underline{p}$ and maximum $\overline{p}$ powers of the BESS as follows:

$$\underline{p} \leq p_{d,t}^{\mathrm{b}} \leq \overline{p}, \quad \forall t \in \mathcal{T} \tag{24}$$

The power converter is a two-terminal device that transfers power at a certain efficiency. The conversion efficiency in the forward and reverse directions $\eta \in (0, 1)$ for terminals 1 and 2 is characterized by:

$$p_2 = \max\{-\eta p_1, -(1/\eta)p_1\}, \tag{25}$$

$$\underline{p} \leq p_1 \leq \overline{p}. \tag{26}$$

We approximate these *non*convex constraints with their convex hull:

$$p_1 + p_2 \geq (1-\eta)p_1, \tag{27}$$

$$p_1 + p_2 \leq 2\overline{p}\frac{1-\eta}{1+\eta}. \tag{28}$$

Similarly, typically nonconvex chance constraints are computed with conservative approximations [42]. Here, we apply chance constraints to the unsupplied net load demand:

$$\mathbf{Prob}(p^{\mathrm{out}} \geq 0) \leq 1 - \gamma, \tag{29}$$

where γ is a high probability. With this constraint, we target the probability of a deficient power balance during an outage to be less than $1 - \gamma$.

3) IMPLEMENTATION DETAILS

The optimization problem is formulated and solved using a collection of Python-based software packages for convex optimization, namely *cvxpy* [43], *cvxpower* [41], and *cvxstoc* [42], where *cvxpy* is a modeling language for convex optimization problems; *cvxpower* provides a declarative language for describing and optimizing power networks; and *cvxstoc* is a modeling framework for specifying and solving convex stochastic programs. We use 100 Monte Carlo samples for an approximation of the expression expectation and the chance constraints. The chance constraint probability is equal to 95%.

The simulation data are selected to represent the real-life operating environment of the MG. The wholesale market price is retrieved for the Finnish bidding area for the year 2019 using Nordpool's historical market data. The static values of the electricity tariff are taken from actual retail tariffs and Elenia's distribution tariffs. The characteristics of the BESS are chosen based on the peak load demand of the MG and interpolation of the reference scenario for the development of the parameters of a stationary $LiFePO_4$ BESS to the year 2021 [44]. The charging/discharging efficiency of the BESS is 96%, the battery investment cost C^{inv} is 378.64 €/kWh, and the number of equivalent life cycles n_{cyc} is 10^4 cycles. The leakage rate of 0.1% of the BESS capacity per day is equally distributed among T time periods and applied at any time t as $\alpha = 0.001/T$. With the allowed DoD of 90 %, the marginal cost of the battery degradation β is 0.021 €/kWh. The maximum number of time periods for the expected duration of outages $\tau_{\max}$ is determined from the relation of BESS energy capacity to nominal power and equals 1 and 2 hours. The unit cost of the demand not supplied consists of the unit cost for the amount and duration of unexpected interruptions in Finland, which are together equal to 12.1 €/kWh [45], and the profit loss from the distribution fees C^{nsc} not received. This value for the duration of unexpected interruptions is given in the 2005 value of money and is not adjusted using the consumer price index. All the static cost data used in the optimization are provided in Table 5. The implementation source codes and some real-world historical data are available online.[3]

TABLE 5. Values of costs used in the optimization of the MG operation management.

Cost	C^{nsc}, €/kWh	C^{etax}, €/kWh	C^{rm}, €/kWh	C^{fic}, €/kWh	β, €/kWh	C^{ens}, €/kWh
Value	0.0521	0.0279	0.0024	0.0007[a]	0.0210	12.1521

[a] If the nominal power of the power plant is less than 50 kVA, no distribution fee will be charged.

Four test scenarios are considered for the operation management of the MG: *economical*, *reliable*, *uncertain*, and *perfect foresight*. The former two assume the usage of the BESS solely for the objective functions of cost reduction (i.e., $\lambda = 0$ in Eq. (8)) or outage reduction (i.e., $\lambda = 1$ in Eq. (8)), whereas the latter two are described by Eq. (8) with the predicted (i.e., uncertain scenario) and known (i.e., perfect foresight scenario) outage probability λ. Importantly, the chance constraint is not applied for the economical scenario. The objective functions in Eq. (8) are normalized for the uncertain scenario using weighted min-max normalization [46] applied to prosumer flexibility modeling in [39]. For instance, in the case of the cost reduction objective, the minimum value is acquired from the economical scenario, whereas the maximum is derived from the reliable scenario. The same logic holds for the outage reduction objective.

V. RESULTS AND DISCUSSION

A. TEST SCENARIOS

In this paper, we used real interruption data obtained from several substations in Finland. For the sake of simplicity, the MG was theoretically placed at the centroid of fault clusters where the interruption data were obtained to produce fair

[3] https://git.io/Jundm

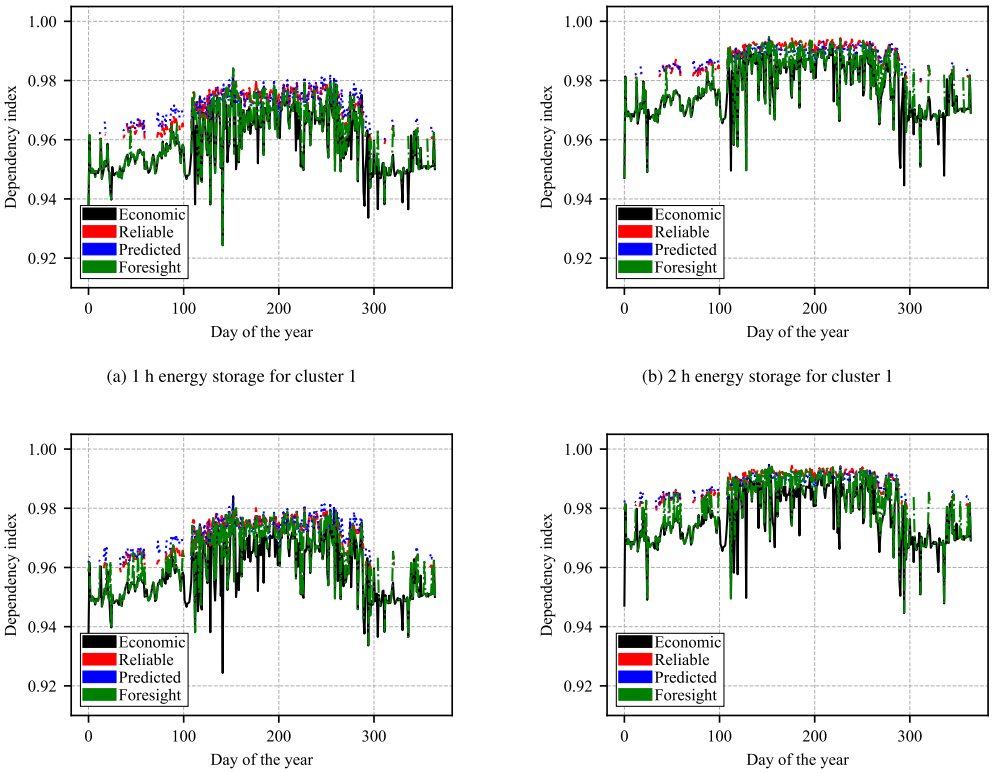

(a) 1 h energy storage for cluster 1

(b) 2 h energy storage for cluster 1

(c) 1 h energy storage for cluster 6

(d) 2 h energy storage for cluster 6

FIGURE 8. Daily dependency index (R_L) for the year 2013.

results. The scenarios chosen are the five clusters with the best accuracy and the one with the lowest accuracy from Fig. 4 as follows:

- Cluster 1: highest accuracy cluster ≈ 78%
- Cluster 2: accuracy cluster ≈ 75%
- Cluster 3: #1 accuracy cluster ≈ 73%
- Cluster 4: #2 accuracy cluster ≈ 73%
- Cluster 5: accuracy cluster ≈ 72%
- Cluster 6: lowest accuracy cluster ≈ 56%

Each cluster prediction is used independently for the optimization as explained above in Section IV-A.

B. RESILIENCE

The daily resilience metric calculated using Eq. (2) for the year 2013 is shown in Fig. 8, which depicts the combined use of the proposed predictive interruption model and the economical approach (predicted); considering only the economical approach (economical); the reliability model approach (reliable); and faults to be known (foresight). The daily resilience metric gives a granular view of how the prior knowledge of the operational behavior of the microgrid can enhance the MG resilience over a period of time. We analyzed the faults in the region under study and found that 2 h for T_D explains more than 90% of the interruption time for outages occurring in the region, and $T_U = 24 - T_D$, because the daily index analysis covers a period of 24 h. The variation seen in the daily resilience illustrated in Fig. 8 is due the variation in the load and in the energy stored in the battery.

Fig. 8 presents a comparison between the above-mentioned approaches between clusters 1 and 6 (the highest and lowest accuracies). Fig. 8 shows how the combination of economical and predicted approaches faults yields a better dependency and thus, the microgrid is more resilient to upcoming events by having more energy available when a fault occurs. The above-discussed trade-off maintains a balance that results in a more robust grid but also considering the energy prices.

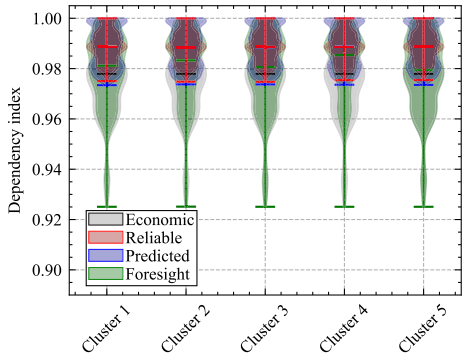

FIGURE 9. Violin plot for R_L in the highest accuracy clusters for the year 2013.

From only the economical perspective, there is a significant decrease in dependency when faults occur for that specific day, thereby reducing the resilience. Furthermore, Figs. 8b and 8d show how increasing the value of the battery storage enhances the dependency index for all approaches.

A closer look at the all-year-round dependency for the approaches is analyzed in Fig. 9: the economical and foresight approaches are very similar having a lower adjacent value smaller than the other two approaches and more outside points. Moreover, the dependency data for the economical approach is more distributed on the axes meaning that it is not dependent on resilience. The reliable and predicted approaches follow a resilient strategy and thereby a narrow distance between adjacent values. Their medians are almost the same but have variations in the first and third quartiles with the predictive one having greater values closer to 1. There is no difference between clusters for the economical approach because it does not consider interruption data, whereas for the other approaches the difference is almost negligible because of the smaller discrepancies in the interruption accuracy.

The violin plot shown in Fig. 10 contains the plots of the dependency index based on a 24 h ahead horizon and calculated hourly for five days (five without faults and five with faults) for five clusters with a higher accuracy. The scenarios plotted were the economical approach and the proposed predictive approach. We can see that when a fault occurs in these two scenarios, the proposed approach becomes slightly more conservative, thereby narrowing the upper and lower adjacent values and maintaining the median at higher levels of dependency. The economical approach does not distinguish a possible upcoming fault event, meaning that the lower adjacent value is smaller. The tendency of the proposed predicted approach to be more conservative with the available energy shows an increase in the resilience especially for the days that

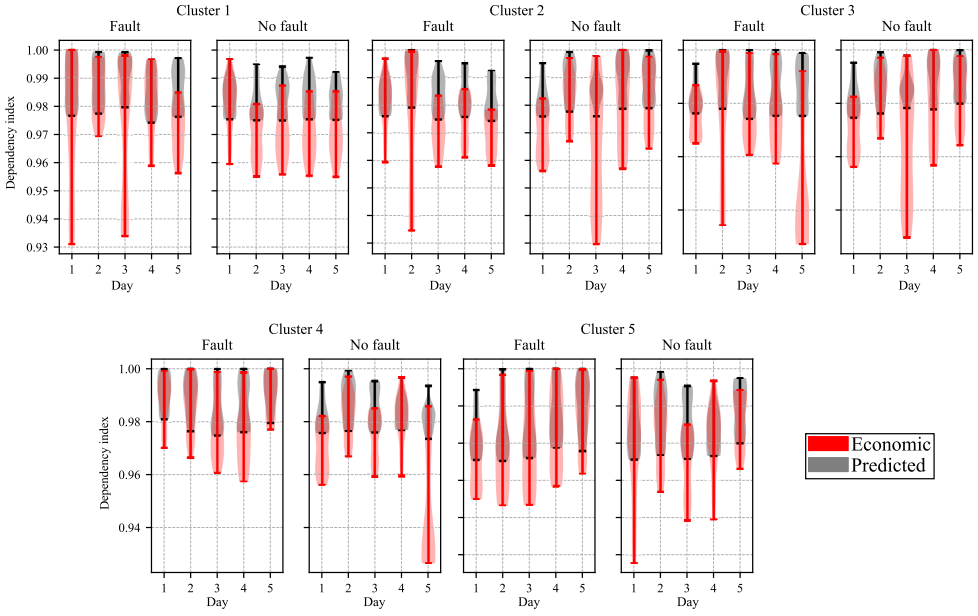

FIGURE 10. Violin plot for R_L in five clusters calculated hourly for days with and without a fault.

have a high probability of a fault occurrence. The scenario plotted in Fig. 10 considers 2 h of energy available in the battery.

VI. CONCLUSION

Preparation of a grid against severe fault conditions is one of the least investigated actions to take account of when increasing the overall resilience in an MG. The reason behind this is the unpredictable and probabilistic nature of these events. In this paper, weather-based decision-making for charging a BESS in an MG was developed. The methodology includes three different models: interruption prediction, load demand, and solar PV production forecast. We were able to effectively predict an upcoming interruption in the system with 78% accuracy and thereby implement a multiobjective chance constraint optimization to schedule the microgrid battery storage according to the prediction. The proposed optimization approach takes into consideration two objectives: resilience to possible supply interruptions and economic dispatch so that we can guarantee a safe and economical operation of the grid.

We also proposed daily quantification of the resilience metric of dependency, which measures on a daily basis the energy stored in the BESS revealing for the day ahead how independent the MG will be from the main grid. We showed that when compared with the economical, reliable, and foresight approaches, our control policy can improve the overall resilience for short and long periods of time in regard to an interruption in the main grid so that the MG operates in the island mode. When calculating the resilience index in our proposed approach, the probability of the occurrence of a fault determines whether we can prepare the MG for the upcoming events. Fault data are not usually available for all places where microgrids are located or they are designed to be built; this is due to companies' polices that prevent the data being shared, or data are simply nonexistent for the region. The more data are available, the more precise are the outcomes from outage models, meaning better results in the MG resilience. Having this type of data, we can see from our approach that a trade-off between an economical and resilient MG can be possible by employing multiobjective BESS optimization. An overall resilience improvement can only be achieved by correctly assessing the framework cycle and its individual pillars described in detail in the paper.

In summary, using interruption and economic dispatch ensures that the microgrid does not operate oversized when there is no risk of a fault occurrence and that it also enters into a hardening state, which increases the amount of energy stored in the BESS in the case of a high probability of a fault occurrence, thereby supplying energy for longer periods when operating in the island mode.

REFERENCES

[1] M. K. Senapati, C. Pradhan, S. R. Samantaray, and P. K. Nayak, "Improved power management control strategy for renewable energy-based DC micro-grid with energy storage integration," *IET Gener., Transmiss. Distrib.*, vol. 13, no. 6, pp. 838–849, Mar. 2018.

[2] H. Mahmood and J. Jiang, "Decentralized power management of multiple PV, battery, and droop units in an islanded microgrid," *IEEE Trans. Smart Grid*, vol. 10, no. 2, pp. 1898–1906, Mar. 2017.

[3] Y. Zhang, C. Zhang, T. Wang, Y. Qu, W. Wang, L. Bai, J. Hao, and S. Guan, "A strategy for day-ahead prediction of residual capacity of energy storage unit of micro grid in islanded state," in *Proc. IEEE Int. Conf. Mechatronics Autom.*, Aug. 2016, pp. 2652–2657.

[4] A. A. Bajwa, H. Mokhlis, S. Mekhilef, and M. Mubin, "Enhancing power system resilience leveraging microgrids: A review," *J. Renew. Sustain. Energy*, vol. 11, no. 3, May 2019, Art. no. 035503.

[5] M. Chaudry, P. Ekins, K. Ramachandran, A. Shakoor, J. Skea, G. Strbac, X. Wang, and J. Whitaker, "Building a resilient U.K. Energy system," U.K. Energy Res. Centre, Res. Rep., Apr. 2011.

[6] A. Berkeley and S. Jackson, "A framework for establishing critical infrastructure resilience goals: Final goals and recommendations," Nat. Infrastruct. Advisory Council, Washington, DC, USA, NIAC Rep., 2010.

[7] L. Wen, K. Zhou, S. Yang, and X. Lu, "Optimal load dispatch of community microgrid with deep learning based solar power and load forecasting," *Energy*, vol. 171, pp. 1053–1065, Mar. 2019.

[8] G. R. Athira and V. R. Pandi, "Energy management in islanded DC microgrid using fuzzy controller to improve battery performance," in *Proc. Int. Conf. Technol. Advancements Power Energy (TAP Energy)*, Dec. 2017, pp. 1–6.

[9] I. Alsaidan, A. Khodaei, and W. Gao, "Distributed energy storage sizing for microgrid applications," in *Proc. IEEE/PES Transmiss. Distrib. Conf. Exposit. (T&D)*, May 2016, pp. 1–5.

[10] A. Khodaei, "Resiliency-oriented microgrid optimal scheduling," *IEEE Trans. Smart Grid*, vol. 5, no. 4, pp. 1584–1591, Jul. 2014.

[11] M. Khederzadeh, "Distribution grid restoration by forming resiliency-oriented less-vulnerable microgrids," in *Proc. CIRED Workshop*, 2016.

[12] H. Wang, Z. Yan, M. Shahidehpour, X. Xu, and Q. Zhou, "Quantitative evaluations of uncertainties in multivariate operations of microgrids," *IEEE Trans. Smart Grid*, vol. 11, no. 4, pp. 2892–2903, Jul. 2020.

[13] U. B. Tayab, F. Yang, M. El-Hendawi, and J. Lu, "Energy management system for a grid-connected microgrid with photovoltaic and battery energy storage system," in *Proc. Austral. New Zealand Control Conf. (ANZCC)*, Dec. 2018, pp. 141–144.

[14] M. Tostado-Véliz, D. Icaza-Alvarez, and F. Jurado, "A novel methodology for optimal sizing photovoltaic-battery systems in smart homes considering grid outages and demand response," *Renew. Energy*, vol. 170, pp. 884–896, Jun. 2021.

[15] R. Wu and G. Sansavini, "Integrating reliability and resilience to support the transition from passive distribution grids to islanding microgrids," *Appl. Energy*, vol. 272, Aug. 2020, Art. no. 115254.

[16] F. H. Jufri, V. Widiputra, and J. Jung, "State-of-the-art review on power grid resilience to extreme weather events: Definitions, frameworks, quantitative assessment methodologies, and enhancement strategies," *Appl. Energy*, vol. 239, pp. 1049–1065, Apr. 2019.

[17] M. Panteli and P. Mancarella, "The grid: Stronger, bigger, smarter?: Presenting a conceptual framework of power system resilience," *IEEE Power Energy Mag.*, vol. 13, no. 3, pp. 58–66, May 2015.

[18] H. Farzin, M. Fotuhi-Firuzabad, and M. Moeini-Aghtaie, "Role of outage management strategy in reliability performance of multi-microgrid distribution systems," *IEEE Trans. Power Syst.*, vol. 33, no. 3, pp. 2359–2369, May 2018.

[19] A. Younesi, H. Shayeghi, P. Siano, A. Safari, and H. H. Alhelou, "Enhancing the resilience of operational microgrids through a two-stage scheduling strategy considering the impact of uncertainties," *IEEE Access*, vol. 9, pp. 18454–18464, 2021.

[20] G. Liu, T. B. Ollis, Y. Zhang, T. Jiang, and K. Tomsovic, "Robust microgrid scheduling with resiliency considerations," *IEEE Access*, vol. 8, pp. 153169–153182, 2020.

[21] H. Hesse, R. Martins, P. Musilek, M. Naumann, C. Truong, and A. Jossen, "Economic optimization of component sizing for residential battery storage systems," *Energies*, vol. 10, no. 7, p. 835, Jun. 2017.

[22] W. I. Schmitz, M. Schmitz, L. N. Canha, and V. J. Garcia, "Proactive home energy storage management system to severe weather scenarios," *Appl. Energy*, vol. 279, Dec. 2020, Art. no. 115797.

[23] A. M. Madni and S. Jackson, "Towards a conceptual framework for resilience engineering," *IEEE Syst. J.*, vol. 3, no. 2, pp. 181–191, Jun. 2009.
[24] A. Kwasinski, "Quantitative model and metrics of electrical grids' resilience evaluated at a power distribution level," *Energies*, vol. 9, no. 2, p. 93, Feb. 2016.
[25] F. Pedregosa, G. Varoquaux, A. Gramfort, V. Michel, B. Thirion, O. Grisel, M. Blondel, P. Prettenhofer, R. Weiss, V. Dubourg, and J. Vanderplas, "Scikit-learn: Machine learning in Python," *J. Mach. Learn. Res.*, vol. 12, pp. 2825–2830, Jan. 2011. [Online]. Available: http://jmlr.org/papers/v12/pedregosa11a.html
[26] *World Weather Online*. Accessed: Dec. 2020. [Online]. Available: https://www.worldweatheronline.com/
[27] *World Weather Online Historical Weather Data API Wrapper*. Accessed: Dec. 2020. [Online]. Available: https://github.com/ekapope/WorldWeatherOnline
[28] O. Lammi, *Coordinate System Functions*. Accessed: Dec. 2020. [Online]. Available: http://users.jyu.fi/~vesal/riippu/matka02/fetch_map/coordinates.py
[29] C. Brester, H. Niska, R. Ciszek, and M. Kolehmainen, "Weather-based fault prediction in electricity networks with artificial neural networks," in *Proc. IEEE Congr. Evol. Comput. (CEC)*, Jul. 2020, pp. 1–8.
[30] L. Breiman, *Mach. Learn.*, vol. 45, no. 1, pp. 5–32, 2001.
[31] G. Ke, Q. Meng, T. Finley, T. Wang, W. Chen, W. Ma, Q. Ye, and T.-Y. Liu, "LightGBM: A highly efficient gradient boosting decision tree," in *Proc. Adv. Neural Inf. Process. Syst.*, vol. 30, 2017, pp. 3146–3154.
[32] LightGBM. (2019). *Light Gradient Boosting Machine*. Accessed: Jun. 15, 2019. [Online]. Available: https://github.com/microsoft/LightGBM/
[33] S. Makridakis, E. Spiliotis, and V. Assimakopoulos, "The M5 accuracy competition: Results, findings and conclusions," *Int. J. Forecasting*, 2020.
[34] J. Bergstra, D. Yamins, and D. Cox, "Hyperopt: A Python library for optimizing the hyperparameters of machine learning algorithms," in *Proc. 12th Python Sci. Conf.*, vol. 13, 2013, p. 20.
[35] S. Pfenninger and I. Staffell, "Long-term patterns of European PV output using 30 years of validated hourly reanalysis and satellite data," *Energy*, vol. 114, pp. 1251–1265, Nov. 2016.
[36] M.-L. Honkola, N. Kukkurainen, L. Saukkonen, A. Petäjä, J. Karasjärvi, T. Riihisaari, R. Tervo, M. Visa, J. Hyrkkänen, and R. Ruuhela, "The finnish meteorological institute: Final report for the open data project," Tech. Rep., 2013.
[37] M. Kubli, "Squaring the sunny circle? On balancing distributive justice of power grid costs and incentives for solar prosumers," *Energy Policy*, vol. 114, pp. 173–188, Mar. 2018.
[38] R. Wu and G. Sansavini, "Integrating reliability and resilience to support the transition from passive distribution grids to islanding microgrids," *Appl. Energy*, vol. 272, Aug. 2020, Art. no. 115254.
[39] A. Mashlakov, E. Pournaras, P. H. J. Nardelli, and S. Honkapuro, "Decentralized cooperative scheduling of prosumer flexibility under forecast uncertainties," *Appl. Energy*, vol. 290, May 2021, Art. no. 116706.
[40] G. Liu, M. Starke, B. Xiao, X. Zhang, and K. Tonsovic, "Microgrid optimal scheduling with chance-constrained islanding capability," *Electr. Power Syst. Res.*, vol. 145, pp. 197–206, Apr. 2017.
[41] N. Moehle, E. Busseti, S. Boyd, and M. Wytock, "Dynamic energy management," in *Large Scale Optimization in Supply Chains and Smart Manufacturing*. Cham, Switzerland: Springer, 2019, pp. 69–126.
[42] A. Ali, J. Z. Kolter, S. Diamond, and S. P. Boyd, "Disciplined convex stochastic programming: A new framework for stochastic optimization," in *Proc. UAI*, 2015, pp. 62–71.
[43] S. Diamond and S. Boyd, "CVXPY: A Python-embedded modeling language for convex optimization," *J. Mach. Learn. Res.*, vol. 17, no. 83, pp. 1–5, 2016.
[44] P. Ralon, M. Taylor, A. Ilas, H. Diaz-Bone, and K. Kairies, "Electricity storage and renewables: Costs and markets to 2030," Int. Renew. Energy Agency, Abu Dhabi, UAE, Tech. Rep., 2017.
[45] Energiavirasto. (2015). *Regulation Methods in the Fourth Regulatory Period of 1 January 2016–31 December 2019 and the Fifth Regulatory Period of 1 January 2020–31 December 2023*. Accessed: Apr. 14, 2021. [Online]. Available: https://www.energiavirasto.fi/
[46] R. T. Marler and J. S. Arora, "Function-transformation methods for multi-objective optimization," *Eng. Optim.*, vol. 37, no. 6, pp. 551–570, Sep. 2005.

DANIEL GUTIERREZ-ROJAS (Student Member, IEEE) received the B.Sc. degree in electrical engineering from the University of Antioquia, Colombia, in 2016, and the M.Sc. degree in protection of power systems from the University of São Paulo, Brazil, in 2017. He is currently pursuing the Ph.D. degree with the School of Energy Systems, LUT University, Finland. From 2017 to 2019, he worked as a Security of Operation and Fault Analyst for Colombia's National Electrical Operator. His research interests include predictive maintenance, power systems, microgrids, mobile communication systems, and electrical protection systems.

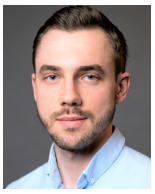

ALEKSEI MASHLAKOV received the double M.Sc. (tech.) degree in electrical engineering from the National Research University "Moscow Power Engineering Institute," Moscow, Russia, and Lappeenranta–Lahti University of Technology LUT, Lappeenranta, Finland, in 2017. He is currently pursuing the D.Sc. (tech.) degree in energy market and solar economy from the LUT University.

His research focuses on ICT-centred solutions for flexibility aggregation of local energy systems to provide network management and system balancing services. His research interests include data-driven probabilistic energy forecasting, power grid modeling, and optimization under uncertainty.

CHRISTINA BRESTER received the master's degree in system analysis and control from Reshetnev Siberian State Aerospace University, Krasnoyarsk, Russia, in 2014, and the Ph.D. degree in technical sciences, in 2016. She is currently pursuing the Ph.D. degree with the Research Group of Environmental Informatics, University of Eastern Finland (UEF), Kuopio. She is currently a Researcher at UEF. Her research interests include data-driven modeling and optimization methods applied to various practical problems, such as human emotion recognition from speech, predicting bacterial abundances in drinking water distribution systems, fault and load prediction in energy grids, and cardiovascular predictive modeling.

HARRI NISKA received the M.Sc. and Ph.D. degrees in environmental science and technology from the University of Eastern Finland, in 2002 and 2012, respectively. He is currently the Project Director and a Research Manager at the University of Eastern Finland. He has involved into a range of national and EU-level research and development projects related to sustainable energy and environment. His research interests include intelligent data processing, predictive analytics, machine learning, optimization, and related applications. He has published over 50 international and refereed publications on these topics. In recent years, he has been mainly focusing on the research on data-driven modeling in the field of smart grids.

MIKKO KOLEHMAINEN received the degree in software engineering and the Ph.D. (D.Sc.Tech.) degree from the Helsinki University of Technology, in 1987 and 2004, respectively. During his career, he has first worked as a System Analyst and the Chief Software Engineer in the software industry, developing solutions for energy companies. In the 90's, he has moved to the academic world, working as a Researcher both in bioinformatics and environmental sciences, followed by a nomination to the Research Director of environmental informatics (a new and emerging field). Currently as a Professor, he is leading the Research Group of Environmental Informatics, University of Eastern Finland. Since 2001, the research group has been carrying out industry related projects using artificial intelligence methods to solve data-based problems related to the environment. He has also worked as the CTO of a start-up company helping the companies to utilize the AI in their operation. He was the Chair of ICANNGA'09.

ARUN NARAYANAN (Member, IEEE) received the B.E. degree in electrical engineering from the Visvesvaraya National Institute of Technology, Nagpur, India, in 2002, the M.Sc. degree in energy technology from the Lappeenranta University of Technology (LUT), Lappeenranta, Finland, in 2013, and the Ph.D. degree from the School of Energy Systems, LUT University, in 2019.

He is currently a Postdoctoral Researcher with the Research Group of Cyber-Physical Systems Group, LUT University. His research interests include renewable energy-based smart microgrids, electricity distribution and markets, demand-side management, energy management systems, and information and communications technology. He focuses on applying optimization, computational concepts, and artificial intelligence techniques to renewable electrical energy problems.

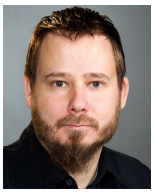

SAMULI HONKAPURO received the M.Sc. (tech.) and D.Sc. (tech.) degrees in electrical engineering from the Lappeenranta–Lahti University of Technology LUT, Lappeenranta, Finland, in 2002 and 2008, respectively.

He is currently a Professor (tenured) of energy markets at LUT University. He has been active in academic research related to electricity distribution business and electricity markets for over 15 years. His present research interests include business and market models for integration of distributed energy resources in energy markets.

PEDRO H. J. NARDELLI (Senior Member, IEEE) received the B.S. and M.Sc. degrees in electrical engineering from the State University of Campinas, Brazil, in 2006 and 2008, respectively, and the Ph.D. degree from the University of Oulu, Finland, and the State University of Campinas, following a dual degree agreement, in 2013. He is currently an Assistant Professor (tenure track) in the IoT in energy systems at LUT University, Finland, and holds a position of an Academy of Finland Research Fellow with a project called building the energy internet as a large-scale IoT-based cyber-physical system that manages the energy inventory of distribution grids as discretized packets via machine-type communications (EnergyNet). He leads the Cyber-Physical Systems Group, LUT, and the Project Coordinator of the CHIST-ERA European Consortium Framework for the Identification of Rare Events via Machine Learning and IoT Networks (FIREMAN). He is also an Adjunct Professor at the University of Oulu in the topic of "communications strategies and information processing in energy systems." His research interests include wireless communications, particularly applied in industrial automation and energy systems. He received the Best Paper Award of IEEE PES Innovative Smart Grid Technologies Latin America, in 2019, in the track "Big Data and Internet of Things." For more information, see his personal website (https://sites.google.com/view/nardelli/).

Publication III

Gutierrez-Rojas, D., Christou, I.T., Dantas, D., Narayanan, A.,
Nardelli, P. H. J. and Yang, Y.
Performance evaluation of machine learning for fault selection in power transmission lines

Reprinted with permission from
Knowledge and Information Systems
Vol. 64, pp. 859–883, Feb. 2022

Knowledge and Information Systems (2022) 64:859–883
https://doi.org/10.1007/s10115-022-01657-w

REGULAR PAPER

Performance evaluation of machine learning for fault selection in power transmission lines

Daniel Gutierrez-Rojas[1] · Ioannis T. Christou[2,3] · Daniel Dantas[4] · Arun Narayanan[1] · Pedro H. J. Nardelli[1] · Yongheng Yang[5]

Received: 10 February 2021 / Revised: 10 January 2022 / Accepted: 15 January 2022 /
Published online: 19 February 2022

Abstract
Learning methods have been increasingly used in power engineering to perform various tasks. In this paper, a fault selection procedure in double-circuit transmission lines employing different learning methods is accordingly proposed. In the proposed procedure, the discrete Fourier transform (DFT) is used to pre-process raw data from the transmission line before it is fed into the learning algorithm, which will detect and classify any fault based on a training period. The performance of different machine learning algorithms is then numerically compared through simulations. The comparison indicates that an artificial neural network (ANN) achieves remarkable accuracy of 98.47%. As a drawback, the ANN method cannot provide explainable results and is also not robust against noisy measurements. Subsequently, it is demonstrated that explainable results can be obtained with high accuracy by using rule-based learners such as the recently developed quantitative association rule mining algorithm (QARMA). The QARMA algorithm outperforms other explainable schemes, while attaining an accuracy of 98%. Besides, it was shown that QARMA leads to a very high accuracy of 97% for highly noisy data. The proposed method was also validated using data from an actual transmission line fault. In summary, the proposed two-step procedure using the DFT combined with either deep learning or rule-based algorithms can accurately and successfully perform fault selection tasks but indicating remarkable advantages of the QARMA due to its explainability and robustness against noise. Those aspects are extremely important if machine learning and other data-driven methods are to be employed in critical engineering applications.

Keywords Fault selection · Deep learning · QARMA · Power system protection

✉ Daniel Gutierrez-Rojas
Daniel.Gutierrez.Rojas@lut.fi

1 LUT University, Yliopistonkatu 34, 53850 Lappeenranta, Finland

2 The American College of Greece, Athens, Greece

3 Research and Innovation Development, NetCompany-Intrasoft, Luxembourg City, Luxembourg

4 The University of Manchester, Oxford Rd, Manchester M13 9PL, UK

5 Zhejiang University, Zheda Rd. 38, Hangzhou 310058, China

1 Introduction

Transmission lines are a fundamental part of today's power systems, as they ensure power supply to end consumers by connecting them to far-off large generation plants. Hence, it is crucial to have an adequate protective system that is capable of isolating faults quickly and reliably to prevent any possible damage to other electrical components [29]. The most commonly used device for protection of transmission lines is the distance relay, whose operation relies on the impedance between the fault location and relay installation point. Depending on the network conditions, looped segments, and double circuit lines that share towers [4], short lines, and in-feed from the other end of the line, the measured fault impedance can suffer from certain transitory variations that can cause incorrect operation of the distance relay.

Many transmission line protection schemes are used, but they do not provide intrinsic phase selection (e.g., negative-sequence and zero-sequence line differential, neutral over-current protections). However, information of the faulty phase is required to enable single-pole tripping. As any action performed by the protective system during real-time operations will directly affect the grid dynamics, correct tripping is critical to maintain the system stability and reliability [30]. Distance relaying depends on a fault selector to calculate the impedance in the loop that would lead to line triggering when the protective zone requirements are met. Therefore, a reliable distance relaying protection system for transmission networks must have a high-accuracy fault selector for correct operations in any protective zone for fast trip decision-making. In particular, faults in double-circuit and high-impedance faults rarely pose technical challenges in terms of fault selection and proper relay operation [14, 25, 32]. In addition, mutual impedance from double-circuit transmission lines may affect relay performance. When a fault to ground occurs, the zero-sequence currents from one line induce a voltage in the coupled adjacent line, thereby causing a current to flow in the opposite direction, which may add or subtract to the existing zero-sequence current [20].

Both researchers and relay manufacturers have made great efforts to improve fault classification algorithms to perform fault selection and thereby increase the system robustness. The main difficulty for selecting the correct fault is related to the effects of high resistance on the fault parameters at any given point. This leads to a situation where the fault currents are similar to each other in magnitude, and thus, their classification becomes a difficult computational task. Fault selection methods using one-end recordings can be classified according to the algorithm [27]. Following this approach, they can be divided into two broad classes: classical and emerging methods, primarily differing with respect to the balance between speed and accuracy. Some algorithms can perform the fault selection faster than the time taken by a cycle of the system frequency, but at lower accuracy. On the other hand, others perform the fault selection with high accuracy, but they lack speed and even post-protective actions, and therefore are not suitable for real-time protection and trip decision making based on the faulted loop (distance relays) [28]. These algorithms consider all measurements available, if not, approaches like shown in [21] can deal with missing values.

One remarkable example of a classical method is the symmetrical component angle comparison which checks whether the magnitude of sequence currents is sufficient to reliably perform the task by comparing with a threshold. Depending on the currents that are above the threshold, the fault is selected by comparing the angles, as illustrated in Fig. 1. In particular, either negative- and positive-sequence currents (I_{2F} and I_{1F}, respectively; see Fig. 1a), or negative- and zero-sequence (I_{2F} and I_{0F}, respectively; see Fig. 1b) currents are compared. Both cases must be consistent to perform fault selection.

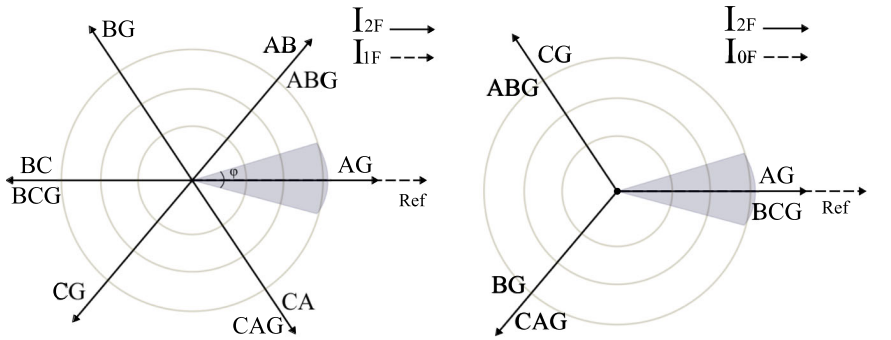

(a) Angle comparison between I_{2F}, I_{1F} **(b)** Angle comparison between I_{2F}, I_{0F}

Fig. 1 Fault selection method based on symmetrical currents

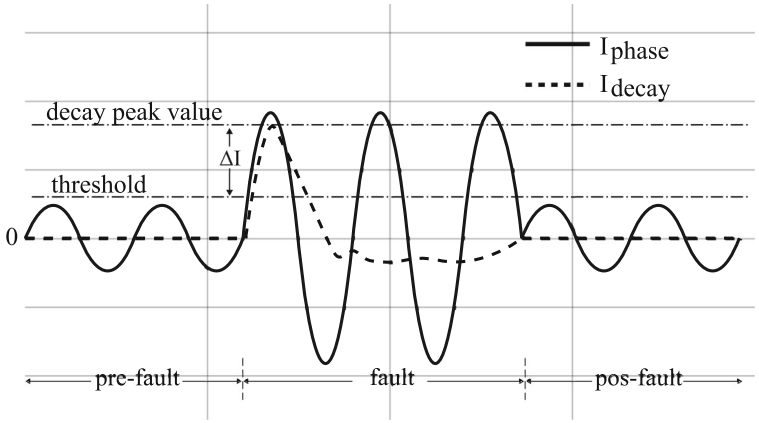

Fig. 2 Fault current from any phase and its associated decaying current

Another classical method is the so-called delta method that uses transient components from faulty continuous currents or voltage signals are used as prefault components. The output components employed in this method are, for example, decaying memory function (as illustrated in Fig. 2), superimposed signals, or Fourier transforms.

One of the most common classical method is the impedance-based algorithm. Its main advantage is to achieve a speed below one cycle of the system frequency, making it very popular in distance relays, being it implemented by different commercial products used for single pole tripping actions. In this method, current and voltage measurements from the fault condition are used to determine the respective zone of operation for each phase (in the case of a single phase-earth fault) or multiple phases in the loop $R - X$ diagram. These measurements are extensively used in numerical relays. Single phase-earth impedance loop characteristics for relays, such as plain impedance, quadrilateral, self-polarised mho [15], offset mho/lenticular, fully cross-polarized mho, or partially cross-polarized mho, can be defined depending on the manufacturer and system conditions.

The other class of fault classification methods and electric power applications are based on emerging computational approaches such as machine learning (ML) or deep learning (DL) [5, 7, 17, 18]. For example, in [6], the authors introduced a non-intrusive fault identification

method in power transmission lines using PS-HST to extract high-frequency fault components. A feed-forward artificial neural network (ANN) was used to select the fault classes. The authors calculated the HST coefficients and obtained a power spectrum based on the Parseval's theorem. In [1], a semi-supervised ML approach based on co-training of two classifiers is presented. The fault selection was performed in both transmission and distribution systems. Feature extraction was performed using a wavelet transform of the current and voltage signals, and a nature-inspired meta-heuristic, harmony search, was used for determining the optimal parameters of the wavelets.

Another emerging method is pattern recognition, having shown promising results compared with conventional methods. For instance in [8], a summation-Gaussian extreme learning machine (SG-ELM) was used for transmission line diagnosis, which includes fault classification and fault location, by means of an iterative back-propagation learning algorithm. In [27], an intrinsic time decomposition (ITD) algorithm was employed to analyze the frequency and time of non-stationary signals, and subsequently, a probabilistic neural network (PNN) to implement fault classification was developed. The advantage of this approach lies in its training speed that enables the entire process to be performed in real time. A power-spectrum-based hyperbolic S-transform (PS-HST) and back-propagation artificial neural network (ANN) were used in [6] to extract high-frequency components of the electric signal generated by an electric fault to improve fault selection coefficients, and fault classes in power transmission networks were then identified with one-end recordings. Three ML models—naive Bayes classifier, support vector (SV), and extreme learning machine—were compared in [26] for fault classification based on the Hilbert–Huang Transform.

Hybrid techniques can also play an important role. Control strategies that involve two or more of the methods described above can be used to increase the reliability and accuracy of fault selection. New numerical relays (with higher processing capabilities) are often employed to effectively select the proper fault and avoid undesirable tripping. Strategies based on ML use classic methods for pre-processing to improve their models [6].

Here, we will give particular attention to the quantitative association rule mining algorithm (QARMA), which has not yet been employed for the fault selection in transmission lines. QARMA has already been tested in several application scenarios and use-cases in the health domain and in predictive maintenance applications in particular (see [10, 11] for results relating to predicting tool Remaining Useful Life in the auto-motive manufacturing industry from the recently concluded PROPHESY project). Within the context of the EU-funded QU4LITY[1] project, QARMA results have been tested against real-world data-sets ranging from tool wear-and-tear to body measurements to compute morphotype fit scores in the fashion industry.

The main reason therefore for choosing QARMA as a tool to study its applicability in the given domain is the success that QARMA-based classifiers and regressors obtained in such varied domains, and given the natural appeal that the output of QARMA offers, in the form of easy-to-understand rules, that we consider are more directly explainable than higher-order approaches to explainability/interpretability such as Shapley values for explaining otherwise black-box models. Still, we compare our main two approaches, namely deep neural networks and QARMA to several other well-known classification algorithms, see Sect. 4.2. The main criteria for the choice of these other algorithms were their prior use in this domain as established in the literature, their overall popularity in the ML field in general, as established by the number of results returned in Google Search for the respective terms, and finally, their explainability/interpretability.

[1] https://qu4lity-project.eu/.

This paper extends the above contributions by proposing a two-stage method. The first stage is the delta method discrete Fourier transform (DM-DFT) that is used to pre-process the raw data from the transmission. The second stage performs a machine learning algorithm for fault selection. We studied different techniques in terms of accuracy and explainability. Our main contributions, also presented in Sect. 4, are as follows:

- We propose a general hybrid methodology based on DM-DFT algorithm that works independent of network topology.
- We test and compare the performance of well-known ML algorithms techniques such as decision trees, neural networks, and support vector machines (SVM).
- We develop a fully explainable method that employs the quantitative association rule mining algorithm (QARMA) [12, 13] and compare its performance with the state-of-the-art ML algorithms (mostly not-explainable).
- We demonstrate with several numerical examples, including real-world data that fault classification task can be solved by QARMA with very high accuracy even when only one-end currents are available, or when the measurements are subject to high levels of noise.

The rest of this paper is divided as follows. Section 2 introduces proposed methodology. Section 3 details the machine learning algorithms employed here, including a detailed description of QARMA. Section 4 presents the numerical results, while Sect. 5 concludes this paper.

2 Proposed method

2.1 Step 1: delta method discrete Fourier transform

To extract fault features (currents and voltages), a combined DM-DFT is employed to identify the fault instance. The DFT maps a given point of the input signal (i.e., current or voltage) into two points in the output signal. For N samples, considering the pair x_n (input signal) and X_k (its DFT)

$$X_k = \sum_{n=0}^{T-1} x_n e^{-2\pi i k n/T}, \tag{1}$$

where $0 \leq k \leq T-1$, and T is the number of samples per cycle and n represents current phase (a, b or c). The DM-DFT uses a moving window of length T instead of the complete signal, thus allowing faster fault recognition. The fault point requires to be within a fault time, which is considered here to be approximately 3.5 cycles. The sampling rate is 4 kHz, i.e., about 80 samples per cycle (which is usually used in commercial relays). To obtain a highly accurate signal point 1.5 cycles or about 120 samples after fault occurrence are needed. When a transmission line is in a faulty state, magnitudes of currents and voltages (which are the features used in the fault classification task) can suddenly change depending on the type of fault and its characteristics. Figure 3 illustrates a cycle in the periodic sinusoidal signal where the DFT calculations are performed. Once the DFT is calculated, variations in the frequency domain can be detected as follows:

$$\text{threshold} = 1.5 I_{n(j)}, \tag{2}$$

$$\Delta I_n = I_{n(j+T)} - \text{threshold}, \tag{3}$$

$$F_i = j + T \leftrightarrow \Delta I \geq 0 \tag{4}$$

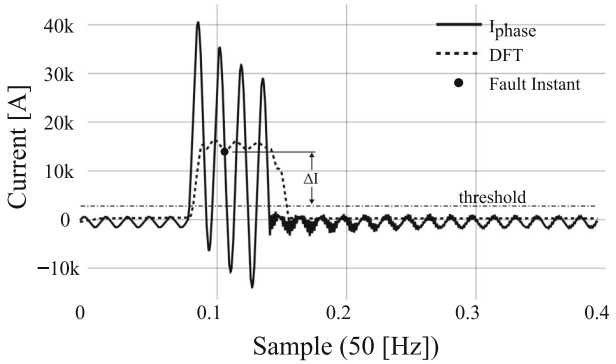

Fig. 3 DM-DFT cycle calculation

where "threshold" refers to the current signal; ΔI_n are the changes in the current signal; $I_{n(j)}$ is the current Fourier value of the jth sample with $0 \leq j \leq S - T$; S is the total number of samples in the signal; and F_i indicates the fault instance. Threshold for the ongoing signal calculation is given by 1.5 times the Fourier pre-fault signal value. A different threshold value is selected based on the experimental results for different fault conditions. The DM-DFT is applied to the three-phase currents without considering if ΔI_n have similar values; it only considers values above the threshold. If multiple ΔI_n are positive, the fault instant is chosen from the phase n that has the highest value. If $\Delta I_n \leq 0$ for all three phases, then it is assumed that there is no fault and the feature extraction is taken randomly from one of the samples of each signal. Delta methods can be seen as detection of high fluctuation of any quantity (like temperature, current, or even monetary value) and is only used to identify faulted point and then method continues with feature extraction. At this stage, it is possible to miss fault points (miscalculation of a given phasor due to wrong time series point) because of threshold values. However, for the data-set obtained in this process, all the faults were detected successfully.

Note that the DFT phasor estimation is less sensitive to noise than the individual measurements, and it is robust to the presence of harmonics [23]. Also the threshold selection can perform even if parallel lines are out of service or if it is applied to transmission lines with different parameters or ratings [16]. That means the threshold is independent of the topology and geometry of the structure. Traditional protection relays use the DFT for protection calculations [23], therefore using the same pre-processing technique to minimize hardware requirements, while providing sufficient information to the neural network. However, the DFT is dependent on the sample frequency, which might be problematic for real-time applications because of the computational time limitations. It means, the DFT calculation might take longer than 20 ms to calculate, which is the time where the trip decision is made in a real-time transmission line scenario.

The process is applied to data-sets (like the one obtained from simulations to be explained in Sect. 4.1) that contain currents and voltages, either with or without a faulted state. The selection is automatically done after DFT procedure is completed. For data-sets with faults, the voltages and current feature extraction are selected at the fault instant point; for the ones without faults, a random point within the signal is selected. The output data-set, listed in Table 1, is the input for the ML methods to be described next. Table 1 contains the absolute values of currents and voltages of local and remote ends of the transmission line. The neutral currents were estimated as a phasorial sum of the *abc* currents.

Table 1 Output from DM-DFT including all datasets with and without faults

Feature	File 1	File 2	…	Last file
$L_{I_A}, L_{I_B}, L_{I_C} \ldots R_{V_C}$	Value	Value	…	Value
Target variable				
Fault type	Value	Value	…	Value

2.2 Step 2: machine learning methods

A number of different established algorithms are then considered for the supervised learning: decision trees, artificial neural networks (both shallow and deep), support vector machines, rule-extraction systems (Ripper-k and QARMA), naive Bayes, logistic regression, and finally ensemble methods (AdaBoost). As already mentioned, the main criteria for selecting the above methods were their prior use in the domain, as established in the current literature, their popularity in the machine learning field, and their explainability/interpretability properties.

These algorithms have different accuracy levels and time to train each model. Moreover, the "explainability" of their models also varies. For example, explainable methods, such as decision trees, usually have poorer accuracy than ANNs. On the other hand, when the training data-set is large enough, an ANN often gives very high accuracy, but it is time consuming, and the resulting model offers little in terms of explainability to humans. The algorithm should then be selected depending on the requirements set between accuracy, time, as well as explainability of the outcome.

In this paper, the focus is on representatives from the class of DL methods and the "explainable artificial intelligence (AI)" families—for an exposition to the latter class, see [22]. We built and tested models with multiple hidden layers of feed-forward nodes trained by mini-batch-based optimization methods (including classical stochastic gradient descent with momentum as well as the Adam [24] optimizer); we also built rule sets extracted using the QARMA algorithm for quantitative association rule mining [13]. These choices were made because of the proven capability of DL methods to obtain very high accuracy given enough data, and also because QARMA is an algorithm that has already been successfully tested for Predictive Maintenance (PdM) related tasks in industrial settings. The output data-set from the DM-DFT is used in all cases, and it contains all the produced features. The target variable, i.e., the fault type (see Table 1), is encoded into eleven different classes (ten fault types plus one no_fault mode) as it has string values (one-hot encoding). Figure 4 presents the flowchart of the proposed two-step method. The DM-DFT is employed for all cases as the preprocessing stage, while the second stage is the different ML algorithms presented here.

3 Selected learning algorithms

This section starts with the algorithm that is expected to have the highest accuracy: the ANN as proposed in [9]. Then, the QARMA algorithm [12] is presented in brief, as it is expected to provide reasonably high accuracy but with the added benefit of explainable outcomes.

3.1 Artificial neural networks

Artificial neural networks (ANN) and in particular feed-forward ANNs, also known as multilayer perceptrons, are a powerful ML tool and have been used extensively for fault diagnosis

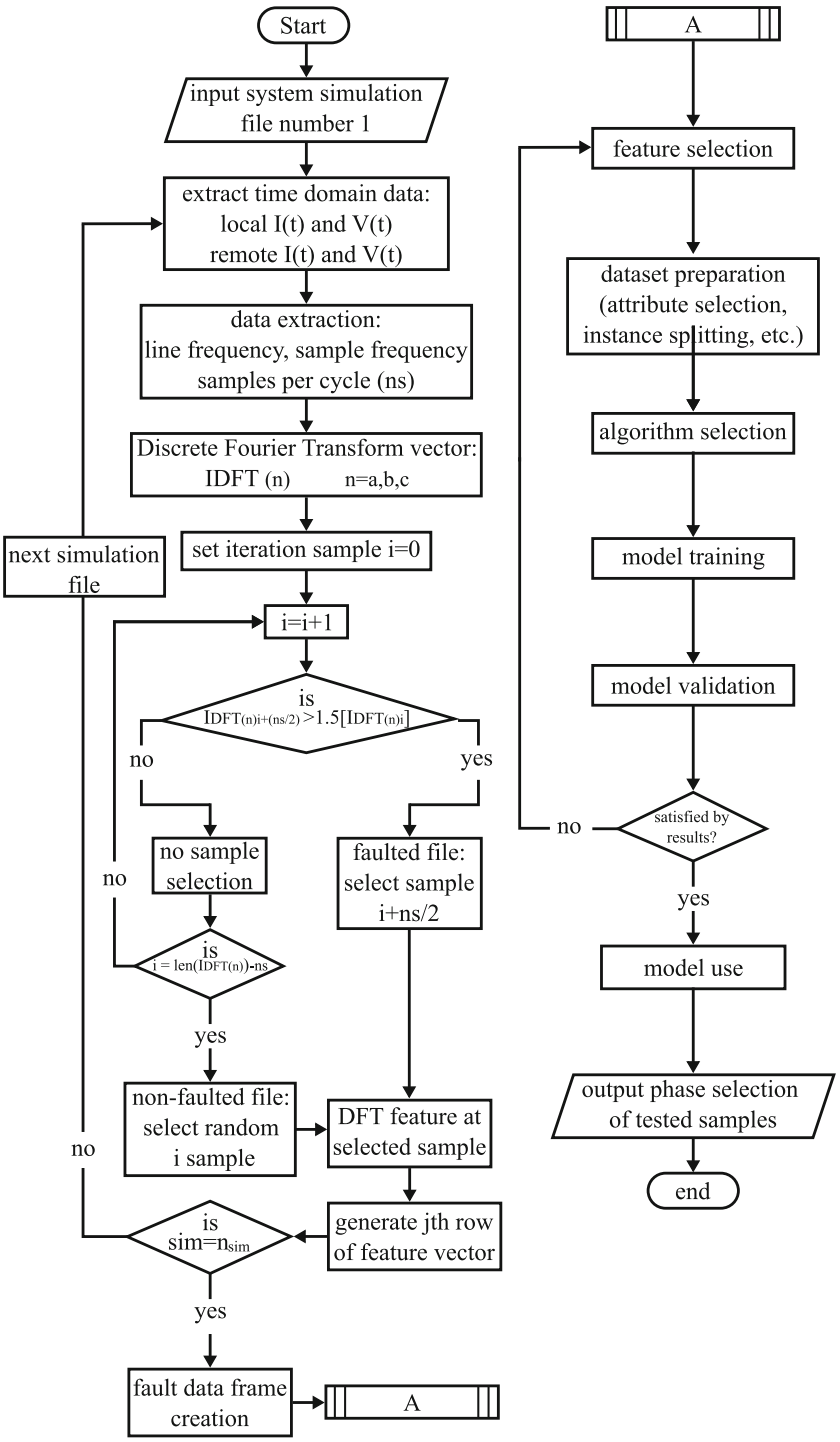

Fig. 4 Flowchart of the fault classification process using ML

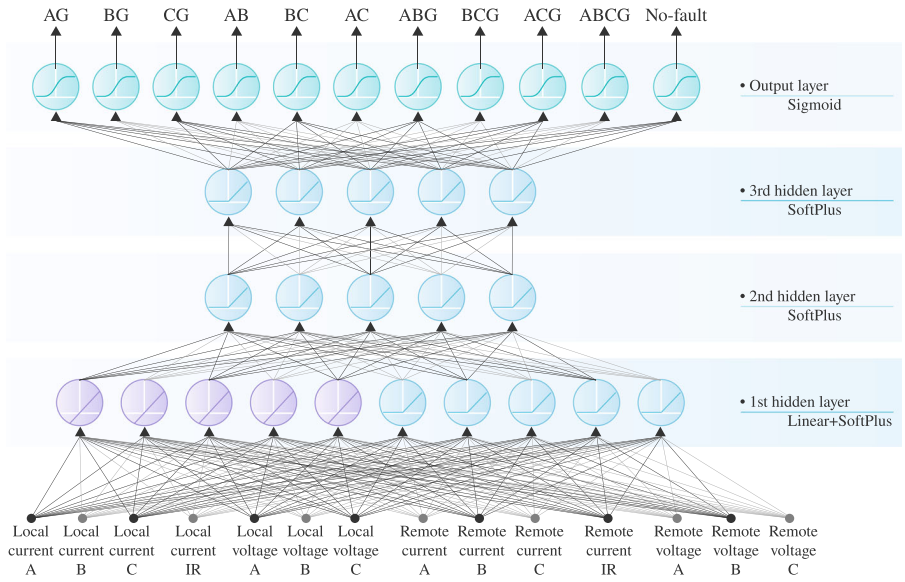

Fig. 5 Structure of a three-stages feed-forward neural network

problems such as the ones mentioned before. The ANN is a feed-forward neural network consisting of three stages. The first stage is the input layer containing the voltages and currents from both ends at the time of fault occurrence given by the DM-DFT along with a fault tag coded into binary form. The second stage is the set of hidden layers, where every node in a particular layer receives inputs from all the nodes in the layer immediately below that layer and sends its output to all nodes in the layer immediately above it. We have experimented with various architectures, shallow and deep, using the Open-Source library popt4jlib (https://github.com/ioannischristou/popt4jlib) that allows for parallel and distributed evaluation of training instance pairs of both the network output as well as the gradient of the network computed via the classical back-propagation algorithm. The third and final stage is the output layer that returns fault type (or no_fault) signals that are encoded back into the phase selection tag. Figure 5 illustrates the procedure, where "Local current A" refers to the current signal of phase *A* measured at the left end of the transmission line (see Fig. 6), while "Remote Current A" refers to the current signal of phase *A* measured at the right end of the transmission line and subsequently with voltages and phase *B* and *C*. Together, they form the features of the data-set. The multi-layer ANN in [9] has the following parameters: two fully connected layers with a rectifier linear unit (ReLU) activation, one output layer with *softmax* activation, categorical cross-entropy loss function, and *adam* optimizer.

In our experiments, the best topology was achieved with a deeper network consisting of 4 layers in total: the first hidden layer consisting of a mixture of 5 linear activation units and 5 SoftPlus activation units (smoother version of ReLU), and the other two hidden layers consisting of 5 SoftPlus activation units each. The output layer, using one-hot encoding, comprised of 11 sigmoid (logistic) activation units, each one corresponding to one of the possible classification results for the problem (10 different fault types and one no_fault type.)

3.2 Quantitative association rule mining for fault diagnosis

Association rule mining (ARM) is a major and still very active research area; implementations of the algorithms developed over the years are found in most popular software packages for data mining, such as WEKA, MOA, KEEL, and Orange. ARM works on datasets that contain subsets of "items." A typical dataset applicable for ARM is a database containing super-market basket data, i.e., the items in customers' shopping carts during check-out. Its major objective is to discover statistical rules that relate the presence of a set of such items to the presence of other items, and a typical association rule for such market basket data would be $Buys(\text{“}Milk\text{”}) \implies Buys(\text{“}Bread\text{”})$ where the implication is understood to hold in a statistical sense, so that the rule means that the percentage of baskets that contain both milk and bread is above a minimum threshold (support of the rule) as well as that the ratio of all baskets that contain both milk and bread over the number of baskets that contain at least milk is above another threshold (confidence of the rule.) The a priori [3] algorithm is a famous early algorithm for discovering all such rules satisfying minimum support and confidence in a given dataset. In the following years, many different authors improved upon this first algorithm (see [19] for a notable example).

However, the above notion of association rules is a "qualitative" one: any possible quantitative attribute belonging to the items is not taken into account. Quantitative association rule mining (QARM) is an extension of the standard ARM that allows for items to quantify any attributes they may have in the rule antecedents and/or consequences, for more precise rules.

An illustrative example of a quantitative association rule would then be $Buys(Milk).price \leq 0.9 \wedge Buys(Bread).price \leq 0.25 \Rightarrow Buys(Sugar).price \leq 0.1$ which says that (for a percentage of customers above the specified support) customers who buy milk at a price less than or equal to $USD\$.9$ and bread at a price less than or equal to $USD\$.25$ will also purchase sugar at a price less than or equal to $USD\$.1$. This is significantly more information than simply knowing that when a customer buys bread and milk they are also likely to buy sugar.

QARMA [12, 13] is a family of efficient novel cluster–parallel algorithms for mining quantitative association rules with a single consequent item, and many antecedent items with different attributes in large multidimensional datasets. Using the standard support-confidence framework of qualitative association rule mining [2], it extends the notions of support, confidence, and many other "interestingness" metrics so that they apply to quantitative rules.

QARMA is configured to produce rules of the form $I_1.attr_1 \in [l_{1,1}, h_{1,1}] \wedge \cdots \wedge I_n.attr_m \in [l_{n,m}, h_{n,m}] \implies J_0.p \in [l_0, h_0]$ or alternatively to produce rules of the form: $I_1.attr_1 \in [l_{1,1}, h_{1,1}] \wedge \cdots \wedge I_n.attr_m \in [l_{n,m}, h_{n,m}] \implies J_0.p = v$. The latter form is very useful in supervised classification problems where the value of the target item attribute is essentially the class variable that is being learned.

QARMA (fully specified in [13], and then extended in [12]) within the particular context of grid fault diagnosis, works as follows:

First, all subsets of variables including the target variable (fault indicator) of length 2, then 3, then 4, up to a user-specified length are constructed, and called "itemsets." Then, the algorithm proceeds sequentially to produce all valid quantitative association rules from each itemset of length 2, then 3, then 4…Within each phase of producing all valid rules of length $l = 2, 3, \ldots$, the algorithm considers in parallel all frequent itemsets of length l. For a given itemset, it produces all possible rules (with each attribute in the rule being un-quantified in the beginning); for each such initially unquantified rule, a possibly different CPU core runs a procedure called $QUANTIFY\_RULE()$ maintaining a local rule set R (initially empty) and runs a modified breadth-first Search procedure that first assigns the consequent attribute

to the highest possible value, and, as long as the resultant partially quantified rule has support above the threshold required, adds it to a queue data structure T.

While this queue is not empty, the first rule inserted in the queue is retrieved and removed from the queue. For each attribute that has not been quantified in it yet, the algorithm creates as many new rules as there are different values in the dataset for the attribute being examined in an ascending attribute order value and enters the queue T in this order, but only if the newly quantified rule exceeds the minimum support requirement. If the partially quantified rule also meets minimum confidence (or any other metric), then it is checked against the current set of local rules R to see if it is dominated by another rule in R. If no other rule in R dominates the current rule, the current rule is added to the set R. After having run this BFS process in parallel for all frequent itemsets of length l, the various CPUs participating in the run synchronize to obtain all rules from all the other ones before moving to process the frequent itemsets of length $l + 1$.

The resulting rule set has the theoretical property that it maximally covers the dataset it has worked on: there is no other rule outside the produced dataset in the form described above that can cover even a single extra instance in the dataset while having the required minimum support and confidence (or other specified interestingness metrics) required. Once the set of all non-dominated rules has been computed, a classifier based on their ensemble works as follows:

1. Select all the rules whose antecedent conditions are satisfied by this instance and add them to the set F;
2. Sort out the rule-set F in decreasing order of confidence and decreasing order of support on the training set;
3. Remove all but the top-100 rules of the sorted set F;
4. Each rule in F carries a weight equal to its confidence on the training set;
5. The weighted majority vote of the rules in F decides the class of the instance.

4 Simulation results

4.1 Test system description

A 400-kV, 50-Hz power system (Fig. 6) was simulated to extract features and then generate the dataset of currents and voltages based on the DFT at a fault point (when there is a fault). Under this setting, 10 different faults can occur involving the electrical phases A, B or C and ground G of the transmission line: three-phase faults (ABCG), bi-phase faults (ABG, BCG, CAG, AB, BC and CA) and mono-phase faults (AG, BG and CG). They differ from each other due to the phases involved and their parameters. The electrical system under study is composed of a double-circuit transmission line typical, for example, in Finland and other European countries. It has two lines connected to a local end marked as L and remote end R. At each end, a source is connected representing a transmission network. These types of lines represent a challenge for correct fault identification and selection owing to the strong impact of mutual impedance on the fault resistance. As for the communication channel, data were gathered by intelligent electronic devices (IED) from both ends and sent via a wireless link (e.g., 4G or 5G) to the fault selector, as shown in Fig. 6. It also presents the data flow blocks how the fault selection is performed and retrieved back to the smart devices for protective actions. The training and testing data-sets were collected in the preprocessing phase.

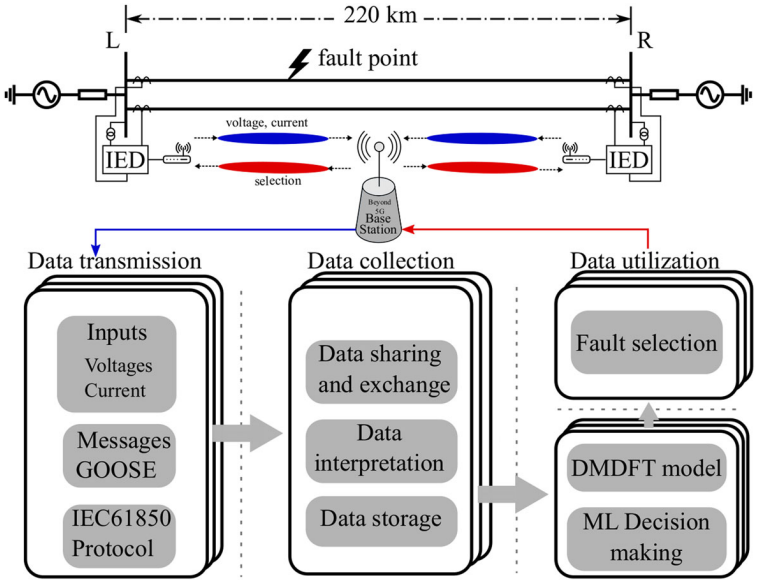

Fig. 6 A 400-kV double-circuit transmission line and data flow

Table 2 Simulation input parameters

Parameter	Training data set	Testing data set
Fault type	None, AG, BG, CG, ABG, BCG, CAG, AB, BC, CA, ABC	None, AG, BG, CG, ABG, BCG, CAG, AB, BC, CA, ABC
Fault resistance (Ω)	0.01, 0.1, 1, 5[a]	Random
Fault distance (%)	10–90 (steps of 10)	Random
Fault inception angles	2 (45° and 90°)	Random
Power flow variation	2	Random
Line parameter error	5	Random
Total size	15,120	5040

[a]Fault resistances from 10–200 Ω (steps of 10 Ω) are only applied for single-phase faults

All the simulations were carried out in MATLAB/Simulink. The simulations were prepared with the specifications shown in Table 2, the transmission line parameters in Table 3. Both normal operations and different fault types (10 in total) were simulated along with different fault resistances (24), fault inception angles (2), line parameter errors (5), high and low power flow (2), and fault locations along the line (9). The simulation comprised 20160 rounds to collect data of both fault and non-faulted systems whose details are presented in Table 2. The resulting data-set is already publicly available.[2]

[2] https://github.com/ioannischristou/popt4jlib/tree/master/testdata/grid_fault.

Table 3 Transmission line parameters

Parameter	Transmission line L–R
Voltage (kV)	400
Length (km)	220
Positive-sequence resistance (Ω/km)	0.0033564
Positive-sequence inductance (H/km)	0.00057347
Positive-sequence capacitance (F/km)	$2.0423e^{-8}$
Zero-sequence resistance (Ω/km)	0.27073
Zero-sequence inductance (H/km)	0.0039052
Zero-sequence capacitance (F/km)	$7.9939e^{-9}$

4.2 Results

Two simulation scenarios and a real fault from a transmission line were used to test the proposed methodology. Note that, for these experiments, all machine learning algorithms ran on the same machine. However, the proposed implementations are fully parallel and do take advantage of all CPU cores available in the computer running the codes. This makes it more computation-efficient. Specifically, QARMA does not require any hyper-parameters to run.

This is not the case for the ANN, though, for which, the architecture (number of layers, number of nodes in each layer, type of each node and so on) must be specified in advance, and forms the set of hyper-parameters that need to be fine-tuned through experimentation and best-practice guidance.

Nevertheless, it is worth mentioning that we do not claim that the parameters of our ANN model are optimal, as they were found by manual search in repeated experiments; they only provided excellent accuracy, and it is only this best set of results for the ANN that we report in this paper. Further, regarding the hyper-parameters required for the other classification algorithms that we experimented with, Naive Bayes requires no hyper-parameters, Ripper-k requires only the number of FOLD iterations which is by default set to 2, Decision Trees, Logistic Regression and Support Vector Machines are famous for requiring very few hyper-parameters (gain criterion function, and penalty factors "w" and "C," respectively); finally, for the AdaBoost.M1 method, that does require the base weak learners to be fully specified, we left the default settings specified in the WEKA package.

Besides, all simulation scenarios were based on typical topologies and parameters used in the specialized literature, which represent real transmission lines and their operation.

4.2.1 Test system 1

In the first test system, the generated data-set was split into two subsets: 75% of a random shuffle of the data-set was kept for training and the remaining 25% was used to validate the accuracy of the trained models. The exact same split was used for all simulations with all different algorithms. Experiments with fivefold cross-validation gave essentially identical results. Table 4 shows the results of running the above-mentioned algorithms for supervised learning on the produced data-set; Fig. 7 shows the results for the classification task. The accuracy achieved with the DL model setup was remarkably high, 98.33%. It was achieved by a 4-layer deep network, with 10 nodes in the first hidden layer (5 linear and 5 SoftPlus units), 5 SoftPlus units in the second layer, and 5 SoftPlus units in the third layer; the output layer had 11 sigmoid units corresponding to each of the 11 fault class types (including the

Table 4 ML results on the fault-grid dataset

Classifier	Accuracy (%)
Decision tree	94.62
ANN (1 hidden layer)	95.18
ANN (3 hidden layer)	**98.33**
SVM	89.05
Ripper-k	86.17
Naïve Bayes	59.42
Logistic regression	78.47
AdaBoost.M1	17.81
QARMA	**98**

Bold indicates the two best accuracy methods

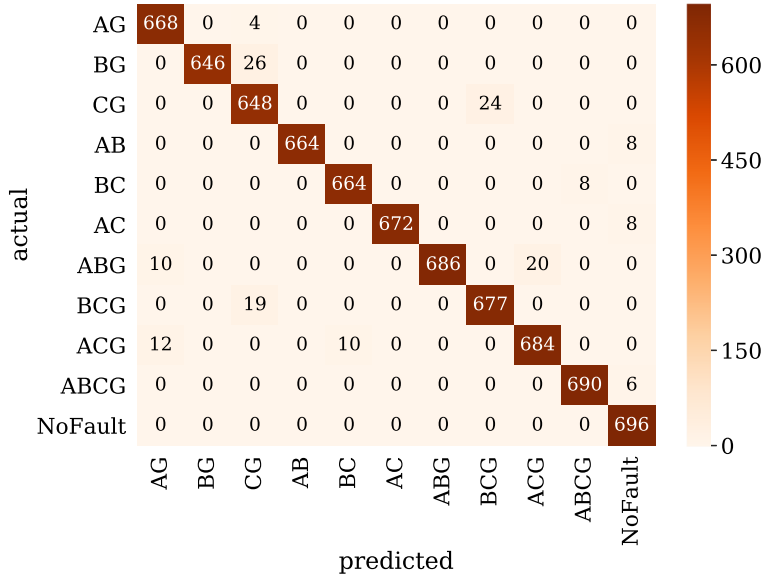

Fig. 7 Fault classification task confusion matrix for test system 1

"no-fault" type). This particular architecture was determined via trial-and-error, as the best observed among 50 different architectures. The total cost function of the network was the sum of square errors of each output node over all training instances. The entire network was trained via stochastic gradient descent (SGD) as the weights optimization algorithm. The backpropagation algorithm was used to compute the overall function gradient (derivatives corresponding to each data instance within a batch computed in parallel and then summed together to form the total gradient). The open-source library popt4jlib (https://github.com/ioannischristou/popt4jlib) was used to train this network, and it also contains the simulation datasets used in this paper. Note that simpler methods such as Naive Bayes or logistic regression did not perform well on this dataset. This happens because the relatively deep neural network employed here has enough layers to produce an intermediate representation that makes it easy for the final layer to classify correctly the 11 different classes; and that

Table 5 Feature selection on original data-set

Round	Feature
1	All features (local and remote current and voltages including I_R)
2	$L_{I_A}, L_{I_B}, L_{I_C}, L_{I_R}$
3	$R_{I_A}, R_{I_B}, R_{I_C}, R_{I_R}$
4	$L_{I_A}, L_{I_B}, L_{I_C}, L_{V_A}, L_{V_B}, L_{V_C}$
5	$R_{I_A}, R_{I_B}, R_{I_C}, R_{V_A}, R_{V_B}, R_{V_C}$
6	$L_{I_A}, L_{I_B}, L_{I_C}$
7	$R_{I_A}, R_{I_B}, R_{I_C}$
8	$L_{V_A}, L_{V_B}, L_{V_C}$
9	$R_{V_A}, R_{V_B}, R_{V_C}$

the large number of produced high-confidence rules leads to majority votes that are usually correctly predicting the fault.

The SGD method was used with a mini-batch size of 50 instances. In addition, normalization of the gradient vector $g(w) = \nabla E(w)$ to 1 before the steepest gradient descent rule $w \leftarrow w - \alpha g(w)$ was important for quick convergence; the learning rate α decayed as the epochs progressed according to the formula $\alpha \leftarrow \alpha 500/(500 + \text{epoch})$. The remarkable validation accuracy was achieved after only 10 epochs in less than 8.6 s of wall-clock training time on an Intel i-9 10920X processor, using all its 24 logical cores. This high accuracy is due to the large size of the simulated fault dataset and equally importantly because of the *balance between the sample sizes of the various classes*. The strong success of the DL model is also because all the voltages and currents from both lines were available, including neutral currents. The faults that were not selected properly were all single-phase-to-ground faults. This can be explained as follows: in those fault cases where the fault resistance took the larger value, only one of the phases changed slightly compared to the other two phases making the feature variation difficult for the model to detect. Further, perfect communication and without any problems related to latency, availability, or synchronization was considered.

With this setup, the importance of availability of all features was tested. Table 5 lists the number of features tested, and Fig. 8 shows the results with an ANN.

With fewer features, the ANN does not perform as well, emphasizing the importance of neutral current estimation. However, when only one-end currents are available, the validation error of the algorithm is still adequate for the task.

We also ran an experiment to test the sensitivity of the neural network to measurement noise; we progressively added more Gaussian white noise (with zero mean and increasing sigma values) to each of the features in our training and/or test data except for the class attribute (fault type.) The results are tabulated in Table 6 and show that for small σ values less than 10, the trained model is still able to classify test data with nearly the same accuracy as when there is no noise in the measurements; however, for large $\sigma = 100$, the neural network accuracy drops significantly, to around 89% which indicates that the trained model is no longer able to accurately identify fault types when measurement noise reaches such high levels. The situation is the same or worse when the training data-set itself suffers from measurement noise: when the training data-set is "polluted" with white noise with small $\sigma = 10$, even when the test data have no noise at all, the accuracy of the trained model

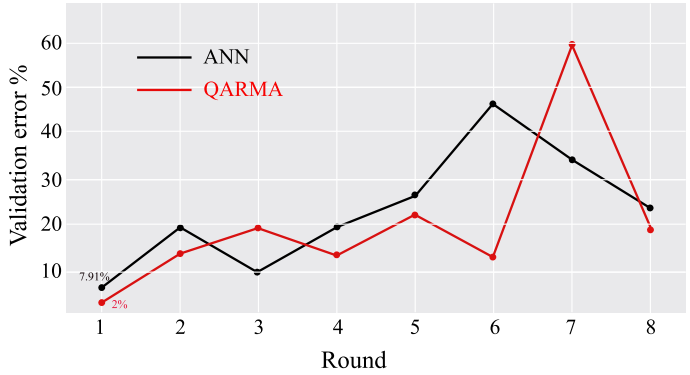

Fig. 8 Validation error obtained with same model parameters using less features

Table 6 Neural network performance under different noise levels in the data

Training σ	Testing σ	NN error%	QARMA error%
0	0.01	2.98	2
0	1	3	2
0	10	3.14	2.01
0	100	11.7	2.23
0.01	0	3.04	2
1	0	3.04	2
10	0	6.1	2.01
100	0	17.84	2.47
100	100	20.67	2.89

drops to less than 94%. When both training and test data are "polluted" with white noise with $\sigma = 100$, the neural network accuracy drops to less than 80%.

We ran QARMA on the same training set with the user-defined support threshold of 3.5%, and the confidence threshold of 90% to obtain 5333 rules covering 97.8% of the entire training set. Then, a slight variant of the decision making algorithm described in the previous section, based on weighted voting, was used: for each instance in our test set, as long as the instance is covered by more than 100 rules, the instance's class is decided upon by the majority vote of the *top 10 firing rules having the highest confidence on the training set; instances that fail the minimum coverage requirement are not classified*. This algorithm resulted in high accuracy comparable with the one obtained by the DL, around 98% but at the following cost: a longer training time (around 15 min of wall clock time on the same i-9 10920X CPU with 24 logical cores.) For a small percentage of testing instances, approximately 4%, QARMA was not able to provide a decision, because of the small number of rules firing on them. However, we expect that QARMA and its decision-making components will compare equally well or even outperform deep learning techniques in training sets that are more highly skewed.

Another advantage of QARMA relates to the sensitivity of the produced rules with respect to noise in the data. We already saw that when the training and testing data suffer from Gaussian white noise with $\sigma = 100$ the performance of the neural network drops just below 80%. On the other hand, when QARMA ran on the same noise-polluted training dataset with $\sigma = 100$, and then the resulting rule-ensemble asked to classify an equally noise-polluted

testing data-set (with $\sigma = 100$), surprisingly, QARMA performance remained very high at 97.11% making QARMA much more robust to noise in the measurements than the neural network. QARMA performance is then very little affected by noise in absolute terms, ranging from 2% of error in the best studied case (first row of Table 6) to 2.9% in the worst (last row).

Even though more research and experiments are needed to fully explain why this might happen, we believe that the answer about the cause of the difference of robustness between the two classifiers is probably lying on the underlying models' complexity: the NN being a deeply composite function of many variables (connection weights and bias thresholds) when optimized on a noise-polluted training data-set is easier to over-fit, and "learn" some of the noise in its weights. On the other hand, QARMA being a rule extractor that learns rules that have only a small number of different features in their antecedent conditions provides an ensemble of simple if-then decision rules that are more likely to hold true in the presence of noise.

Besides, QARMA produces a model with a set of quantitative rules that are much easier to understand and reason about than most of the other models, and DL models in particular; this makes QARMA results much easier to explain to humans than any other model. Every extracted rule is trivially checked against the training data-set for validation purposes, and it is also trivial to understand "what it means" since the preconditions of the rule are nothing more than a conjunction of the restrictions of the attributes that comprise the rule's antecedents to certain intervals. This ease of understanding of rules is what has made them particularly attractive since the beginning of AI and ML research. In fact, already since the 1980s, there have been attempts to extract the knowledge that is embedded in neural network models into sets of rules [31] since such rule sets were recognized from the beginning as the most obvious knowledge representation that can exist. Therefore, QARMA is, in general, a particularly good fit for the newly emerging "eXplainable Artificial Intelligence" (XAI) paradigm, the term "explainable" meaning that the resulting model that the algorithm produces can be easily understood by humans.

4.2.2 Test system 2

A different line configuration was also tested in order to evaluate the generalization capabilities. The test system 2 consists of a single-circuit 400-kV transmission line connected to two Thevenin equivalents. Although this is a simpler system that does not have the same impact of mutual impedance of double-circuit transmission lines, the inclusion of this simulation in the data-set allows the analysis of generalizing the solution to different systems. A data-set containing 990 rows was used for testing the original model; the ANN achieved an accuracy of 98.8% while QARMA achieved 98.1% for all faulty classes and non-faults in this system. The results were slightly better than the test performed on the original data-set, showing the viability of DMFT for fault detection and the ANN/QARMA for classification. The confusion matrix of the mentioned test can be seen in Fig. 9.

We also ran a symmetrical algorithm method using the model data-set for this paper. This method is used as the basis for comparison of our proposed approach because it is employed by one top relay manufacturer. The results can be seen in Fig. 10 (note that a confusion matrix like the one presented in Fig. 9 cannot be used for comparing all faults using the symmetrical method because the datasets have different lengths; only AC, BC and CG faults can be compared in that way). The accuracy of this method for single-phase faults can is represented in Table 7 along with the false positive single-phase detection. False positive in this context is seen as the number of single-phase faults selected by the symmetrical method

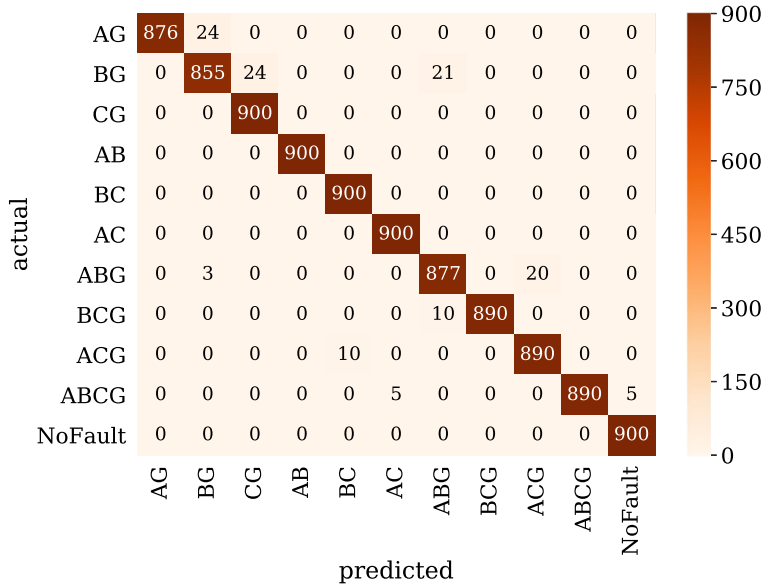

Fig. 9 Fault classification task confusion matrix for test system 2

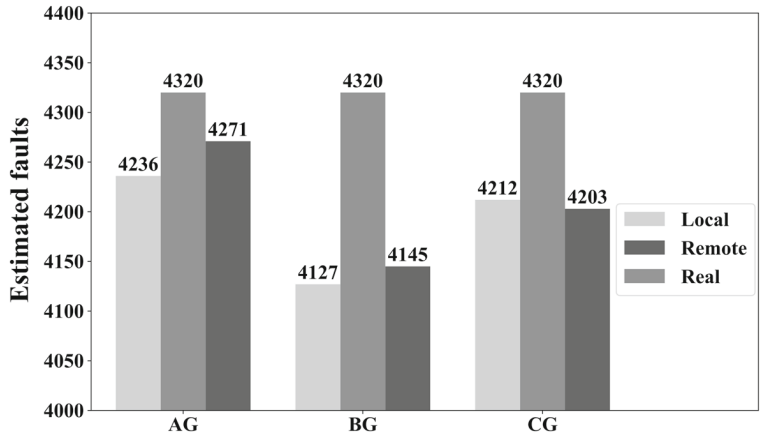

Fig. 10 Fault classification by symmetrical angle method

given that the real fault involved at least 2 phases. Under those conditions, the classification strategy takes the system to a situation less secure than with a tripolar tripping.

In summary, the results shown in Fig. 7 indicate that the errors in the proposed method occurred in the form of lack of identification of some faults. Since fault selection systems are meant to be associated with protection algorithms, those errors can cause an unnecessary tripolar breaker opening—security error. Considering an interconnected system, security errors are less likely to cause system-wide power outages than protection dependability errors. Therefore, in comparison with the symmetric method, the proposed solution will promote better system stability than the traditional method's results depicted in Table 7.

Table 7 Results obtained by replicating symmetrical method

	Dependability		Security	
	Local end (%)	Remote end (%)	Local end	Remote end
AG	98.05	98.86	910	910
BG	95.53	95.94	896	909
CG	97.50	97.29	880	880

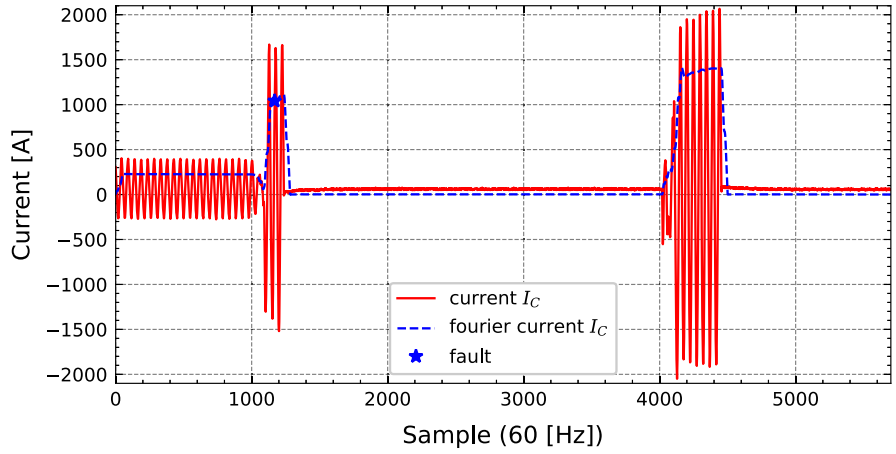

Fig. 11 Phase C and DFT of real transmission system fault

4.2.3 Real fault file

To test the proposed procedure, we used a real fault file from a transmission system located in Brazil, whose exact location cannot be disclosed. Real faults are usually gathered by fault recorders in *.cvg* files, we used an algorithm to convert into matrices (*.mat*) for easier processing. Once the voltages and currents matrices are obtained, they can be injected in DM-DFT algorithm that yields the fault point and extracts the features as seen in Fig. 11.

In real situations, faults can suddenly reappear for reasons as re-closure or reinsertion. This is the case on the CG-type fault we see in Fig. 11. The algorithm detects successfully the first fault occurrence and also locate the exact sample where the phasors are extracted to perform selection. The NN and QARMA techniques were applied in the real fault data with a successful result: both correctly classify the fault as CG. Particularly with QARMA, it yielded 1100 rules that predicted the class of the fault, which resulted in the overall correct classification of the test case. One of the highest confidence rules for this test case was,

$$\begin{aligned} &[\text{local\_voltage}_A >= 235730.0266612848] \\ &\text{AND } [\text{local\_voltage\_}B >= 231130.0132737731] \\ &\text{AND } [\text{remote\_ir} >= 321.3212781340371] \\ &\quad \Rightarrow [\text{fault\_type} = \text{CG}]. \end{aligned} \tag{5}$$

The support of this rule on the training set is 2.72%, and it holds with confidence 100%.

4.3 Discussion

4.3.1 Implications of the results

Current implementations for real-time use cases, such as relay 21 in transmission lines, usually employ a full cycle of phasor estimation and around 4 ms of angle comparison between current/voltage components, as reported by some manufacturers. With either of the studied methods (DL or QARMA), once the model is generated based on historical data of the target system, the time taken to perform phase evaluation given a single-phase fault in the system is as small as 4 ms. Therefore, both methods can reliably select the faulty phase in the relay to make additional trip decisions. The algorithms described in this paper that are commonly implemented in relays in operation today employ a full cycle Fourier phasor estimation for both the protection and the phase estimation. Because the phasor calculation is done in real time, it is based on the Fourier transform (or another filter with a similar output) that provides the root-mean-square (RMS) value required for the proposed phase estimation, implying that only the phase selection itself has to be calculated.

Distance relays (ANSI 21) require 4 ms of angle comparison between current/voltage components, as reported by some manufacturers. The process to utilize the algorithms' outputs only requires multiplications and additional operations, making it more computationally efficient than most phasor operations and suitable for use in real-time applications.

4.3.2 Communication systems

As for the requirements for a communication setup where one can perform phase selection, no communication is needed between the two ends as a signal input, because once the model is generated, the validation is performed at the end. However, there is still a need for communication for data gathering from both ends for phasor estimation. Current mobile communication advances could enable wireless communication between the ends for instantaneous data gathering of currents and voltages, and interface diversity could enable a centralized system that is cheaper to implement in a communication architecture, as shown in Fig. 6.

4.3.3 Explainable results

When comparing the results of the DL method against the ones provided by QARMA, it is clear that the rule set produced by QARMA leads to a slightly lower accuracy than the DL method, while still being highly accurate. However, the resulting QARMA model is by default much more "explainable" than the DL model and has the extra advantage that it can be "reverse-engineered" much more easily than any other model. As an example, consider the following QARMA produced rule:

$$\begin{aligned} &\text{local\_current\_}A \in [433.89, 589.99] \\ &\quad \wedge \text{ local\_current\_}B \in [433.96, 564.25] \\ &\quad \Longrightarrow \text{ fault\_type} = 10 \text{ (no\_fault)} \end{aligned} \tag{6}$$

which holds with support 3.66% and confidence 91.84% on the training set. This rule is highly statistically significant as it has conviction 1,115.06, and lift equal to 10.13. It is also obvious to a human what it means. As another example, consider the rule:

$$\text{local\_current\_}A \geq 438.39$$

$$\wedge\ \text{local\_voltage\_}B \geq 235721.9\ \wedge \text{local\_voltage\_}C \geq 225592.7$$
$$\Longrightarrow\ \text{fault\_type} = 0\,(\text{AG}) \tag{7}$$

holding with support 4.19% and confidence 95.06%. Again, a human can understand what the rule means instantly.

When the QARMA rule set leads to a false diagnosis, it is trivial to see which set of rules led to the wrong decision. These rules can then be individually checked by human experts to see if their validity still holds in the face of new data and/or operating system conditions. Thus, at least, in principle, the entire model can be monitored and "debugged" in real time by human experts when it is put in production. This contrasts with models that make decisions based on the output of a highly nonlinear equation.

When less features are available in the training set, it has been shown that performance drops as expected. In certain cases, the performance degrades gracefully, but it can also be more serious. This performance degradation could be mitigated to a larger extent if we performed our simulations allowing the design of the deep network to vary with all hyper-parameters, from the number of layers and the number of epochs chosen, to the optimization algorithm used for the learning of the network weights and threshold biases. However, with such an approach, the ML process shown in Fig. 4 would essentially have to be repeated anew. Instead, we show how a network with predefined hyper-parameters, in particular those proposed in Sect. 3, performs when trained on different subsets of the original training dataset containing less features, such as local only information (local currents or local voltages and so on.)

Moreover, we also presented key aspects related to the real dataset from a transmission line and how the proposed method can be used by power engineers on their operational decision-making, including the association rules provided by QARMA that "explain" the fault selection. Results from association rules improve the knowledge on how power systems work in face of stressful events. This is indeed an important step if traditional engineering fields would rely more on machine learning methods. This sort of new explaining knowledge is to become evermore frequent in real-world applications as well as in academic research.

5 Conclusion

In this paper, we have proposed and analyzed a two-step methodology for selecting faults in double-circuit transmission lines. In the first step, the DFT was used to pre-process the raw data from the transmission lines. Subsequently, different learning algorithms were employed in the second step to detect and classify any fault based on a training period, and their performances were compared through numerical simulations. The presented two-step approach has been proven to be highly robust against high resistance faults and faults that occur in lines with high mutual impedance. The results have shown high phase selection for all types of faults and even identified recordings that do not present faulty states.

Among the different benchmarked learning methods, deep neural networks have reached an accuracy of 98.33% of correct selection, while the QARMA reached 98% accuracy. However, interestingly, the QARMA is also an explainable algorithm (i.e., the outcomes have explainable explicit internal relations between features) and also robust against noisy measurements unlike ANNs. This makes QARMA a highly suitable approach to achieve high robustness and high accuracy with explainable model outcomes. Future work will include the communication delay of the current and voltage signals sent to the central processing unit from the IEDs to evaluate the performance of the proposed method.

Acknowledgements This paper is partly supported by Academy of Finland (AKA) via EnergyNet Research Fellowship n.321265/n.328869. This work is also part of FIREMAN project supported by the CHIST-ERA Grants: (a) CHIST-ERA-17-BDSI-003 (b) T9EPA3-00017 and by Academy of Finland (n. 326270). We would like to thank Dr. Hanna Niemelä for valuable comments and for helping to proofread this paper.

Funding Open Access funding provided by LUT University (previously Lappeenranta University of Technology (LUT))

Declarations

Conflict of interest The authors declare that they have no conflict of interest.

References

1. Abdelgayed TS, Morsi WG, Sidhu TS (2018) Fault detection and classification based on co-training of semi-supervised machine learning. IEEE Trans Ind Electron 65(2):1595–1605
2. Adamo J-M (2001) Data mining for association rules and sequential patterns. Springer, New York
3. Agrawal R, Srikant R (1994) Fast algorithms for mining association rules. In: 20th International conference on very large databases, pp 487–499
4. Bak CL, da Silva FF (2018) Deploying correct fault loop in distance protection of multiple-circuit shared tower transmission lines with different voltages. J Eng 2018(15):1087–1090
5. Chamoso P, De Paz JF, Bajo J, Villarrubia G (2018) Agent-based tool to reduce the maintenance cost of energy distribution networks. Knowl Inf Syst 54(3):659–675
6. Chang H-H, Linh NV, Lee W-J (2018) A novel non-intrusive fault identification for power transmission networks using power-spectrum-based hyperbolic s-transform—part I: fault classification. IEEE Trans Ind Appl 54(6):5700–5710
7. Chen K, Hu J, He J (2018) Detection and classification of transmission line faults based on unsupervised feature learning and convolutional sparse autoencoder. IEEE Trans Smart Grid 9(3):1748–1758
8. Chen YQ, Fink O, Sansavini G (2018) Combined fault location and classification for power transmission lines fault diagnosis with integrated feature extraction. IEEE Trans Ind Electron 65(1):561–569
9. Chollet F (2018) Deep learning mit Python und Keras: Das Praxis-Handbuch vom Entwickler der Keras-Bibliothek. MITP-Verlags GmbH & Co. KG, Blaufelden
10. Christou I et al (2020) End-to-end industrial iot platform for actionable predictive maintenance. In: 4th IFAC Workshop on advanced maintenance engineering, services and technologies. IFAC
11. Christou I et al (2020) Predictive and explainable machine learning for industrial internet of things applications. In: IEEE Distributed computing on sensor systems conference on, workshop on IoT applications and industry 4.0. IEEE
12. Christou IT (2019) Avoiding the hay for the needle in the stack: online rule pruning in rare events detection. In: 16th International symposium on wireless communication systems (ISWCS). IEEE, pp 661–665
13. Christou IT, Amolochitis E, Tan Z-H (2018) A parallel/distributed algorithmic framework for mining all quantitative association rules. arXiv preprint arXiv:1804.06764
14. da Silva FF, Bak CL (2017) Distance protection of multiple-circuit shared tower transmission lines with different voltages—part II: fault loop impedance. IET Gener Transm Distrib 11(10):2626–2632
15. Domzalski MJ, Nickerson KP, Rosen PR (2001) Application of mho and quadrilateral distance characteristics in power systems [relay protection]. In: 2001 Seventh international conference on developments in power system protection (IEE), pp 555–558

16. Fan X, Zhu Y (2010) Study on fault phase selection based on FFT and phase-separation current phase difference of high-voltage transmission lines. In: 2010 IEEE International conference on mechatronics and automation. IEEE, pp 762–767
17. Gashteroodkhani O, Majidi M, Etezadi-Amoli M (2020) A combined deep belief network and time-time transform based intelligent protection scheme for microgrids. Electric Power Syst Res 182:106239
18. Gururajapathy S, Mokhlis H, Illias H (2017) Fault location and detection techniques in power distribution systems with distributed generation: a review. Renew Sustain Energy Rev 74:949–958
19. Han J, Pei J, Yin Y (2000) Mining frequent patterns without candidate generation. ACM SIGMOD Record 29(2):1–12
20. Holbeck JI, Lantz MJ (1943) The effects of mutual induction between parallel transmission lines on current flow to ground faults. Electr Eng 62(11):712–715
21. Huang H, Yan Q, Zhao Y, Lu W, Liu Z, Li Z (2017) False data separation for data security in smart grids. Knowl Inf Syst 52(3):815–834
22. Jia Y, Bailey J, Ramamohanarao K, Leckie C, Ma X (2019) Exploiting patterns to explain individual predictions. Knowl Inf Syst 62(3):927–950
23. Junior GM, Di Santo SG, Rojas DG (2016) Fault location in series-compensated transmission lines based on heuristic method. Electric Power Syst Res 140:950–957
24. Kingma DP, Ba J (2017) Adam—a method for stochastic optimization. arXiv preprint arXiv:1412.6980
25. Mahfouz MM, El-Sayed MA (2016) Smart grid fault detection and classification with multi-distributed generation based on current signals approach. IET Gener Transm Distrib 10(16):4040–4047
26. Mishra M, Rout PK (2018) Detection and classification of micro-grid faults based on HHT and machine learning techniques. IET Gener Transm Distrib 12(2):388–397
27. Pazoki M (2018) A new fault classifier in transmission lines using intrinsic time decomposition. IEEE Trans Ind Inform 14(2):619–628
28. Price E, Einarsson T (2008) The performance of faulted phase selectors used in transmission line distance applications. In: Proceedings of 61st annual conference for protective relay engineers, pp 484–490
29. Rajaraman P, Sundaravaradan N, Meyur R, Reddy MJB, Mohanta D (2016) Fault classification in transmission lines using wavelet multi-resolution analysis. IEEE Potentials 35(1):38–44
30. Taheri MM, Seyedi H, Mohammadi-ivatloo B (2017) DT-based relaying scheme for fault classification in transmission lines using MODP. IET Gener Transm Distrib 11(11):2796–2804
31. Towell GG, Shavlik J (1994) Knowledge-based artificial neural networks. Artif Intell 70(1–2):119–165
32. Vyas BY, Das B, Maheshwari RP (2016) Improved fault classification in series compensated transmission line: comparative evaluation of Chebyshev neural network training algorithms. IEEE Trans Neural Netw Learn Syst 27(8):1631–1642

Daniel Gutierrez-Rojas received the B.Sc. degree in Electrical Engineering from University of Antioquia, Colombia in 2016 and the M.Sc. degree in Protection of Power Systems University of São Paulo, Brazil, in 2017. From 2017 to 2019, he worked as security of operation and fault analyst for Colombia's National electrical operator. He is currently working toward the Ph.D. degree at the School of Energy Systems at LUT University, Finland. His research interests include predictive maintenance, power systems, microgrids, mobile communication systems and electrical protection systems.

Ioannis T. Christou received the Dipl. Ing. degree in electrical engineering from the National Technical University of Athens, Greece, in 1991, the MSc and PhD degrees in computer sciences from the University of Wisconsin at Madison in 1993 and 1996, respectively, and the MBA degree from NTUA and Athens University of Economics and Business in 2006. He has been with Delta Technology, Inc., as a senior developer, with Intracom S.A. as an area leader in data and knowledge engineering, and with Lucent Technologies Bell Labs as a member of technical staff. He has also been an adjunct assistant professor with the Department of Computer Engineering and Informatics, University of Patras, Greece, adjunct professor at the Information Networking Institute of Carnegie-Mellon University in Pittsburgh, PA, and professor of big data at Athens Information Technology. He is currently a Sr. research data scientist at the Dept. of Research and Innovation Development at NetCompany-Intrasoft (Luxemburg), and an associate professor at the American College of Greece (Greece). He has published more than 80 papers in high-impact journals and conferences in the areas of computational intelligence, data mining, optimization, and parallel computing.

Daniel Dantas received the B.S. degree in electric and electronic engineering from the University of Brasilia, in 2012 and the Ph.D. degree in electrical power systems from the University of São Paulo, in 2019. He worked in protection and control systems in different capacities for utilities in Brazil, Canada, and as a researcher in the University of Manchester. Currently, he is at National Grid UK.

Arun Narayanan received his B.E. degree in Electrical Engineering from Visvesvaraya National Institute of Technology, Nagpur, India and M.Sc. in Energy Technology from Lappeenranta University of Technology (LUT), Finland, in 2002 and 2013, respectively. He subsequently completed his Ph.D. from the School of Energy Systems, LUT University, in 2019. He is currently a Postdoctoral researcher with LUT University, Lappeenranta, Finland, in the research group "Cyber-Physical Systems Group." His research interests include renewable energy-based smart microgrids, electricity distribution and markets, demand-side management, energy management systems, and information and communications technology. He focuses on applying optimization, computational concepts, and artificial intelligence techniques to renewable electrical energy problems.

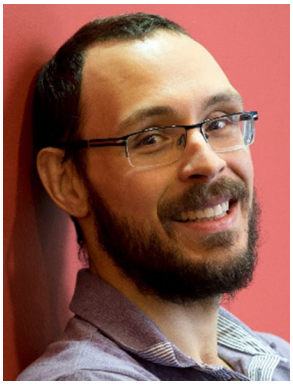

Pedro H. J. Nardelli received the B.S. and M.Sc. degrees in electrical engineering from the State University of Campinas, Brazil, in 2006 and 2008, respectively. In 2013, he received his doctoral degree from University of Oulu, Finland, and State University of Campinas following a dual degree agreement. He is currently Associate Professor (tenure track) in IoT in Energy Systems at LUT University, Finland, and holds a position of Academy of Finland Research Fellow with a project called Building the Energy Internet as a large-scale IoT-based cyber-physical system that manages the energy inventory of distribution grids as discretized packets via machine-type communications (EnergyNet). He leads the Cyber-Physical Systems Group at LUT and is Project Coordinator of the CHIST-ERA European consortium Framework for the Identification of Rare Events via Machine Learning and IoT Networks (FIREMAN). He is also Adjunct Professor at University of Oulu in the topic of "communications strategies and information processing in energy systems". His research focuses on wireless communications particularly applied in industrial automation and energy systems. He received a best paper award of IEEE PES Innovative Smart Grid Technologies Latin America 2019 in the track "Big Data and Internet of Things". He is also IEEE Senior Member. More information: https://sites.google.com/view/nardelli/

Yongheng Yang received the B.Eng. degree in Electrical Engineering and Automation from Northwestern Polytechnical University, China, in 2009and the Ph.D. degree in Energy Technology (power electronics and drives) from Aalborg University, Denmark, in 2014. He was a postgraduate student with Southeast University, China, from 2009 to 2011. In 2013, he spent three months as a Visiting Scholar at Texas A&M University, USA. Since 2014, he has been with the Department of Energy Technology, Aalborg University, where he became a tenured Associate Professor in 2018. In January 2021, he joined Zhejiang University, China, where he is currently a ZJU100 Professor with the Institute of Power Electronics, College of Electrical Engineering. His current research interests include the grid-integration of photovoltaic systems and control of power converters, in particular, the mechanism and control of grid-forming power converters and systems. Dr. Yang was the Chair of the IEEE Denmark Section (2019-2020). He is an Associate Editor for several IEEE Transactions/Journals. He is a Deputy Editor of the IET Renewable Power Generation for Solar Photovoltaic Systems. He was the recipient of the 2018 IET Renewable Power Generation Premium Award and was an Outstanding Reviewer for the IEEE TRANSACTIONS ON POWER ELECTRONICS in 2018. He received the 2021 Richard M. Bass Outstanding Young Power Electronics Engineer Award from the IEEE Power Electronics Society (PELS). In addition, he has received two IEEE Best Paper Awards. He is currently the Secretary of the IEEE PELS Technical Committee on Sustainable Energy Systems.

Publication IV

Gutierrez-Rojas, D., Räsänen, P., Belisario, A. B., Dzaferagic,
M., Almeida, G. M. and Nardelli, P. H. J.

Improving Fault Detection in Industrial Processes by Event-Driven Data Acquisition

Reprinted with permission from
IEEE Access
Vol. 10, pp.80918–80931, Jul. 2022

IEEE Access
Multidisciplinary ⋮ Rapid Review ⋮ Open Access Journal

Received 27 June 2022, accepted 18 July 2022, date of publication 21 July 2022, date of current version 5 August 2022.

Digital Object Identifier 10.1109/ACCESS.2022.3192972

RESEARCH ARTICLE

Improving Fault Detection in Industrial Processes by Event-Driven Data Acquisition

DANIEL GUTIERREZ-ROJAS[1], (Student Member, IEEE), PEKKA RÄSÄNEN[1], ANA BRANDÃO BELISÁRIO[2], MERIM DZAFERAGIC[3], GUSTAVO MATHEUS DE ALMEIDA[2], AND PEDRO H. J. NARDELLI[1], (Senior Member, IEEE)

[1]Department of Electrical Engineering, School of Energy Systems, LUT University, 53850 Lappeenranta, Finland
[2]Department of Chemical Engineering, School of Engineering, Federal University of Minas Gerais, Belo Horizonte 31270-901, Brazil
[3]CONNECT, Trinity College Dublin, Dublin 2, D02 PN40 Ireland

Corresponding author: Daniel Gutierrez-Rojas (daniel.gutierrez.rojas@lut.fi)

This work was supported in part by the Academy of Finland through the EnergyNet Research Fellowship under Grant 321265 and Grant 328869, in part by the Academy of Finland through the FIREMAN Consortium under Grant 326270, and in part by the CHIST-ERA under Grant CHIST-ERA-17-BDSI-003.

ABSTRACT Data acquisition in process industries usually takes place at each sampling. The disadvantage is that a considerable amount of data without new information about the state of the process is continuously transmitted and processed. This negatively affects the communication system and computational power, which is more critical nowadays given the number of variables measured, even in seconds. One solution concerns the event-driven paradigm, in which only relevant data according to a pre-defined criterion is forwarded for further processing. This work investigated the event-based threshold and delta methods in the context of fault detection. The data transmission rate was also analyzed. The well-know Tennessee Eastman problem (TEP) was used as a case study. The fault detection system was based on PCA (principal component analysis), which is widely used for this purpose in this benchmark. The results were compared with the commonly used time-based approach, for a fixed false alarm rate. The threshold rule provided similar results, but with much less data. For the delta rule, significant MDR (missed detection rate) gains of up to 74% were obtained for five of the six hard-to-detect faults, and of up to 69%, for two of the three very hard-to-detect faults. MDR values very close to zero were reached for two of the three intermediate detection faults and two of the hard-to-detect faults. The detection time was also evaluated. In this regard, considerably lower values were obtained for all intermediate detection faults, three of the hard-to-detect faults and all very hard-to-detect faults. In short, the delta method was able to improve fault detection performance, especially for hard-to-detect faults, with a considerably lower data transmission rate, around 20% on average. Event-driven data acquisition can be very attractive for process industries.

INDEX TERMS Data acquisition, event-driven, signal reconstruction, fault detection, PCA, Tennessee benchmark.

I. INTRODUCTION

Data acquisition based on a fixed time interval is commonly used in continuous process industries worldwide [1]. The disadvantage of this procedure is that a fair amount of data without new information about the state of the process is continuously transmitted and processed. This data can overwhelm system communication and limit computing power, resulting in information loss. Currently, high frequency data sampling nowadays through a multitude of industrial sensors, even within seconds, exacerbates this problem. In this context, the challenge is to select only data that carry new information for transmission and further processing.

Event-based data acquisition is an alternative to periodic procedure, since events are asynchronous in nature [2].

The associate editor coordinating the review of this manuscript and approving it for publication was Baoping Cai.

An event refers to a significant change in a signal according to a predefined threshold [3]. In process industries, a considerable change in a measured variable is often associated with new information about the state of the process, which would actually require processing. Variables measurements can be used directly, or their variations (derived). This strategy favors communication and data processing, which in turn can result in energy savings and running more tasks in parallel [4]. The event-based paradigm emerged in the context of system control [5]–[10]. More information can be found in [3], [4].

Several potential advantages using event-driven data acquisition strategies have been reported in the literature. They pertain to data storage, channel bandwidth, signal reconstruction, communication system, and sensor power consumption, to name a few. Below are examples of works from different areas of knowledge. [11] used an event-driven mechanism to update information about unreliable links in network switched systems. The authors reported a gain in network security and bandwidth. [12] described an event-based analysis of a solar distribution feeder integrated into distribution substations. The authors highlighted an improvement in event detection, analysis of the impact of solar production, and understanding of the dynamics of the solar feeder control system. [13] employed smart meters through event-driven sampling for data acquisition and feature extraction to disregard redundant information. The authors reported that this data filtering facilitated the identification of energy consumption patterns of devices by vector support machines. [14] designed an event-based model predictive control strategy to more efficiently reconfigure production logic in real-time. An industrial sewing machine production plant was used as a case study, focusing on smart factories. [15] investigated event-based sampling techniques for more efficient node communication and power consumption in wireless sensor networks (WSN). The application involved air quality monitoring. According to the authors, smarter data acquisition would contribute to increasing the life cycle of sensor nodes, since data transmission is currently the main source of energy consumption. [16] compared time- and event-based sampling strategies in electricity grids. The authors reported that the latter was able to perform the signal reconstruction satisfactorily. [17] used Monte Carlo simulation to perform component reliability analysis in complex and dynamic systems using dynamic fault tree. As this is time consuming, an event-driven simulation approach was applied disregarding the gate simulations without significant changes in the output. The authors reported that this data filtering increased computational efficiency. [18] presented an event-driven architecture in the context of Industry 4.0 for manufacturing systems. The focus was on more efficient integration of data from devices and services at all levels for more flexible and timely decisions. [19] developed an information system to detect significant events in collaborative processes in modern business environments. The authors aimed to provide more agile responses to improve interaction between people, devices and organizations. [20] applied an event-driven strategy, in combination with MPCA (multiway principal component analysis), to monitor a SBR (sequencing batch reactor) wastewater process, which outperformed the time-based approach. [21] investigated techniques for developing event-oriented control systems for batch processes. The authors reported gains in engineering and economics aspects. [22] proposed a reduction in the number of events and decision variables using a context-based definition of what an event would be. This more rational concept was used in a MILP (mixed integer linear programming) problem to model batch scheduling with respect to multi-product/stage machine processes. [23] considered a series of sensors to monitor the thermal control system of a space station. To reduce the amount of data to be processed, the authors adopted an event-driven simulation, computing only the events that could actually contribute to reaching an alarm level. In summary, all works reported that the event-based paradigm can be an efficient strategy to reduce the amount of data before further processing. This is also the case for fault detection ([15], [17], [20]), which is the focus of this work.

Process monitoring, and more specifically fault detection, is an essential activity in process industries. Due to the inherent complexity of the processes, being multivariable, nonlinear and only partially known, this task is still challenging from a practical point of view [24]. Many process variables are currently measured continuously, even within seconds, which is very beneficial on the one hand [25]. However, problems with the resulting massive amount of data also arise from the other side. Packet collision and high latency are examples involving data transmission in communication systems [26]. As far as information is concerned, more data does not necessarily mean more quality. Process noisy, missing values, measurement errors and imbalanced classes (operation modes), to name a few, occur frequently [27]. In this context, process industries can benefit greatly from the event-driven paradigm, reducing the amount of data to be transmitted and processed. Unlike the fixed-time data acquisition procedure, the input data for the fault detection system would only be updated in the case of new process information, according to a predefined criterion.

This work investigates the event-driven data acquisition strategy for fault detection in continuous industrial systems. The threshold [28] and delta [29] event-based methods were evaluated under different data transmission rates. The well-known Tennessee Eastman Process (TEP) benchmark served as the case study [30]. Several techniques and strategies have been used for fault detection purposes in this benchmark. To name a few, DPCA (dynamic principal component analysis) with decorrelated residuals [31], a combination of PCA (principal component analysis) and k-NN (k-nearest neighbors) [32], a combination of PCA with fuzzy logic [33], a sparse auto-encoder [34], RNN (recurrent neural network) and CNN (convolutional neural network) deep learning models [35], and image processing using MLP (multilayer perceptron) and RBF (radial basis function) neural networks

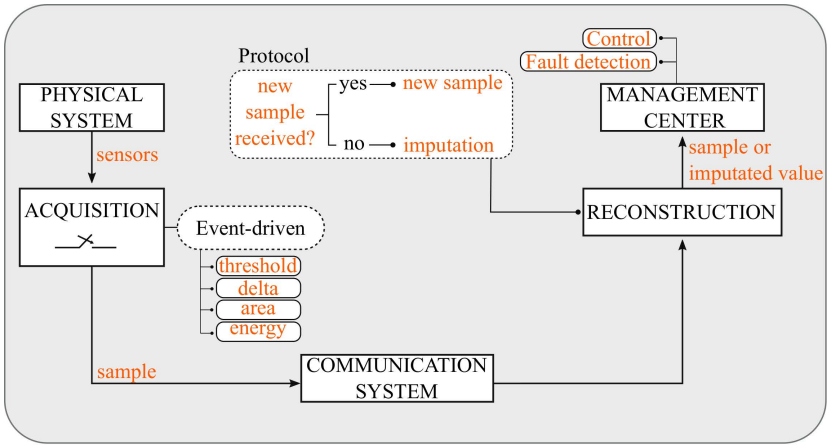

FIGURE 1. Proposed approach for event-driven data acquisition.

based classifiers [36]. A common point among all these works is the use of the fixed-time approach. The following works are reviews on fault detection and diagnosis using data-driven modeling in various fields of engineering: photovoltaic system [37], power transformer [38], HVAC (heating, ventilation and air conditioning) system [39], building energy system [40], marine current turbine [41], gear system [42], thermal system [43], industrial system [44] and high-speed trains in intelligent transportation [45]. The present work made use of PCA, as it is the most applied technique for fault detection in the TEP benchmark. [31], [32], [46]–[48] are examples of recent works, which also employed periodic data acquisition. In this sense, the results obtained with the event-based methods were compared with this commonly used fixed-time approach. The classic work in [49] was used for this purpose. To have the same basis of comparison, the percentage of variance explained by the PCA model was approximately 55% and the false alarm rate was set at 1%. In addition, the missed detection rate (MDR) and detection time (delay) were used as performance metrics. This work shows, as its main contribution, the possibility of obtaining a better performance in fault detection with considerably low data transmission rates. Event-driven applications in process industries are often related to process control and instrumentation. To the best of the authors' knowledge, there is no systematic study of its use for fault detection in continuous industrial systems.

This paper is organized as follows. Section II shows the proposed event-driven framework for data acquisition. The methodology is depicted in section III. The event-based methods used in this work are described in section IV. Section V refers to the TEP (Tennessee Eastman Process) benchmark used as a case study. Section VI presents the results and discussion of the fault detection performance, including a comparison between the event- and the time-based approaches. An analysis of the data transmission rate is given in section VII. Final considerations are given in section VIII.

II. EVENT-DRIVEN DATA ACQUISITION FRAMEWORK

To properly design an event-driven data acquisition procedure, it is necessary to characterize the measured signals. This can be done explicitly by knowing the math function or directly from the data. The latter is generally used due to the complexity of industrial processes. The main question in this case concerns how to "filter" the signals to consider only the sampling points associated with new information about the state of the process. Predefined thresholds based on individual values, or signal variations or accumulations over time, are used to identify these relevant events [3], [4]. As part of the data acquisition phase, event-driven strategies have the potential to significantly reduce the amount of data to be transmitted and processed. In this sense, applications of Cyber-Physical Systems (CPS) involving large amounts of data can be greatly benefited [50]. Figure 1 depicts the proposed event-based data acquisition system with a focus on continuous industrial processes. Each element is described below.

A. PHYSICAL SYSTEM

This initial element refers to the real-world system of interest. It is very important to have information about the measured variables, the location of the sensors and the dynamics of the process.

B. DATA ACQUISITION

The input to this step is the sampled values collected continuously by a series of sensors in the physical system using a fixed time interval. The selection of samples to be transmitted containing new information about the state of the process is based on a predefined event-based strategy. This data filtering

can be applied locally in the case of smart sensors or at a remote center. Examples of event-based methods are given by the threshold, delta, area, and energy approaches (described in the IV section). The first two were used in this work with different data compression rates, which determines the amount of data to be transmitted for further processing.

C. COMMUNICATION SYSTEM

This system is responsible for transmitting the previously selected values. Wired or wireless systems can be used. This data filtering contributes to more efficient management of memory, latency and packet collision, to name a few, which is most critical in the case of networks with limited bandwidth. The communication system infrastructure and its challenges are outside the scope of this work.

D. SIGNAL RECONSTRUCTION

The signal at this point may contain missing values as the values of some variables may not have been transmitted. This occurs when they do not exceed the respective event-based method limits. For signal reconstruction, a data imputation protocol should then be used [51]. The present work adopted the last value sent by the communication system. This procedure is also beneficial in case of signal loss.

E. MANAGEMENT CENTER

This unit receives and processes the previously reconstructed signal, according to the purpose of the application. This can refer to process modeling, simulation, control, optimization or monitoring. Given the objective of this work, a fault detection system is part of this unit in the present work. Central units like this are even more important nowadays, given the concept of a cyber-physical system in the context of Industry 4.0 [50]. This system integration can be useful for offline and real-time applications. Event-based strategies also favor the computational power needed in this case, given the smaller amount of data to be processed.

III. METHODOLOGY

Figure 2 depicts the methodology adopted in this work. There are three main steps: model identification, control limits definition, and fault detection itself. Each step is described below.

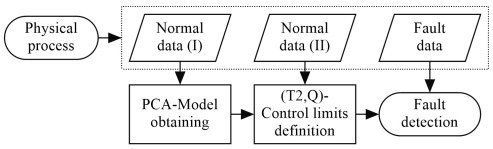

FIGURE 2. Methodology steps.

A. MODEL IDENTIFICATION

The fault detection system was based on PCA (Principal Component Analysis). This technique have been the most used for fault detection in industrial applications [52]–[55]. The case study in this work used the Tennessee benchmark problem [30], described in section V. In this case, a first data set (normal data I), characteristic of the normal operating condition, was used to obtain the PCA model. The approximate number of twelve principal components, which explain about 55% of the total variance in the original data, was adopted for comparison purposes [49].

B. CONTROL LIMITS DEFINITION

The multivariate control charts for the T^2 and Q statistics were used for fault detection [44], [56], [57]. Their respective control limits were calculated from a second data set (normal data II), also characteristic of the normal operating condition. For this, the false alarm rate was set at 1% [49], being determined by the 99th percentile. Both previous steps considered fixed-time sampling. *Fault detection:* The event-based data acquisition framework (Figure 1) was used in this step. At each sampling, the measured value of the variable is transmitted only if it is considered an event. Otherwise, the last value sent to the variable is used during signal reconstruction. This procedure is repeated for each variable. The reconstructed signal is then fed into the previous PCA model, and the corresponding values of T^2 and Q are calculated and plotted on the respective control charts. All twenty-one faults available in the benchmark were investigated (using the respective fault data set). The results were compared with the classical time-based data acquisition approach [49]. The missed detection rate and detection time performance metrics were used for this purpose. The event-based strategies used in this work are described in section IV.

In short, PCA is a dimensionality reduction technique belonging to multivariate statistics [58]. Its principle resides in an orthogonal rotation of the coordinate system given by the original variables. The rotated axes, called principal components, are defined according to a criterion of maximum variance. The first component explains as much of the total variance of the original data as possible, the second, which is orthogonal to the first, as much of the remaining unexplained variance, and so on. Given a required amount of explained variance, the first k components are used as the final PCA model. With regard to fault detection, this model is obtained with normal data, being, therefore, characteristic of the normal operating condition. When fed with fault data, it is expected to recognize such a condition, which is normally accomplished through control charts for the T^2 and Q statistics.

IV. EVENT-DRIVEN METHODS

Event-based methods are generally provided by the following strategies: send-on-delta (SoD) [29], send-on-prediction (SoP) [59], [60], send-on-area (SoA) [61], send-on-energy (SoE) [62], and a simple threshold definition. In SoD, the current value is transmitted when a minimum difference from the last value sent is reached. SoP is an extension of the previous strategy, in which a predicted value from the last update

TABLE 1. Process disturbances [30], [49].

Fault	Process variable	Fault type
1	A/C feed ratio, B composition constant (stream 4)	Step
2	B composition, A/C ratio constant (stream 4)	Step
3	D feed temperature (stream 2)	Step
4	Reactor cooling water inlet temperature	Step
5	Condenser cooling water inlet temperature	Step
6	A feed loss (stream 1)	Step
7	C header pressure loss - Reduced availability (stream 4)	Step
8	A, B, C feed composition (stream 4)	Random variation
9	D feed temperature (stream 2)	Random variation
10	C feed temperature (stream 4)	Random variation
11	Reactor cooling water inlet temperature	Random variation
12	Condenser cooling water inlet temperature	Random variation
13	Reaction kinetics	Slow drift
14	Reactor cooling water valve	Sticking
15	Condenser cooling water valve	Sticking
16	Unknown	Unknown
17	Unknown	Unknown
18	Unknown	Unknown
19	Unknown	Unknown
20	Unknown	Unknown
21	The valve for Stream 4 was fixed at the steady state position	Constant position

is used. SoA and SoE are two other common extensions. The triggering criterion in the first is given by the integral of the absolute difference and, in the second, by the energy of the difference. Another method is provided by the use of a predefined threshold [28]. The event trigger in this case occurs when the current value crosses a cut-off point. This work investigated the threshold and delta strategies. The use of the others is straightforward.

A. THRESHOLD-BASED METHOD

The threshold method employs a cut-off point as a decision rule for data acquisition. The measured value is only transmitted if it exceeds this reference, whose definition uses the mean (S_{avg}), minimum (S_{min}) and maximum (S_{max}) statistics of the signal (S) under the normal operating condition. The resulting lower (T_l) and upper (T_u) thresholds are shown in Equation 1. To investigate the effect of the magnitude of the differences ($S_{max}-S_{avg}$; $S_{avg}-S_{min}$) on data transmission rate and fault detection performance, a parameter p ($0 < p < 1$) was varied as follows: $[5, 10 : 10 : 90, 95]\%$. The higher, the lower the number of values transmitted. This procedure is repeated for each variable separately.

$$T_u = S_{avg} + (S_{max} - S_{avg}) \times p \tag{1a}$$
$$T_l = S_{avg} - (S_{avg} - S_{min}) \times p \tag{1b}$$

The reconstruction of the signal (S'_t) is performed according to Equation 2. The value of the variable (S_t) is transmitted if it exceeds the lower or upper thresholds; otherwise, the last value sent (S'_{t-1}) is used. The threshold definition and signal reconstruction steps follow the event-based data acquisition framework shown in Figure 1.

$$S'_t = \begin{cases} S_t, & \text{if } (S_t < T_l) \text{ or } (S_t > T_u) \\ S'_{t-1}, & \text{if } T_l \leq S_t \leq T_u \end{cases} \tag{2}$$

The threshold method (with $p = 50\%$) is illustrated for feed A (stream 1), which is one of the variables of the TEP benchmark. Figures 3a and 3b show the original and filtered signals, respectively, given fault 5 (Table 1).

B. DELTA-BASED METHOD

The send-on-delta (SoD) method is based on the difference between the current value and the one previously sent by the data acquisition system. Equation 3 shows the definition of the reference value in this case, which is given by the maximum absolute difference (Δ max) between consecutive values (S_t, S_{t-1}) considering the signal under the normal operating condition. The parameter p was used as before. This procedure is applied to each variable separately.

$$\Delta \max = \max(\mid S_t - S_{t-1} \mid) \times p \tag{3}$$

The next step concerns the reconstruction of the signal (S'_t), according to Equation 4. The value of the variable (S_t) is transmitted only if the corresponding difference is greater than Δ max; otherwise, the last value sent (S'_{t-1}) is used. The delta rule is detailed in Figure 4. This procedure is applied to each variable separately. It also follows the event-based data acquisition framework shown in Figure 1.

$$S'_t = \begin{cases} S_t, & \text{if } \mid S_t - S_{t-1} \mid > (\Delta \max) \\ S_{t-1}, & \text{if } \mid S_t - S_{t-1} \mid \leq (\Delta \max) \end{cases} \tag{4}$$

Figure 3c illustrates the use of the delta rule for A feed (stream 1), with $p = 50\%$, given fault 5 (Table 1). A low resolution signal can be verified in comparison to the threshold rule (Figure 3b).

V. CASE STUDY: TENNESSEE EASTMAN PROCESS (TEP) BENCHMARK

The Tennessee benchmark problem [30] has often been used for the development of fault detection systems [35], [54], [55], [63], [64]. Based on a real industrial process, it involves

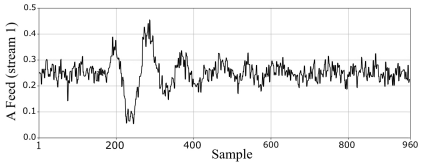

(a) Original signal.

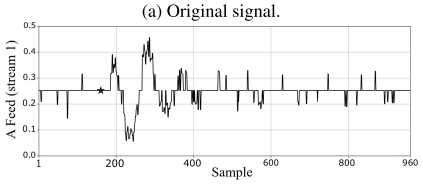

(b) Filtered signal: Threshold rule ($p = 50\%$).

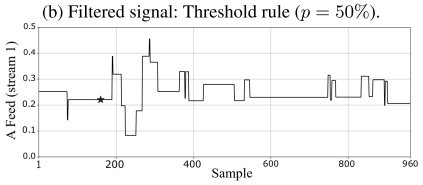

(c) Filtered signal: Delta rule ($p = 50\%$).

FIGURE 3. Event-based data acquisition for A feed (stream 1), which is one of the variables of the case study (section V), given fault 5 (Table 1) (⋆: Fault start up at $t = 160$).

a reactor, a condenser, a vapor-liquid separator, a recycle compressor and a stripper column (Figure 5). The objective is to obtain the liquid (l) products, G and H, from the gaseous (g) reactants, A, C, D and E. This is achieved by a set of four irreversible and exothermic chemical reactions, as shown below. Components B (not shown) and F are an inert and a by-product, respectively.

$$\begin{aligned} A_{(g)} + C_{(g)} + D_{(g)} &\rightarrow G_{(l)}(product1) \\ A_{(g)} + C_{(g)} + E_{(g)} &\rightarrow H_{(l)}(product2) \\ A_{(g)} + E_{(g)} &\rightarrow F_{(l)}(byproduct) \\ 3\,D_{(g)} &\rightarrow 2\,F_{(l)}(byproduct) \end{aligned}$$

There are fifty-two measurements, where twenty-two are process variables, eleven are manipulated variables, and nineteen are laboratory parameters. The variables and parameters are collected every three and six minutes, respectively. Twenty-one faults are available (Table 1) [1], [49], occurring one at a time. The normal and fault data sets are composed of 500 and 960 observations, which correspond to twenty-five and forty-eight hours of simulation, respectively. Each fault occurs at $t = 160$, that is, after eight hours under normal operation. Gaussian noise is introduced into all measurements.

VI. RESULTS AND DISCUSSION

The results obtained with the event-driven methods, namely, threshold and delta rules, were compared with the time-based approach. The PCA model (step 1 in Figure 2), characteristic of the normal operating condition, as well as the respective

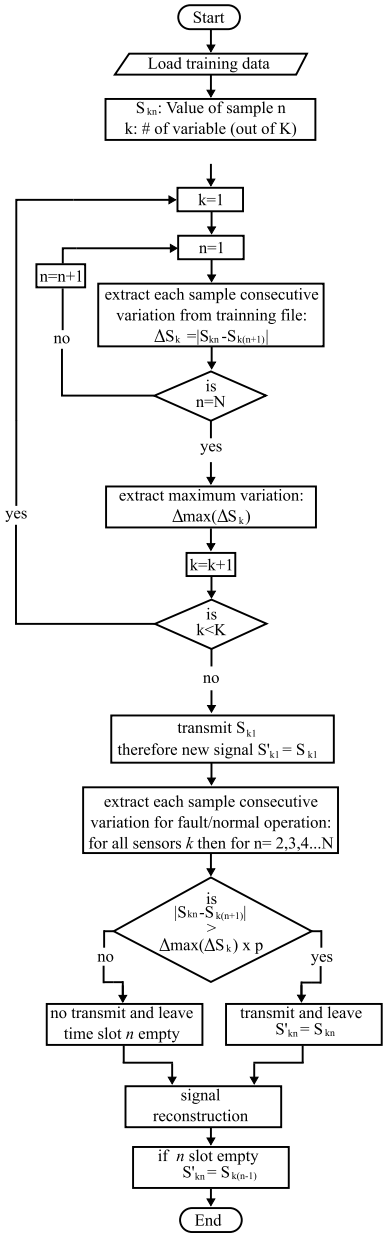

FIGURE 4. Flowchart of the delta event-driven method for data acquisition.

upper control limits for the statistics T^2 and Q (step 2), were common to both cases. This model is given by twelve

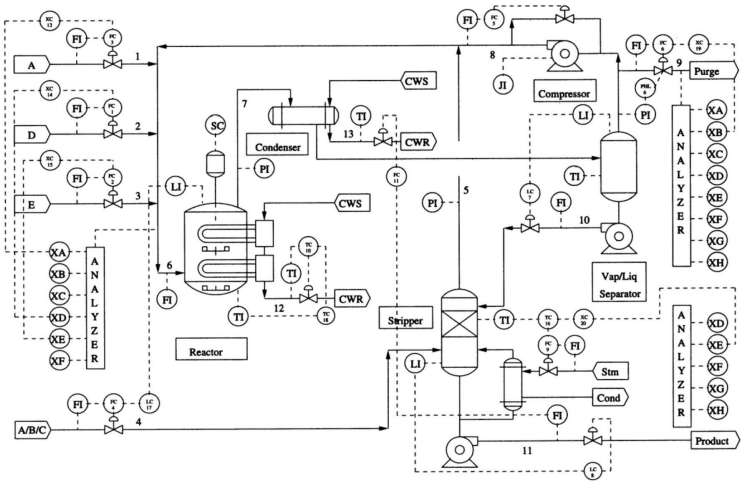

FIGURE 5. Process flowchart of the Tennessee benchmark problem [1].

TABLE 2. MDR (missed detection rate) for the T^2 statistic.

Fault	Time-based approach	Event-based delta approach (p in %)											Absolute gain
		5	10	20	30	40	50	60	70	80	90	95	
1	0.008	**0.008**	**0.008**	**0.008**	**0.008**	**0.008**	**0.008**	0.009	**0.008**	**0.008**	0.010	0.010	0%
2	0.020	**0.020**	**0.020**	**0.020**	**0.020**	0.023	0.023	**0.020**	0.023	0.023	0.023	0.023	0%
3	0.998	0.999	0.996	0.996	1.000	**0.993**	1.000	1.000	0.996	1.000	1.000	1.000	1%
4	0.956	0.961	0.959	0.960	0.973	0.969	0.939	0.934	**0.905**	0.999	0.999	0.999	**5%**
5	0.775	0.774	0.771	0.770	0.766	0.764	0.766	0.773	0.729	0.683	**0.604**	0.701	**17%**
6	0.011	0.011	0.011	0.011	0.011	0.011	0.011	**0.008**	0.009	0.009	0.009	0.009	0%
7	0.085	0.079	0.076	0.079	0.065	0.045	0.051	0.161	**0.000**	**0.000**	**0.000**	**0.000**	**9%**
8	0.034	0.033	**0.031**	0.034	**0.031**	0.033	**0.031**	**0.031**	**0.031**	0.043	0.054	0.045	0%
9	0.994	0.998	0.996	0.991	0.993	0.998	0.984	0.984	**0.979**	1.000	1.000	1.000	2%
10	0.666	0.653	0.653	**0.646**	0.655	0.671	0.678	0.679	0.694	0.744	0.806	0.826	2%
11	0.794	0.789	0.786	0.796	0.793	0.794	0.761	**0.688**	0.876	0.886	0.899	0.926	**11%**
12	0.029	0.021	0.021	0.023	**0.019**	0.024	0.026	0.021	0.035	0.034	0.059	0.056	1%
13	0.060	**0.060**	**0.060**	0.061	0.061	0.061	0.061	0.063	0.061	0.063	0.076	0.078	0%
14	0.158	0.120	0.125	0.111	0.114	0.096	**0.094**	0.106	0.095	0.154	0.149	0.154	**6%**
15	0.988	0.979	0.978	0.984	0.983	0.993	**0.940**	0.974	0.984	0.996	1.000	1.000	**5%**
16	0.834	0.833	0.833	0.851	0.844	0.834	0.860	0.809	**0.733**	0.920	0.934	0.946	**10%**
17	0.259	0.254	0.251	0.258	0.260	**0.249**	0.261	0.255	0.273	0.338	0.261	0.324	1%
18	0.113	0.113	0.113	0.111	**0.110**	0.113	0.116	0.118	0.113	0.113	0.121	0.121	0%
19	0.996	0.999	0.999	1.000	0.999	0.996	0.993	0.998	**0.885**	0.988	0.996	1.000	**11%**
20	0.701	0.704	0.710	0.709	0.718	0.725	0.684	0.731	**0.650**	0.766	0.754	0.805	**5%**
21	0.736	0.694	0.693	0.691	0.691	0.696	0.690	**0.651**	0.716	0.786	0.865	0.876	**8%**

Gray cells: False alarm rate $> 5\%$ (Table 4).

principal components, which explains about 56% of the total variance of the original data. This percentage was adopted for comparison purposes [49]. The difference between them concerns the input information for the fault detection system (step 3). All values sampled periodically are used in the time-based procedure, while they are filtered in the event-based approach (Figure 1).

The threshold method performed slightly better compared to the fixed-time approach over the entire range of the p parameter (results not shown due to lack of space). The benefit in this case concerns the use of a much smaller amount of data, which favors online applications, especially nowadays, given the era of big data.

Tables 2 and 3 show the missed detection rate (MDR) obtained with the delta rule for the T^2 and Q statistics, respectively. The best result for each fault is in bold. For example, the best MDR values for fault 5 were equal to 0.604 (for T^2 and $p = 0.90$) and 0.001 (for Q and $p = 0.80$). Absolute differences from the respective MDR values obtained with the periodic approach are also presented. The greater this difference, the better the result obtained by the delta rule. For example, the gains for fault 5 were equal to about 17% (=0.775 − 0.604) and 74% (=0.746 − 0.001) for the statistics T^2 and Q, respectively. For the Q statistic, it can be seen that the MDR value obtained with the event-driven delta rule is very close to zero (0.001), as desired, while the

TABLE 3. MDR (missed detection rate) for the Q statistic.

Fault	Time-based approach	Event-based delta approach (p in %)											Absolute gain
		5	10	20	30	40	50	60	70	80	90	95	
1	0.003	0.003	0.003	0.003	0.003	**0.001**	0.003	0.003	0.003	0.006	0.004	0.004	0%
2	0.014	0.014	0.014	0.015	0.011	0.011	**0.010**	0.018	0.000	0.023	0.023	0.023	0%
3	0.991	0.990	0.990	0.985	0.975	0.830	0.949	0.160	0.461	**0.876**	0.926	0.995	**11%**
4	0.038	0.035	**0.031**	0.040	0.038	0.031	0.033	0.046	0.006	0.063	0.000	0.470	1%
5	0.746	0.745	0.743	0.743	0.720	0.644	0.303	0.164	0.000	**0.001**	0.000	0.008	**74%**
6	0.000	**0.000**	**0.000**	**0.000**	**0.000**	**0.000**	0.000	**0.000**	**0.000**	**0.000**	**0.000**	**0.000**	0%
7	0.000	**0.000**	**0.000**	**0.000**	**0.000**	**0.000**	**0.000**	**0.000**	**0.000**	**0.000**	**0.000**	**0.000**	0%
8	0.024	0.025	0.025	0.021	0.023	**0.019**	0.025	0.000	0.025	0.025	0.026	0.026	1%
9	0.981	0.979	0.983	0.979	0.966	0.915	0.675	0.711	0.484	**0.501**	1.000	1.000	**48%**
10	0.659	0.650	0.653	0.648	0.578	0.465	0.255	**0.061**	0.065	0.226	0.454	0.464	**60%**
11	0.356	0.340	0.335	0.335	0.329	0.290	0.198	**0.099**	0.320	0.313	0.519	0.635	**26%**
12	0.025	0.025	0.025	0.029	0.031	0.018	**0.009**	0.005	0.014	0.016	0.016	0.016	2%
13	0.045	0.045	0.045	0.045	0.048	**0.041**	0.044	0.054	0.053	0.055	0.055	0.060	0%
14	0.000	**0.000**	**0.000**	**0.000**	**0.000**	**0.000**	**0.000**	0.001	0.001	0.001	0.001	0.001	0%
15	0.973	0.970	0.971	0.968	0.948	0.855	0.756	0.251	**0.279**	0.954	0.956	0.884	**69%**
16	0.755	0.744	0.740	0.728	0.661	0.574	**0.290**	0.210	0.174	0.536	0.633	0.546	**47%**
17	0.108	0.098	0.103	0.100	0.100	0.064	**0.034**	0.054	0.043	0.083	0.086	0.094	**7%**
18	0.101	0.103	0.100	0.101	0.096	0.076	0.031	0.048	**0.034**	0.063	0.114	0.114	**7%**
19	0.873	0.863	0.856	0.869	0.821	0.666	0.539	**0.526**	0.628	0.845	0.711	0.740	**35%**
20	0.550	0.546	0.538	0.529	0.509	0.448	0.286	0.169	**0.135**	0.138	0.376	0.354	**42%**
21	0.570	0.578	0.571	0.570	0.535	**0.456**	0.309	0.505	0.555	0.610	0.614	0.704	**11%**

Gray cells: False alarm rate $>$ 5% (Table 5).

TABLE 4. FAR (false alarm rate) for the T^2 statistic.

Fault	Time-based approach	Event-based delta approach (p in %)										
		5	10	20	30	40	50	60	70	80	90	95
1	0	**0**	**0**	**0**	**0**	**0**	**0**	0	**0**	**0**	0	0
2	0	**0**	**0**	**0**	**0**	0.013	0	**0**	0	0	0	0
3	0.006	0.006	0.006	0	0	**0**	0	0	0	0	0	0
4	0.006	0.006	0.006	0.006	0.006	0.006	0	0	**0**	0	0	0
5	0.006	0.006	0.006	0.006	0.006	0.006	0	0	0	0	**0**	0
6	0	0	0	0	0	0	0	**0**	0	0	0	0
7	0	0	0	0	0	0	0	0	**0**	**0**	**0**	**0**
8	0	0	**0**	0	**0**	0	**0**	**0**	**0**	0	0	0
9	0.019	0.019	0.019	0.025	0.013	0	0	0	**0**	0	0	0
10	0	0	0	**0**	0	0	0	0	0	0	0	0
11	0	0	0	0	0	0	0	**0**	0	0	0	0
12	0	0	0	0	**0**	0	0.013	0	0	0	0	0
13	0	**0**	**0**	0	0	0	0	0	0	0	0	0
14	0	0	0	0	0	0	**0**	0	0	0	0	0
15	0	0	0	0	0	0	**0**	0	0	0	0	0
16	0.044	0.050	0.056	0.056	0.044	0.038	0	0	**0**	0	0	0
17	0	0	0	0	0	**0**	0	0	0	0	0	0
18	0	0	0	0	**0**	0	0	0	0	0	0	0
19	0	0	0	0	0	0	0	0	**0**	0	0	0
20	0	0	0	0	0	0	0	0	**0**	0	0	0
21	0	0	0	0	0	0	0	**0**	0	0	0	0

Gray cells: False alarm rate $>$ 5%.

corresponding value for the time-fixed procedure is considerably high (0.746). A gray cell means the result was not considered valid due to a false alarm rate (FAR) above 5%. Tables 4 and 5 show the FAR values for the T^2 and Q statistics, respectively. For example, for fault 5 and statistic T^2, FAR is equal to 0.006 and zero ($p = 0.90$) for the temporal and delta approaches, respectively. The corresponding values for the Q statistic are equal to 0.006 and 0.013 ($p = 0.80$), respectively. The vast majority of FAR values were comparable to those obtained with the time-based approach. This point is critical when comparing fault detection strategies. Tables 6 and 7 show the detection time (or detection delay) for the statistics T^2 and Q, respectively. A fault was recognized after the occurrence of six consecutive points beyond the control limit, the detection time being calculated from the first [49]. For fault 5 and statistic T^2, it was equal to 16 and 15 ($p = 0.90$) sampling units given the periodic and delta procedures, respectively. That is, there was a gain of one sampling unit in this case. A detailed analysis of the event-based delta strategy is presented below, along with a comparison with the time-fixed approach.

From the MDR results obtained from the statistics T^2 and Q with PCA for the fixed-time approach (2nd column of Tables 2 and 3), the set of twenty-one faults of the Tennessee benchmark problem can be grouped into four subsets according to the level of detection difficulty. Group 1 refers to easy faults (1, 2, 4, 6, 7, 8, 12, 13, 14); group 2, to intermediate faults (11, 17, 18); group 3, to hard faults (5, 10, 16, 19, 20, 21); and group 4, to very hard faults (3, 9, 15).

First, significant MDR gains were verified for eight faults, all related to the Q statistic. Namely, faults 5 (74%; $p = 0.80$), 9 (48%; $p = 0.80$), 10 (60%; $p = 0.60$), 11 (26%; $p = 0.60$),

TABLE 5. FAR (false alarm rate) for the Q statistic.

Fault	Time-based approach	Event-based delta approach (p in %)										
		5	10	20	30	40	50	60	70	80	90	95
1	0	0	0.006	0.013	0.031	**0.044**	0.006	0	0	0	0	0
2	0.006	0.006	0.006	0.013	0.025	0.069	**0.006**	0.006	0.375	0	0	0
3	0.013	0.013	0.006	0.019	0.050	0.100	0	0.475	0.106	**0**	0	0
4	0.006	0.006	**0.006**	0.006	0.013	0.094	0.150	0.044	0.200	0.013	0.294	0
5	0.006	0.006	0.006	0.006	0.013	0.094	0.150	0.044	0.200	**0.013**	0.294	0
6	0	**0**	**0**	**0**	**0**	**0**	0.056	**0**	**0**	**0**	**0**	**0**
7	0	**0**	**0**	**0**	**0**	**0.031**	**0.031**	**0.031**	**0**	**0**	**0**	**0**
8	0.006	0	0.006	0.013	0.025	**0.019**	0	0.069	0	0	0	0
9	0.006	0.006	0.006	0.006	0.013	0.106	0.400	0.044	0.169	**0**	0	0
10	0	0	0	0	0.019	0.038	0.006	**0.006**	0.038	0	0	0
11	0.006	0.006	0.006	0.006	0.019	0.056	0.131	**0**	0	0	0	0
12	0	0	0	0.006	0.006	0.006	**0.031**	0.188	0	0	0	0
13	0	0	0	0	0	**0**	0	0	0	0	0	0
14	0	**0**	**0**	**0.006**	**0**	**0.013**	**0**	0	0	0	0	0
15	0.006	0.006	0	0	0	0.038	0.013	0.063	**0.038**	0	0	0
16	0.006	0.006	0.006	0.006	0.019	0.100	**0**	0.188	0.106	0	0	0
17	0.013	0.013	0.013	0.006	0.019	0.044	**0.044**	0.038	0	0	0	0
18	0.006	0.006	0.006	0.006	0.006	0.019	0.063	0	**0**	0	0	0
19	0	0	0	0.006	0.006	0.019	0	**0.019**	0	0	0	0
20	0	0	0	0	0.006	0.044	0	0.006	**0**	0	0	0
21	0.019	0.019	0.019	0.019	0.038	**0.038**	0.369	0	0	0	0	0

Gray cells: False alarm rate $> 5\%$.

15 (69%; $p = 0.70$), 16 (47%; $p = 0.50$), 19 (35%; $p = 0.60$) and 20 (42%; $p = 0.70$) (Table 3). For example, for fault 10, the MDR values were equal to 0.659 and 0.061 ($p = 0.60$) for the periodic and delta strategies, respectively. The difference between them corresponds to the gain of 60%. The respective FAR values were considerably low, equal to 0.013, zero, 0.006, zero, 0.038, zero, 0.019 and zero, respectively (Table 5). Faults 5, 10, 16, 19 and 20 are hard-to-detect (group 3), and faults 9 and 15 are very hard-to-detect (group 4). Figure 6 shows the Q control charts obtained with the event-based delta rule for faults 5, 10, 16 and 20 (on the left). Corresponding charts for the usual fixed-time approach are also presented for comparison purposes (on the right).

Furthermore, it can be noted that the best MDR values are a function of the parameter p. However, they are concentrated at $0.50 < p < 0.80$. This result suggests an optimal range for p, which is positive in the sense of defining a single value. For example, the MDR for fault 5, initially equal to 0.001 ($p = 0.80$), is equal to 0.164 for the most usual value of p, equal to 0.60 (Table 3). The gain in the latter would still be high, around 58% (=0.746 − 0.164), with a FAR value still considerably low, equal to 0.044 (Table 5). An ensemble approach using an interval for p can also be considered.

There are cases where the gain is not relatively large; however, MDR tends to zero as desired. This was verified for fault 7, with an MDR of zero for $p = 0.70$, 0.80, 0.90 and 0.95, given the T^2 statistic (Table 2). The value corresponding to the periodic approach is relatively higher, equal to 0.085. For the Q statistic, it occurred for faults 17 and 18, both with an MDR of 0.034 for $p = 0.50$ and 0.70, respectively (Table 3). The corresponding values for the cyclic procedure are relatively larger, equal to 0.108 and 0.101, respectively. The MDR values for faults 5, 10 and 11, which showed significant gains (previous analysis), were also relatively low. Namely, 0.001 ($p = 0.80$), 0.061 ($p = 0.60$) and 0.099 ($p = 0.60$), respectively (Table 2). On the other hand, the values corresponding to the time-based approach are considerably high, equal to 0.746, 0.659 and 0.356, respectively. The FAR values in all cases were close to zero (Tables 4 and 5). Faults 11, 17 and 18 belong to group 2 (intermediate detection), and faults 5 and 10 to group 3 (hard detection).

Another performance metric concerns detection time. Tables 6 and 7 summarize the results for the statistics T^2 and Q, respectively. As before, a gray cell means it was not considered valid due to a false alarm rate above 5%. Shorter detection times were generally associated with lower MDR values (Tables 2 and 3), as expected. Relatively high MDRs and therefore low gains were obtained for faults 11, 16 and 21, given the T^2 statistic. The respective MDR gains were equal to 11% (=0.794 − 0.688; $p = 0.60$), 10% (=0.834 − 0.733; $p = 0.70$) and 8% (=0.736 − 0.651; $p = 0.60$) (Table 2), with FAR values equal to zero for all (Table 4). However, the main result in this case concerns the detection time, with gains of 208 (=304 − 96), 26 (=312 − 286) and 49 (=563 − 514) sampling units, respectively, in relation to the fixed-time approach (Table 6). That is, these faults were detected in advance, through the delta rule. Fault 11 belongs to group 2 (intermediate detection) and faults 16 and 21 to group 3 (hard detection). More, the detection times for faults 4, 9, 15 and 19 were equal to 447 ($p = 0.70$), 734 ($p = 0.70$), 646 ($p = 0.50$) and 444 ($p = 0.70$) sampling units, respectively, given the T^2 statistic (Table 6), with FAR values equal to zero for all (Table 4). These values are still relatively high, but these faults were not detected (ND) by the time-fixed approach (Table 6). For the Q statistic, this occurred for faults 3, 9 and 19, with detection times of 307 ($p = 0.80$), 233 ($p = 0.80$) and 217 ($p = 0.60$) sampling units, respectively (Table 7), with all FAR values close to zero (Table 5). These faults were also not detected (ND) by the time-based approach (Table 7). Fault 19 is hard-to-detect (group 3) and faults 3, 9 and 15 are very hard-to-detect (group 4). Furthermore, as described earlier, faults 10,

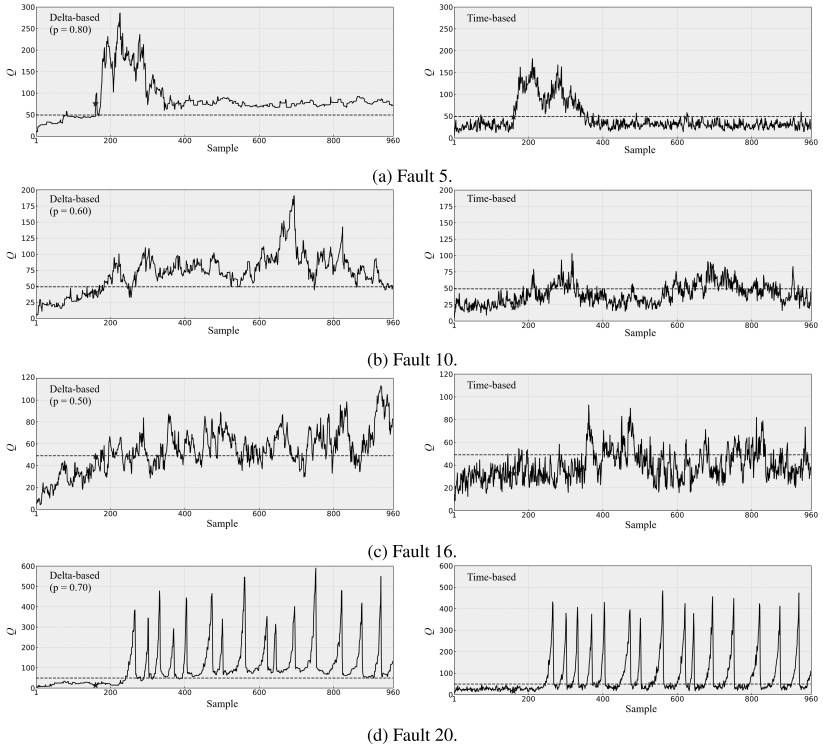

(a) Fault 5.

(b) Fault 10.

(c) Fault 16.

(d) Fault 20.

FIGURE 6. ***Q*** **control charts for the event-based delta method (on the left) and time-based approach (on the right) for hard-to-detect faults (⋆: Fault start up at** $t = 160$**).**

15 and 16 showed significant MDR gains, given the Q statistic (Table 3). Thus, they also showed considerable gains in terms of detection time. Namely, 25 ($=49-24$; $p = 0.60$), 662 ($=740-78$; $p = 0.70$) and 161 ($=197-36$; $p = 0.50$) sampling units, respectively (Table 7), with FAR values close to zero for all (Table 5). Faults 10 and 16 are hard-to-detect (group 3), and fault 15 are very hard-to-detect (group 4). Intermediate faults 17 and 18 (group 2), with MDR gains of 7% (Table 3), also presented reasonable gains for detection time, given the Q statistic. Namely, 16 ($=25-9$; $p = 0.50$) and 72 ($=84-12$; $p = 0.70$) sampling units, respectively (Table 7), with FAR values close to zero (Table 5). Slightly longer detection times were observed for some faults in relation to the periodic procedure. Namely, for fault 14, equal to -1 sampling unit ($=4-5$; $p = 0.50$), and for fault 20, equal to -3 sampling units ($=87-90$; $p = 0.70$), given the T^2 statistic (Table 6). However, the respective MDR gains were equal to 6% ($=0.158-0.094$) and 5% ($=0.701-0.650$) (Table 2), with FAR values equal to zero (Table 4).

Two event-based systems were analyzed in this work, namely, the threshold and delta rules. The threshold method provided at least the same fault detection performance compared to the time-based approach, but with much less data. On the other hand, the delta rule yielded significantly superior performance, including hard-to-detect faults. This analysis also showed that the delta rule led to significantly superior performance, including hard-to-detect faults. This performance can be explained as follows. For the usual case of fixed-time data acquisition procedure, at each sampling interval, all measured samples of all monitored variables compose the input vector fed to the PCA-based fault detection system, which is characteristic of normal operating condition. With respect to the event-based data acquisition approach, only values beyond their respective limits are used in the input vector. The values not transmitted are replaced by the last ones sent for signal reconstruction. This second input vector generally presents more discrepant deviations from the normal condition compared to the first one provided by the fixed-time approach. This fact contributes to improve the fault detection performance. In other words, the most relevant changes in fault signals come earlier, favoring fault detection. This is in agreement with the best results generally obtained

TABLE 6. Time to detection (in sampling units) for the T^2 statistic.

Fault	Time-based approach	Event-based delta approach (p in %)											Absolute gain
		5	10	20	30	40	50	60	70	80	90	95	
1	7	**7**	**7**	**7**	**7**	**7**	**7**	7	**7**	**7**	9	9	0
2	17	**17**	**17**	**17**	**17**	19	19	**17**	19	19	19	19	0
3	–	–	–	–	–	–	–	–	–	–	–	–	**ND**
4	–	–	–	–	–	–	65	470	**447**	–	–	–	**ND**
5	16	13	13	13	16	15	14	1	13	1	**15**	19	1
6	10	10	10	10	10	10	10	**7**	8	8	8	8	3
7	1	1	1	1	1	1	1	1	**1**	**1**	**1**	**1**	0
8	23	23	**23**	23	**23**	25	**23**	**25**	**25**	25	27	27	0
9	–	–	–	–	–	–	781	782	**734**	–	–	–	**ND**
10	96	96	96	**96**	73	74	96	95	96	99	101	102	0
11	304	304	304	304	197	197	197	**96**	325	146	146	146	**208**
12	22	22	22	22	**22**	22	22	22	22	22	30	22	0
13	49	**49**	**49**	49	49	49	49	51	50	51	58	59	0
14	4	4	4	4	4	5	**5**	6	6	6	6	6	-1
15	–	–	–	–	–	–	**646**	781	–	–	–	–	**ND**
16	312	312	312	313	312	310	308	305	**286**	310	310	311	**26**
17	29	29	29	30	29	**29**	29	31	29	31	31	31	0
18	93	93	93	93	**89**	93	94	99	99	94	99	99	4
19	–	–	–	–	–	–	–	–	**444**	–	–	–	**ND**
20	87	87	87	87	87	87	90	87	**90**	90	91	91	-3
21	563	563	563	558	560	550	546	**514**	564	566	696	702	**49**

ND = Not detected by the time-based approach.
Gray cells: False alarm rate $> 5\%$.

TABLE 7. Time to detection (in sampling units) for the Q statistic.

Fault	Time-based approach	Event-based delta approach (p in %)											Absolute gain
		5	10	20	30	40	50	60	70	80	90	95	
1	3	3	3	3	3	**2**	3	3	3	6	6	4	1
2	12	12	12	13	11	11	**12**	15	1	19	19	19	0
3	–	–	–	–	–	86	-	43	88	**307**	320	–	**ND**
4	3	5	**3**	3	3	3	1	15	1	1	1	30	0
5	1	2	2	2	1	1	1	1	1	**1**	1	11	0
6	1	**1**	**1**	**1**	**1**	**1**	1	**1**	**1**	**1**	**1**	**1**	0
7	1	**1**	**1**	**1**	**1**	**1**	**1**	**1**	**1**	**1**	**1**	**1**	0
8	20	22	22	19	20	**16**	21	1	21	21	22	22	4
9	–	–	–	–	–	685	1	386	199	**233**	–	–	**ND**
10	49	49	49	49	48	45	47	**24**	27	43	75	75	**25**
11	11	11	11	10	10	6	6	**7**	48	25	25	12	4
12	8	8	8	8	7	7	**7**	8	8	22	22	22	1
13	37	37	37	37	41	**35**	38	44	43	45	45	49	2
14	1	**1**	**1**	**1**	**1**	**1**	**1**	2	2	2	2	2	0
15	740	–	–	–	–	573	99	1	**78**	-	746	586	**662**
16	197	196	196	196	196	13	**36**	36	13	195	258	247	**161**
17	25	25	25	25	24	24	**9**	24	24	24	24	24	**16**
18	84	85	84	85	85	15	1	8	**12**	17	92	92	**72**
19	–	–	–	–	–	15	18	**217**	110	550	478	557	**ND**
20	87	87	87	87	85	82	75	15	**82**	87	87	87	5
21	285	285	285	285	285	**283**	1	398	245	489	492	564	2

ND = Not detected by the time-based approach.
Gray cells: False alarm rate $> 5\%$.

for intermediate values for the parameter p (Equation 4). While values of p close to zero produce similar results to the fixed-time approach, values close to one constitute a strong constraint for the initial detection of the faults. That is, the data transmission rate plays a considerable role in fault detection, and p can be seen as a sensitivity parameter. The highest performance was mostly for hard-to-detect faults.

VII. DATA TRANSMISSION RATE ANALYSIS

Data transmission in industrial systems has become increasingly critical due to the huge amount of continuously measured variables nowadays [65]. Greater efficiency is therefore crucial for better management of networking and computing aspects, among others. For example, with respect to latency and bandwidth, as well as memory allocation and processing power. These issues are also essential for advancing cyber-physical systems (CPS) applications. One way to reduce the amount of data to be transmitted and processed is through the event-based paradigm [4]. The motivation is that significant process changes are usually not periodic. This approach can also improve fault detection performance, as shown in this work mainly for hard-to-detect faults.

Figure 7a shows the average number of values transmitted in each sampling interval as a function of the parameter p (Equation 3). All fifty-two variables and twenty-one faults of the TEP benchmark were considered. The time-based approach ($p = 0$), in which all sampled values are passed

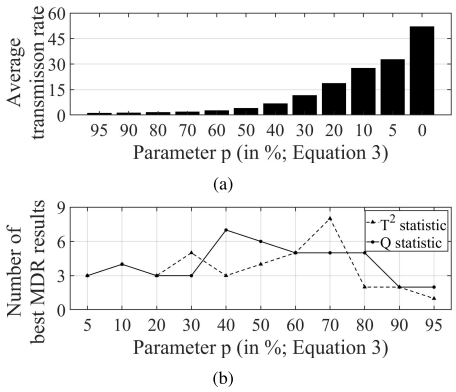

FIGURE 7. Effect of the parameter p (Equation 3) (a) on the average number of sampled values transmitted per sampling unit and (b) on the number of best MDR results, given the event-based delta rule (Equation 4).

continuously, serves as a reference. For the more restrictive case ($p = 0.95$) of the event-based delta method (Equation 4), less than five measured values are forwarded on average. The higher the value of this parameter, the lower the data transmission rate.

The best MDR results (section VI) were obtained for a range of values for p considering all twenty-one faults. Its definition must be a compromise between data transmission rate and fault detection performance. Figure 7b shows the number of best MDR values as a function of the p parameter. For example, there were three best MDR values for $p = 0.05$ (or 5%), given the T^2 statistic. They refer to faults 1, 2 and 13 (Table 2). This was also the case for the Q statistic, with faults 6, 7 and 14 (Table 3). A best result can be counted more than once, as it can occur for an interval of p, given a fault. For example, for fault 13, this occurs for $p = 0.05$ and 0.10 (MDR = 0.06) (Table 2). For T^2, the value of p with the highest number of best MDR values was equal to 0.70 (with eight faults), followed by 0.30 and 0.60 (with five). Given Q, the best score occurred for $p = 0.40$ (with seven faults), followed by $p = 0.50$ (with six) and $p = 0.60$, 0.70 and 0.80 (with five). In general, the best results were found for intermediate values of p, for both statistics. On the one hand, this means that it is not necessary to forward all sampled values ($p = 0$), and on the other hand, values of p close to one degrade the fault detection performance as it is very restrictive. The data transmission rate for intermediate values of p ($0.30 < p < 0.80$) varied between less than five and about ten observations on average, that is, around a maximum of 20% ($\approx 10/52$; Figure 7a). This number is considerably lower in relation to the full set of fifty-two values sampled. In addition to the benefit in terms of data transmission rate, an intermediate value of p also improved the fault detection performance compared to the usual fixed-time approach (section VI).

VIII. CONCLUSION

Data transmission in process industries usually occurs at every sampling interval. The problem is that a considerable amount of data without new process information is continually forwarded and processed. This adversely affects the communication system and computing power. For example, regarding network latency and bandwidth, and memory allocation and processing capacity. This is more critical nowadays, given the era of big data and cyber-physical systems (CPS) in the context of Industry 4.0. An efficient way to reduce the amount of data to be transmitted can be provided by the event-based paradigm. In this strategy, only sampled data associated with significant changes (events) in the process state are forwarded for further processing.

This work proposed an event-driven data acquisition framework for continuous industrial systems. Two methods were considered, namely, threshold and delta rules.Furthermore, the level of data filtering was varied in both. They were applied in the context of fault detection, using the Tennessee benchmark problem as a case study. The fault detection system was based on PCA (principal component analysis), which has been widely used for process monitoring. The threshold method provided similar results to the classical data acquisition time-based approach, with the advantage of using much less data. On the other hand, the delta method was generally better. Significant results, including mostly hard-to-detect faults, were achieved for considerably low data transmission rates, around 20% on average. In short, the event-based delta rule was able to reduce the amount of data to be transmitted and, at the same time, improve the fault detection performance compared to the fixed-time procedure.

Future work may be related to the search for an optimal value for the parameter p used for data filtering, sensor technology and communication systems, and signal reconstruction. This work adopted the PCA technique, which is commonly used for fault detection in the TEP benchmark problem. Artificial intelligence techniques can also be evaluated. Furthermore, while fault detection is still a major practical challenge, how the event-driven paradigm affects fault diagnosis is another point of investigation.

Concluding, event-driven data acquisition can be very attractive for process industries, given the large amount of variables measured continuously, even in seconds. The proposed event-based data acquisition framework can be applied directly to similar systems.

REFERENCES

[1] L. H. Chiang, R. D. Braatz, and E. L. Russel, *Fault Detection and Diagnosis in Industrial Systems*. 2001.
[2] F. Marvasti, *Nonuniform Sampling: Theory and Practice*. Springer, 2001.
[3] Y. Tsividis, "Event-driven data acquisition and digital signal processing—A tutorial," *IEEE Trans. Circuits Syst. II, Exp. Briefs*, vol. 57, no. 8, pp. 577–581, Aug. 2010.
[4] M. Miskowicz, *Event-Based Control and Signal Processing*. Boca Raton, FL, USA: CRC Press, 2015.

[5] X.-M. Zhang, Q.-L. Han, and B.-L. Zhang, "Adaptive sampling based on amplitude sensitivity," *IEEE Trans. Ind. Informat.*, vol. 13, no. 1, pp. 4–16, 2017.
[6] Z. Heng, P. Chen, Z. Jin, and Z. Chu, "Event-triggered control in networked control systems: A survey," in *Proc. 27th Chin. Control Decis. Conf. (CCDC)*, May 2015, Art. no. 15340402.
[7] K.-E. Årzén, "A simple event-based PID controller," in *Proc. 14th IFAC World Congr.*, vol. 18, 1999, pp. 423–428.
[8] R. Tomovic and G. Bekey, "Adaptive sampling based on amplitude sensitivity," *IEEE Trans. Autom. Control*, vol. 11, no. 2, pp. 282–284, Apr. 1966.
[9] R. Dorf, M. Farren, and C. Phillips, "Adaptive sampling frequency for sampled-data control systems," *IRE Trans. Autom. Control*, vol. 7, no. 1, pp. 38–47, Jan. 1962.
[10] P. Ellis, "Extension of phase plane analysis to quantized systems," *IRE Trans. Autom. Control*, vol. AC-4, no. 2, pp. 43–54, Nov. 1959.
[11] W. Xie, X. Zhang, and K. Shi, "Resilient security filtering for networked switched systems with event-driven measurements," *IEEE Access*, vol. 9, pp. 43434–43443, 2021.
[12] P. Khaledian, A. Aligholian, and H. Mohsenian-Rad, "Event-based analysis of solar power distribution feeder using micro-PMU measurements," in *Proc. IEEE Power Energy Soc. Innov. Smart Grid Technol. Conf. (ISGT)*, Feb. 2021, pp. 1–5.
[13] S. M. Qaisar, F. Alsharif, A. Subasi, and A. Bensenouci, "Appliance identification based on smart meter data and event-driven processing in the 5G framework," *Proc. Comput. Sci.*, vol. 182, pp. 103–108, Jan. 2021.
[14] W. Chen, H. Liu, and E. Qi, "Discrete event-driven model predictive control for real-time work-in-process optimization in serial production systems," *J. Manuf. Syst.*, vol. 55, pp. 132–142, Apr. 2020.
[15] C. Santos, J. Jiménez, and F. Espinosa, "Effect of event-based sensing on IoT node power efficiency. Case study: Air quality monitoring in smart cities," *IEEE Access*, vol. 7, pp. 132577–132586, 2019.
[16] M. de Castro Tomé, P. H. J. Nardelli, and H. Alves, "Long-range low-power wireless networks and sampling strategies in electricity metering," *IEEE Trans. Ind. Electron.*, vol. 66, no. 2, pp. 1629–1637, Feb. 2019.
[17] E. Gascard and Z. Simeu-Abazi, "Quantitative analysis of dynamic fault trees by means of Monte Carlo simulations: Event-driven simulation approach," *Rel. Eng. Syst. Saf.*, vol. 180, pp. 487–504, Dec. 2018.
[18] A. Theorin, K. Bengtsson, J. Provost, M. Lieder, C. Johnsson, T. Lundholm, and B. Lennartson, "An event-driven manufacturing information system architecture for industry 4.0," *Int. J. Prod. Res.*, vol. 55, no. 5, pp. 1297–1311, Mar. 2017.
[19] A.-M. Barthe-Delanoë, S. Truptil, F. Bénaben, and H. Pingau, "Event-driven agility of interoperability during the run-time of collaborative processes," *Decis. Support Syst.*, vol. 59, pp. 171–179, Mar. 2014.
[20] L. Zhao, T. Chai, and Q. Cong, "Event-driven operation process monitoring of SBR wastewater process," in *Proc. 16th Triennial World Congr.* Amsterdam, The Netherlands: Elsevier, 2005, pp. 149–154.
[21] A. Sanchez, G. Rotstein, N. Alsop, J. P. Bromberg, C. Gollain, S. Sorensen, S. Macchietto, and C. Jakeman, "Improving the development of event-driven control systems in the batch processing industry. A case study," *ISA Trans.*, vol. 41, no. 3, pp. 343–363, Jul. 2002.
[22] S. Wand and M. Guignard, "Redefining event variables for efficient modeling of continuous-time batch processing," *Ann. Oper. Res.*, vol. 116, pp. 113–126, Oct. 2002.
[23] R. Doyle, L. Charest, N. Rouquette, J. Wyatt, and C. Robertson, "Causal modeling and event-driven simulation for monitoring of continuous systems," in *Proc. 9th Comput. Aerosp. Conf.* Reston, VA, USA: American Institute of Aeronautics and Astronautics, 1993, p. 4525.
[24] S. Yin and O. Kaynak, "Big data for modern industry: Challenges and trends [point of view]," *Proc. IEEE*, vol. 103, no. 2, pp. 143–146, Feb. 2015.
[25] V. Venkatasubramanian, "Drowning in data: Informatics and modeling challenges in a data-rich networked world," *AIChE J.*, vol. 55, no. 1, pp. 2–8, 2009.
[26] F. Zezulka, P. Marcon, Z. Bradac, J. Arm, T. Benesl, and I. Vesely, "Communication systems for industry 4.0 and the IIoT," *IFAC-PapersOnLine*, vol. 51, no. 6, pp. 150–155, Jan. 2018.
[27] J. Liu, J. Li, W. Li, and J. Wu, "Rethinking big data: A review on the data quality and usage issues," *ISPRS J. Photogramm. Remote Sens.*, vol. 115, pp. 134–142, May 2016.
[28] K. J. Astrom and B. M. Bernhardsson, "Comparison of Riemann and Lebesgue sampling for first order stochastic systems," in *Proc. 41st IEEE Conf. Decis. Control*, vol. 2, Dec. 2002, pp. 2011–2016.
[29] M. Miskowicz, "Send-on-delta concept: An event-based data reporting strategy," *Sensors*, vol. 6, no. 1, pp. 49–63, 2006.
[30] J. J. Downs and E. F. Vogel, "A plant-wide industrial process control problem," *Comput. Chem. Eng.*, vol. 17, no. 3, pp. 245–255, Mar. 1993.
[31] T. J. Rato and M. S. Reis, "Fault detection in the Tennessee Eastman benchmark process using dynamic principal components analysis based on decorrelated residuals (DPCA-DR)," *Chemometrics Intell. Lab. Syst.*, vol. 125, pp. 101–108, Jun. 2013.
[32] C. Zhang, Q. Guo, and Y. Li, "Fault detection in the Tennessee Eastman benchmark process using principal component difference based on k-nearest neighbors," *IEEE Access*, vol. 8, pp. 49999–50009, 2020.
[33] M. Ammiche, A. Kouadri, and A. Bakdi, "A combined monitoring scheme with fuzzy logic filter for plant-wide Tennessee Eastman process fault detection," *Chem. Eng. Sci.*, vol. 187, no. 12, pp. 269–279, 2018.
[34] H. Ren, Y. Chai, J. Qu, K. Zhang, and Q. Tang, "An intelligent fault detection method based on sparse auto-encoder for industrial process systems: A case study on Tennessee Eastman process chemical system," in *Proc. 10th Int. Conf. Intell. Hum.-Mach. Syst. Cybern. (IHMSC)*, Aug. 2018, pp. 2037–2042.
[35] I. Lomov, M. Lyubimov, I. Makarov, and L. E. Zhukov, "Fault detection in Tennessee Eastman process with temporal deep learning models," *J. Ind. Inf. Integr.*, vol. 23, Sep. 2021, Art. no. 100216.
[36] P. Hajihosseini, M. M. Anzehaee, and B. Behnam, "Fault detection and isolation in the challenging Tennessee Eastman process by using image processing techniques," *ISA Trans.*, vol. 79, pp. 137–146, Aug. 2018.
[37] Y.-Y. Hong and R. A. Pula, "Methods of photovoltaic fault detection and classification: A review," *Energy Rep.*, vol. 8, pp. 5898–5929, Nov. 2022.
[38] A. R. Abbasi, "Fault detection and diagnosis in power transformers: A comprehensive review and classification of publications and methods," *Electr. Power Syst. Res.*, vol. 209, Aug. 2022, Art. no. 107990.
[39] J. Chen, L. Zhang, Y. Li, Y. Shi, X. Gao, and Y. Hu, "A review of computing-based automated fault detection and diagnosis of heating, ventilation and air conditioning systems," *Renew. Sustain. Energy Rev.*, vol. 161, Jun. 2022, Art. no. 112395.
[40] L. Zhang, M. Leach, Y. Bae, B. Cui, S. Bhattacharya, S. Lee, P. Im, V. Adetola, D. Vrabie, and T. Kuruganti, "Sensor impact evaluation and verification for fault detection and diagnostics in building energy systems: A review," *Adv. Appl. Energy*, vol. 3, no. 25, 2021, Art. no. 100055.
[41] T. Xie, T. Wang, Q. He, D. Diallo, and C. Claramunt, "A review of current issues of marine current turbine blade fault detection," *Ocean Eng.*, vol. 218, no. 15, 2020, Art. no. 108194.
[42] O. D. Mohammed and M. Rantatalo, "Gear fault models and dynamics-based modelling for gear fault detection—A review," *Eng. Failure Anal.*, vol. 117, Nov. 2020, Art. no. 104798.
[43] G. Faure, M. Vallée, C. Paulus, and T. Q. Tran, "Fault detection and diagnosis for large solar thermal systems: A review of fault types and applicable methods," *Sol. Energy*, vol. 197, pp. 472–484, Feb. 2020.
[44] Y.-J. Park, S.-K. S. Fan, and C.-Y. Hsu, "A review on fault detection and process diagnostics in industrial processes," *Ind. Eng. Chem. Res.*, vol. 8, no. 9, pp. 1–26, 2020.
[45] H. Chen and B. Jiang, "A review of fault detection and diagnosis for the traction system in high-speed trains," *IEEE Trans. Intell. Transp. Syst.*, vol. 21, no. 2, pp. 450–465, Feb. 2020.
[46] Y. Du and D. Du, "Fault detection and diagnosis using empirical mode decomposition based principal component analysis," *Comput. Chem. Eng.*, vol. 115, pp. 1–21, Jul. 2018.
[47] S. Gajjar, M. Kulahci, and A. Palazoglu, "Real-time fault detection and diagnosis using sparse principal component analysis," *J. Process Control*, vol. 67, pp. 112–128, Jul. 2018.
[48] Y. Liu, G. Zhang, and B. Xu, "Compressive sparse principal component analysis for process supervisory monitoring and fault detection," *J. Process Control*, vol. 50, pp. 1–10, Feb. 2017.
[49] E. L. Russell, L. H. Chiang, and R. D. Braatz, "Fault detection in industrial processes using canonical variate analysis and dynamic principal component analysis," *Chemometrics Intell. Lab. Syst.*, vol. 51, no. 1, pp. 81–93, 2000.
[50] D. Serpanos, "The cyber-physical systems revolution," *Computer*, vol. 51, no. 3, pp. 70–73, Mar. 2018.
[51] C. Kalalas and J. Alonso-Zarate, "Sensor data reconstruction in industrial environments with cellular connectivity," in *Proc. IEEE 31st Annu. Int. Symp. Pers., Indoor Mobile Radio Commun. (PIMRC)*, Aug. 2020, pp. 1–6.

[52] M. El Koujok, A. Ragab, H. Ghezzaz, and M. Amazouz, "A multiagent-based methodology for known and novel faults diagnosis in industrial processes," *IEEE Trans. Ind. Informat.*, vol. 17, no. 5, pp. 3358–3366, May 2021.
[53] J. Jiao, W. Zhen, W. Zhu, and G. Wang, "Quality-related root cause diagnosis based on orthogonal kernel principal component regression and transfer entropy," *IEEE Trans. Ind. Informat.*, vol. 17, no. 9, pp. 6347–6356, Sep. 2021.
[54] R. Marino, C. Wisultschew, A. Otero, J. M. Lanza-Gutierrez, J. Portilla, and E. D. L. Torre, "A Machine-Learning-Based distributed system for fault diagnosis with scalable detection quality in industrial IoT," *IEEE Internet Things J.*, vol. 8, no. 6, pp. 4339–4352, Mar. 2021.
[55] Z. Chen, Y. Cao, K. Zhang, T. Koenings, T. Peng, C. Yang, W. Gui, and S. X. Ding, "A distributed canonical correlation analysis-based fault detection method for plant-wide process monitoring," *IEEE Trans. Ind. Informat.*, vol. 15, no. 5, pp. 2710–2720, May 2019.
[56] K. Serverson, P. Chaiwatanodom, and R. D. Braatz, "Perspectives on process monitoring of industrial systems," *Annu. Rev. Control*, vol. 42, pp. 190–200, Dec. 2016.
[57] Z. Ge, Z. Song, and F. Gao, "Review of recent research on data-based process monitoring," *Ind. Eng. Chem. Res.*, vol. 52, no. 10, pp. 3543–3562, 2013.
[58] I. T. Jolliffe, *Principal Component Analysis*. Springer, 2002.
[59] K. Staszek, S. Koryciak, and M. Miskowicz, "Performance of send-on-delta sampling schemes with prediction," in *Proc. IEEE Int. Symp. Ind. Electron.*, Jun. 2011, pp. 2037–2042.
[60] Y. S. Suh, "Send-on-delta sensor data transmission with a linear predictor," *Sensors*, vol. 7, no. 4, pp. 537–547, 2007.
[61] V. H. Nguyen and Y. S. Suh, "Networked estimation with an area-triggered transmission method," *Sensors*, vol. 8, no. 2, pp. 897–909, 2008.
[62] M. Miskowicz, "Efficiency of event-based sampling according to error energy criterion," *Sensors*, vol. 10, no. 3, pp. 2242–2261, Mar. 2010.
[63] J. Zhou and Y. Zhu, "Identification based fault detection: Residual selection and optimal filter," *J. Process Control*, vol. 105, pp. 1–14, Sep. 2021.
[64] A. Hamadouche, "Model-free direct fault detection and classification," *J. Process Control*, vol. 87, pp. 130–137, Mar. 2020.
[65] S. J. Qin, "Process data analytics in the era of big data," *AIChE J.*, vol. 60, no. 9, pp. 3092–3100, 2014.

DANIEL GUTIERREZ-ROJAS (Student Member, IEEE) received the B.Sc. degree in electrical engineering from the University of Antioquia, Colombia, in 2016, and the M.Sc. degree in protection of power systems from the University of São Paulo, Brazil, in 2017. He is currently pursuing the Ph.D. degree with the School of Energy Systems, LUT University, Finland. From 2017 to 2019, he worked as a Security of Operation and Fault Analyst with Colombia's National Electrical Operator. His research interests include predictive maintenance, power systems, microgrids, mobile communication systems, and electrical protection systems.

PEKKA RÄSÄNEN received the B.Sc. degree in automation from the EVTEK University of Applied Sciences of Vantaa, Finland, in 2008, and the M.Sc. degree in electrical engineering (the industrial IoT) from the LUT University of Lappeenranta, Finland, in 2020. He worked with ABB Drives as an Electrical Designer, from 2010 to 2015; with ABB Marine as an Electrical Designer, from 2015 to 2019; and with the Electrical Steering Unit, Azipod, as a Lead Engineer, from 2019 to 2021. Since 2021, he has been working with ABB Drives as a Global Process Owner of electrical engineering as well as a Global Owner for electrical, mechanical and thermal tools.

ANA BRANDÃO BELISÁRIO received the B.Sc. and M.Sc. degrees in chemical engineering from the Federal University of Minas Gerais, Brazil, in 2017 and 2020, respectively. During the bachelor's degree, she received an Exchange Scholarship to study at Hochschule Niederrhein, Germany, and during the master's degree, a research grant to develop a part of her work at the LUT University of Lappeenranta, Finland. She currently works with data science, machine learning and statistics in chemistry and chemical engineering. Her research interests include mixture-process design of experiments and predictive chemistry.

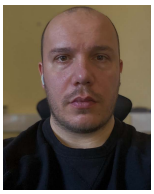

MERIM DZAFERAGIC received the B.Sc. and M.Sc. degrees in telecommunications engineering from the University of Sarajevo, Bosnia and Herzegovina, in 2011 and 2013, respectively, and the Ph.D. degree in telecommunications engineering from Trinity College Dublin, Ireland, in 2020. His work has focused on complex system science and machine learning applied to communication networks. His work has been focused on the impact of topological structures on the overall network performance, as well as the use of different machine learning approaches to support the operation of the industrial IoT networks. As part of his Ph.D., he has been working on the concept of emergence, distributed optimization, and self-organization solutions for communication networks. His most recent work focuses on intelligent control in cellular networks.

GUSTAVO MATHEUS DE ALMEIDA received the B.Sc. and M.Sc. degrees in chemical engineering from the Federal University of Minas Gerais, Brazil, in 2003 and 2006, respectively, and the Ph.D. degree in chemical engineering from the University of São Paulo, Brazil, in 2006. He was a Postdoctoral Fellow at the Federal University of Minas Gerais, from 2006 to 2008; a Professor at the Federal University of São João del-Rei, Brazil, from 2009 to 2014; and a Visiting Professor at the University of Coimbra, Portugal, in 2011. Since 2015, he has been a Professor at the Department of Chemical Engineering, Federal University of Minas Gerais, and since 2017, he has been a Co-ordinator of the Research Group on Data Analysis. His research interests include data-driven modeling, industrial statistics, data visualization, and process monitoring in continuous process industries.

PEDRO H. J. NARDELLI (Senior Member, IEEE) received the B.S. and M.Sc. degrees in electrical engineering from the State University of Campinas, Brazil, in 2006 and 2008, respectively, and the Ph.D. degree from the University of Oulu, Finland, and the State University of Campinas, following a Dual Degree Agreement, in 2013. He is currently an Assistant Professor (Tenure Track) in the IoT in energy systems at LUT University, Finland, and holds a position of the Academy of Finland Research Fellow with a project called Building the Energy Internet as a Large-Scale IoT-Based Cyber-Physical System that manages the energy inventory of distribution grids as discretized packets via machine-type communications (EnergyNet). He leads the Cyber-Physical Systems Group, LUT, and is a Project Co-ordinator of the CHIST-ERA European Consortium Framework for the Identification of Rare Events via Machine Learning and IoT Networks (FIREMAN). He is also an Adjunct Professor at the University of Oulu in the topic of communications strategies and information processing in energy systems. His research interest includes wireless communications particularly applied in industrial automation and energy systems. He received the Best Paper Award of IEEE PES Innovative Smart Grid Technologies Latin America 2019 in the track Big Data and Internet of Things. More information can be found at https://sites.google.com/view/nardelli/.

Publication V

Gutierrez-Rojas, D., Nardelli, P. H., Mendes, G., and Popovski, P.
Review of the State of the Art on Adaptive Protection for Microgrids Based on Communications

Reprinted with permission from
IEEE Transactions on Industrial Informatics
Vol. 17, no. 3, pp. 1539–1552, Mar. 2021

Review of the State of the Art on Adaptive Protection for Microgrids Based on Communications

Daniel Gutierrez-Rojas, *Student Member, IEEE*, Pedro Henrique Juliano Nardelli, *Senior Member, IEEE*, Goncalo Mendes, and Petar Popovski, *Fellow, IEEE*

***Abstract*—The dominance of distributed energy resources in microgrids and the associated weather dependence require flexible protection. They include devices capable of adapting their protective settings as a reaction to (potential) changes in the state of the system. Communication technologies have a key role in this system, since the reactions of the adaptive devices shall be coordinated. This coordination imposes strict requirements: communications must be available and ultrareliable with bounded latency in the order of milliseconds. This article reviews the state of the art in the field and provides a thorough analysis of the main related communication technologies and optimization techniques. We also present our perspective on the future of communication deployments in microgrids, indicating the viability of 5G wireless systems and multiconnectivity to enable adaptive protection.**

***Index Terms*—Adaptive protection, communication systems, distributed energy resources (DER), microgrids, renewable energy sources (RES), ultrareliable and low-latency communications (URLLC), 5G.**

Nomenclature

DER	Distributed energy resources.
DoS	Denial of service.
DPN3	Distributed network protocol.
GOOSE	Generic object-oriented substation event.
IEDs	Intelligent electronic devices.
IoT	Internet of things.
LAN	Local area network.
MPMC	Microgrid protection management controller.
NS	Network slicing.
RES	Renewable energy sources.
RTPS	Real-time publish–subscribe.
SCADA	Supervisory control and data acquisition.
SMV	Sampled measured values.
SNTP	Simple network time protocol.
URLLC	Ultrareliable and low-latency communications.

Manuscript received December 17, 2019; revised May 26, 2020 and June 19, 2020; accepted June 29, 2020. Date of publication July 3, 2020; date of current version November 20, 2020. This work was supported in part by the Academy of Finland through the ee-IoT Project under Grant 319009, FIREMAN consortium under Grant CHIST-ERA/326270, and EnergyNet Fellowship under Grant 321265 and Grant 328869, and in part by the DIGI-USER research platform. Paper no. TII-19-5321. *(Corresponding author: Pedro Henrique Juliano Nardelli.)*

Daniel Gutierrez-Rojas, Pedro Henrique Juliano Nardelli, and Goncalo Mendes are with the Lappeenranta-Lahti University of Technology, 53850 Lappeenranta, Finland (e-mail: daniel.gutierrez.rojas@lut.fi; Pedro.Nardelli@lut.fi; Goncalo.Mendes@lut.fi).

Petar Popovski is with the Department of Electronic Systems, Aalborg University, 9220 Aalborg, Denmark (e-mail: petarp@es.aau.dk).

Color versions of one or more of the figures in this article are available online at https://ieeexplore.ieee.org.

Digital Object Identifier 10.1109/TII.2020.3006845

I. Introduction

THE ELECTRIFICATION of energy systems based on RES contributes toward reaching United Nations Sustainable Development Goal 7—*ensure access to affordable, reliable, sustainable and modern energy for all*. Furthermore, building transmission lines and distribution lines, as well as new communication infrastructure to serve the traditional power systems, is becoming more and more challenging owing to, for instance, growing pressures over environmental licensing, funding allocation, etc. It has been suggested that the centralized paradigm of energy delivery is reaching its technical boundaries and no longer seems to constitute the most effective approach for granting continuous and reliable power supply to customers located at the edge of the grid, especially in countries with a high percentage of nonurban area installations [1]. The above-mentioned trends have led to increasing interest in installing small-scale generation closer to the consumption nodes—DER.

Practical modernization of the electrical grid usually refers to small-scale cluster integration of DER and customer demand at the distribution level—microgrids. Microgrids are localized electrical systems with autonomous control and enhanced grid–demand interaction, which are also able to operate in a grid-connected and islanded mode [2], [3]. Sophisticated features of microgrids as advanced power electronics and complex control configurations impose substantial technical challenges. Protection schemes and strategies against internal and external faults, which can harm system elements or consumer equipment, are among those challenges. Microgrid operational conditions may vary rapidly due to DER contribution with low inertia of nonrotating elements and rapid changes in weather conditions (wind and solar radiation) [4] or due to sudden state changes between connected and islanded modes. External faults are normally cleared using conventional protection schemes at the distribution

level, but these schemes may not be suitable to microgrid internal faults [5].

To ensure safe and appropriate operation, all variables of the microgrid elements shall be monitored, and required changes shall be applied to the device protection settings dynamically when the operating conditions of the grid change (e.g., due to fault occurrence). Conventional protection schemes, however, rely on large inertia and long transient periods, which are insufficient in this new microgrid context dominated by DER. Thus, adaptive schemes become necessary [6], [7]. The self-implemented changes by adaptive protection devices are based on "intelligent" algorithms that process the available data, making the microgrid a cyber–physical system. This leads to an additional concern about the cyber domain: failures in algorithms may stress or even harm physical components [8].

In microgrids that rely on a central management controller, the communication of IEDs is used to keep the system updated on the current state of the grid, tracking the operating currents and making proper fault detection [7], [9], [10]. A reliable communication between the system elements is, therefore, needed. In fact, any type of electrical protection scheme that relies on communication requires robustness, a virtually full-time availability, and strictly bounded latency [11]. Those stringent requirements associated with communications are hard to meet for any current communication system (either wired or wireless). Latency as low as 10 ms, high reliability (i.e., packet error rate lower than 99.999%), high availability (≈99.999%), and time synchronization are some of the key requirements that the fifth generation (5G) of wireless mobile networks promise to achieve for safe operation of electrical protection systems and that previous technologies alone cannot satisfy due to lack of performance and cost-effective solutions. In particular, the integration of different existing technologies with 5G with other wireless interfaces (e.g., WiFi, LTE, or NB-IoT) to exploit the *interface diversity* also known as multiconnectivity offers an already feasible solution for many applications that require high reliability with latency at order of milliseconds, as shown in [12]. Such a performance is only becoming possible due to major advancements in machine-type communications, adopting specific solutions for different regimes related to data rates, coverage, availability, reliability, and latency. The deployment of NS and different types of control messages to establish connections are also examples of wireless communication engineering solutions to comply with the aforementioned strict quality of service requirements.

It is also important to consider the different protocols available for communications in grid protection. The Standard IEC 61850 includes messaging protocols for control and grid automation that are ideal for adaptive protection. Although various review papers on adaptive microgrid protection and their communication schemes have been published [6], [7], [13], [14], none of them actually considers the possibility of using emerging 5G mobile communications as part of their proposed solutions. We try here to fill this gap by reviewing of the state of the art of adaptive protection focusing on the communication aspects and how 5G technologies can be deployed as an enabling technology.

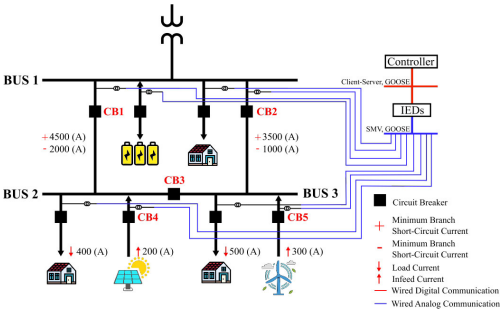

Fig. 1. Generic case of a microgrid adaptive setting with fault and load current.

The rest of this article is organized as follows. Section II presents a generic case that highlights the need for adaptive protection schemes in microgrids. Section III presents a review of techniques for adaptive protection and communication approaches in microgrids. Section IV discusses finding done in previous chapters, introduces how 5G can become a reliable communication system for adaptive microgrid protection, and elaborates on outstanding issues and challenges in this area. Finally, Section V concludes this article.

II. Adaptive Protection Schemes in Microgrids

The most common type of protection in electrical distribution systems today is overcurrent-based protection. This mission-critical application requires from the communication system a latency between 12 and 20 ms with 99.999% of reliability for sensing/metering and control purposes [15]. Overcurrent protection is impacted more than any other protection function by connection of DER [16] due to bidirectional current flow to the faulted point. The state of the different circuit breakers in the electrical grid also plays a significant role in the protection settings. Consider a generic case representation of a microgrid depicted in Fig. 1 with a common IEC 61850 communication setup.

A. Adaptive Setting

The electrical system in Fig. 1 is composed of three main circuit breakers (CB1, CB2, and CB3), which are responsible for maintaining the power supply within the microgrid and two circuits breakers (CB4 and CB5) at the DER infeed. Consider overcurrent protection functions for CB1 and CB2 associated with an IED located at BUS 1 and three different cases for their setting and reclosing.

1) Case 1. CB1 and CB2 are Closed and CB3, CB4, and CB5 are Opened: Without any infeed from DER at CB4 and CB5, apply the rule of thumb where the overcurrent settings (CB_S) are inside the interval of double the magnitude of load

current I_l and half of the minimum current fault I_f, as follows:

$$\mathrm{CB}_S = \left[I_l \times 2, \frac{I_f}{2} \right] \tag{1}$$

where currents are measured in Amperes.

At CB1, the protection setting in relation to the current is given by

$$\mathrm{CB}_{S1} = \left[400 \times 2, \frac{2000}{2} \right] \Rightarrow [800, 1000]. \tag{2}$$

For CB1, the rule of thumb applies correctly, and then, we only have to choose a setting value given inside the limits showed in (2).

Likewise, for CB2, we have

$$\mathrm{CB}_{S2} = \left[500 \times 2, \frac{1000}{2} \right] \Rightarrow [1000, 500]. \tag{3}$$

In this case, when we do not have an optimal interval, in order to find a setting, we sum the minimum fault current 500 A and load current 1000 A divided by 2, which returns a setting of 750 A. The setting must be above load current and below minimal fault current.

2) Case 2. CB2 and CB3 Closed and CB1, CB4, and CB5 are Opened: With CB3 closed, the setting at CB2 has lower margin from minimum fault current due to the increase in load current. Having 900 A of load current and 1000 A as minimum fault current, we must find a middle point for setting at 950 A. As establish before, a setting below the maximum load current could make the protective device operate under normal operating conditions, and in a setting above minimal current fault, the protective device would not be able to identify and clear any fault under faulty conditions. This means an increase in the setting at CB2, while the previous setting is inadequate for this case because, at some point, the load current may be seen as fault current by the IED causing complete isolation of both loads.

3) Case 3. CB2, CB3, CB4, and CB5 are Closed and CB1 is Opened: With the infeed of DER into the microgrid, the protection setting at CB2 can also change. A total infeed of 500 A leaves the maximum load seen from the IED at 400 A and, consequently, a bigger margin for setting overcurrent protection function at CB2.

These different cases within a simple microgrid configuration shows the necessity of awareness of the IED to know operation conditions of the network, so they can adapt to its actual state by changing their overcurrent settings and guarantee a reliable protection for all elements. This means complete fault isolation, including selectivity. Considering case 3 microgrid state, if there is a fault at BUS 2, both loads (or part of the load, if DER had a manageable way to supply part of the load at BUS 3) would get disconnected by operation of CB2, but with a centralized wireless proposed scheme, as shown in the following sections, that situation could be avoided, and power supply of load at BUS 3 could be ensured, by having a lower overcurrent setting at CB2 and operation of CB3 instead.

4) Auto-Reclosing: Once a fault in a given microgrid network is cleared by protective devices, it is important to reclose as fast as possible to minimize the lack of power supply and provide stability to the system. Auto-reclosing, though, can degrade the life of some elements or even cause permanent damage if the attempt is unsuccessful. The auto-reclosing action is mostly a control function that can be easily performed at the MPMC level to mitigate any possible damage to the system; the line branches that have less current contribution are the ones to reclose first. This implies that the MPMC has to know the current state of the circuit breakers of the microgrid, along with real-time operation currents and fault currents, so that the line branches that reclose first can be determined. Since the current measuring is performed at IEDs, these devices need to communicate with the MPMC. Similarly to the protective system for fault clearance, wireless communication seems to be a more suitable solution for this task due to its flexibility.

B. Adaptive Protection Algorithms

Traditional distribution systems are designed to have radial configuration, in order to supply power from a single power source at a time. This means that current will flow only in one direction, i.e., from the source (distribution feeders) to the load (consumer). Protection functions for radial configuration usually include nondirectional overcurrent relays or IEDs, with fixed settings and no need for communication within protective elements [17]. As microgrids start to proliferate and DER penetration in distribution networks increases, power flow and, therefore, fault current become bidirectional. Adaptive protection schemes appear as an option to solve the fault clearance challenges that are imposed in this scenario.

Fig. 2 shows the flowchart of a typical adaptive protective scheme implementation. First, the real-time data gathered by the IEDs are collected and sent through a wired communication channel (usually Ethernet-based), where these are received by the MPMC (see Fig. 3) [20], which will analyze whether a trip action was made and whether it was from a fault occurrence. Then, the microgrid state is evaluated for possible temporary conditions in the system after any possible reclose from the circuit breakers. Based on the fault currents, the system will update the settings at the decision-making table, and depending of the state of circuit breakers, a signal could be sent back to the IEDs to rewrite their actual settings for the new ones.

Additionally, in [19], after the measurements are gathered, a block of artificial neural networks and another of support vector machine algorithms estimate whether there is a fault and its location, respectively. A least-squares estimation is employed for comparison before updating the decision table. In [21], the whole tripping process is shown by dividing the flowchart into two main blocks (relay agent and central controller agent) performing an examination of grid state and updating the values of relays. After a fault occurs, the new state is evaluated to calculate new relay settings. A calculation of the average of total communication latency that involves the previous described blocks was described in [20]. Adaptive protection schemes use different methods to solve their setting adjustment when needed. Those methods also rely on different optimization techniques to find an efficient but fast method to change a predetermined variable of the IED. Examples include

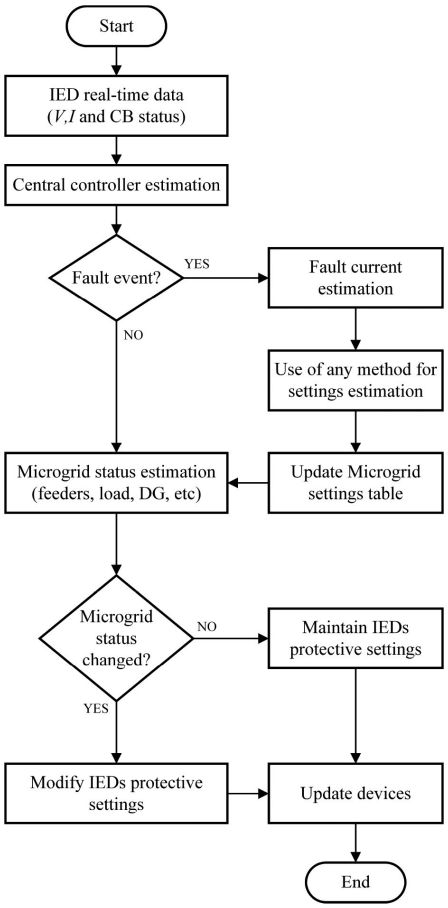

Fig. 2. Typical adaptive protection scheme (adapted from [18] and [19]).

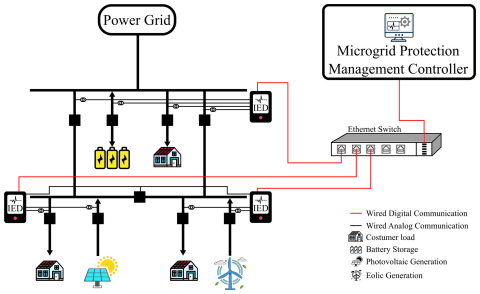

Fig. 3. Implementation of wired Ethernet-based communications for an overcurrent adaptive protection scheme (adapted from [18]).

TABLE I
WIRED AND WIRELESS COMMUNICATION FOR SUBSTATION AUTOMATION

Characteristics	Wired	Wireless
Reliability	- Once the installation is complete, probability to fail is very low	- Redundancy can lower probability to fail
Stability	- Not distorted by other connections or objects	- Variation in the latency could be experienced depending on the interference by other networks
Visibility	- Not visible by other wired connections but could be connected by nodes to facilitate data transfer	- Might be visible to other wireless connections depending of the bandwidth
Speed	- Independent cables avoid unexpected and unnecessary data making transfer faster	- Latency of 5G deployments can perform equal or better than wired networks
Security	- Firewall and other applications provide enough security when the installation is monitored	- Signals that propagate through can be intercepted. Proper encryption technologies can avoid this
Cost	- Design, space adequation and installation could be costly	- Cost of installation relatively inexpensive
Mobility	- Stationary without possibility of fast reallocation	- Flexible and easy to add new components or reallocation
Installation	- Depending on size and requirements, it can take longer to set up	- Requires less equipment and fast installation
Maintenance	- Potentially costly depending of number of elements	- Due to less elements, less costly and less frequent maintenance

differential search algorithm [22], fuzzy logic and genetic algorithm [23], and modified particle swarm optimization [24].

III. EXISTING COMMUNICATION APPROACHES IN ADAPTIVE PROTECTION SYSTEMS

A. Wired and Wireless Implementations

In wired-communication-based automation and adaptive protection implementations, the data transfer between IEDs and the MPMC takes place through cables installed at the substation level. Wireless communication, in contrast, operates based on radio frequency signals. Both implementations have advantages and disadvantages, and whether one is more appropriate than the other depends entirely on the use case. Table I presents a comparison between wired and wireless applications of some of the characteristics of substation control that are relevant for adaptive protection.

Wired connections are generally considered to be highly reliable, but their total cost and lack of flexibility impose additional challenges when new equipment is installed at the substation. Wired and wireless communication can also be combined to enhance the tasks performed by each element of the network, such as in [25], where a mix of technologies such as Fiber Optics, Broadband Power Line over medium voltage, and WiFi are used

for control and measuring. However, most work found in the literature adopts less sophisticated physical wired communications, for high reliability and low latency.

In this context, the role of emerging technologies in wireless communications (5G and integration of 5G other wireless communication interfaces) can be groundbreaking. These will be able not only to efficiently address the drawbacks from legacy wireless communications, but also to significantly enhance its capabilities. Furthermore, the discussion on the need for more versatile communication technologies, i.e., applicable to the generality of implementation use cases, increasing efficiency and reducing costs, is a valid one. Thus, the authors propose a change of paradigm of microgrid automation and control toward a scenario of prevalent adaptive protection implementations, which, as explained, constitute a significant departure from contemporary wired installations.

B. Traditional Communication Architectures

Recent literature on adaptive protection of microgrids has revealed a variety of approaches for analyzing the performance of the respective algorithms and methodologies. Some approaches focus on centralized or decentralized management for data processing and control, while others focus on the communication infrastructure to reduce times of online settings adjustment. Most of the utilized algorithms were tested in grid-connected operation conditions. A small set, however, can also work under an islanded mode, in order to test control robustness of adaptive protection in the case of communication failures or disconnection from the grid, when DER are present.

Table II summarizes the aforementioned approaches to adaptive protection in microgrids, in the last five years. In [19], a centralized approach is chosen. The article states that the methodology requires a database available beforehand, and it is obtained through simulation. It proposes a data mining methodology to quantitatively extract meaningful information from the database.

As for the implementation, the authors used a wired communication approach, along with SNTP and SCADA, which includes the IEC 61850 standard. The authors considered both grid-connected and island operation modes. A fractionalization of microgrid protection is made in [28] to avoid dependence of centralized management and to improve reliability, which can also work in grid-connected and island operation modes. In [20] and [25], a decentralized methodology is proposed using the IEC 61850 standard for grid-connected operation mode. A combination of adaptive communication-based decentralized (precontingency) and centralized (post-contingency) protection schemes is shown in [21], which is suitable for both grid-connected and islanded operation modes. In addition, in this article, the IEC 61850 is used for communication between the elements.

When a microgrid is in the island mode, it often loses its communication capabilities with a central server, leaving all protection devices operating with stationary settings or not being adjusted to the lower setting, which means that the fault will not be detected. To overcome this problem, in the case of communication failure, Habib *et al.* [54] propose a solution using a supercapacitor with a bidirectional voltage-source converter to contribute to the fault current and increase the current value to a certain level, which is sensed by the relay, and a comparison between high and low settings can be made. In [58], numerical relays and a global system for mobile communication modem are connected to communicate with each other (schematic shown in [102]) and perform a decentralized adaptive protective action due to very good coverage. In addition, in [43], the authors propose a SCADA system with advanced meter infrastructure (AMI) and 4G wireless communication.

The SCADA system is used to perform the online adaptive feature, by obtaining measurements from DER output and AMI. To acquire the mentioned data from the distribution system to the control center, a 4G wireless communication system was used. Finally, in their work, Bari and Jawale [75] suggest that the information exchange between the elements can be accomplished by a wireless sensor network.

Fig. 4 offers a quantitative analysis of the communication approaches used in adaptive protection of microgrids in recent literature, based on 85 compiled papers from the last five years. The analysis is expressed in terms of communication technology (wired or wireless), control approach (centralized or decentralized), and operation mode (grid-connected, islanded, or both operation modes). It is important to make the remark that the literature review spans from January 2015 to July 2019, i.e., publications compiled for 2019 do not reflect an entire year. The findings from this analysis are further discussed in Section IV.

C. Communication Standards and Protocols for Substation Automation and Control

When it comes to communications architecture, the IEC 61850 is a widely accepted standard for automation and equipment of power utilities and DER, specifically for defining protocols for IEDs at electrical substations [103]. There are three main protocols defined by the IEC 61850.

1) *GOOSE:* It is used to send data from IED to IED or from IED to circuit breakers due to its high-speed and high-priority characteristics, suitable for tasks such as command trips or alarms.
2) *SMV:* It is used to transfer the analog channels of current and voltage to the IED.
3) *Manufacturing message specification:* It is used for applications that are non-time-critical, such as communications between the controller and substations.

IEC 61850 also defines generic substations events, which is a control model that provides a fast and reliable mechanism for data transferring over the electrical substation network. The generic substation event model is divided into earlier described GOOSE and generic substation state events. All of the above tasks, performed inside communication layers within a power system, are adequate for protection-related applications. The three protocols run over transmission control protocol, Internet protocol, or a LAN that can use high-speed switched Ethernet like in [18].

TABLE II
MAPPING OF COMMUNICATION APPROACHES USED IN ADAPTIVE PROTECTION SCHEMES FOR MICROGRIDS

Reference		Controller		Communication			Operation Mode	
Year	Cite	Centralized	Decentralized	Wired	Wireless	Standard/Protocol	Grid-connected	Islanded
2019	[19]	✓		✓		IEC 61850, SNTP	✓	✓
	[26]	✓		✓		IEC 61850	✓	
	[27]	✓		—	—	—	✓	
	[28]		✓	✓		—	✓	✓
	[29]	✓		✓		—	✓	
	[30]	✓		✓		RTPS		✓
	[31]		✓				✓	
	[32]		✓				✓	✓
2018	[33], [34]		✓	—	—	—	✓	
	[35]		✓	✓		—	✓	
	[36]–[38]	✓		—	—	IEC 61850, DPN3	✓	✓
	[39]	✓		✓		IEC 61850	✓	✓
	[40]	✓		✓		—	✓	✓
	[41]	✓		✓		Telnet	✓	
	[42]	✓		✓		—	✓	
	[20]		✓	✓		IEC 61850	✓	
	[43], [44]	✓			✓	IEC 61850,60870-5-101	✓	
	[21]	✓	✓	✓		IEC 61850	✓	✓
	[23]	✓		—	—	IEC 61850,60870-5-101	✓	
	[7]		✓	✓				✓
	[25]		✓	✓	✓	IEC 61850	✓	
	[45]		✓	—	—	—	✓	✓
	[46]	—	—	—	—	—	✓	
	[47]–[53]	—	—	—	—	—	—	—
2017	[54]	✓	✓	—	—	—	✓	✓
	[55]	✓		—	—	—	✓	✓
	[56]	✓		—	—	IEC 61850, DPN3	✓	✓
	[57]		✓	✓		—	✓	
	[58]		✓		✓	—	✓	
	[59]	✓	✓	—	—	—	✓	✓
	[60]		✓	✓		—	✓	✓
	[61]	✓		✓		—	✓	
	[62]		✓	✓		Point-to-Point	✓	
	[63]	✓		✓		—	✓	✓
	[24], [64]–[68]	—	—	—	—	—	✓	
2016	[69]–[71]	✓		✓		—	✓	
	[72]	✓		✓		IEC 61850	✓	✓
	[73]	✓		✓		IEC 61850, DPN3	✓	✓
	[22]	✓		✓		IEC 61850	✓	
	[74]	✓		✓		IEC 61850, DPN3	✓	
	[75]	—	—		✓	—	✓	
	[76]	✓		—	—	IEC 61850, IEEE 1588	✓	✓
	[77]	✓		—	—	—	✓	✓
	[78]	—	—	—	—	—	✓	✓
	[79]–[84]	—	—	—	—	—	✓	
2015	[85]	✓		✓		IEC 61850	✓	
	[86]	✓		—	—	IEC 61850	✓	✓
	[87]	✓		—	—	—	✓	✓
	[88]	✓					✓	✓
	[89], [90]	✓		✓		—	✓	
	[91]						✓	
	[92]							✓
	[93], [94]	✓		—	—	—	✓	
	[18], [95], [96]	✓		✓		IEC61850	✓	✓
	[97]	✓	✓	—	—	—	✓	✓
	[98]	—	—	—	—	—	✓	✓
	[99]–[101]	—	—	—	—	—	✓	

— Not specified. Their main features are discussed throughout Section III.

IEC 61850 entails additional features, such as data modeling, reporting schemes, fast transfer of events, setting groups, sampled data transfer, commands, and data storage, which justify its use in substations and grid protection. A communication setup using IEC 61850 standard makes it relatively simple to achieve low latency, normally around 4 ms, which is ideal for protection purposes. Although many of the current implementations using this standard use wired Ethernet or fiber-optic physical layers, wireless communication may also be implemented using IEC 61850 for communications between the substation elements.

Other standards used are, for instance, the IEEE 1588, which describes a hierarchical master–slave architecture for clock distribution and introduces precision time protocol (PTP), used to synchronize clocks throughout a computer network. On a LAN,

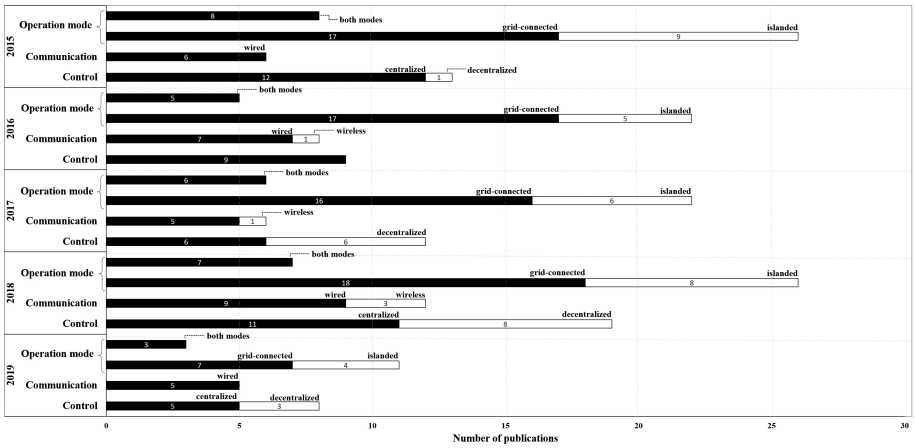

Fig. 4. Communication approaches found in microgrid adaptive protection literature, expressed in the number of publications per year.

it achieves clock accuracy in the submicrosecond range, making it suitable for measurement and control system applications [104].

The PTP supports the transmission of GOOSE messages over an Ethernet network using IEC 61850. This is generally implemented in SCADA systems, where several substations can be covered. For instance, Liu *et al.* [105] show that monitoring three pulses per second signals from master to slave can be synchronized within 200 ns and deliver accurate time stamps below 500 ns. Note that this delay has a much lower order of magnitude compared to the adaptive protection needs (order of milliseconds), making them negligible. In addition, the IEC 60870-5 defines systems used for telecontrol, supervisory control, and data acquisition in electrical engineering and power system automation applications. It provides the communication architecture for sending basic telecontrol messages between two elements (e.g., IED and MPMC) that have permanent connected communication channels. IEC 60870-5-101 specifically refers to companion standards for basic telecontrol tasks, which are commonly used in substation control and protection in SCADA systems.

Other protocols used for control purposes found in the literature and listed in Table II are the following.

1) *DPN3:* It is used mainly for communication between a master and remote terminal unit or IEDs. It provides multiplexing, data fragmentation, error checking, link control, prioritization, and layer 2 addressing services for user data. The protocol is robust, efficient, and compatible with many elements, which is suitable for SCADA systems. Depending on the elements and the applications, it can become very complex.
2) *Telnet:* It is an application protocol used in Internet or LAN to provide interactive text-oriented communication systems using a virtual terminal connection and data being interspersed in-band with control information over an 8-byte transmission control protocol. Telnet was often used to perform remote connection applications. It does not use, however, any form of encrypting mechanism, which makes it vulnerable in modern security terms.
3) *RTPS:* It is a protocol that provides two main communication models: the publish–subscribe protocol that transfers data from publishers to subscribers, and the composite state transfer protocol that transfers states. It features characteristics such as modularity, scalability, and extensibility, and it is suitable for real-time applications running over standard internet protocol networks.
4) *Peer-to-peer*: It allows us to connect a large number of users over a LAN. The scalability is no longer limited by the server. Its functions are distributed among a number of client peers, communicating in a multicast mode. Messages are sent from one client directly to another client, without relying on a central server.

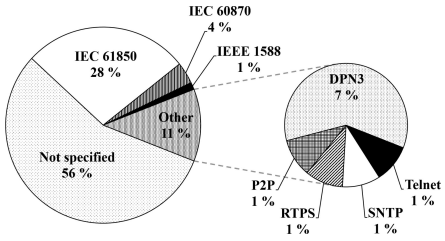

Fig. 5. Percent distribution of communication standards and protocols used in microgrid adaptive protection literature.

Fig. 5 shows the percent distribution of communication standards and protocols used in recent microgrid adaptive protection

literature (based on the same 85-research-paper sample). An immediate observation is the dominance of the IEC 61850 standard, which suggests that its protocols are suitable for adaptive protection tasks even in the case of wireless deployments, as shown in Table II.

One additional consideration to communication standards and protocols is the physical capability of network elements. Adaptive protection requires robust and flexible elements for data gathering and control. Due to their ability to receive and send data to form the closed loop of the adaptive process, IEDs comply fully with these strict requirements. IEDs must also count with sufficient flash memory capabilities to read/write protective settings [16] and successfully achieve the communication data exchange. Bari and Jawale [75] also mention that IEDs should have the ability of logging voluminous information about system parameters. In [43] and [44], the authors selected the most suitable wireless technology for collecting data in real time and transfer it to the central controller, based on synergies with SCADA systems.

D. Cyber-Security

The transition of microgrids to the cyber-physical domain comes with a number of cyber-security risks. Communication systems are vulnerable to malicious cyber-attacks. If the protection systems in place do not perform appropriately, such attacks can potentially harm the physical domain [13]. Cyber-attacks can be classified into two main categories: network security attacks and GOOSE and SMV message attacks [7]. Three types of attacks related to network security are as follows.

1) *DoS:* DoS prevents authorized users to access a service and affects the timeliness of the information exchange, which can cause packet losses. Peng *et al.* [106] address the case of load frequency control in a power system, where supply is limited from DoS attacks by transferring the model of multiarea power systems to a dependent time-delay model, in order to tolerate a certain degree of data losses induced by energy-limited DoS. Many classical approaches address this type of attacks by using distribute topology formation techniques that are based upon the cooperation between IED nodes [107].
2) *Password cracking attempts:* This method is based on attempts to gain access to system devices (such as IEDs) to gain control over them, performing tripping actions or blocking them from protective signals. For techniques to detect type of attacks, see [108].
3) *Eavesdropping attacks:* This type of attack is done by accessing the communication link between the control center and the substation and can be performed in both wired and wireless communication implementations. The data packets are intercepted by the intruder, who is able to replace real data for fabricated one. Then, the controller can send back to the IEDs tripping signals out of wrong information provided by the intruder [109].

For GOOSE and SMV attacks, we have the following.

1) *GOOSE and SMV modification attacks:* In this type of attack, the intruder modifies the message data between the IED (GOOSE sender) and the circuit breaker (GOOSE receiver) without any notice. And as SMV, the intruder can send wrong information about the analog variables of the system. In [110], a case where the minimum capabilities an intruder needs to inject a single message and perform undesirable actions is presented.
2) *GOOSE and SMV DoS attacks:* The intruder can prevent the correct operation of the IED by sending a great amount of messages to an IED target causing communication collapse and making it unable to respond to other messages.
3) *GOOSE and SMV replay attacks:* Fault information packets are kept from the intruder and then sent back to the elements under normal operation, causing undesirable tripping and possible substation outages.

When a communication failure resulting from cyber-attacks takes place in a microgrid, it would usually trigger microgrid islanding, which poses challenges to protective devices. Habib *et al.* [7] envision such a scenario, devising an approach to handle relying on energy storage. Under service of energy storage, the IEDs may be able to reach the overcurrent fixed setting to perform tripping actions in the case of fault condition, guaranteeing protection actuation and, therefore, no damages to the microgrid.

The literature is abundant in terms of proposed approaches for evaluating and preventing cyber-attack in electrical networks [111]. However, for the sake of effectiveness and robustness of operations, cyber-security should be approached holistically and from a project design stage. Therefore, to prevent those attacks, guaranteeing a reliable cyber-physical protective system embedded in the communication architecture of microgrids, substantial improvements, and thus investments in prevention, detection, mitigation, and resilience must still be undertaken.

IV. Discussion, Open Issues, and Challenges

The increasing penetration of RES in electrical networks and the dissemination of microgrids are generating interest in developing communication technologies tailored to new uses and functionalities. For instance, islanded operation will become more relevant (as seen in Fig. 4), driving the need for further adaptability in protective units for system elements. Unprecedented changes have taken place in the ways in which people communicate during the last two decades. Changes in the communication infrastructure of distribution systems and microgrids are also important and ruled by the need for greater flexibility and more cost-effective solutions. The research presented in this article highlights the predominance of wired centralized communication approaches for adaptive protection in microgrids. In contrast, it reveals no identifiable changing trend in terms of adopted communication technology (wired or wireless) in recent practical and theoretical research (see Fig. 4). There is a dominant use of IEC 61850 standard because it addresses necessary communication protocols in the substation domain 5. IEC 61850 is suitable for wireless communications and can be used for future implementation of protection and control systems. Many further developments such as the IoT, augmented reality, telemedicine, virtual reality, and unmanned driving have been applied to real businesses. These developments have brought significant changes to society, and their mobile communication requirements became higher [112]–[114].

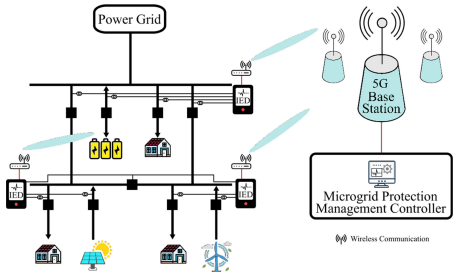

Fig. 6. Wireless 5G communications deployment with interface diversity in an overcurrent adaptive protection scheme.

Section III showed that current microgrid sensoring and monitoring rely largely on wired communications, even though wireless systems can meet increasing quality of service requirements (as ongoing discussions on 5G suggest). On a related note, the recent appearance of mobile 5G wireless communications, an evolution of 4G, as proposed by the latest realization of the 3rd Generation Partnership Project, has revealed highly promising for various vertical use cases, with reported efficient technical and economical solutions [115]. In the years to come, 5G networks shall include features targeted at improved performance for specific vertical use cases (as the case of energy and automation verticals). Advantages of 5G communication infrastructure include cost savings (no wired physical connections are needed), network virtualization, improved response time, efficiency, flexibility, redundancy, and its platform approach, where a single interface is used to provide different types of connectivity [116]. Microgrid protection will eventually benefit from 5G technology developments, as it matures, since all network communications within the different elements from traditional protection or adaptive protection can be made using a centralized scheme, as shown in Fig. 6.

In particular, 5G is framed as having three cornerstones:

1) *enhanced mobile broadband:* more data rate and connectivity than previous technology (4G);
2) *massive machine-type communication (mMTC):* larger number of devices connected than 4G and possibility of machine-to-machine communications;
3) *URLLC:* 1-ms latency and 99.999% reliability.

All the above features are relevant and will play a key role in substation control and grid automation. For instance, system operators can connect devices that are located in zones with difficult access. 5G would also allow for protection to become more distributed by installing IEDs at points closer to consumption and DER generation without having to build new communication infrastructure. mMTC schemes could be used by IEDs to communicate without having to rely on central servers for actuation purposes (e.g., reclosing schemes or informing the current state of a branch), as well as including one or multiples IEDs to the network, maintaining the same base stations (scalability). If one considers a large network deployment, as in a big city, massive connectivity between the elements is needed.

However, URLLC is the most promising regime for adaptive protection in microgrids. Previous work shows that message latency should be constrained by two cycles (i.e., 40 ms for a 50-Hz power system) [117], while other indicates a stricter requirement between 12 and 20 ms [15], both considering high reliability. Current 4G systems can deliver an end-to-end latency of 20 ms, at best, which is a result of the constraint from the frame structure. For example, tests in a 4G industrial private network achieved in the most favorable settings a delay of 26 ms (in comparison to a wired Ethernet scenario that achieved a delay of 3 ms) [118]. It is important to mention that, although 5G URLLC targets latencies as low as 1 ms, our particular application is less strict requiring 12-ms latency at the most stringent cases.

In terms of reliability, the performance of 4G is dependent on several parameters, from the size of the message to the number of users. In [12], the authors have proposed a quantitative relation between these key parameters based on field measurements. The URLLC regime in 5G relates latency and reliability in a sense that the target reliability should be achieved within a very low latency constraint; originally, this constraint was 1 ms, but in the later years, it has been relaxed according to some more elaborate requirements for industrial IoT (see, e.g., [119, Table 1]). Even these more relaxed versions, including the one we are using for the adaptive protection case, cannot be met by 4G.

In this case, the data-driven reliability guarantees based on a statistical learning framework seems a more suitable approach than the "deterministic" 1 ms potentially provided in the URLLC regime [120]. Depending on the application, ultrareliability is critical, but the low latency is more flexible; the adaptive protection exemplifies this. Besides, recent results have proved that interface diversity where 5G combined with other wireless interfaces can provide ultrareliability with bounded delay, which would satisfy the adaptive protection requirements [12].

The integration of these different quality of service can be done by NS, which is a concept that finds an efficient way for serving a determined application with 5G features on a common infrastructure [121], [122]. Various works in fields of communication for applications in Industry 4.0 show that NS using programmability and flexibility can be used to reduce complexity. This allows getting the best feature from a communication network, depending on the requirements from specific applications [123]. A slice can be considered an independent network, with corresponding advantages; in microgrid protection, it could be divided in many slices depending on the availability, latency, or message type, as shown in [124]. This concept makes communications even more flexible. As RES penetration increases in distribution systems, particularly in microgrids, the bidirectional fault current magnitudes become bigger, more sensors need to be installed, and, therefore, more signals need to be monitored. It then becomes a growing challenge for communication systems to deliver different messages from sensing devices to controllers and actuators. NS architectures may be able to efficiently deal with the complexity of handling such different and demanding requirements, which can range from high reliability and low latency to high data rates on the same industrial application.

All in all, new ways to incorporate wireless technology in substation automation and control need to be researched in

the upcoming years, to accompany the rapid changes electrical distribution systems are already undergoing. The wired communication infrastructure will not be able to catch up, due to the lack of scalability and further prohibitive characteristics. A good approach would be multiconnectivity that combines wired and wireless, as those technologies have different failure patterns. 5G communications will open new frontiers in how these systems can be effectively integrated to perform tasks such as adaptive protection with very stringent requirements [125]. In particular, ultrareliable communications with latency constraints required to perform adaptive protection should coexist with other applications with multiple requirements, including massive connectivity of machine-type devices and more traditional broadband applications. While current 5G solutions are not yet capable of reaching the demanded performance in protection applications, upcoming releases of 5G—and even of 6G—are expected to focus on specific vertical applications and application-specific requirements. In this context, fast technological developments, including potentially groundbreaking concepts, such as semantic filters [126] and edge intelligence, are expected to take place in the upcoming years[127]. These developments should allow for tailored wireless communication solutions, i.e., based on specific applications and their particular requirements, that coexist and share the same resources.

Usually, societal paradigm changes take place decades after key technologies (such as 5G) have been developed, and rapid adoption is limited by conservative and progressive investment. The adoption of wireless connectivity in energy sector has not yet become mainstream. Some solutions such as 4G and WiFi are deployed for some applications (mainly monitoring, metering, and demand response), but not for adaptive protection, due to their performance limitations. Upgrading infrastructure to add 5G capabilities would bring additional capital costs considering incremental deployment in the existing grid infrastructure. In contrast, it is expected that 5G brings down the operational costs related to communication network operations, due to its modularity and scalability [128]. In 5G, the concept of local operator and private cellular networks indicates the tendency of third-party service providers, which is expected to decrease the operational costs related to the communication network, compared to more expensive deployment and maintenance of wired networks [129].

5G has many potential advantages, but also some challenges related to its effective implementation. These challenges are commonly associated with cyber-security. Careful examination of communication technologies has to be taken into consideration during a control and protection project design stage. The authors suggest this step to be essential for the economic viability of the project, since it can greatly reduce costs. This design should also include a robust system architecture to prevent or avoid possible cyber-attacks, given the vulnerability of wireless communication systems over wired communication systems. The reason for this is the wireless air propagation channel, where signals can be picked up from nearby locations without interfering in any hardware equipment.

It is worth restating that the proposed adaptive protection scheme can greatly reduce costs associated with the communication network, bringing more flexibility in comparison to the traditional wired solutions. The benefits of using 5G would also be combined with already deployed solutions, leading to gains from multiconnectivity, which is a popular way of attaining now that there are many wireless interfaces available [12]. In summary, we argue that the proposed solution generally complies with the current deployments, which yields a smooth transition that will bring not only technical benefits but also economical ones.

V. Conclusion

This article presented key technical aspects related to the communication system that is needed to perform adaptive protection in microgrids with high penetration of DERs. We particularly focused on different exiting solutions for adaptive protection systems, which were dominantly based on wired solutions. We covered the traditional communication architectures (e.g., centralized or decentralized) and standards (e.g., GOOSE, SMV, and RTPS, among others). We also discussed aspects related to cyber-security, including potential threats and types of attacks. What is remarkable, though, is that current approaches mostly rely on wired networks despite the unquestionable performance gains of wireless technologies during the last decade. In this sense, we argue that 5G in combination with other existing solutions (e.g., WiFi) can already achieve the required reliability of 99.999% with a bounded latency as low as 12 ms so that they should be seriously considered as a feasible enabler of adaptive protection applications. In the near future, we expect that these solutions will take over many traditionally wired applications, since wireless solutions tend to be cheaper, more flexible, and easier to implement than wired ones to perform the same tasks, including mission-critical ones. All in all, this review highlighted the state of the art in the field indicating possible research directions that shall be taken to effectively deploy adaptive protection using wireless communications.

References

[1] H. Lee *et al.*, "An energy management system with optimum reserve power procurement function for microgrid resilience improvement," *IEEE Access*, vol. 7, pp. 42577–42585, 2019.
[2] C. Marnay and J. Lai, "Serving electricity and heat requirements efficiently and with appropriate energy quality via microgrids," *Elect. J.*, vol. 25, pp. 7–15, 2012.
[3] P. H. Nardelli *et al.*, "Models for the modern power grid," *Eur. Phys. J. Special Topics*, vol. 223, no. 12, pp. 2423–2437, 2014.
[4] M. A. Haj-ahmed and M. S. Illindala, "The influence of inverter-based DGs and their controllers on distribution network protection," in *Proc. IEEE Ind. Appl. Soc. Annu. Meeting*, Oct. 2013, pp. 1–9.
[5] M. Soshinskaya, W. H. J. Crijns -Graus, J. M. Guerrero, and J. C. Vasquez, "Microgrids: Experiences, barriers and success factors," *Renew. Sustain. Energy Rev.*, vol. 40, pp. 659–672, 2014.
[6] T. S. Ustun, C. Ozansoy, and A. Zayegh, "A microgrid protection system with central protection unit and extensive communication," in *Proc. 10th Int. Conf. Environ. Elect. Eng.*, May 2011, pp. 1–4.
[7] H. F. Habib, C. R. Lashway, and O. A. Mohammed, "A review of communication failure impacts on adaptive microgrid protection schemes and the use of energy storage as a contingency," *IEEE Trans. Ind. Appl.*, vol. 54, no. 2, pp. 1194–1207, Mar./Apr. 2018.
[8] M. H. Cintuglu, O. A. Mohammed, K. Akkaya, and A. S. Uluagac, "A survey on smart grid cyber-physical system testbeds," *IEEE Commun. Surv. Tuts.*, vol. 19, no. 1, pp. 446–464, First Quarter 2017.
[9] H. Wan, K. K. Li, and K. P. Wong, "An adaptive multiagent approach to protection relay coordination with distributed generators in industrial power distribution system," *IEEE Trans. Ind. Appl.*, vol. 46, no. 5, pp. 2118–2124, Sep./Oct. 2010.

[10] H. F. Habib, T. Youssef, M. H. Cintuglu, and O. A. Mohammed, "Multi-agent-based technique for fault location, isolation, and service restoration," *IEEE Trans. Ind. Appl.*, vol. 53, no. 3, pp. 1841–1851, May/Jun. 2017.

[11] M. Baranwal, A. Askarian, S. Salapaka, and M. Salapaka, "A distributed architecture for robust and optimal control of DC microgrids," *IEEE Trans. Ind. Electron.*, vol. 66, no. 4, pp. 3082–3092, Apr. 2019.

[12] J. J. Nielsen, R. Liu, and P. Popovski, "Ultra-reliable low latency communication using interface diversity," *IEEE Trans. Commun.*, vol. 66, no. 3, pp. 1322–1334, Mar. 2018.

[13] S. Beheshtaein, R. Cuzner, M. Savaghebi, and J. M. Guerrero, "Review on microgrids protection," *IET Gener, Transmiss. Distrib.*, vol. 13, no. 6, pp. 743–759, Mar. 2019.

[14] S. Beheshtaein, R. M. Cuzner, M. Forouzesh, M. Savaghebi, and J. M. Guerrero, "DC microgrid protection: A comprehensive review," *IEEE J. Emerg. Sel. Topics Power Electron.*, to be published, doi: 10.1109/JESTPE.2019.2904588.

[15] Y. Yan, Y. Qian, H. Sharif, and D. Tipper, "A survey on smart grid communication infrastructures: Motivations, requirements and challenges," *IEEE Commun. Surv. Tuts.*, vol. 15, no. 1, pp. 5–20, First Quarter 2013.

[16] R. Moxley and F. Becker, "Adaptive protection what does it mean and what can it do?" in *Proc. 71st Annu. Conf. Protective Relay Eng.*, Mar. 2018, pp. 1–4.

[17] R. Bansal, *Power System Protection in Smart Grid Environment.* Boca Raton, FL, USA: CRC Press, 2019.

[18] C. Ozansoy, "A methodology for determining fault current impact coefficients of distributed energy resources in an adaptive protection scheme," in *Proc. 9th Int. Conf. Elect. Electron. Eng.*, Nov. 2015, pp. 479–483.

[19] H. Lin, K. Sun, Z. Tan, C. Liu, J. M. Guerrero, and J. C. Vasquez, "Adaptive protection combined with machine learning for microgrids," *IET Gener., Transmiss. Distrib.*, vol. 13, no. 6, pp. 770–779, 2019.

[20] X. Jin, R. Gokaraju, R. Wierckx, and O. P. Nayak, "High speed digital distance relaying scheme using FPGA and IEC 61850," *IEEE Trans. Smart Grid*, vol. 9, no. 5, pp. 4383–4393, Sep. 2018.

[21] M. J. Daryani, A. E. Karkevandi, and O. Usta, "Multi-agent approach to wide-area integrated adaptive protection system of microgrid for pre- and post-contingency conditions," in *Proc. IEEE PES Innovative Smart Grid Technol. Conf. Eur.*, Oct. 2018, pp. 1–6.

[22] M. Singh, T. Vishnuvardhan, and S. Srivani, "Adaptive protection coordination scheme for power networks under penetration of distributed energy resources," *IET Gener., Transmiss. Distrib.*, vol. 10, no. 15, pp. 3919–3929, Nov. 2016.

[23] N. E. Naily, S. M. Saad, T. Hussein, K. El-Arroudi, and F. A. Mohamed, "On-line adaptive protection scheme to overcome operational variability of DG in smart grid via fuzzy logic and genetic algorithm," in *Proc. 9th Int. Renew. Energy Congr.*, Mar. 2018, pp. 1–6.

[24] A. I. Atteya, A. M. E. Zonkoly, and H. A. Ashour, "Optimal relay coordination of an adaptive protection scheme using modified PSO algorithm," in *Proc. 19th Int. Middle East Power Syst. Conf.*, Dec. 2017, pp. 689–694.

[25] A. A. de Sotomayor, D. D. Giustina, G. Massa, A. Dedè, F. Ramos, and A. Barbato, "IEC 61850-based adaptive protection system for the MV distribution smart grid," *Sustain. Energy, Grids Netw.*, vol. 15, pp. 26–33, Sep. 2018.

[26] M. N. Alam, "Adaptive protection coordination scheme using numerical directional overcurrent relays," *IEEE Trans. Ind. Inform.*, vol. 15, no. 1, pp. 64–73, Jan. 2019.

[27] S. Teimourzadeh, F. Aminifar, M. Davarpanah, and M. Shahidehpour, "Adaptive protection for preserving microgrid security," *IEEE Trans. Smart Grid*, vol. 10, no. 1, pp. 592–600, Jan. 2019.

[28] M. Singh and P. Basak, "Adaptive protection methodology in microgrid for fault location and nature detection using q0 components of fault current," *IET Gener., Transmiss. Distrib.*, vol. 13, no. 6, pp. 760–769, 2019.

[29] V. Nougain, S. Mishra, and A. K. Pradhan, "MVDC microgrid protection using a centralized communication with a localized backup scheme of adaptive parameters," *IEEE Trans. Power Del.*, vol. 34, no. 3, pp. 869–878, Jun. 2019.

[30] H. Habib, M. M. Esfahani, and O. A. Mohammed, "Investigation of protection strategy for microgrid system using lithium-ion battery during islanding," *IEEE Trans. Ind. Appl.*, vol. 55, no. 4, pp. 3411–3420, Jul./Aug. 2019.

[31] A. E. Momesso, W. M. S. Bernardes, and E. N. Asada, "Fuzzy adaptive setting for time-current-voltage based overcurrent relays in distribution systems," *Int. J. Elect. Power Energy Syst.*, vol. 108, pp. 135–144, 2019.

[32] R. R. Ferreira, P. J. Colorado, A. P. Grilo, J. C. Teixeira, and R. C. Santos, "Method for identification of grid operating conditions for adaptive overcurrent protection during intentional islanding operation," *Int. J. Elect. Power Energy Syst.*, vol. 105, pp. 632–641, Feb. 2019.

[33] S. A. Hosseini, A. Nasiri, and S. H. H. Sadeghi, "A decentralized adaptive scheme for protection coordination of microgrids based on team working of agents," in *Proc. 7th Int. Conf. Renew. Energy Res. Appl.*, Oct. 2018, pp. 1315–1320.

[34] S. Paladhi and A. K. Pradhan, "Adaptive zone-1 setting following structural and operational changes in power system," *IEEE Trans. Power Del.*, vol. 33, no. 2, pp. 560–569, Apr. 2018.

[35] S. AsghariGovar, S. Heidari, H. Seyedi, S. Ghasemzadeh, and P. Pourghasem, "Adaptive CWT-based overcurrent protection for smart distribution grids considering CT saturation and high-impedance fault," *IET Gener., Transmiss. Distrib.*, vol. 12, no. 6, pp. 1366–1373, 2018.

[36] C. Chandraratne, W. L. Woo, T. Logenthiran, and R. T. Naayagi, "Adaptive overcurrent protection for power systems with distributed generators," in *Proc. 8th Int. Conf. Power Energy Syst.*, Dec. 2018, pp. 98–103.

[37] K. Sedghisigarchi and K. T. Sardari, "An adaptive protection strategy for reliable operation of microgrids," in *Proc. IEEE Int. Energy Conf.*, Jun. 2018, pp. 1–6.

[38] M. Amaratunge, D. U. Y. Edirisuriya, A. L. A. P. L. Ambegoda, M. A. C. Costa, W. L. T. Peiris, and K. T. M. U. Hemapala, "Development of adaptive overcurrent relaying scheme for IIDG microgrids," in *Proc. 2nd Int. Conf. Elect. Eng.*, Sep. 2018, pp. 71–75.

[39] R. Shah, P. Goli, and W. Shireen, "Adaptive protection scheme for a microgrid with high levels of renewable energy generation," in *Proc. Clemson Univ. Power Syst. Conf.*, Sep. 2018, pp. 1–7.

[40] W. L. T. Peiris, W. H. Eranga, K. T. M. U. Hemapala, and W. D. Prasad, "An adaptive protection scheme for small scale microgrids based on fault current level," in *Proc. 2nd Int. Conf. Elect. Eng.*, Sep. 2018, pp. 64–70.

[41] K. Q. da Silva *et al.*, "An adaptive protection system for distribution network with distributed generation," in *Proc. Simposio Brasileiro de Sist. Eletricos*, May 2018, pp. 1–6.

[42] M. Zanjani, K. Mazlumi, and I. Kamwa, "Application of μPMUs for adaptive protection of overcurrent relays in microgrids," *IET Gener., Transmiss. Distrib.*, vol. 12, no. 18, pp. 4061–4068, 2018.

[43] K. Xu and Y. Liao, "Intelligent method for online adaptive optimum coordination of overcurrent relays," in *Proc. Clemson Univ. Power Syst. Conf.*, Sep. 2018, pp. 1–5.

[44] K. Xu and Y. Liao, "Online adaptive optimum coordination of overcurrent relays," in *Proc. Clemson Univ. Power Syst. Conf.*, Apr. 2018, pp. 1–5.

[45] Z. Zhonghua, J. Zhen, C. Jun, S. Zhiwei, and W. Yanguo, "Topology self-identification and adaptive operation method of distribution network protection and self-healing system," in *Proc. Int. Conf. Power Syst. Technol.*, Nov. 2018, pp. 3087–3092.

[46] J. Ma, J. Liu, Z. Deng, S. Wu, and J. S.Thorp, "An adaptive directional current protection scheme for distribution network with DG integration based on fault steady-state component," *Int. J. Elect. Power Energy Syst.*, vol. 102, pp. 223–234, Nov. 2018.

[47] Y. Cai, Z. Cai, C. Guo, Y. Huang, and G. Dai, "Research on adaptive protection and control algorithm for distribution network based on network description model," in *Proc. Int. Conf. Power Syst. Technol.*, Nov. 2018, pp. 142–147.

[48] Y. Kang and Z. Duan, "New algorithm for adaptive current protection setting of fan connected to distribution network," in *Proc. Electron. Autom. Control Conf IEEE 3rd Adv. Inf. Technol.*, Oct. 2018, pp. 1415–1419.

[49] Z. Linli *et al.*, "Adaptive tripping for distribution network based on fault indicator recording data," in *Proc. China Int. Conf. Electricity Distribution*, Sep. 2018, pp. 1659–1664.

[50] A. K. Upadhiya, S. Sarangi, G. K. Rao, and S. Painuli, "Adaptive fault location algorithm for double circuit line," in *Proc. Int. Conf. Power Energy Environ. Intell. Control*, Apr. 2018, pp. 801–806.

[51] X. He, Q. Qian, Y. Wang, Y. Wang, and S. Shi, "Adaptive traveling waves based protection of distribution lines," in *Proc. 2nd IEEE Conf. Energy Internet Energy Syst. Integr.*, Oct. 2018, pp. 1–5.

[52] W. M. Elhadad, A. Y. Hatata, and E. A. Badran, "A proposed adaptive distance relay model in ATPDraw," in *Proc. 20th Int. Middle East Power Syst. Conf.*, Dec. 2018, pp. 754–759.

[53] J. Zhao and R. Bian, "A new method of adaptive current protection for distribution lines with wind turbines," in *Proc. IEEE 3rd Adv. Inf. Technol. Electron. Autom. Control Conf*, Oct. 2018, pp. 269–273.

[54] H. F. Habib, A. A. S. Mohamed, M. E. Hariri, and O. A. Mohammed, "Utilizing supercapacitors for resiliency enhancements and adaptive microgrid protection against communication failures," *Electr. Power Syst. Res.*, vol. 145, pp. 223–233, Apr. 2017.

[55] E. Purwar, D. N. Vishwakarma, and S. P. Singh, "A new adaptive inverse-time protection scheme for modern distribution systems with distributed generation," in *Proc. IEEE Power Energy Soc. Innovative Smart Grid Technol. Conf.*, Apr. 2017, pp. 1–5.

[56] B. A. Pacheco, M. A. I. Martins, C. Q. Pica, and N. Rodrigues, "A case study of adaptive microgrid protection during transitions and operations," in *Proc. Brazilian Power Electron. Conf.*, Nov. 2017, pp. 1–5.

[57] K. A. Wheeler, S. O. Faried, and M. Elsamahy, "A microgrid protection scheme using differential and adaptive overcurrent relays," in *Proc. IEEE Elect. Power Energy Conf.*, Oct. 2017, pp. 1–6.

[58] N. E. Naily, S. M. Saad, J. Wafi, A. Elhaffar, and N. Husseinzadch, "Adaptive overcurrent protection to mitigate high penetration of distributed generation in weak distribution systems," in *Proc. 9th IEEE-GCC Conf. Exhib.*, May 2017, pp. 1–9.

[59] S. Gaber, K. Hassan, and A. Megahed, "A novel adaptive wide area protection scheme for smart grids with distributed generation," in *Proc. 19th Int. Middle East Power Syst. Conf.*, Dec. 2017, pp. 802–810.

[60] U. Orji *et al.*, "Adaptive zonal protection for ring microgrids," *IEEE Trans. Smart Grid*, vol. 8, no. 4, pp. 1843–1851, Jul. 2017.

[61] E. C. Piesciorovsky and N. N. Schulz, "Fuse relay adaptive overcurrent protection scheme for microgrid with distributed generators," *IET Gener., Transmiss. Distrib.*, vol. 11, no. 2, pp. 540–549, 2017.

[62] W. Tang and H. Yang, "Self-adaptive protection strategies for distribution system with DGs and FCLs based on data mining and neural network," in *Proc. IEEE Int. Conf. Environ. Elect. Eng. IEEE Ind. Commercial Power Syst. Eur.*, Jun. 2017, pp. 1–5.

[63] H. Muda and P. Jena, "Sequence currents based adaptive protection approach for DNs with distributed energy resources," *IET Gener. Transmiss. Distrib.*, vol. 11, no. 1, pp. 154–165, 2017.

[64] E. C. Piesciorovsky and N. N. Schulz, "Comparison of ,real-time and real-time simulators with relays in-the-loop for adaptive overcurrent protection," *Electr. Power Syst. Res.*, vol. 143, pp. 657–668, Feb. 2017.

[65] S. Shen *et al.*, "An adaptive protection scheme for distribution systems with DGs based on optimized thevenin equivalent parameters estimation," *IEEE Trans. Power Del.*, vol. 32, no. 1, pp. 411–419, Feb. 2017.

[66] S. P. George and S. Ashok, "Over current relay coordination in a real system with wind farm integration using hybrid genetic algorithm approach," in *Proc. IET Int. Conf. Resilience Transmiss. Distrib. Netw.*, Sep. 2017, pp. 1–6.

[67] X. Song, Y. Zhang, S. Zhang, S. Song, J. Ma, and W. Zhang, "Adaptive protection scheme for distributed systems with DG," *J. Eng.*, vol. 2017, no. 13, pp. 1432–1436, 2017.

[68] A. Tjahjono *et al.*, "Adaptive modified firefly algorithm for optimal coordination of overcurrent relays," *Transmiss. Distribution IET Gener.*, vol. 11, no. 10, pp. 2575–2585, 2017.

[69] S. Misak, J. Stuchly, J. Vramba, T. Vantuch, and D. Seidl, "A novel approach to adaptive active relay protection system in single phase AC coupling off-grid systems," *Electr. Power Syst. Res.*, vol. 131, pp. 159–167, Feb. 2016.

[70] H. S. Sanca, F. C. Souza, B. A. Souza, and F. B. Costa, "Comparison frequency estimation methods on adaptive protection architecture applied on systems with distributed generation," in *Proc. 13th Int. Conf. Develop. Power Syst. Protection*, Mar. 2016, pp. 1–6.

[71] H. Leite, E. Almeida, and N. Silva, "Real-time closed-loop test to adaptive protection in a smart-grid context," in *Proc. 13th Int. Conf. Develop. Power Syst. Protection*, Mar. 2016, pp. 1–5.

[72] Z. Liu and H. K. Hidalen, "A simple multi agent system based adaptive relay setting strategy for distribution system with wind generation integration," in *Proc. 13th Int. Conf. Develop. Power Syst. Protection*, Mar. 2016, pp. 1–6.

[73] H. Lin, J. M. Guerrero, C. Jia, Z.-hua Tan, J. C. Vasquez, and C. Liu, "Adaptive overcurrent protection for microgrids in extensive distribution systems," in *Proc. 42nd Annu. Conf. IEEE Ind. Electron. Soc.*, Oct. 2016, pp. 4042–4047.

[74] M. Y. Shih, A. C. Enrquez, Z. M. Leonowicz, and L. Martirano, "Mitigating the impact of distributed generation on directional overcurrent relay coordination by adaptive protection scheme," in *Proc. IEEE 16th Int. Conf. Environ. Elect. Eng.*, Jun. 2016, pp. 1–6.

[75] N. A. Bari and S. D. Jawale, "Smart and adaptive protection scheme for distribution network with distributed generation: A scoping review," in *Proc. Int. Conf. Energy Efficient Technol. Sustainability*, Apr. 2016, pp. 569–572.

[76] O. V. G. Swathika and S. Hemamalini, "Prims-aided Dijkstra algorithm for adaptive protection in microgrids," *IEEE J. Emerg. Sel. Topics Power Electron.*, vol. 4, no. 4, pp. 1279–1286, Dec. 2016.

[77] H. Muda and P. Jena, "Real time simulation of new adaptive overcurrent technique for microgrid protection," in *Proc. Nat. Power Syst. Conf.*, Dec. 2016, pp. 1–6.

[78] M. Pujiantara *et al.*, "Optimization technique based adaptive overcurrent protection in radial system with DG using genetic algorithm," in *Proc. Int. Seminar Intell. Technol. Appl.*, Jul. 2016, pp. 83–88.

[79] S. Chen, N. Tai, C. Fan, S. Hong, and J. Liu, "An adaptive current protection for distributed network with wind generators," in *Proc. IEEE Power Energy Soc. Gen. Meeting*, Jul. 2016, pp. 1–5.

[80] J. H. He, Y. H. Cheng, J. Hu, and H. T. Yip, "An accelerated adaptive overcurrent protection for distribution networks with high DG penetration," in *Proc. 13th Int. Conf. Develop. Power Syst. Protection*, Mar. 2016, pp. 1–5.

[81] N. V. Grebchenko, D. Y. Osipov, A. G. Teslya, J. B. Bozok, and I. I. Koval, "Adaptive current short-circuit protection in electric systems with distributed generation," in *Proc. Int. Symp. Power Electron., Elect. Drives, Autom. Motion*, Jun. 2016, pp. 1279–1283.

[82] T. Bujanovic and P. Ghosh, "Adaptive algorithm for microprocessor based distance relays in smart grid," in *Proc. IEEE Smart Energy Grid Eng.*, Aug. 2016, pp. 358–364.

[83] X. Guo, B. Han, J. Lei, and G. Wang, "A novel adaptive zero-sequence current protection for low resistance grounding system," in *Proc. IEEE PES Asia-Pacific Power Energy Eng. Conf.*, Oct. 2016, pp. 2523–2528.

[84] D. Jiandong, S. Lei, C. Shuaishuai, H. Yu, and L. Wuji, "Research on adaptive current instantaneous trip protection for active distribution network line with DFIGs," in *Proc. China Int. Conf. Elect. Distrib.*, Aug. 2016, pp. 1–5.

[85] D. D. Giustina, A. Ded, A. A. de Sotomayor, and F. Ramos, "Toward an adaptive protection system for the distribution grid by using the IEC 61850," in *Proc. IEEE Int. Conf. Ind. Technol.*, Mar. 2015, pp. 2374–2378.

[86] H. Lin, J. M. Guerrero, J. C. Vasquez, and C. Liu, "Adaptive distance protection for microgrids," in *Proc. 41st Annu. Conf. IEEE Ind. Electron. Soc.*, Nov. 2015, pp. 725–730.

[87] K. Vijitha, M. P. Selvan, and P. Raja, "Short circuit analysis and adaptive zonal protection of distribution system with distributed generators," in *Proc. Int. Conf. Energy, Power Environ.: Towards Sustain. Growth*, Jun. 2015, pp. 1–6.

[88] M. Farsadi, A. Y. Nejadi, and A. Esmaeilynasab, "Reducing over-current relays operating times in adaptive protection of distribution networks considering DG penetration," in *Proc. 9th Int. Conf. Elect. Electron. Eng.*, Nov. 2015, pp. 463–468.

[89] V. A. Papaspiliotopoulos, G. N. Korres, and N. D. Hatziargyriou, "Protection coordination in modern distribution grids integrating optimization techniques with adaptive relay setting," in *Proc. IEEE Eindhoven PowerTech*, Jun. 2015, pp. 1–6.

[90] A. Gupta, A. Varshney, O. V. G. Swathika, and S. Hemamalini, "Dual simplex algorithm aided adaptive protection of microgrid," in *Proc. Int. Conf. Comput. Intell. Commun. Netw.*, Dec. 2015, pp. 1505–1509.

[91] W. Fan, Z. Wu, X. Dou, Y. Shi, Y. Wang, and M. Zhou, "Preliminary study on adaptive fast-tripping current protection for microgrid," in *Proc. IEEE Innovative Smart Grid Technol.*, Nov. 2015, pp. 1–6.

[92] R. R. Ferreira, A. P. Grilo, J. C. Teixeira, and R. C. Santos, "Method for adaptive overcurrent protection of distribution systems with distributed synchronous generators," in *Proc. IEEE Power Energy Soc. Gen. Meeting*, Jul. 2015, pp. 1–5.

[93] S. P. George and S. Ashok, "Multiagent based adaptive relaying for distribution network with distributed generation," in *Proc. Int. Conf. Energy, Power Environ.: Towards Sustain. Growth*, Jun. 2015, pp. 1–6.

[94] J. P. Nascimento, N. S. D. Brito, and B. A. de Souza, "An adaptive protection algorithm for distribution systems with distributed generation," in *Proc. IEEE PES Innovative Smart Grid Technol. Latin Amer.*, Oct. 2015, pp. 165–170.

[95] C. Ozansoy, "Design of an adaptive protection system for microgrids with distributed energy resources in accordance with IEC 61850-7-420," in *Proc. 9th Int. Conf. Elect. Electron. Eng.*, Nov. 2015, pp. 474–478.

[96] F. Coffele, C. Booth, and A. Dyko, "An adaptive overcurrent protection scheme for distribution networks," *IEEE Trans. Power Del.*, vol. 30, no. 2, pp. 561–568, Apr. 2015.

[97] B. P. Bhattarai, B. Bak-Jensen, S. Chaudhary, and J. R. Pillai, "An adaptive overcurrent protection in smart distribution grid," in *Proc. IEEE Eindhoven PowerTech*, Jun. 2015, pp. 1–6.
[98] N. Tummasit, S. Premrudeepreechacharn, and N. Tantichayakorn, "Adaptive overcurrent protection considering critical clearing time for a microgrid system," in *Proc. IEEE Innovative Smart Grid Technol.*, Nov. 2015, pp. 1–6.
[99] P. Esmaili, A. A. b. M. Zin, and O. Shariati, "On-line overcurrent relays setting approach in distribution networks by implementing new adaptive protection algorithm," in *Proc. IEEE 10th Int. Conf. Intell. Sens., Sens. Netw. Inf. Process.*, Apr. 2015, pp. 1–6.
[100] D. S. Kumar, B. M. Radhakrishnan, D. Srinivasan, and T. Reindl, "An adaptive fuzzy based relay for protection of distribution networks," in *Proc. IEEE Int. Conf. Fuzzy Syst.*, Aug. 2015, pp. 1–6.
[101] J. López, Y. Hsiao, T. Hsiao, and C. Lu, "Adaptive system protection scheme using generalized pattern search," in *Proc. 18th Int. Conf. Intell. Syst. Appl. Power Syst.*, Sep. 2015, pp. 1–6.
[102] A. Elhaffar, N. El-Naily, and K. El-Arroudi, "Management of distribution system protection with high penetration of DGs," in *Energy Systems and Management*. New York, NY, USA: Springer, 2015, pp. 279–291.
[103] *IEEE Standard Test Methods for Use in the Evaluation of Message Communications Between Intelligent Electronic Devices in an Integrated Substation Protection, Control and Data Acquisition System*, IEEE Standard C37.115-2003, 2003.
[104] *IEEE Standard for a Precision Clock Synchronization Protocol for Networked Measurement and Control Systems*," IEEE Standard 1588-2002, Oct. 2002, pp. 1–154.
[105] Y. Liu, R. Zivanovic, S. Al-Sarawi, C. Marinescu, and R. Cochran, "A synchronized event logger for substation topology processing," in *Proc. Australas. Univ. Power Eng. Conf.*, 2009, pp. 1–6.
[106] C. Peng, J. Li, and M. Fei, "Resilient event-triggering h_∞ load frequency control for multi-area power systems with energy-limited DoS attacks," *IEEE Trans. Power Syst.*, vol. 32, no. 5, pp. 4110–4118, Sep. 2017.
[107] P. Srikantha and D. Kundur, "Denial of service attacks and mitigation for stability in cyber-enabled power grid," in *Proc. IEEE Power Energy Soc. Innov. Smart Grid Technol. Conf.*, 2015, pp. 1–5.
[108] J. Hong and C.-C. Liu, "Intelligent electronic devices with collaborative intrusion detection systems," *IEEE Trans. Smart Grid*, vol. 10, no. 1, pp. 271–281, Jan. 2019.
[109] Y. Zhang, L. Wang, Y. Xiang, and C.-W. Ten, "Power system reliability evaluation with SCADA cybersecurity considerations," *IEEE Trans. Smart Grid*, vol. 6, no. 4, pp. 1707–1721, Jul. 2015.
[110] J. G. Wright and S. D. Wolthusen, "Stealthy injection attacks against IEC61850s GOOSE messaging service," in *Proc. IEEE PES Innovative Smart Grid Technol. Conf. Eur.*, Oct. 2018, pp. 1–6.
[111] M. S. Rahman, M. A. Mahmud, A. M. T. Oo, and H. R. Pota, "Multi-agent approach for enhancing security of protection schemes in cyber-physical energy systems," *IEEE Trans. Ind. Inform.*, vol. 13, no. 2, pp. 436–447, Apr. 2017.
[112] P. H. J. Nardelli *et al.*, "Energy internet via packetized management: Enabling technologies and deployment challenges," *IEEE Access*, vol. 7, pp. 16909–16924, 2019.
[113] P. Wang, M. Liu, Z. Cheng, Y. Yang, and S. Zhang, "Key technology research on 5G mobile communications power system," in *Proc. IEEE Int. Telecommun. Energy Conf.*, Oct. 2017, pp. 142–148.
[114] G. Durisi, T. Koch, and P. Popovski, "Toward massive, ultrareliable, and low-latency wireless communication with short packets," *Proc. IEEE*, vol. 104, no. 9, pp. 1711–1726, Sep. 2016.
[115] P. Popovski *et al.*, "Wireless access for ultra-reliable low-latency communication: Principles and building blocks," *IEEE Netw.*, vol. 32, no. 2, pp. 16–23, Mar./Apr. 2018.
[116] P. Hovila *et al.*, "5G networks enabling new smart grid protection solutions," in *Proc. 25th Int. Conf. Elect. Distrib.*, Madrid, Spain, Jun. 2019. [Online]. Available: https://www.cired-repository.org/handle/20.500.12455/816
[117] T. S. Ustun, R. H. Khan, A. Hadbah, and A. Kalam, "An adaptive microgrid protection scheme based on a wide-area smart grid communications network," in *Proc. IEEE Latin-Amer. Conf. Commun.*, Nov. 2013, pp. 1–5.
[118] F. Polunin, D. C. Melgarejo, T. Lindh, A. Pinömaa, P. H. Nardelli, and O. Pyrhonen, "Demonstrating the impact of LTE communication latency for industrial applications," in *Proc. IEEE 17th Int. Conf. Ind. Inform.*, 2019, vol. 1, pp. 977–982.
[119] 5G for Connected Industries and Automation, 5G Alliance for Connected Industries and Automation, Frankfurt am Main, Germany, 2018.
[120] M. Angjelichinoski, K. F. Trillingsgaard, and P. Popovski, "A statistical learning approach to ultra-reliable low latency communication," *IEEE Trans. Commun.*, vol. 67, no. 7, pp. 5153–5166, Jul. 2019.
[121] X. Foukas, G. Patounas, A. Elmokashfi, and M. K. Marina, "Network slicing in 5G: Survey and challenges," *IEEE Commun. Mag.*, vol. 55, no. 5, pp. 94–100, May 2017.
[122] A. E. Kalør, R. Guillaume, J. J. Nielsen, A. Mueller, and P. Popovski, "Network slicing in industry 4.0 Applications: Abstraction methods and end-to-end analysis," *IEEE Trans. Ind. Inform.*, vol. 14, no. 12, pp. 5419–5427, Dec. 2018.
[123] P. Popovskii, K. F. Trillingsgaard, O. Simeone, and G. Duris, "5G wireless network slicing for eMBB, URLLC, and mMTC: A communication-theoretic view," *IEEE Access*, vol. 6, pp. 55765–55779, 2018.
[124] H. V. K. Mendis, P. E. Heegaard, and K. Kralevska, "5G network slicing for smart distribution grid operations," in *Proc. 25th Int. Conf. Elect. Distrib.*, Madrid, Spain, Jun. 2019. [Online]. Available: https://www.cired-repository.org/handle/20.500.12455/658
[125] L. Thrybom and Á. Kapovits, "5G and energy," *5GPPP White Paper*, 2015.
[126] P. Popovski *et al.*, "Wireless access in ultra-reliable low-latency communication (URLLC)," *IEEE Trans. Commun.*, vol. 67, no. 8, pp. 5783–5801, Aug. 2019.
[127] J. Park, S. Samarakoon, M. Bennis, and M. Debbah, "Wireless network intelligence at the edge," *Proc. IEEE*, vol. 107, no. 11, pp. 2204–2239, Nov. 2019.
[128] G. Bag, L. Thrybom, and P. Hovila, "Challenges and opportunities of 5G in power grids," *CIRED-Open Access Proc. J.*, vol. 2017, no. 1, pp. 2145–2148, 2017.
[129] Y. Siriwardhana, P. Porambage, M. Liyanage, J. S. Walia, M. Matinmikko-Blue, and M. Ylianttila, "Micro-operator driven local 5G network architecture for industrial internet," in *Proc. IEEE Wireless Commun. Netw. Conf.*, 2019, pp. 1–8.

Daniel Gutierrez-Rojas (Student Member, IEEE) received the B.Sc. degree in electrical engineering from the University of Antioquia, Medelln, Colombia, in 2016, and the M.Sc. degree in protection of power systems from the University of São Paulo, São Paulo, Brazil, in 2017. He is currently working toward the Ph.D. degree with the School of Energy Systems, Lappeenranta-Lahti University of Technology, Lappeenranta, Finland.

From 2017 to 2019, he worked as Security of Operation and Fault Analyst with Colombias National Electrical Operator. His current research interests include predictive maintenance, power systems, microgrids, mobile communication systems, and electrical protection systems.

Pedro Henrique Juliano Nardelli (Senior Member, IEEE) received the B.S. and M.Sc. degrees in electrical engineering from the State University of Campinas, Campinas, Brazil, in 2006 and 2008, respectively, and the doctoral degree in communication engineering from the University of Oulu, Oulu, Finland, and the State University of Campinas, in 2013, following a dual-degree agreement.

He is currently an Assistant Professor (tenure track) in Internet of Things (IoT) in Energy Systems with the Lappeenranta-Lahti University of Technology (LUT), Lappeenranta, Finland, and holds a position of Academy of Finland Research Fellow with a project called Building the Energy Internet as a large-scale IoT-based cyber–physical system that manages the energy inventory of distribution grids as discretized packets via machine-type communications (EnergyNet). He leads the Cyber–Physical Systems Group with LUT and is the Project Coordinator of the CHIST-ERA European Consortium Framework for the Identification of Rare Events via Machine Learning and IoT Networks (FIREMAN). He is also an Adjunct Professor with the University of Oulu in the topic of communications strategies and information processing in energy systems. His current research interests include wireless communications particularly applied in industrial automation and energy systems.

Dr. Nardelli received a Best Paper Award of the IEEE Power and Energy Society Innovative Smart Grid Technologies Latin America 2019 in the track Big Data and Internet of Things.

Goncalo Mendes received the Ph.D. degree in sustainable energy systems (MIT Portugal Program) from the University of Lisbon, Lisbon, Portugal, 2017.

He is currently a Postdoctoral Researcher with the School of Energy Systems, Lappeenranta-Lahti University of Technology, Lappeenranta, Finland. He has recently received a Fulbright scholarship to investigate regulatory challenges faced by multistakeholder microgrid projects and to derive novel enabling policies from these lessons. He is a representative for Europe at the International Steering Committee of the annual Microgrid Symposiums and a member of CIREDs Working Group on Microgrid Business Models and Regulatory Issues. His main research interests include intersection of local energy systems with policy and business aspects.

Petar Popovski (Fellow, IEEE) received the Dipl.Ing and M.Sc. degrees in communication engineering from Saints Cyril and Methodius University, Skopje, North Macedonia, in 1997 and 2000, respectively, and the Ph.D. degree in wireless communications from Aalborg University, Aalborg, Denmark, in 2005.

He is currently a Professor with Aalborg University, where he is heading the section on connectivity. He has authored or coauthored more than 300 papers in journals, conference proceedings, and edited books. He was featured in the list of Highly Cited Researchers 2018, compiled by Web of Science. He holds more than 30 patents and patent applications. He has recently published the book entitled *Wireless Connectivity: An Intuitive and Fundamental Guide* (Hoboken, NJ, USA: Wiley, 2020). His current research interests include wireless communication, communication theory, and Internet of things.

Prof. Popovski received an ERC Consolidator Grant (2015), the Danish Elite Researcher Award (2016), the IEEE Fred W. Ellersick Prize (2016), the IEEE Stephen O. Rice Prize (2018), and the Technical Achievement Award from the IEEE Technical Committee on Smart Grid Communications. He is currently a Steering Committee Member of the IEEE International Conference on Communications, Control, and Computing Technologies for Smart Grids (SmartGridComm) and IEEE TRANSACTIONS ON GREEN COMMUNICATIONS AND NETWORKING. He previously served as a Steering Committee Member of the IEEE INTERNET OF THINGS JOURNAL. He is an Area Editor for the IEEE TRANSACTIONS ON WIRELESS COMMUNICATIONS. He was the General Chair of the IEEE SmartGridComm 2018 and the IEEE Communication Theory Workshop 2019. Since 2019, he has been a Member-at-Large of the Board of Governors of the IEEE Communications Society.

ACTA UNIVERSITATIS LAPPEENRANTAENSIS

1036. KARUPPANNAN GOPALRAJ, SANKAR. Impacts of recycling carbon fibre and glass fibre as sustainable raw materials for thermosetting composites. 2022. Diss.

1037. UDOKWU, CHIBUZOR JOSEPH. A modelling approach for building blockchain applications that enables trustable inter-organizational collaborations. 2022. Diss.

1038. INGMAN, JONNY. Evaluation of failure mechanisms in electronics using X-ray imaging. 2022. Diss.

1039. LIPIÄINEN, SATU. The role of the forest industry in mitigating global change: towards energy efficient and low-carbon operation. 2022. Diss.

1040. AFKHAMI, SHAHRIAR. Laser powder-bed fusion of steels: case studies on microstructures, mechanical properties, and notch-load interactions. 2022. Diss.

1041. SHEVELEVA, NADEZHDA. NMR studies of functionalized peptide dendrimers. 2022. Diss.

1042. SOUSA DE SENA, ARTHUR. Intelligent reflecting surfaces and advanced multiple access techniques for multi-antenna wireless communication systems. 2022. Diss.

1043. MOLINARI, ANDREA. Integration between eLearning platforms and information systems: a new generation of tools for virtual communities. 2022. Diss.

1044. AGHAJANIAN, SOHEIL. Reactive crystallisation studies of CaCO3 processing via a CO2 capture process: real-time crystallisation monitoring, fault detection, and hydrodynamic modelling. 2022. Diss.

1045. RYYNÄNEN, MARKO. A forecasting model of packaging costs: case plain packaging. 2022. Diss.

1046. MAILAGAHA KUMBURE, MAHINDA. Novel fuzzy k-nearest neighbor methods for effective classification and regression. 2022. Diss.

1047. RUMKY, JANNATUL. Valorization of sludge materials after chemical and electrochemical treatment. 2022. Diss.

1048. KARJUNEN, HANNU. Analysis and design of carbon dioxide utilization systems and infrastructures. 2022. Diss.

1049. VEHMAANPERÄ, PAULA. Dissolution of magnetite and hematite in acid mixtures. 2022. Diss.

1050. GOLOVLEVA, MARIA. Numerical simulations of defect modeling in semiconductor radiation detectors. 2022. Diss.

1051. TREVES, LUKE. A connected future: The influence of the Internet of Things on business models and their innovation. 2022. Diss.

1052. TSERING, TENZIN. Research advancements and future needs of microplastic analytics: microplastics in the shore sediment of the freshwater sources of the Indian Himalaya. 2022. Diss.

1053. HOSEINPUR, FARHOOD. Towards security and resource efficiency in fog computing networks. 2022. Diss.

1054. MAKSIMOV, PAVEL. Methanol synthesis via CO2 hydrogenation in a periodically operated multifunctional reactor. 2022. Diss.

1055. LIPIÄINEN, KALLE. Fatigue performance and the effect of manufacturing quality on uncoated and hot-dip galvanized ultra-high-strength steel laser cut edges. 2022. Diss.

1056. MONTONEN, JAN-HENRI. Modeling and system analysis of electrically driven mechatronic systems. 2022. Diss.

1057. HAVUKAINEN, MINNA. Global climate as a commons — from decision making to climate actions in least developed countries. 2022. Diss.

1058. KHAN, MUSHAROF. Environmental impacts of the utilisation of challenging plastic-containing waste. 2022. Diss.

1059. RINTALA, VILLE. Coupling Monte Carlo neutronics with thermal hydraulics and fuel thermo-mechanics. 2022. Diss.

1060. LÄHDEAHO, OSKARI. Competitiveness through sustainability: Drivers for logistics industry transformation. 2022. Diss.

1061. ESKOLA, ROOPE. Value creation in manufacturing industry based on the simulation. 2022. Diss.

1062. MAKARAVA, IRYNA. Electrochemical recovery of rare-earth elements from NdFeB magnets. 2022. Diss.

1063. LUHAS, JUKKA. The interconnections of lock-in mechanisms in the forest-based bioeconomy transition towards sustainability. 2022. Diss.

1064. QIN, GUODONG. Research on key technologies of snake arm maintainers in extreme environments. 2022. Diss.

1065. TAMMINEN, JUSSI. Fast contact copper extraction. 2022. Diss.

1066. JANTUNEN, NIKLAS. Development of liquid–liquid extraction processes for concentrated hydrometallurgical solutions. 2023. Diss.

1067. GULAGI, ASHISH. South Asia’s Energy [R]evolution – Transition towards defossilised power systems by 2050 with special focus on India. 2023. Diss.

1068. OBREZKOV LEONID. Development of continuum beam elements for the Achilles tendon modeling. 2023. Diss.

1069. KASEVA, JANNE. Assessing the climate resilience of plant-soil systems through response diversity. 2023. Diss.

1070. HYNNINEN, TIMO. Development directions in software testing and quality assurance. 2023. Diss.

1071. AGHAHOSSEINI, ARMAN. Analyses and comparison of energy systems and scenarios for carbon neutrality - Focus on the Americas, the MENA region, and the role of geo-technologies. 2023. Diss.

1072. LAKANEN, LAURA. Developing handprints to enhance the environmental performance of other actors. 2023. Diss.

1073. ABRAMENKO, VALERII. Synchronous reluctance motor with an axially laminated anisotropic rotor in high-speed applications. 2023. Diss.

LUT University

ISBN 978-952-335-933-8
ISBN 978-952-335-934-5 (PDF)
ISSN 1456-4491 (Print)
ISSN 2814-5518 (Online)
Lappeenranta 2023